PRECISION FARMING TECHNOLOGIES FOR ENHANCING AIR QUALITY AND MONITORING BEHAVIORS AND WELFARE IN CAGE-FREE HENS

by

RAMESH BAHADUR BIST

(Under the Direction of Lilong Chai)

ABSTRACT

As the poultry industry is shifting towards cage-free farming practices, various challenges arise regarding air quality, management, behavior, and welfare. In response, this study investigates novel strategies to enhance indoor air quality, manage floor eggs, and monitor footpad health, behaviors, and welfare conditions. The objective of this dissertation study was to evaluate the performance of electrostatic particle ionization (EPI) systems with different lengths, placement heights, and electric supply duration on reducing air pollutants such as particulate matter (PM) and ammonia (NH_3), which are detrimental to both hen welfare and worker health. Moreover, the research delved into the application of advanced monitoring systems for detecting health and welfare issues such as mortality, floor egg-laying behavior (FELB), piling behavior (PB), bumblefoot, and footpad dermatitis (FPD). For this study, 800 hens were raised in 4 cage-free research rooms and arranged in different experimental designs per research objectives. The results demonstrated no significant difference in NH_3 concentrations among treatments. However, it shows a significant reduction in $PM_{2.5}$ (up to 31.7%), PM_{10} (up to 32.7%), small particles (up to 32.4%), and large particles (up to 33.3%) using longer EPI systems, highlighting the critical role of precise technology application in enhancing air quality. Additionally, the

study revealed no significant differences in PM reduction across various EPI heights but underscored the importance of prolonged operation for optimal PM mitigation. The development and testing of You Only Look Once (YOLO) models showcased higher accuracy (up to 99.6%) in mortality, FELB, PB, BFD detections, and automatic FPD scoring, offering promising tools for real-time health and behavior monitoring. In conclusion, this dissertation emphasizes the transformative impact of precision farming technologies in advancing poultry welfare and environmental conditions within cage-free rooms. By integrating EPI technology, and cutting-edge monitoring systems, the research provides a holistic approach to tackling the challenges of modern poultry farming, paving the way for more ethical, efficient, and environmentally friendly production practices.

INDEX WORDS: Precision farming, Computer vision, Cage-free, Laying hens, Air quality, Behaviors and welfare

PRECISION FARMING TECHNOLOGIES FOR ENHANCING AIR QUALITY AND MONITORING BEHAVIORS AND WELFARE IN CAGE-FREE HENS

by

RAMESH BAHADUR BIST

B.Sc. in Zoology, Siddhanath Science Campus, Tribhuvan University, Kanchanpur, Nepal, 2014

M.Sc. in Animal Science, Arkansas State University, Jonesboro, Arkansas, 2018

A Dissertation Submitted to the Graduate Faculty of the University of Georgia in Partial Fulfillment of the Requirement for the Degree of

DOCTOR OF PHILOSOPHY

ATHENS, GEORGIA

2024

PRECISION FARMING TECHNOLOGIES FOR ENHANCING AIR QUALITY AND MONITORING BEHAVIORS AND WELFARE IN CAGE-FREE HENS

by

RAMESH BAHADUR BIST

Major Professor:	Lilong Chai
Committee:	Casey W. Ritz
	Woo K. Kim
	Prafulla Regmi
	Deana R. Jones

Electronic Version Approved:

Ron Walcott
Vice Provost for Graduate Education and Dean of the Graduate School
The University of Georgia
May 2024

DEDICATION

I want to dedicate this dissertation to my beloved father (Tej Bahadur Bist), mother (Madhavi Devi Bist), brother (Harish Bahadur Bist), sister (Puja Bist), sister-in-law (Nidhi Baral), friend (Keshav Bist), and my cherished wife (Salina Thapa Magar) along with my daughter (Reeva Bist). Your unwavering love, encouragement, and support have been the pillars of my strength and perseverance throughout these years, making this achievement possible. Thank you from the bottom of my heart.

म यो शोधपत्र मेरो प्यारो बुबा (तेज बहादुर बिष्ट), आमा (माधवी देवी बिष्ट), भाइ (हरिश बहादुर बिष्ट), बहिनी (पुजा बिष्ट), बुहारी (निधि बराल), साथी (केशव बिष्ट), र मेरी प्यारी श्रीमती (सलिना थापा मगर) साथै मेरी छोरी (रिभा बिष्ट)लाई समर्पित गर्न चाहन्छु। यी वर्षहरूमा तपाईंहरूको अटल माया, प्रोत्साहन र समर्थनले मलाई शक्ति र धैर्य प्रदान गरेको छ, जसले यो उपलब्धि सम्भव बनाएको छ। तपाईंहरूप्रति मेरो हृदयको गहिराइबाट धन्यवाद।

ACKNOWLEDGEMENTS

First of all, my deepest appreciation goes to Dr. Lilong Chai, my supervisor, who opened the doors to my dreams and guided me toward the right paths. His enduring support has shaped who I am today. More than a supervisor, Dr. Chai has been an elder brother and a true leader, introducing me to research, paper writing, oral presentations, leadership, and extension works. His generosity in providing resources and personal guidance transformed me from a novice into a productive Poultry Science student capable of conducting and documenting significant research. Dr. Chai's readiness to assist in experiments, celebrate academic milestones, and meticulously review countless documents has been invaluable. I wish him immense success at The University of Georgia.

I extend my gratitude to all committee members and supervisors for their invaluable support. Dr. Casey W. Ritz, your kindness and guidance have been indispensable, especially in research and academic writing. Your contributions created a conducive environment for my Ph.D. journey. Dr. Woo K. Kim, your assistance in my research, from research lab support to feed formulation, has been crucial. Dr. Prafulla Regmi, thank you for your patience with my mistakes on the farm, for correcting my misunderstandings, and for sharing your expertise in animal behavior and welfare. Your equipment and advice significantly enhanced my research quality. Dr. Deana R. Jones, although known for your strictness, was the perfect choice for me, offering invaluable research methodology suggestions that elevated the quality of my work.

My heartfelt thanks to the scholars who supported me academically. Dr. Kristen Navara, your guidance through my graduate journey and towards graduation was pivotal. Dr. Guoming Li,

your example of positivity and kindness, helpful advice, and class support have greatly influenced my academic career. Ms. Kerry A. Banks, Ms. Stacy Minie, and Ms. Kim Kotkiewicz, your responsiveness in financial matters was crucial for the progress of my experiments. Dr. Amit K. Singh, your unconditional support and familial treatment were unforgettable, especially your help with statistical analysis in my early career stages.

To the graduate students who were part of my Ph.D. journey, your help was invaluable. Mr. Milan K. Sharma, my brother, your guidance in the early stages and assistance with feed formulation were much appreciated. Dr. Yangyang Guo, your support in setting up the lab and experiments was foundational. Mr. Sachin Subedi, my younger brother, your selfless assistance and prioritization of my projects were truly supportive. Mr. Xiao Yang, your daily data collection and sampling assistance greatly eased my Ph.D. journey.

I'm grateful for the farm staff's support. Ms. Lindsey Rackett, Mr. Jesse Hank, and Mr. Matthew Mac Smith, your management of the farm operations and care for the experimental chickens were essential. Mr. Christopher A. McKenzie, your support with feed mixing and delivery was key to the timely success of my research.

My acknowledgment extends to support from Nepal, particularly Mr. Keshav Bist, whose expertise in programming was crucial. Your programming assistance and algorithmic suggestions were instrumental in my machine learning and deep learning projects. Your teaching style in the step-by-step process of machine learning helped me a lot. Your readiness to solve programming challenges has been a beacon of support.

I'm thankful for the project's sponsors, including the Egg Industry Center, Georgia Research Alliance (Venture Fund), Oracle America, USDA-NIFA AFRI, UGA CAES Dean's Office Research Fund, UGA COVID Recovery Research Fund, USDA Hatch projects, UGA Rural

Engagement Seed Grant & UGA Global Engagement Fund, whose financial support made this research possible.

Lastly, my heartfelt gratitude to my parents, beloved wife Salina Thapa Magar, brothers, sisters, sisters-in-law, father-in-law, mother-in-law, maternal uncles, and all relatives for their endless support and sacrifices. My wife's daily assistance, unwavering support through challenges, and exceptional parenting have been a cornerstone of my success. This journey would not have been possible without each of you. Your contributions have been the bedrock of my Ph.D. career, and I stand today because of your unwavering faith and assistance.

अन्त्यमा, साथ दिनुहुने मेरा आमाबुवा, मेरी प्यारी श्रीमती, दाजुभाइ, दिदी बहिनी, बुहारी, सासु, ससुरा, मामा, र मेरा सम्पूर्ण आफन्तजनहरूमा हार्दिक धन्यवाद ज्ञापन गर्दछु। मेरो आमाबुवालाई उहाँहरूको अथक प्रयास र त्यागहरूको लागि म हृदयदेखि धन्यवाद दिन्छु जसले मलाई यो सफलताको बिन्दुमा पुऱ्याएको छ। साथै मलाई यो सफलता प्राप्त गर्नको लागि धेरै त्याग गर्नुहुने मेरी प्यारी पत्नी (सलिना थापा मगर) लाई विशेष धन्यवाद दिन चाहन्छु। दैनिक कार्यहरूमा तपाईंको सहयोग, कठिनाइ र तनावपूर्ण क्षणहरूमा स्थिर समर्थन, र छोरीको पालनपोषणको लागि फेरि पनि धन्यवाद।

TABLE OF CONTENTS

Page

APPENDICES

LIST OF TABLES

Page

LIST OF FIGURES

Page

CHAPTER 1

PRECISION POULTRY FARMING TECHNOLOGIES: LITERATURE REVIEW

1.1 INTRODUCTION

Poultry farming plays a vital role in securing global food supplies, especially with the ongoing growth of the world's population. As this population surge unfolds, the need for more intelligent approaches to produce sufficient protein becomes increasingly paramount. Poultry products (encompassing meat and eggs) are a cost-effective and readily accessible alternative protein source in the USA. In particular, eggs serve as the main protein source in the human diet, with consumption increasing by 4.8% since 2000, significantly impacting the United States economy (UEP, 2022). As of January 1, 2024, the United States saw a 1% increase in the total number of layers from the last year, reaching 379 million. Among these layers, 312 million were producing table or market-type eggs, 63.6 million were broiler-type hatching eggs, and 3.83 million were layer hatching eggs (USDA, 2024). In addition, there has been a trend of increasing cage-free hen numbers compared to cage-hen numbers (Figure 1.1) (USDA, 2023). Each hen lays on average 300 eggs annually and 79.3 eggs per 100 hens daily (USDA, 2024). An increase in the human population and a broader egg industry shift toward a cage-free system might affect egg production. The target is to raise cage-free (CF) production to 66% by 2026 to meet demand (UEP, 2022). However, moving from caged to cage-free production comes with various

challenges and complexities that need to be addressed.

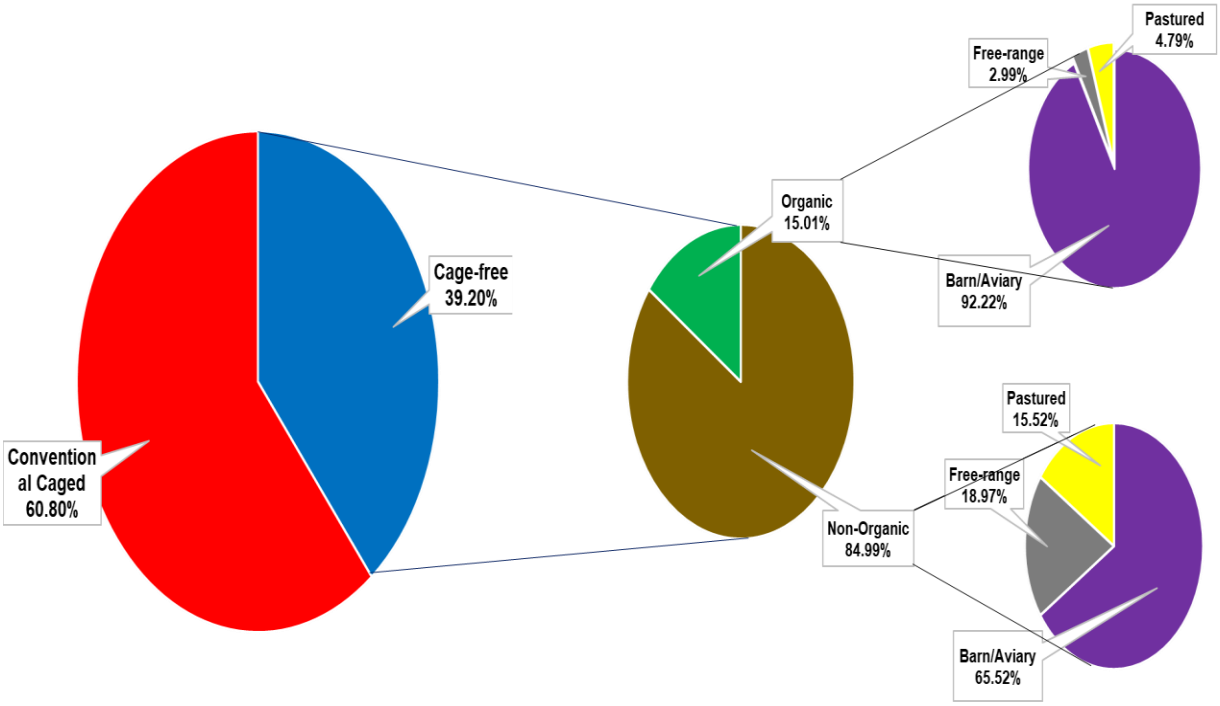

Figure 1.1: Distribution of laying hens across various poultry housing (USDA 2024).

Shifting from caged systems to cage-free housing presents a notable challenge of the increased presence of air pollutants like particulate matter (PM) and ammonia (Zhao et al., 2011; Xin, 2016; Chai et al., 2018). Research suggests that CF environments demonstrate significantly higher PM and ammonia emissions than conventional cage and enriched colony systems (Zhao et al., 2015). Additionally, CF housing shows elevated concentrations of airborne bacteria due to PM acting as the primary carrier. Airborne contaminants such as dust, ammonia, and pathogens can accumulate in poultry houses, leading to respiratory issues, stress, and reduced bird productivity (Patterson, 2005). Maintaining optimal air quality ensures birds' and farm workers' health and well-being (Xin, 2016; Chai et al., 2018; Bist and Chai, 2022; Bist et al., 2023b). As a

result, the research should focus on prioritizing strategies that mitigate emissions in CF housing. Recommendations suggest keeping ammonia levels below 10 ppm and not to exceed 25 ppm daily within the laying hen house (UEP, 2006). Furthermore, adherence to the PM occupational exposure limit (human) is crucial, not exceeding 35 $\mu g/m^3$ 24-hour mean for $PM_{2.5}$ and 150 $\mu g/m^3$ 24-hour mean for PM_{10} (US EPA, 2022). Therefore, controlling PM and ammonia emissions is crucial for protecting animal welfare and human health in poultry farming environments. Furthermore, managing floor eggs, common in cage-free systems, poses logistical challenges that impact hygiene, egg quality, and labor efficiency. Additionally, ensuring hens' behavior and welfare in cage-free environments requires continuous monitoring of behavior, social dynamics, and environmental conditions to address potential stressors and promote natural behaviors.

Berckmans (2014) and Li et al. (2019) highlighted that poultry management in intensive production systems is complex and dynamic. Individual birds can exhibit varied behaviors (pecking, foraging, dustbathing, mislaying) depending on the rearing systems and environmental conditions, challenging manual inspection (Oliveira et al., 2019). Moreover, within the same setting, poultry may respond differently to their surroundings, and their behavior patterns can change throughout the day (Tolkamp et al., 2011). Precision animal farming tools, acting as constant monitors, offer invaluable assistance to farmers by observing chickens, reporting abnormalities, and providing early warnings to prevent adverse outcomes (Berckmans, 2014).

Poultry behaviors carry crucial information that can inform facility design and animal-driven management practices for enhanced production (Li et al., 2020a). For instance, preening

and gentle pecking can indicate normal behavior (Appleby et al., 2004). However, severe pecking can result in cannabilism and death of the bird. Therefore, observing normal behavior can give an idea of abnormal behaviors on the farm when the behaviors deviate from normal standards. While manual observation remains the gold standard for studying poultry behaviors, it is labor-intensive and prone to human bias (Tuyttens et al., 2014). Precision animal farming tools offer a solution by automatically and objectively detecting poultry behaviors, enabling continuous monitoring and analysis.

Precision poultry farming (PPF) is an innovative approach that utilizes advanced technologies and data-driven approach within the poultry sector to address various challenges in the bird management, environment, waste management, behavior monitoring, health, nutrition, and welfare assessment (Zhao et al., 2022). The landscape of poultry farming is transforming with the advent of precision technology. PPF collects real-time data on birds using different technologies. This new wave of technologies integrates cutting-edge advancements, including smart robots, advanced computers, artificial intelligence, and sensor technology, to revolutionize the efficiency of poultry farming. The overarching objective of precision technology is to ensure that chickens receive precisely tailored environments to perform their natural behaviors and produce safe, high-quality foods. To achieve this, farms leverage data to monitor the health and behaviors of each bird to enhance the growth and overall health of chickens. This means that PPF can help improve animal welfare by detecting early stages of diseases and stressful situations during bird management and allowing steps to be taken quickly enough to limit the adverse effects. Precision technology represents a significant stride toward optimizing poultry farming practices. This innovative method tackles the increasing worldwide need for protein

while establishing a more sustainable and effective system to fulfill the nutritional requirements of a burgeoning world population. The precision tools showcased in this study play a pivotal role in the early detection of issues related to animal welfare. They contribute significantly to enhancing and expediting management decisions, ultimately leading to a reduction in economic losses.

This study's primary goal is to emphasize the growing importance of precision techniques in poultry farming, providing an insightful tour through the dynamic developments in this field. Precision technologies hold immense promise in poultry farming, where challenges such as air quality and monitoring behaviors and welfare are paramount. This literature review explores the precision farming technologies utilized in poultry production, specifically focusing on improving air quality, management, and behavior monitoring and welfare within cage-free hen rooms.

1.2 ELECTROSTATIC CHARGING SYSTEM

Traditional application of electrostatic ionization technology involves managing particulate matter (PM) levels within animal feeding operations. However, it has also found application in poultry housing environments (Mitchell et al., 2004; Ritz et al., 2006; Winkel et al., 2012; Manuzon et al., 2014). This method, based on electrostatic principles, functions by generating charged particles. These generated charged particles attract and neutralize airborne contaminants like dust, dander, ammonia, and bacteria within poultry houses (Mitchell et al., 2004; Ritz et al., 2006). Previous studies have demonstrated its efficacy in reducing airborne PM and bacteria (Mitchell et al., 2002, 2004; Mitchell and Waltman, 2003). By creating cleaner and healthier indoor environments, these systems minimize respiratory issues and stress among birds,

thus enhancing their overall well-being and productivity. Furthermore, reducing airborne pathogens helps mitigate disease transmission, bolstering biosecurity measures on the farm. For instance, Mitchell and Waltman (2003) observed a significant reduction in dust levels by 77–79% with an electrostatic charging system (ESCS) in a hatching cabinet. Similarly, ESCS effectively decreased *Enterobacteriaceae* and Salmonella bacteria in the air by 93 to 96% and 33 to 83%, respectively (Mitchell and Waltman, 2003). Recent research has explored the efficacy of the prototype electrostatic precipitator (ESP) technique across various ventilation and weather conditions, achieving notable reductions in PM2.5 and PM10 levels by up to 97.8% and 99.0%, respectively (Knight et al., 2021). Consequently, various studies on electrostatic ionization have shown significant reductions in PM and airborne bacteria by up to 94% and 96%, respectively (Table 1.1). In addition, one study has shown ammonia reduction by 56% using ESCS (Mitchell et al., 2004). Therefore, an ESCS can be a possible solution to improve air quality by reducing PM, ammonia, and bacterial concentrations. Various research studies have been covered in Table 1.1.

Table 1.1: Air Pollutant reduction with electrostatic charging.

Control Technology	**Charging Units**	**PM 2.5 (%)**	**PM10 (%)**	**Total dust (%)**	**Airborne bacteria (%)**	**Ammonia**	**References**
ESP	13.8, 27.6, and 41.4 kV	86.9 – 97.8	90.8 – 99.0	N/A	N/A	N/A	Knight et al., 2021

Negative ionization system Positive ionization system	Electrode -30kV with 2mA current Electrode +30kV with 2 mA current	49 6	68 0	N/A	N/A	N/A	Winkel et al., 2016
ESP	Electrode +30kV with 0.2-1.0 mA current	45.3	57.0	N/A	N/A	N/A	Winkel et al., 2015
Optimized ESP	9.6 to 13.6 KV with air velocity 0.8 to 2.2 m/s	86	84	82	N/A	N/A	Manuzon et al., 2014
Prototype ESP	+30 kVdc and <1 mA	45	57	N/A	N/A	N/A	Winkel et al., 2012
Air Ionization	−30 kVdc and 0.9 mA	10	36	N/A	N/A	N/A	Cambra-López et al., 2009

ESCS	25K–30K Vdc and 2 mA	N/A	36	48	N/A	N/A	Lim et al., 2008
ESCS	−30 kVdc and 2 mA	N/A	N/A	43	N/A	13	Ritz et al., 2006
ESCS	−30 kVdc and <0.5 mA	N/A	N/A	61	67	56	Mitchell et al., 2004
ESCS	-30 kVdc and 0.2 mA	N/A	N/A	77-79	93-96% Enterobacteriaceae 33-83% Salmonella	N/A	Mitchell and Waltman, 2003
ESCS	−20 kVdc and 0.5 mA	N/A	N/A	94	93% Enterobacteriaceae	N/A	Mitchell et al., 2002

ESP= Electrostatic precipitator, ESCS=Electrostatic Charging System, N/A= not available or not found. Published in Applied Science MDPI journal. Bist, R. B., & Chai, L. (2022). Advanced strategies for mitigating particulate matter generations in poultry houses. *Applied Sciences*, *12*(22), 11323.

Various studies have explored different charging systems in diverse poultry housing setups (Mitchell, 1998; Mitchell et al., 2002; Ritz et al., 2006; Knight et al., 2021). However, these studies lack a comprehensive comparison of air pollutant reduction across different charging systems, considering factors like length, duration, height, and potential synergies with bedding management strategies. In addition, it is essential to acknowledge the limitations of EPI systems, as they may not effectively address all sources of air pollution. Additionally, their efficacy can be influenced by factors like airflow patterns, house design, and maintenance practices, necessitating further research to optimize their deployment for specific poultry production environments.

1.3 IOT AND SENSOR APPLICATIONS

In modern poultry farming, the real-time monitoring of vital environmental parameters is essential for ensuring optimal growth and productivity. Precision agriculture, fueled by Internet of Things (IoT) applications, employs strategically positioned sensors within poultry house to continuously gather data on temperature, humidity, air quality, light intensity, and activity levels (Lashari et al., 2018; Astill et al., 2020; Table 1.2). This data empowers farmers to fine-tune the production environment, creating optimal conditions for bird well-being. Research demonstrates the effectiveness of these technologies, with specific temperature and humidity control improving feed conversion rates and overall growth. Furthermore, IoT applications extend beyond environmental monitoring to track feed consumption (Batuto et al., 2020), water intake (Mohammed et al., 2022), and bird movement patterns (Yang et al., 2022; Gómez et al., 2022), providing valuable insights into behavior (Yang et al., 2023c) and enabling early detection of health issues (Ahmed et al., 2021). For instance, the Li et al. (2020) study highlighted how IoT-

enabled systems facilitated the early detection of abnormal behavior in laying hens, allowing for timely intervention and improved flock health.

Table 1.2: Summary of IoT and sensor technology used in various research.

Sensor types/ Models used	Research objective	Results or conclusion	Reference
Temperature sensor, Ammonia sensor, Carbon dioxide sensor, Dust Monitor	Monitor room temperature, relative humidity, ammonia, carbon dioxide, dust level	It helps to identify and maintain adequate temperature, ammonia, dust, and carbon dioxide levels inside houses	Bist et al., 2022, 2023c; a
Mica2Dot mote radio node, accelerometer	Detection of jumping and landing force	The result found that body-mounted sensors work for detecting hen jumps	Banerjee et al., 2014
Temperature sensors, genetic algorithm of dual-structure coding	Placement of temperature sensors and developed optimized temperature inside housing	Developed accurate temperature-measuring genetic algorithm model	Hu et al., 2022
Body-worn inertial measurement unit modules tailored with time-series data	Automatic recognition of hen's behaviors	The best model reached almost 100% accuracy, highlighting deep learning's	Shahbazi et al., 2023

		potential for improving poultry system management	
Microelectromechanical three-axis accelerometer	Physical activity levels	Physical activities were measured with 98% accuracy and verified using video recordings	Kozak et al., 2016
Accelerometer	Quantify inactivity in laying hen with or without keel-bone fractures	Successfully quantified indifferences between hen with or without keel-bone fractures	Casey-Trott and Widowski, 2018
Accelerometer	Jumping and landing force detection	Accelerometer is feasible for jumping and landing detection	Banerjee et al., 2014
UHF RFID*	Study individual feeding and nesting behaviors	Demonstrated in detecting feeding and nesting behaviors with 86-99% accuracy	Li et al., 2017
Passive RFID	Track and behavior quantification	95% accuracy in tracking the movement trajectories between automated measurement and human labelings	Nakarmi et al., 2014

RFID	Quantifying detection performance	Successfully quantified occupancy of space by 85% or greater	Sales et al., 2015
RFID	Identify laying hens passing the pop-hole	97% of hens identified correctly	Thurner and Wendl, 2008
RFID	Perching behavior monitoring for group-housed poultry	98-100% accuracy	Wang et al., 2019
RFID transponders	Investigate associations between time spent, fear levels, feather damage, and weight	An inverse relationship between fearfulness and the time spent using range area	Hartcher et al., 2016

*RFID- Radio-Frequency Identification.

In poultry, an IoT device widely used to monitor activities and behavior is an accelerometer. Accelerometer sensors, integrated into wearable devices or strategically positioned within poultry housing systems, revolutionize precision technologies by facilitating real-time monitoring of individual birds (Casey-Trott and Widowski, 2018; Pullin et al., 2020). These sensors detect variations in movement, providing farmers with comprehensive insights into bird well-being. By continuously measuring and recording movement and activity levels, accelerometer data offers objective metrics for assessing hen welfare, including early indicators of stress, illness, or environmental disturbances. This allows for timely interventions and targeted

management practices to mitigate welfare risks. In addition, activity level is directly correlated with PM (Costa and Guarino, 2009; Mostafa and Buescher, 2011), and no such study has been done to correlate using accelerometers. However, challenges such as data management, sensor accuracy, price, and scalability hinder widespread adoption in commercial poultry production. Integrating accelerometer data with other sources presents opportunities for holistic management approaches that prioritize productivity and welfare, enhance decision-making processes, and optimize management practices to promote natural behaviors and improve overall welfare outcomes.

1.4 IMAGE PROCESSING TECHNOLOGY

Image processing technology has emerged as a transformative tool in poultry farming, offering farmers automated solutions for monitoring and managing various aspects of production (Neethirajan, 2020; Benos et al., 2021; Subedi et al., 2023a). Cameras installed in poultry houses capture desired views, continuously recording images/videos for further processing (Figure 1.2). By deploying cameras equipped with sophisticated image recognition algorithms, farmers can track flock behavior, assess egg production, and manage housing environments more effectively. Automated egg detection and collection, facilitated by overhead cameras and advanced algorithms, exemplify one of the primary applications of image processing in poultry farming, streamlining the process and minimizing losses. Bird activity can be recorded and processed with minimal human interference using this technology, enhancing operational efficiency and improving animal welfare. Despite its numerous benefits, implementing image processing technology in poultry farming requires careful consideration of cost, infrastructure requirements, and data privacy concerns. Furthermore, challenges such as the complexity of image

backgrounds, environmental conditions, bird sizes, and postures influence the performance of processing algorithms, leading to poor generalization to other settings (Li, 2021). The technology may struggle to differentiate individual poultry in group settings and overlook individual variations within groups, posing challenges for commercial applications and behavior studies. Continued research and development efforts are necessary to address these challenges and improve the accuracy, reliability, and scalability of image processing solutions for poultry production applications.

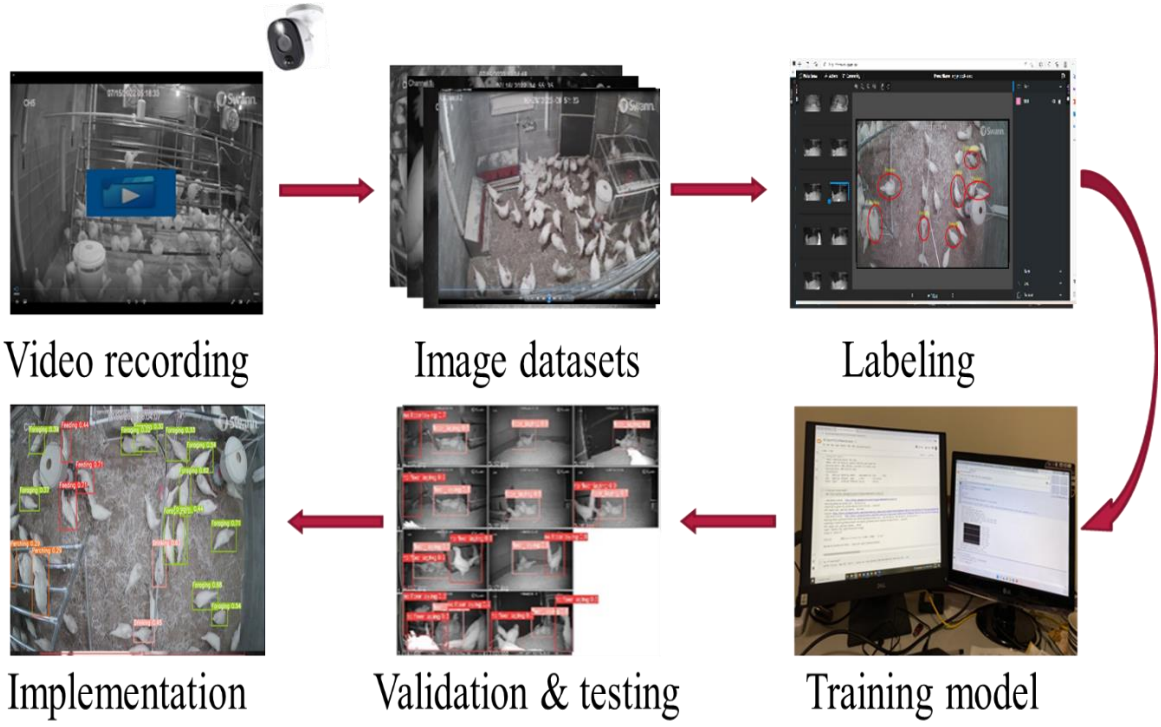

Figure 1.2: Image-processing steps used for machine learning model.

Furthermore, while image processing technology has demonstrated high performance in various applications such as behavior classification (Yang et al., 2023c) and flock distribution evaluation (Yang et al., 2022, 2023a), areas still require further development and evaluation. Specific behaviors, such as laying hen's normal and abnormal behavior monitoring, may

necessitate tailored algorithms based on specific farm settings, highlighting the need for continuous refinement of processing techniques. Challenges such as the inability to differentiate individual poultry in group settings and variations within groups underscore the importance of developing more robust and adaptable algorithms. Despite these challenges, the potential of image processing technology to revolutionize poultry farming by providing valuable insights and automating tasks remains significant. Real-time monitoring and decision-making enabled by this technology enhance operational efficiency and animal welfare, driving ongoing research and innovation. With concerted efforts to overcome limitations and improve performance, image processing technology promises to continue playing a pivotal role in shaping the future of poultry farming, offering farmers unprecedented levels of automation and insight into their operations.

1.5 MACHINE LEARNING

Machine learning algorithms play a pivotal role in unlocking the full potential of precision poultry farming by harnessing data to optimize decision-making and performance (Araujo et al., 2023; Subedi et al., 2023a). These algorithms, spanning supervised, unsupervised, and reinforcement learning techniques, can sift through extensive sensor and video data sets. Their adeptness lies in predicting patterns, identifying irregularities, and refining management approaches. In poultry production, machine learning offers opportunities for enhancing productivity, efficiency, and animal welfare outcomes. Machine learning techniques can be instrumental in developing predictive models for disease detection, establishing early warning systems for welfare issues, and optimizing resource allocation.

Machine learning models have become integral tools for speech recognition (Deng and Li, 2013), text identification (Long et al., 2021), and computer vision (Astill et al., 2020; Yang et al., 2023b). These models have been extensively tested in poultry farming to process poultry-related images (Table 1.3). A prominent machine learning model, YOLO (You Only Look Once), is commonly employed in such tasks (Yang et al., 2022; Subedi et al., 2023a). YOLO models typically consist of input features, a decision boundary, and output labels, including class names, bounding box coordinates, and prediction probabilities. The essence of machine learning lies in learning patterns and relationships from data without explicit programming instructions, allowing for the detection of various elements within poultry-related images. Despite the fundamental principles remaining consistent, the practical applications of machine learning continue to evolve. While machine learning offers robust detection capabilities and can be adapted to different environments, object shapes, sizes, and textures, it also presents computational challenges, particularly during training when dealing with large datasets or complex features. Moreover, selecting the appropriate machine learning algorithm, tuning its parameters, and validating its performance are crucial steps before deployment (Maleki et al., 2020). The successful integration of machine learning in poultry production hinges upon addressing various challenges, including data quality assurance, model interpretability, and efficient utilization of computational resources (Neethirajan, 2023). Moreover, ethical considerations surrounding algorithmic decision-making, such as bias and fairness, necessitate careful deliberation to ensure responsible and transparent utilization of technology (Felzmann et al., 2020). Collaboration among researchers, industry stakeholders, and policymakers is imperative to surmount these challenges and fully harness the transformative potential of machine learning in precision poultry farming.

Table 1.3: Cutting-edge livestock monitoring methods in laying hens using the camera.

Models/ methods	**Objective**	**Result/ Conclusion**	**References**
Real-time and automatic detection of hens using different YOLOv5-hens model	Detect floor hens	Overall accuracy more than 95%	Yang et al., 2022
Automatic monitoring of hens on the floor using YOLOv5 models with different configuration	Monitor and detect hens	Detection precision was 98.2%, recall 92.9%, and mAP_0.50 96.7%	Guo et al., 2023
Spatial distribution of hens using the YOLOv5 model	Spatial distribution of laying hens on the floor in detecting perching, feeding, drinking, and other behaviors	Performance in detecting spatial distribution and behavior detection was obtained up to 94.2%	Yang et al., 2023a
Computer vision-based model using two-stage and single-stage model	Egg grading based on 5 egg sizes and defect detection into 5 categories	Accurately detected the egg and graded it by 94-96%.	Yang et al., 2023b

Monitor applied behaviors using multiple CNN* models	Detect and classify 6 behaviors: feeding, drinking, walking, perching, dustbathing, and nesting.	Received accuracy up to 95.3%	Yang et al., 2023c
Segment anything model (SAM) used to segment hens.	Explore hen tracking	SAM lays the foundation for hen segmentation and tracking	Yang et al., 2023d
YOLOv5 model used to detect pecking behavior	Detect pecking behavior	Yolov5 pecking model results in an accuracy of 78.7%	Subedi et al., 2023a
Machine vision-based YOLO models to detect floor eggs	Floor egg detection	Accurately detected floor eggs by 92.1%	Subedi et al., 2023b
Automatic monitoring of hens on the floor using YOLOv5 models with different configuration	Monitor and detect hens	Detection precision was 98.2%, recall 92.9%, and mAP_0.50 96.7%	Guo et al., 2023

Image processing algorithms developed	Feeding and drinking behavior detection	Achieved above 89% accuracy in detecting bird numbers at feeders and drinkers.	Li et al., 2020d
Faster R-CNN	Pullet drinking behaviors assessment	Drinking behavior detection performance achieved above 88% with a faster R-CNN model.	Li et al., 2020b
Single shot detector, Faster R-CNN, Regional-based fully convolutional network.	Floor egg detection	Faster R-CNN resulted in the best performance with an accuracy of 98%.	Li et al., 2020c
YOLOv4-tiny, YOLOv4	Comfort behavior detection	94% detection mAP for classification on the floor.	Sozzi et al., 2022
KNN[#], Decision Tree, Random Forest, Neural Network	Non-destructive assessment of egg quality	An accuracy of 98% was achieved with Random Forest for egg quality detection.	De Oliveira-Boreli et al., 2023

*CNN- Convolutional neural network; [#]KNN- K-nearest neighbors.

1.6 OBJECTIVES AND OUTLINES OF THE DISSERTATION

The main objective of this dissertation was to explore the integration of precision farming technologies (EPI, image processing, machine learning) for enhancing air quality, behavior monitoring, and animal welfare in cage-free hen environments. The detailed objectives were:

(a) Evaluate the effectiveness of EPI systems in reducing airborne pollutants (ammonia and particulate matter) and improving air quality.

(b) Investigate the application of image processing technology for automated abnormal behavior (mislaying, piling) detection and monitoring.

(c) Develop a machine learning model to detect bumblefoot conditions and automatically score footpad conditions.

This dissertation consists of individual chapters, each published or will be published in different journals and summarized in Chapter 9.

1.7 REFERENCES

Ahmed, G., R. A. S. Malick, A. Akhunzada, S. Zahid, M. R. Sagri, and A. Gani. 2021. An approach towards IoT-based predictive service for early detection of diseases in poultry chickens. Sustainability 13:13396.

Appleby, M. C., J. A. Mench, and B. O. Hughes. 2004. Poultry behaviour and welfare. Cabi.

Araujo, S. O., R. S. Peres, J. C. Ramalho, F. Lidon, and J. Barata. 2023. Machine learning applications in agriculture: current trends, challenges, and future perspectives. Agronomy 13:2976.

Astill, J., R. A. Dara, E. D. G. Fraser, B. Roberts, and S. Sharif. 2020. Smart poultry management: smart sensors, big data, and the internet of things. Computers and

Electronics in Agriculture 170:105291 Available at https://www.sciencedirect.com/science/article/pii/S0168169918316363 (verified 19 October 2023).

Banerjee, D., C. L. Daigle, B. Dong, K. Wurtz, R. C. Newberry, J. M. Siegford, and S. Biswas. 2014. Detection of jumping and landing force in laying hens using wireless wearable sensors. Poultry Science 93:2724–2733 Available at https://www.sciencedirect.com/science/article/pii/S0032579119385220 (verified 8 October 2023).

Batuto, A., T. B. Dejeron, P. D. Cruz, and M. J. C. Samonte. 2020. E-poultry: An IoT poultry management system for small farms.Pages 738–742 in IEEE.

Benos, L., A. C. Tagarakis, G. Dolias, R. Berruto, D. Kateris, and D. Bochtis. 2021. Machine learning in agriculture: A comprehensive updated review. Sensors 21:3758 Available at https://www.mdpi.com/1424-8220/21/11/3758 (verified 16 November 2023).

Berckmans, D. 2014. Precision livestock farming technologies for welfare management in intensive livestock systems. Rev. Sci. Tech 33:189–196.

Bist, R. B., and L. Chai. 2022. Advanced strategies for mitigating particulate matter generations in poultry houses. Applied Sciences 12:11323.

Bist, R. B., L. Chai, X. Yang, S. Subedi, and Y. Guo. 2022. Air quality in cage-free houses during pullets production. Page 1 in American Society of Agricultural and Biological Engineers.

Bist, R. B., P. Regmi, D. Karcher, Y. Guo, A. K. Singh, C. W. Ritz, W. K. Kim, D. R. Jones, and L. Chai. 2023a. Bedding management for suppressing particulate matter in cage-free hen houses. AgriEngineering 5:1663–1676.

Bist, R. B., S. Subedi, L. Chai, and X. Yang. 2023b. Ammonia emissions, impacts, and mitigation strategies for poultry production: A critical review. Journal of Environmental Management 328:116919.

Bist, R. B., X. Yang, S. Subedi, M. K. Sharma, A. K. Singh, C. W. Ritz, W. K. Kim, and L. Chai. 2023c. Temporal variations of air quality in cage-free experimental pullet houses. Poultry 2:320–333.

Cambra-López, M., A. Winkel, J. Van Harn, N. Ogink, and A. Aarnink. 2009. Ionization for reducing particulate matter emissions from poultry houses. Transactions of the ASABE 52:1757–1771.

Casey-Trott, T., and T. Widowski. 2018. Validation of an accelerometer to quantify inactivity in laying hens with or without keel-bone fractures. Animal Welfare 27:103–114.

Chai, L., H. Xin, Y. Zhao, T. Wang, M. Soupir, and K. Liu. 2018. Mitigating ammonia and PM generation of cage-free henhouse litter with solid additive and liquid spray. Transactions of the ASABE 61:287–294.

Costa, A., and M. Guarino. 2009. Particulate matter concentration and emission factor in three different laying hen housing systems. Journal of Agricultural Engineering 40:15–24.

De Oliveira-Boreli, F. P., D. F. Pereira, J. A. Gonçalves, V. Z. da Silva, and I. de A. Nääs. 2023. Non-destructive assessment of hens' eggs quality using image analysis and machine learning. Smart Agricultural Technology 4:100161 Available at https://www.sciencedirect.com/science/article/pii/S2772375522001253 (verified 23 February 2024).

Deng, L., and X. Li. 2013. Machine learning paradigms for speech recognition: An overview. IEEE Transactions on Audio, Speech, and Language Processing 21:1060–1089.

Felzmann, H., E. Fosch-Villaronga., C. Lutz., and A. Tamò-Larrieux. 2020. Towards transparency by design for artificial intelligence. Science and engineering ethics, 26(6), 3333-3361.

Gómez, Y., J. Berezowski, Y. A. Jorge, S. G. Gebhardt-Henrich, S. Vögeli, A. Stratmann, M. J. Toscano, and B. Voelkl. 2022. Similarity in temporal movement patterns in laying hens increases with time and social association. Animals 12:555 Available at https://www.mdpi.com/2076-2615/12/5/555 (verified 16 November 2023).

Guo, Y., P. Regmi, Y. Ding, R. B. Bist, and L. Chai. 2023. Automatic detection of brown hens in cage-free houses with deep learning methods. Poultry Science 102:102784.

Hartcher, K., K. Hickey, P. Hemsworth, G. Cronin, S. Wilkinson, and M. Singh. 2016. Relationships between range access as monitored by radio frequency identification technology, fearfulness, and plumage damage in free-range laying hens. Animal 10:847–853.

Hu, X., L. Gao, L. Huo, L. Li, and M. Er. 2022. Optimal placement of laying hen house temperature sensors based on genetic algorithm. IEEE Access 10:7234–7244.

Knight, R. M., L. Zhao, and H. Zhu. 2021. Modelling and optimisation of a wire-plate ESP for mitigation of poultry PM emission using COMSOL. Biosystems Engineering 211:35–49 Available at https://www.sciencedirect.com/science/article/pii/S1537511021002105 (verified 15 June 2023).

Kozak, M., B. Tobalske, D. Springthorpe, B. Szkotnicki, and A. Harlander-Matauschek. 2016. Development of physical activity levels in laying hens in three-dimensional aviaries. Applied Animal Behaviour Science 185:66–72 Available at

https://www.sciencedirect.com/science/article/pii/S0168159116302842 (verified 24 December 2023).

Lashari, M. H., A. A. Memon, S. A. A. Shah, K. Nenwani, and F. Shafqat. 2018. Iot based poultry environment monitoring system.Pages 1–5 in IEEE.

Li, G. 2021. Developing and applying precision animal farming tools for poultry behavior monitoring. Mississippi State University Available at https://scholarsjunction.msstate.edu/cgi/viewcontent.cgi?article=6119&context=td.

Li, G., X. Hui, F. Lin, and Y. Zhao. 2020a. Developing and evaluating poultry preening behavior detectors via mask region-based convolutional neural network. Animals 10:1762.

Li, G., B. Ji, B. Li, Z. Shi, Y. Zhao, Y. Dou, and J. Brocato. 2020b. Assessment of layer pullet drinking behaviors under selectable light colors using convolutional neural network. Computers and Electronics in Agriculture 172:105333 Available at https://www.sciencedirect.com/science/article/pii/S0168169919317454 (verified 23 February 2024).

Li, G., B. Li, Y. Zhao, Z. Shi, Y. Liu, and W. Zheng. 2019. Layer pullet preferences for light colors of light-emitting diodes. Animal 13:1245–1251.

Li, G., Y. Xu, Y. Zhao, Q. Du, and Y. Huang. 2020c. Evaluating convolutional neural networks for cage-free floor egg detection. Sensors 20:332.

Li, L., Y. Zhao, J. Oliveira, W. Verhoijsen, K. Liu, and H. Xin. 2017. A UHF RFID system for studying individual feeding and nesting behaviors of group-housed laying hens. Transactions of the ASABE 60:1337–1347.

Li, G., Y. Zhao, J. L. Purswell, Q. Du, G. D. Chesser, and J. W. Lowe. 2020d. Analysis of feeding and drinking behaviors of group-reared broilers via image processing. Computers

and Electronics in Agriculture 175:105596 Available at https://www.sciencedirect.com/science/article/pii/S0168169919305745 (verified 23 February 2024).

Lim, T. T., A. J. Heber, J. Ni, L. Zhao, and S. H. Hanni. 2008. Effects of electrostatic space charge system on particulate matter emission from high-rise layer barn. Page 1 in American Society of Agricultural and Biological Engineers.

Long, S., X. He, and C. Yao. 2021. Scene text detection and recognition: The deep learning era. International Journal of Computer Vision 129:161–184.

Maleki, F., N. Muthukrishnan., K. Ovens., C. Reinhold., and R. Forghani. 2020. Machine learning algorithm validation: from essentials to advanced applications and implications for regulatory certification and deployment. Neuroimaging Clinics, 30(4), 433-445.

Manuzon, R., L. Zhao, and C. Gecik. 2014. An optimized electrostatic precipitator for air cleaning of particulate emissions from poultry facilities. ASHRAE Transactions 120.

Mitchell, B. 1998. Effect of negative air ionization on ambient particulates in a hatching cabinet. Applied Engineering in Agriculture 14:551–555.

Mitchell, B., R. Buhr, M. Berrang, J. Bailey, and N. Cox. 2002. Reducing airborne pathogens, dust and Salmonella transmission in experimental hatching cabinets using an electrostatic space charge system. Poultry Science 81:49–55.

Mitchell, B., L. Richardson, J. Wilson, and C. Hofacre. 2004. Application of an electrostatic space charge system for dust, ammonia, and pathogen reduction in a broiler breeder house. Applied Engineering in Agriculture 20:87.

Mitchell, B., and W. Waltman. 2003. Reducing airborne pathogens and dust in commercial hatching cabinets with an electrostatic space charge system. Avian Diseases 47:247–253.

Mohammed, A. Y., H. A. Hussein, and M. L. Shuwandy. 2022. Solving drinking-water challenges: supply and temperature in a smart poultry monitoring system using IoT system. Pages 162–168 in Springer.

Mostafa, E., and W. Buescher. 2011. Indoor air quality improvement from particle matters for laying hen poultry houses. Biosystems Engineering 109:22–36.

Nakarmi, A. D., L. Tang, and H. Xin. 2014. Automated tracking and behavior quantification of laying hens using 3D computer vision and radio frequency identification technologies. Transactions of the ASABE 57:1455–1472.

Neethirajan, S. 2020. The role of sensors, big data and machine learning in modern animal farming. Sensing and Bio-Sensing Research 29:100367.

Neethirajan, S. 2023. Digital phenotyping: A game changer for the broiler industry. Animals, 13(16), 2585.

Oliveira, J., H. Xin, and H. Wu. 2019. Impact of feeder space on laying hen feeding behavior and production performance in enriched colony housing. Animal 13:374–383.

Patterson, P. H. 2005. Management strategies to reduce air emissions: Emphasis—Dust and ammonia. Journal of Applied Poultry Research, 14(3), 638-650.

Pullin, A. N., S. M. Temple, D. C. Bennett, C. B. Rufener, R. A. Blatchford, and M. M. Makagon. 2020. Pullet rearing affects collisions and perch use in enriched colony cage layer housing. Animals 10:1269.

Ritz, C., B. Mitchell, B. Fairchild, M. Czarick III, and J. Worley. 2006. Improving in-house air quality in broiler production facilities using an electrostatic space charge system. Journal of Applied Poultry Research 15:333–340.

Sales, G., A. Green, R. S. Gates, T. M. Brown-Brandl, and R. Eigenberg. 2015. Quantifying detection performance of a passive low-frequency RFID system in an environmental preference chamber for laying hens. Computers and Electronics in Agriculture 114:261–268.

Shahbazi, M., K. Mohammadi, S. M. Derakhshani, and P. W. Groot Koerkamp. 2023. Deep learning for laying hen activity recognition using wearable sensors. Agriculture 13:738.

Sozzi, M., G. Pillan, C. Ciarelli, F. Marinello, F. Pirrone, F. Bordignon, A. Bordignon, G. Xiccato, and A. Trocino. 2022. Measuring comfort behaviours in laying hens using deep-learning tools. Animals 13:33.

Subedi, S., R. Bist, X. Yang, and L. Chai. 2023a. Tracking pecking behaviors and damages of cage-free laying hens with machine vision technologies. Computers and Electronics in Agriculture 204:107545.

Subedi, S., R. Bist, X. Yang, and L. Chai. 2023b. Tracking floor eggs with machine vision in cage-free hen houses. Poultry Science:102637 Available at https://www.sciencedirect.com/science/article/pii/S003257912300161X (verified 10 March 2023).

Thurner, S., and G. Wendl. 2008. Automatic identification and registration of laying hens with RFID technology.Pages 114–117 in Latvia University of Agriculture, Faculty of Engineering.

Tolkamp, B. J., D. J. Allcroft, J. P. Barrio, T. A. Bley, J. A. Howie, T. B. Jacobsen, C. A. Morgan, D. P. Schweitzer, S. Wilkinson, and M. P. Yeates. 2011. The temporal structure of feeding behavior. American Journal of Physiology-Regulatory, Integrative and Comparative Physiology 301:R378–R393.

Tuyttens, F., S. de Graaf, J. L. Heerkens, L. Jacobs, E. Nalon, S. Ott, L. Stadig, E. Van Laer, and B. Ampe. 2014. Observer bias in animal behaviour research: can we believe what we score, if we score what we believe? Animal Behaviour 90:273–280.

UEP. 2006. United egg producers certified animal welfare program. United Egg Producers Available at https://uepcertified.com/ (verified 21 August 2022).

UEP. 2022. Facts & stats. United Egg Producers Available at https://unitedegg.com/facts-stats/ (verified 15 June 2023).

US EPA, O. 2022. NAAQS table. Available at https://www.epa.gov/criteria-air-pollutants/naaqs-table (verified 1 October 2022).

USDA. 2023. USDA ERS - Charts of note. Available at https://www.ers.usda.gov/data-products/charts-of-note/charts-of-note/?topicId=14845 (verified 24 February 2024).

USDA. 2024. Chickens and Eggs. Available at: https://downloads.usda.library.cornell.edu/usda-esmis/files/fb494842n/np194x051/dv141d36t/ckeg0124.pdf (verified 22 February 2024).

Wang, K., K. Liu, H. Xin, L. Chai, Y. Wang, T. Fei, J. Oliveira, J. Pan, and Y. Ying. 2019. An RFID-based automated individual perching monitoring system for group-housed poultry. Transactions of the ASABE 62:695–704.

Winkel, A., J. Mosquera, A. J. Aarnink, P. W. G. Koerkamp, and N. W. Ogink. 2016. Evaluation of oil spraying systems and air ionisation systems for abatement of particulate matter emission in commercial poultry houses. Biosystems Engineering 150:104–122.

Winkel, A., J. Mosquera, P. W. G. Koerkamp, N. W. Ogink, and A. J. Aarnink. 2015. Emissions of particulate matter from animal houses in the Netherlands. Atmospheric Environment 111:202–212.

Winkel, A., J. Mosquera, and N. Ogink. 2012. Removal efficiency of a wire-to-plate electrostatic precipitator for abatement of particulate matter emission from poultry houses. Page 3 in American Society of Agricultural and Biological Engineers.

Xin, H. 2016. Environmental challenges and opportunities with cage-free hen housing systems.Pages 5–9

Yang, X., R. Bist, S. Subedi, and L. Chai. 2023a. A deep learning method for monitoring spatial distribution of cage-free hens. Artificial Intelligence in Agriculture.

Yang, X., R. B. Bist, S. Subedi, and L. Chai. 2023b. A Computer vision-based automatic System for egg grading and defect detection. Animals 13:2354.

Yang, X., R. Bist, S. Subedi, Z. Wu, T. Liu, and L. Chai. 2023c. An automatic classifier for monitoring applied behaviors of cage-free laying hens with deep learning. Engineering Applications of Artificial Intelligence 123:106377 Available at https://www.sciencedirect.com/science/article/pii/S0952197623005614 (verified 29 August 2023).

Yang, X., L. Chai, R. B. Bist, S. Subedi, and Z. Wu. 2022. A Deep learning model for detecting cage-free hens on the litter floor. Animals 12:1983.

Yang, X., H. Dai, Z. Wu, R. Bist, S. Subedi, J. Sun, G. Lu, C. Li, T. Liu, and L. Chai. 2023d. SAM for poultry science. Available at http://arxiv.org/abs/2305.10254 (verified 2 October 2023).

Zhao, Y., A. Aarnink, M. De Jong, N. Ogink, and P. G. Koerkamp. 2011. Effectiveness of multi-stage scrubbers in reducing emissions of air pollutants from pig houses. Transactions of the ASABE 54:285–293.

Zhao, Y., M. Cambra-Lopez., D. J. De Moura., and W. Zheng. 2022. Precision poultry farming. Animals 2076-2615. Available at: https://mdpi-res.com/books/book/5942/Precision_Poultry_Farming.pdf?filename=Precision_Poultry_Farming.pdf.

Zhao, Y., T. A. Shepherd, H. Li, and H. Xin. 2015. Environmental assessment of three egg production systems–Part I: Monitoring system and indoor air quality. Poultry Science 94:518–533.

CHAPTER 2

MISLAYING BEHAVIOR DETECTION WITH DEEP LEARNING TECHNOLOGIES[1]

[1] Bist, R. B., Yang, X., Subedi, S., and Chai, L. 2023. Mislaying behavior detection in cage-free hens with deep learning technologies. *Poultry Science* 102 (7), 102729. https://doi.org/10.1016/j.psj.2023.102729. Reprinted here with permission of the publisher.

ABSTRACT

Floor egg-laying behavior (FELB) is one of the most concerning issues in commercial cage-free (CF) houses because floor eggs (i.e., mislaid eggs on the floor) result in high labor costs and food safety concerns. Farms with poor management may have up to 10% of daily floor eggs. Therefore, it is critical to improve floor egg management. Detecting FELB and non-FELB (NFELB) in a timely manner and identifying the reason behind its cause may address the issue. The primary objectives of this research were to develop and test a new deep-learning model to detect FELB and evaluate the model's performance in four identical research CF rooms (200 Hy-Line W-36 hens per room), where perches and litter floor were provided to mimic commercial tiered aviary system. Five different You Only Look Once version 5 (YOLOv5) models (i.e., YOLOv5n, YOLOv5s, YOLOv5m, YOLOv5l, and YOLOv5x) were trained and compared. According to a dataset of 5400 images (i.e., 3780 for training, 1080 for validation, and 540 for testing), YOLOv5m-FELB and YOLOv5x-FELB models were tested with higher precision (99.9%), recall (99.2%), mAP@0.50 (99.6%), and F1-score (99.6%) than others. However, although it was tested with higher precision, the YOLOv5m-NFELB model has a lower recall than other YOLOv5-NFELB models. Similarly, the speed of data processing (4-45% frame per second) and training time (3-148%) were higher in the YOLOv5s model while requiring less GPU (1.8-4.8 times) than in other models. Furthermore, the camera height of 0.5 m and clean camera outperform compared to 3 m height and dusty camera. Thus, the newly developed and trained YOLOv5s model will be further innovated. Future studies will be conducted to verify the model's performance in commercial CF houses to detect FELB.

Keywords: Cage-free housing; Mislaid egg; Animal behavior; Deep learning; Welfare.

2.1 INTRODUCTION

The laying hen industry is shifting from conventional caged (CC) to cage-free (CF) housing due to various welfare concerns and public demand to improve the behavior and welfare issues (Chai et al., 2018, 2019; Bist et al., 2022, 2023a, 2023b; UEP, 2022). Providing CF housing can improve welfare by providing more space and chances to perform natural behaviors, but there are sometimes some serious downsides to bird welfare and problematic behaviors like mislaid eggs due to floor egg-laying behavior (FELB) of laying hens. Floor egg laying is a natural behavior observed in laying hens where they sit on the floor and lay their eggs. However, laying eggs on the floor increases labor demand and economic losses to the producer because floor eggs have higher chances of contamination with harmful bacteria (Parisi et al., 2015) and are not considered table eggs or for direct sale (Holt et al., 2011). In addition, floor eggs have a higher chance of getting broken and eaten by laying hens.

Several strategies have been implemented to reduce floor eggs. Some of the examples were the use of the nest box (Cox, 2011), perch (Gunnarsson, 1999), light systems (Chai, 2021), and the introduction of experienced hens (Oliveira et al., 2019) to reduce floor eggs. However, the mislaid egg problem still needs to be solved. Vroegindeweij et al. (2018) found that by providing proper training and management practices, the mislaid eggs account for 0.1%-2% of daily egg production. In extreme cases, mislaid eggs can reach 5%-10% of total daily egg production (Vroegindeweij et al., 2018). In any case, the mislaid eggs must be collected manually daily, which is expensive and time-consuming. That is why robots were trained to reduce workload and increase productivity and profitability.

Robots or autonomous navigation systems have shown great potential in improving production in the CF housing system. For example, the Octopus robots (2019) has an autonomous modular system that helps sanitize the poultry houses without human intervention (The Octopus Robots, France). This robot has dramatically reduced mortality and improved welfare by disinfecting the litter by turning and ventilating. Similarly, the Spoutnic robots (Tibot, 2019; TIBOT Technologies, France) were designed to solve the problem of recurring floor eggs by circulating and training laying hens to lay eggs only in nest boxes. This robot has several benefits, including reducing the number of floor eggs and helping improve productivity by increasing movement. According to Li et al. (2022), robot use helped reduce floor eggs by 34% in a two-week experiment. The recently invented and tested robot moves randomly inside the house and helps reduce floor eggs by making hens move around and stop lying on the floor. By moving randomly, the robot can reduce floor eggs but cannot control them entirely because the robot, without detection, will be unable to detect the right FELB. Instead of targeting FELB, the robot moves continuously inside the housing. As a result, the robot can only help push the hens from the open housing areas but cannot reach the birds hiding around the corner or secluded places where most hens lay eggs (Lundberg and Keeling,1999). That is why the robot should incorporate a machine or deep learning model to detect the FELB and primarily target those birds to keep them from lying on the floor.

The rapid development of deep learning has sped up the development of associated techniques, algorithms, and procedures in image processing and computer vision (Horvat et al., 2022). Artificial neural networks are now the industry standard for most computer vision tasks. In the past, various forms of Convolutional Neural Networks (CNNs) like R-CNNs (Region-based

CNNs) and faster R-CNNs were widely used as machine learning models for machine vision and object detection (He et al., 2015). Although these CNNs models effectively detect target objects using a two-stage object recognition model, these models were found to be more complex and computationally intensive compared to single-stage detectors like YOLO (You Only Look Once) models (Horvat et al., 2022). The YOLO is currently well recognized and the most popular form of machine learning due to its small size and faster calculation speed (Jiang et al., 2022; Subedi et al., 2023a, 2023b; Yang et al., 2022). In addition, the YOLO model was best known as the fastest real-time object detection model after the lunch of the YOLOv4 model (Lin et al., 2014; Guo et al., 2020; Wang et al., 2022). The latest YOLO models (YOLOv5, YOLOv6, and YOLOv7) were launched with improved algorithms and more computational functions. There are several benefits or advantages of using the YOLOv5 model compared to previous YOLO models because the YOLOv5 model has a smaller volume and higher precision, speed, and real-time detection efficiency.

Recently, the YOLOv5 model gained attention in the poultry industry for detecting birds, their performance, behavior, welfare status, and productivity. According to Neethirajan (2022), the automatic detection, tracking, and counting of individual birds are very important to ensure farming productivity, health, and animal welfare. The YOLOv5 model was used to develop the ChickTrack model to track 72 birds in poultry housing. Similarly, the YOLOv5 model was used in a research facility to detect individual laying hens with a precision of 96% (Yang et al., 2022). The research done by Gu et al. (2022) found that this model performs efficient and intelligent monitoring for analyzing or detecting health status and behavior. Normal applied behaviors (e.g., sitting, standing, feeding, perching, and drinking) can be easily detected, but abnormal or

problematic behavior is hard to detect with higher speed and accuracy. The problematic behaviors, like pecking behavior, were closely monitored in laying hens, and behavior was detected with high accuracy using the YOLOv5 model (Subedi et al., 2023a). However, no studies have yet been done to detect FELB in CF houses.

This study aimed to develop and optimize a deep learning-based detector for monitoring hens' FELB. The objectives of this study were to: i) develop and test a new deep-learning model to detect FELB and NFELB based on five YOLOv5 models, ii) compare the performances of the five YOLOv5 network models under CF room conditions, and iii) evaluate the performance of the optimal YOLOv5 model under different settings (e.g., environmental conditions and imaging system setting).

2.2 MATERIALS AND METHODS

2.2.1 Housing and Bird Management

The experiment was conducted in four identical research CF rooms (200 Hy-Line W-36 hens per room), where perches and litter floors were provided to mimic the commercial tiered aviary system at the University of Georgia in Athens, GA, USA. Birds were raised from day 1 to day 595 (85 weeks) in each room, measuring 7.3 m L × 6.1 m W × 3 m H (Figure 2.1). The limitation of this dissertation was the availability of 4 rooms to perform all the research. Each room was equipped with feeders, drinkers, lights, a heater, a circulating fan, perch, and nest boxes. Pine shavings (5 cm depth) were spread on the floor as bedding. An automatic digital light dimmer (PLS-2400 MR4, Precision Lighting System, Hot Springs, AR, USA) controlled light systems inside cage-free hen rooms. An A-shaped perch measuring 36.6 meters long with 6 tiers was

installed in each room, providing 0.21 m perch length per bird. The husbandry and management practices followed the recommended Hy-Line W-36 commercial layers guidelines (Hy-Line, 2020). The indoor temperature, relative humidity, light duration (16 hours) and intensity (12-15 lux), and ventilation rates were controlled automatically with a Chore-Tronics Model 8 controller (Chore-Time Equipment, Milford, Indiana, USA). Two ceiling-mounted circulating fans were installed in each room to ensure consistent air and temperature distribution throughout the room. All procedures for this study were conducted at the University of Georgia Poultry Research Center within a laying hen facility and approved by the Institutional Animal Care and Use Committee (IACUC) under approval number A2020 08-014-A2 before the commencement of the study.

Figure 2.1: Experimental cage-free laying hen rooms.

2.2.2 Image Data Acquisition

This study used a night-vision network camera (PRO-1080MSB, Swann Communications USA Inc., Santa Fe Springs, LA, USA) to record the image dataset of hens' behaviors for the main data acquisition tool. Each room had 6 cameras mounted ~3m above the littered floor and two above the ground floor at 0.5m from the ground. The camera records data for 24 hours, but this study took the FELB data acquisition time between 5:00 and 21:00 daily because FELB was mostly observed during light periods. The captured videos were stored in a digital video recorder (DVR-4580, Swann Communications USA Inc., Santa Fe Springs, LA, USA) from 25-50 weeks of age (WOA). The video files were stored in .avi format with a 1920 × 1080 pixels resolution with a sampling rate of 15 frames per second (FPS).

2.2.3 Image Labeling and Data Pre-processing

Video datasets (64.2 terabytes) obtained were converted into images (.jpg) with the help of Free Video to JPG Converter App (ver. 5.0) at a 15 FPS image processing rate. Thus, the obtained image datasets were filtered and separated manually based on FELB observation of the images. The 5400 images were selected and then labeled by an experienced researcher (trained by a previous researcher who worked in machine learning and data labeling) using the image labeler website (Makesense.AI), and labeled data were stored in YOLOv5 format (Guo et al., 2020; Subedi et al., 2023a, 2023b). Those images were labeled manually by putting a square box around the targeted FELB and non-FELB (NFELB) within images. The NFELB is the birds' behavior or activities, like feeding, drinking, sitting, preening, dustbathing, pecking, and foraging (Table 2.1) (Appleby et al., 2004). The two classes (FELB and NFELB) were compared and used for

identification for the model detection. The detailed process of data collection, labeling, pre-processing, training, validation, testing, and implementation is shown in Figure 2.2.

Table 2.1: Ethogram of posture and body orientation in common behaviors of hens.

Behaviors	Posture and body orientation
FELB	Tense or rigid body posture, crouching low to the ground, stretching neck and tail, circling around or pecking at the ground before laying the egg, increased activity levels may be observed, may show signs of stress or discomfort, such as panting or heavy breathing. In addition, FELB is usually observed sitting tightly in a group and exhibits piling-like behavior. In addition, FELB is mostly seen at the corner, near the wall, or close to the nestbox.
Sitting	Relaxed body posture, sitting or perching on the ground or other surfaces, calm and quiet, the body may be oriented in various directions depending on position and surface may be accompanied by grooming or preening behaviors. The hen usually sits far from each other compared to FELB.
Nesting	Sitting in the nest, arranging materials with beaks or feet, may show signs of relaxation, such as closing eyes.
Preening	Standing or sitting with feathers fluffed, using a beak to clean and align feathers, may stretch wings or shake feathers.
Feeding	Pecking at food with a beak may alternate between pecking and lifting the head to swallow, showing excitement or increased activity levels.

Drinking	Drinking water with head lifted up and beak to the nipple may show signs of relief or relaxation.
Foraging	Scratching at the ground with feet and pecking at the ground or objects may show signs of curiosity or exploration.
Dustbathing	Lying on the ground, using legs to dig in the ground, flapping wings to spread dust or dirt on the body, and rolling or wriggling in the dust or dirt may show signs of relaxation or enjoyment.
Perching	Standing or sitting on a perch or roost, gripping the perch with feet, may show signs of rest or sleep.

FELB- floor egg-laying behavior.

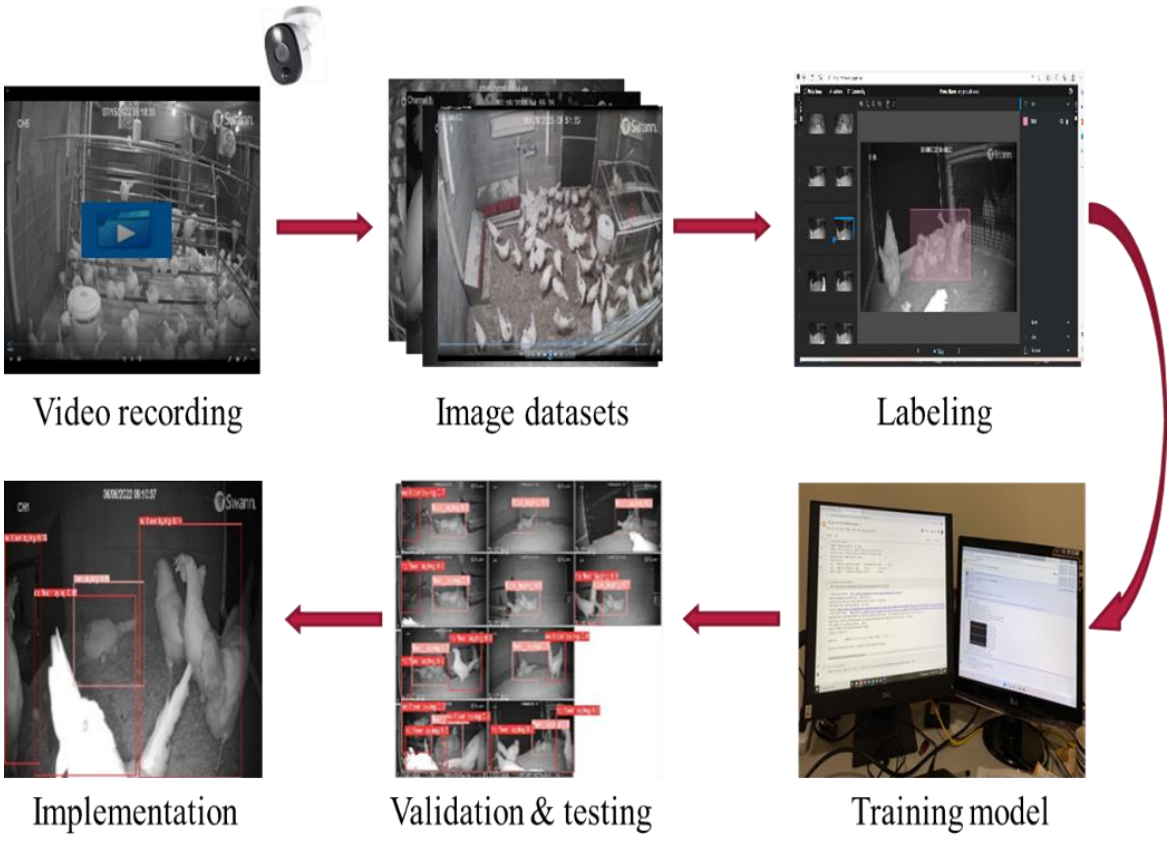

Figure 2.2: Floor egg-laying detection system.

The five YOLOv5 models were obtained from the GitHub repository developed by Ultralytics (Jocher, 2020). The five YOLOv5 models were pretrained with Common Objects in Context (COCO) datasets and can be readily modified into required object detection models through target object training datasets. Before developing the FELB model detector, the experimental configurations were prepared for the model evaluation (Table 2.2). Training datasets were analyzed using Oracle Cloud with different experimental configurations.

Table 2.2: Experimental configuration used for the model evaluation.

Configuration	**Parameters**
CPU	64 core OCPU
Memory (RAM)	1024GB
Drive (2 counts)	7.68 TB NVMe SSD
GPU (4 counts)	4×NVIDIA® A10 (24GB)
Operating system	Ubuntu 22.10 (Kinetic Kudu)
Accelerated environment	NVIDIA CUDA
Libraries	OpenCV-python 4.1.1, Torch 1.7.0, NumPy 1.18.5, Torch-vision 0.8.1

CPU-Central processing unit; GPU- Graphics processing unit; RAM- Random access memory; OCPU- Oracle based CPU.

About 70%, 20%, and 10% of total images (5400 images) were used for training, validation, and testing, respectively (Table 2.3). First, different YOLOv5 models were tested with the $FELB_{Mix}$ datasets (containing all the images from $FELB_{1-4+}$ classes). Then, the obtained best

model was first tested with different classes, as mentioned in Table 2.3, such as comparing those labeled individually vs. grouped. Later, the $FELB_{1\ to\ 4+}$ classes were compared in a group based on the number of hens present for detection. In the same way, the best model was tested based on camera height because height might also affect the detection performance. Finally, the CF rooms environment consists of higher dust particles, which might affect the detection efficiency; we compare images obtained from a clean camera vs. a dusty camera (Figure 2.3).

Table 2.3: Data pre-processing for model detection.

Class[a]	Original dataset	Train (70 %)	Validation (20 %)	Test (10 %)
$FELB_1$	600	420	120	60
$FELB_2$	600	420	120	60
$FELB_3$	600	420	120	60
$FELB_4$	600	420	120	60
$FELB_{4+}$	600	420	120	60
$FELB_{Mix}$	3000	2100	600	300
$FELB_{Height}$	600[b]	420	120	60
$FELB_{Env}$	600[c]	420	120	60

$FELB_{1,2,3,4,4+}$ - floor egg laying behavior number from 1, 2, 3, 4, or 4+ hens; [a]each class or experimental setting were run for 100 epochs with 16 batch size; [b]each 600 images from low (50cm) or ceiling camera (3m); [c]each 600 images from different camera condition due to environmental condition inside CF rooms (clean or dusty camera); Mix- consist the labeled image datasets of $FELB_{1,2,3,4,4+;}$ Env- environmental condition.

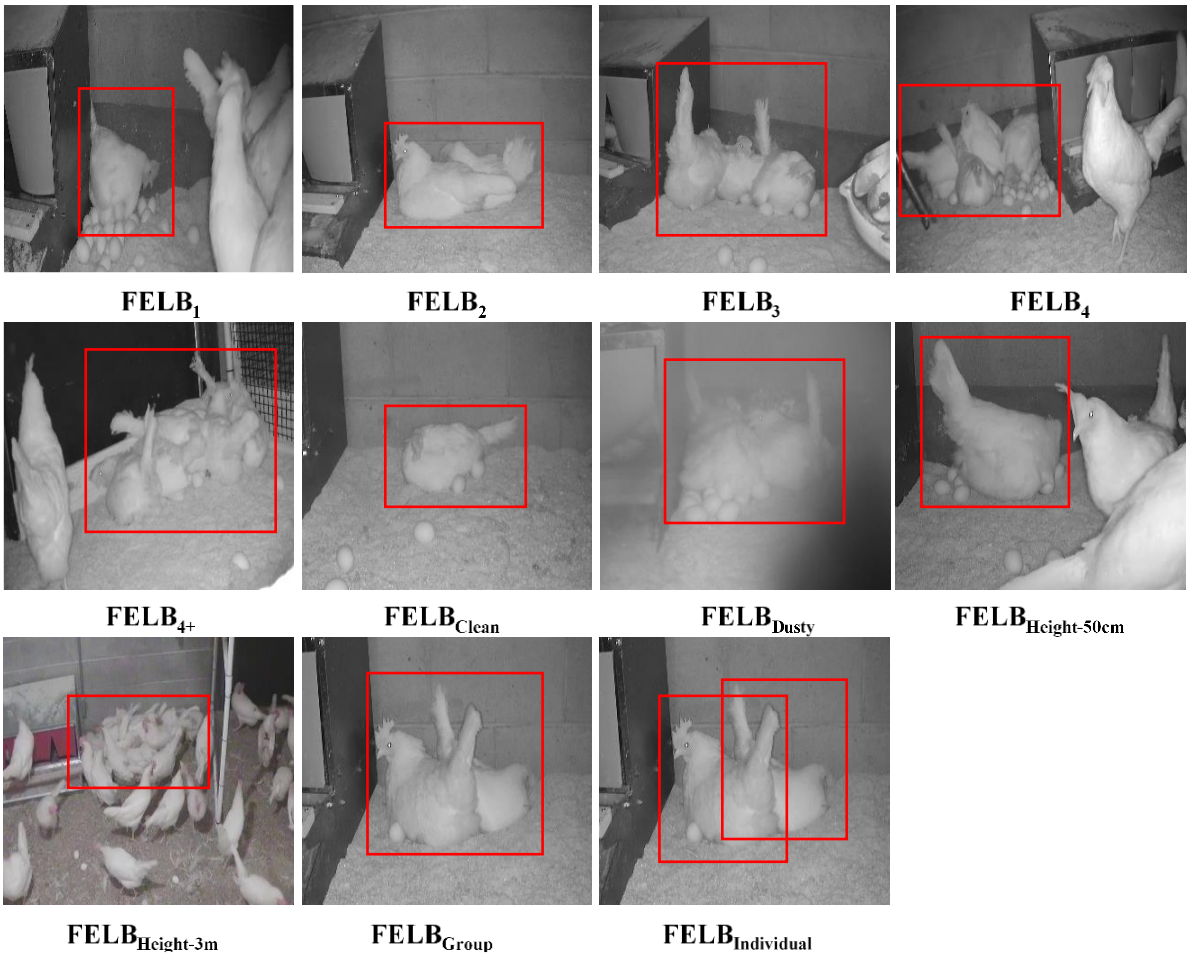

Figure 2.3: Sample images of floor egg-laying behavior (FELB) under various conditions.

2.2.4 Description of the YOLOv5 Models

Before the discovery of the YOLO model, the Region Based Convolutional Neural Networks (R-CNN) series algorithm was widely used to achieve high detection accuracy of the target object (Ting et al., 2021). However, the R-CNN series cannot meet real-time detection requirements at a faster speed because of its two-stage network structure. In 2016, Joseph Redmon and his team developed the single-stage object detection network YOLOv1 model, which can detect objects with higher accuracy and speed and run efficiently in a real-time detection module (Redmon et al., 2016). After the success of the YOLOv1 model, the series of YOLO models

created like YOLOv2, YOLOv3, YOLOv4, and YOLOv5 with various versions with various feature extraction modules, convolutional network, and parameters (Horvat et al., 2022). This study chose the YOLOv5 model because of its high accuracy and speed. Furthermore, the YOLOv5 model has five network models: YOLOv5n, YOLOv5s, YOLOv5m, YOLOv5l, and YOLOv5x for smaller image size detection. That is why we used all the YOLOv5 models to compare and find the best detection model among those. Among these five network models, the internal structure of each model is the same except for the depth and width of multiple parameters, which control the depth of the models and the number of convolution cores (Ting et al., 2021). The different parameters used in this model are in Table 2.4. The Convolution, Batch normalization and Leaky-ReLU (CBL), Spatial Pyramid Pooling (SPP), Concatenate (CONCAT), and Upsample modules are original YOLOv3 and YOLOv4 modules, whereas FOCUS and CSP modules are unique to YOLOv5. The detailed YOLOv5 architecture is mentioned in Figure 2.4.

Table 2.4: Training datasets differ based on the YOLOv5 model used.

Model	**YOLOv5n**	**YOLOv5s**	**YOLOv5m**	**YOLOv5l**	**YOLOv5x**
Type	Nano	Small	Medium	Large	XLarge
Layers	214	214	291	368	445
Parameters	1,766,623	7,025,023	20,875,359	46,143,679	86,224,543
Gradients	1,766,623	7,025,023	20,875,359	46,143,679	86,224,543
GFLOPs	4.2	16.0	48.2	108.2	204.6

Note: YOLO- You only look once; GFLOPs- giga of floating point operations per second.

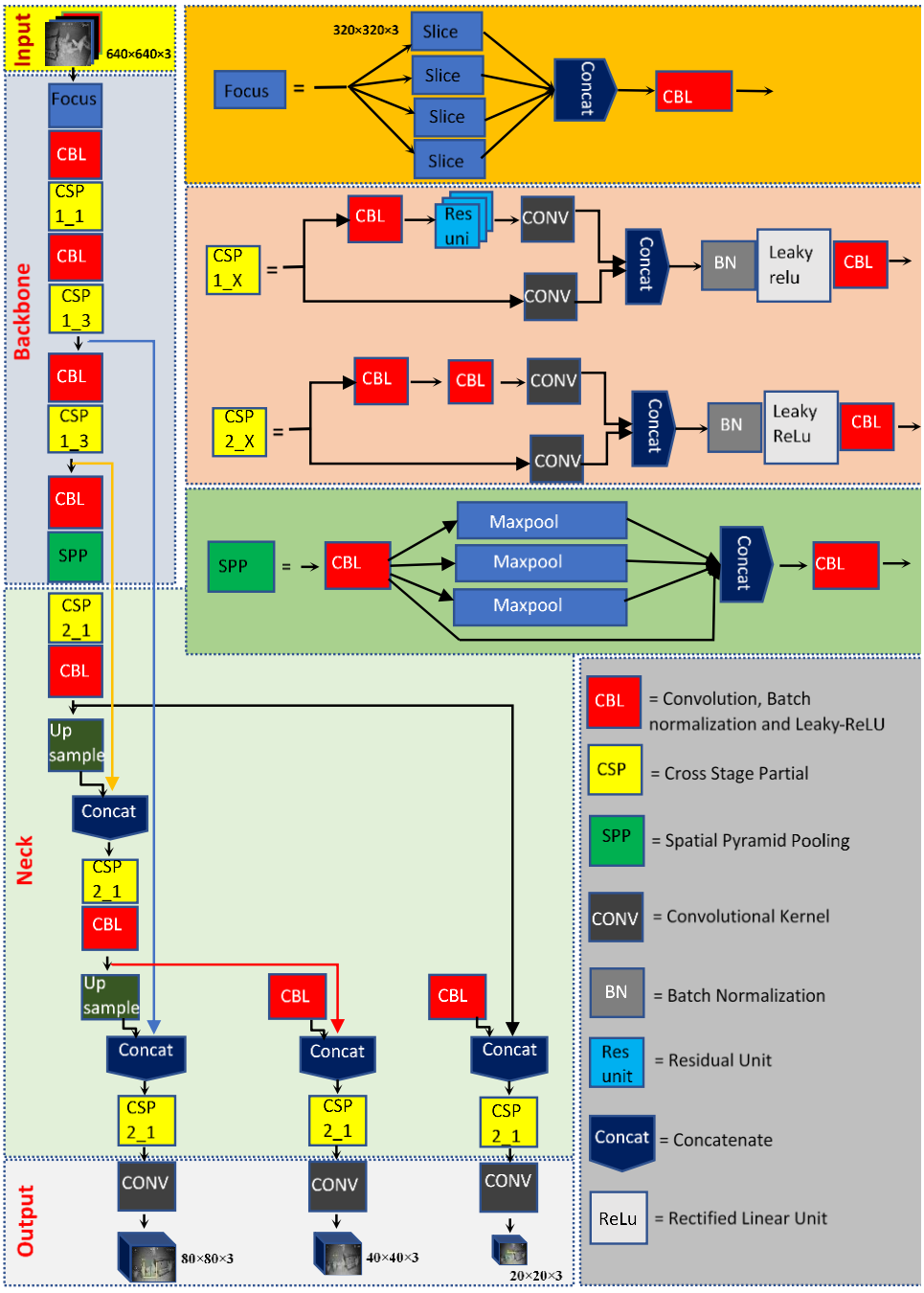

Figure 2.4: YOLOv5 architecture used for the FELB detection.

The YOLOv5 model comprises three main parts: backbone, neck, and head (Jocher, 2020; Subedi et al., 2023a; Yang et al., 2022). Each part functions differently. When the image data is trained as input data, it passes down to the backbone for feature extraction.

2.2.4.1 Backbone

The backbone of the YOLOv5 uses cross stage partial (CSP) Darknet53 convolutional neural network, which uses residual and dense blocks. The CSP network helps reuse denseNet's features and reduces the excessive amount of redundant gradient data (Wang et al., 2020), which improves the egg-laying feature extraction.

2.2.4.2 Neck

The neck of the YOLOv5 consists of two major changes: SPP and Path Aggregation Network (PANet). This PANet variant was modified by incorporating the bottleNeck CSP network strategy. The PANet features a pyramid network and helps enhance information flow. In addition, it helps with proper pixel localization in mask prediction. Similarly, SPP helps improve the network's speed by aggregating the hens' behavior information received as input and returns as a fixed output length without lowering the network speed (He et al., 2015).

2.2.4.3 Head

The head structures in YOLOv3, YOLOv4, and YOLOv5 are the same, consisting of three convolution layers that help to obtain multi-scale predictions as outputs. These layers help to predict the scores, the object classes, and the location of the bounding boxes (x, y, height, width) (Jocher, 2022). The predicted results of floor egg laying were finally taken out through convolutional kernels. The equation used to compute the hens' location or coordinates for the given bounding boxes were as follows:

$$b_x = (2 \times \sigma(t_x) - 0.5) + c_x \qquad (i)$$

$$b_y = (2 \times \sigma(t_y) - 0.5) + c_y \qquad (ii)$$

$$b_w = pw \times (2 \times \sigma(t_w))^2 \qquad (iii)$$

$$b_h = ph \times (2 \times \sigma(t_h))^2 \qquad (iv)$$

Where b_x, b_y, b_w, and b_h represents bounding boxes of x-coordinate, y-coordinate, width, and height.

2.2.5 Model Evaluation

First, the image was trained and validated for the model evaluation to get the necessary outputs (Figure 2.5). The YOLOv5 produces three outputs: the detected hens' classes, bounding boxes, and objectness scores. As a result, it computes the class loss and the objectness loss using Binary Cross Entropy (BCE).

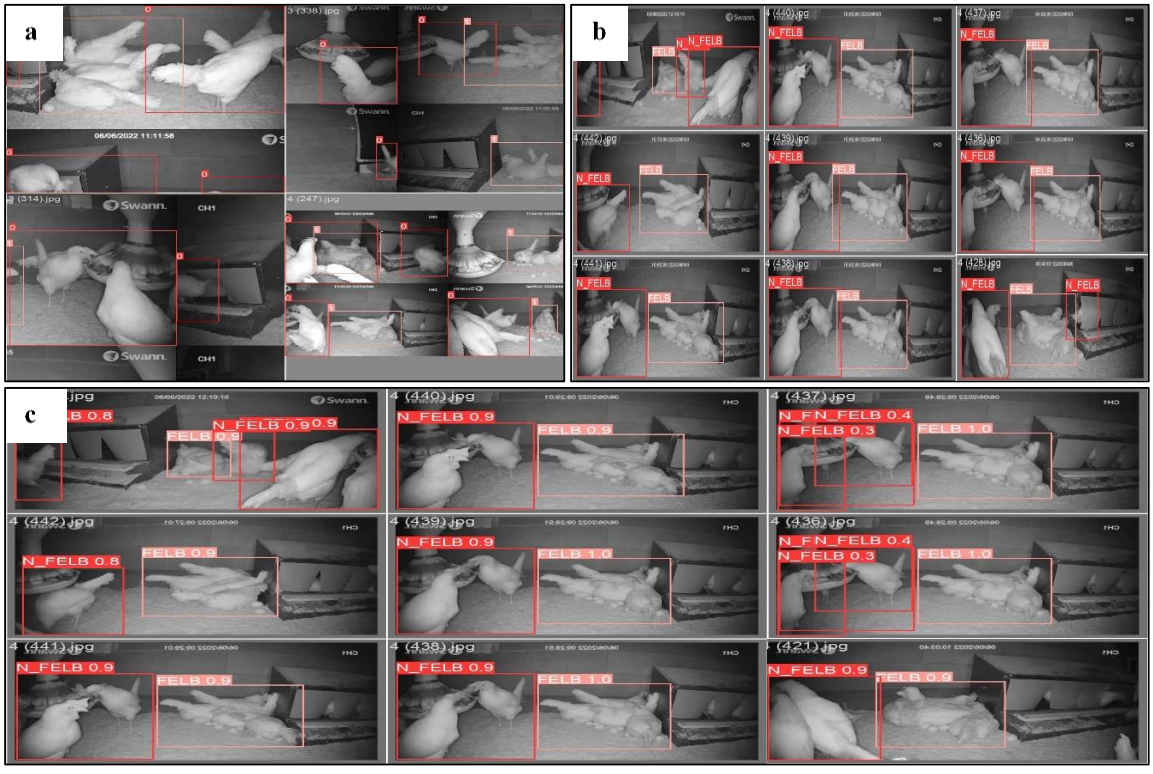

Figure 2.5: Model training (a), validation labels (b), and validation prediction (c).

The location loss is computed using the CIoU (i.e., Complete Intersection over Union) loss. The loss function in YOLOv5 helps to improve detection efficiency by positioning errors. Handling objects of different sizes needs to be strengthened, so loss functions play an important role in solving this issue. The equation of final loss was generated from the following equation:

$$Loss = \lambda_1 L_{cls} + \lambda_2 L_{obj} + \lambda_3 L_{loc} \qquad (v)$$

Similarly, Python 3.10.6 was used for the model evaluation for descriptive statistics and statistical analysis. Precision, recall, F1 score, and mAP were measured for validating data and calculated with the help of the following formulas;

$$Precision = \frac{TP}{TP + FP} \times 100\% \qquad (vi)$$

Precision relates to how much of the bounding box prediction measures correctly from the datasets.

$$Recall = \frac{TP}{TP + FN} \qquad (vii)$$

where, TP, FP, and FN indicate true positive, false positive, and false negative values, respectively.

The recall relates to how much of the true bounding box measure is correctly predicted from the dataset,

$$F1\ Score = \frac{2 \times Recall \times Precision}{Recall + Precision} \qquad (viii)$$

The F1 score for object detection measures a weighted average or harmonic mean of precision and recall.

$$mAP = \frac{\sum_{i-1}^{C} APi}{C} \qquad (ix)$$

where, $\boldsymbol{APi}$ and $\boldsymbol{C}$ represent the average precision of the ith category and the total number of categories, respectively.

The mAP is the mean average precision metric used to evaluate model detection at the intersection over a union (**IoU**) threshold of 0.5 (Map@0.50) or 0.5:0.95 (mAP@0.50:0.95).

To calculate precision and recall, IoU plays an important role. IoU is the proportion of the areas of union and overlaps between bounding boxes of the ground truth and the prediction labels (Figure 2.6).

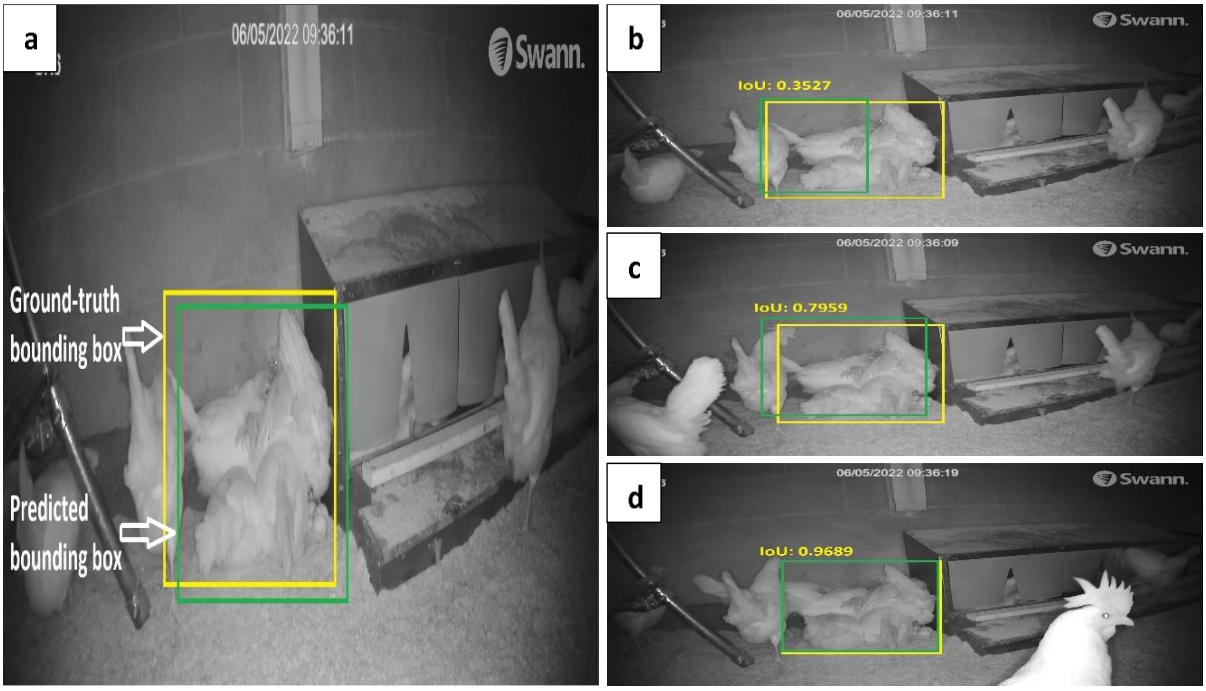

Figure 2.6: An example of the IoU for a) floor egg-laying behavior (FELB) and various bounding boxes indicating b) poor, c) good, and d) bad IoU score.

The IoU threshold, in particular, is used to determine whether the prediction is true positive or false positive. After calculating precision and recall for various IoU thresholds, a precision and recall plot for a single classifier at various IoU thresholds is generated. The precision-recall curve was then used to calculate the average precision. As previously noted, mAP is determined by averaging all classes' average precision (AP).

The higher the values of all the above metrics, the better the detector performance. If model metrics reach almost 100% (F1 score =1.0), then the model performs better in detecting that object without any negative detection. However, getting 100% model metrics is very hard to achieve. Big data and a higher-performance model are required for higher accuracy (Subedi et al., 2023). In addition, cache-to-cache images were used for faster training.

2.3 RESULTS AND DISCUSSION

2.3.1 Comparative Analysis of Different YOLOv5 Models

2.3.1.1 Experimental results of YOLOv5 models

This paper compared five different YOLOv5 models; their results are shown in Table 2.5. Previous research has shown that the YOLOv5x model resulted in higher performance in detecting small-sized objects like chickens, including laying hens (Yang et al., 2022). In this research, with the IoU and confidence threshold of 0.5, the experimental results show the recall value (99.2%) is the same for all the YOLOv5-FELB (YOLOv5n, YOLOv5s, YOLOv5m, YOLOv5l, and YOLOv5x) models, but the YOLOv5-NFELB recall value increases as the size of YOLOv5 model increases except YOLOv5m-NFELB (83.3%). Similarly, mAP@0.50 for all YOLOv5-FELB models is 99.5%, except the YOLOv5l-FELB model (99.4%). Furthermore, the F1 score is highest

in the YOLOv5m and YOLOv5x models, which is 99.6% for FELB. Since the recall, mAP@0.50, and precision well perform in the YOLOv5m and YOLOv5x-FELB model, the result suggests the YOLOv5m and YOLOv5x will be the best model for detecting the target FELB and NFELB on performance level. Since there is no significant difference in performance, we can consider the model of smaller sizes like YOLOv5s and YOLOv5n for faster speed and economy to use (Subedi et al., 2023a).

Table 2.5: Comparison of different YOLOv5 models based on stage all datasets.

Data summary	**YOLOv5n**		**YOLOv5s**		**YOLOv5m**		**YOLOv5l**		**YOLOv5x**	
	FELB	**NFELB**	**FELB**	**NFELB**	**FELB**	**NFELB**	**FELB**	**NFELB**	**FELB**	**NFELB**
Precision (%)	99.2	87.9	99.4	84.3	99.9	90.4	99.1	84.7	99.9	86.2
Recall (%)	99.2	86.0	99.2	86.4	99.2	83.3	99.2	86.4	99.2	87.2
mAP@0.50 (%)	99.5	91.7	99.5	90.9	99.5	91.2	99.4	90.1	99.5	90.9
mAP@0.50-0.95 (%)	74.0	61.4	76.8	62.0	76.0	61.7	76.0	62.5	76.6	63.3
F1-score	99.2	86.9	99.3	85.3	99.6	86.7	99.2	85.5	99.6	86.7

FELB- floor egg laying behavior; NFELB- Non-floor egg laying behavior; mAP- mean average precision.

2.3.1.2 Model performance curves for YOLOv5 models

The precision curves were detected and evaluated based on the epochs. In all models, precision curves seem to be lowest initially and then increase gradually with the increase in epochs (Figure 2.7). As a result, it is found that the average precision curve for FELB and NFELB is highest for YOLOv5n (93.7%), YOLOv5s (94.4%), YOLOv5m (95.13%), YOLOv5l (93.3%), and YOLOv5x (94.2%) at 97, 74, 93, 71, and 47 epochs, respectively. Overall, the precision for the YOLOv5m-FELB and YOLOv5x-FELB were the highest among other models, with a precision of 99.5%. However, the precision reached almost 90.4% for the YOLOv5m-NFELB model by the end of 100 epochs.

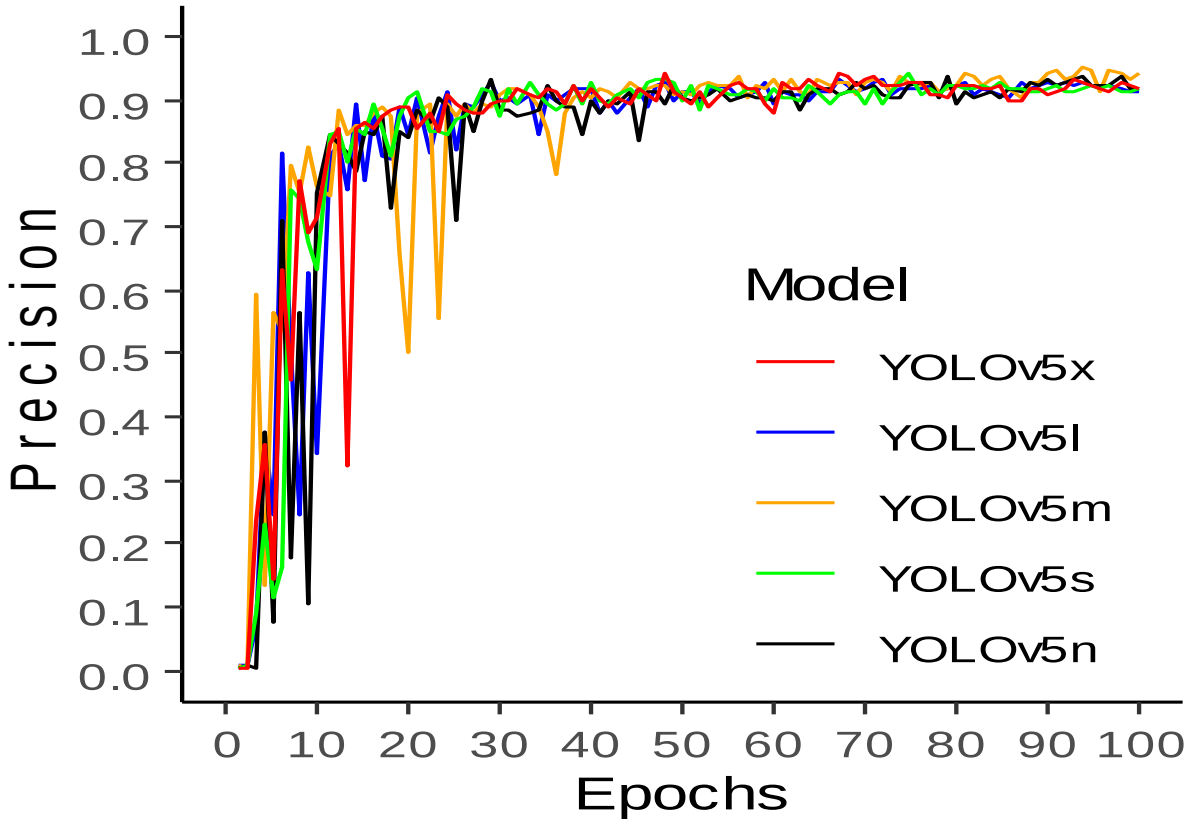

Figure 2.7: Average precision curves of floor egg-laying behavior (FELB) and Non-FELB detected by different models.

Similarly, recall values also increase with increased epoch size (Figure 2.8). The recall helps the model detect all the positive datasets (Subedi et al., 2023). The highest recall confidence curves for all classes (average of FELB and NFELB) for the YOLOv5n (93.9%), YOLOv5s (93.6%), YOLOv5m (93.9%), YOLOv5l (93.5%), and YOLOv5x (93.7%) was at 83, 69, 75, 67, and 46 epochs, respectively. Overall, the recall value for FELB for all the models was the same (99.2%). However, the recall value for NFELB varied per model and was found to be highest for the YOLOv5x model (87.2%).

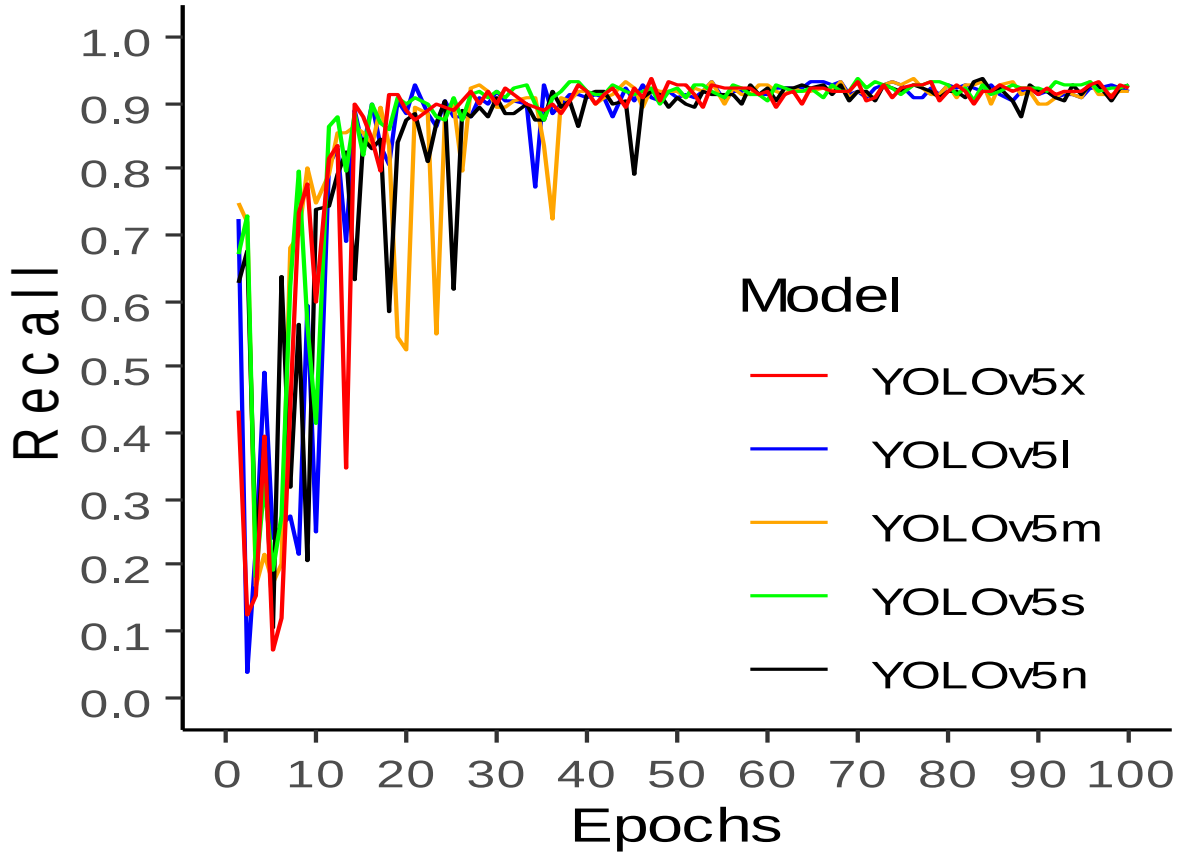

Figure 2.8: Average recall curves of floor egg-laying behavior (FELB) and Non-FELB detected by different models.

The model always requires Precision-Recall curves to predict the FELB. The prediction ability of the YOLOv5 model increases with increasing recall values because the model often needs both high precision and high recall. Similarly, good precision-recall curves should have a greater area under the curve (AUC) shown by the FELB detection model for all the models used. The Precision-recall value for all the classes was highest for the YOLOv5n model and lowest for the YOLOv5l model at mAP@0.50. However, the precision-recall curve for all the YOLOv5-FELB models shows 99.5%, except the YOLOv5l-FELB model (99.4%). Finally, F1 scores are error metrics that help determine the model's robustness and predict model performance for balanced or imbalanced datasets. The F1 score seems to increase the accuracy of the model. The higher the F1 score, the better the accuracy and recall of the model. For the classes FELB and NFELB, the F1-score is highest for YOLOv5x, YOLOv5m, and YOLOv5s, with an F1-score of 93%.

2.3.1.3 Model performance in FELB and NFELB detection

The prediction model is evaluated from the confusion matrix, which consists of four important components (TP, TN, FP, and FN; Figure 2.9). This study uses YOLOv5 models with two classes, FELB and NFELB. The TP for detecting FELB is 0.99 for all models, while it varies for NFELB detection. The highest TN for detecting NFELB is for the YOLOv5x model (0.92) and the lowest for YOLOv5m (0.89). FP and FN values are predicted to be zero for all models except the YOLOv5m-FELB model (0.01). Thus, a higher value of TP gives a higher model performance (Subedi et al., 2023a, 2023b).

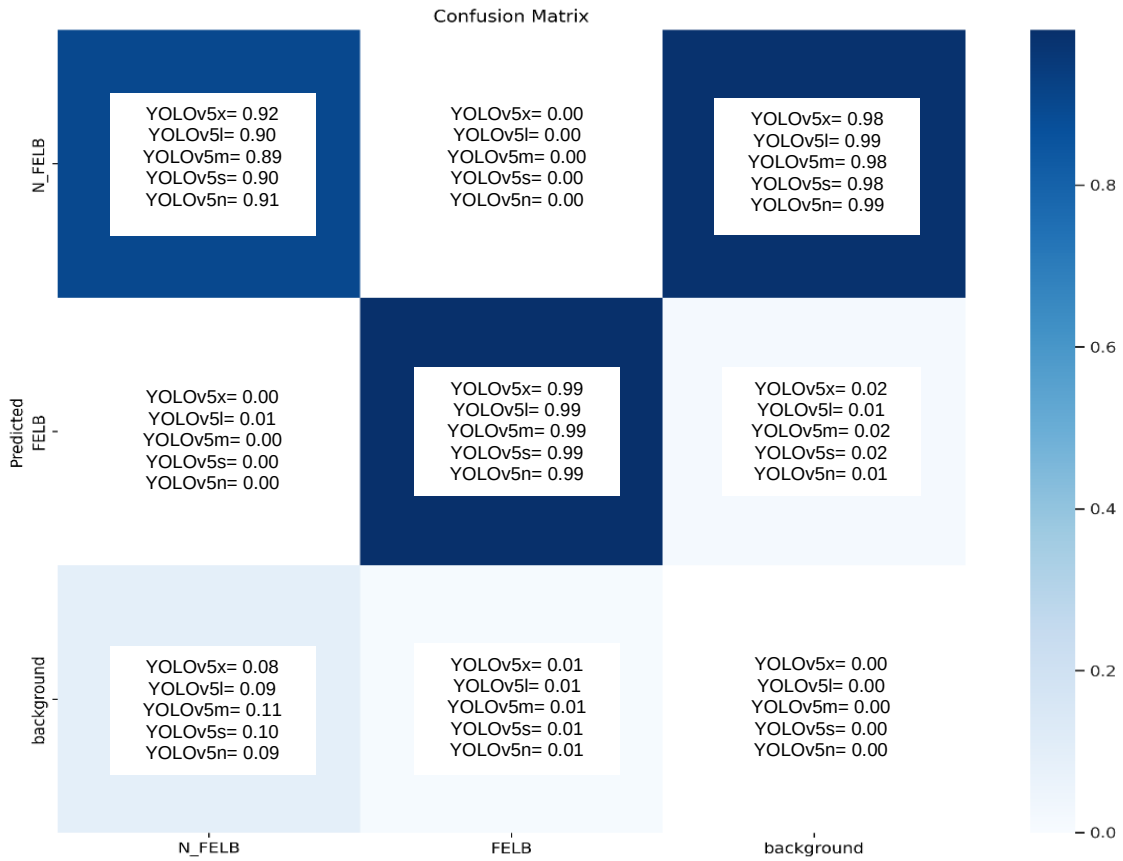

Figure 2.9: Confusion matrices of the five YOLOv5-FELB and YOLOv5-NFELB models.

The test results from the YOLOv5 model comparisons for FELB and NFELB detection are shown in Figure 2.10. The YOLOv5 model has improved the detection of FELB and NFELB in test data. From the several tested and validated images, the YOLOv5s and YOLOv5m show higher detection accuracy for FELB and NFELB detection, whereas the YOLOv5n resulted in the lowest FELB and NFELB detection.

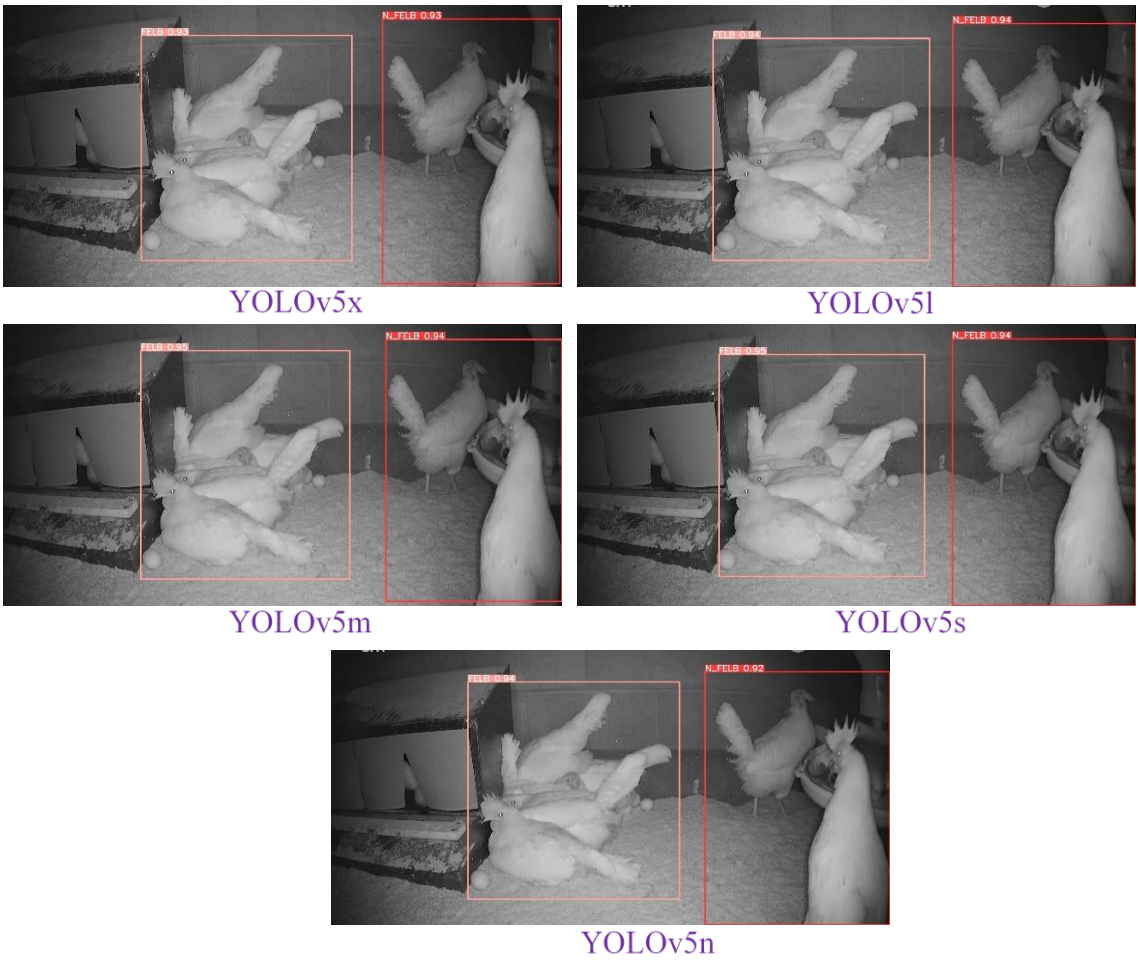

Figure 2.10: YOLOv5 detection results based on each model used for the same image.

Where, pink boxes represent detected FELB and red boxes represent detected NFELB.

2.3.1.4 Performances of YOLOv5 models in data training and validation

In this study, the training and validation of each model's loss function decrease rapidly when run at 100 epochs with a batch size 16. The train box loss, train object loss, train class loss, Val object loss, Val class loss, and Val box loss values in all the YOLOv5 models decrease as the model was trained higher with a higher number of epochs, giving a better performance model. In the process of training the model from 0-100 epochs, the model's performance increased

continuously, giving higher precision, recall, and mAP@0.50 (Figure 2.11). Therefore, to increase the model's performance, all the loss parameters should be at the lowest level or zero.

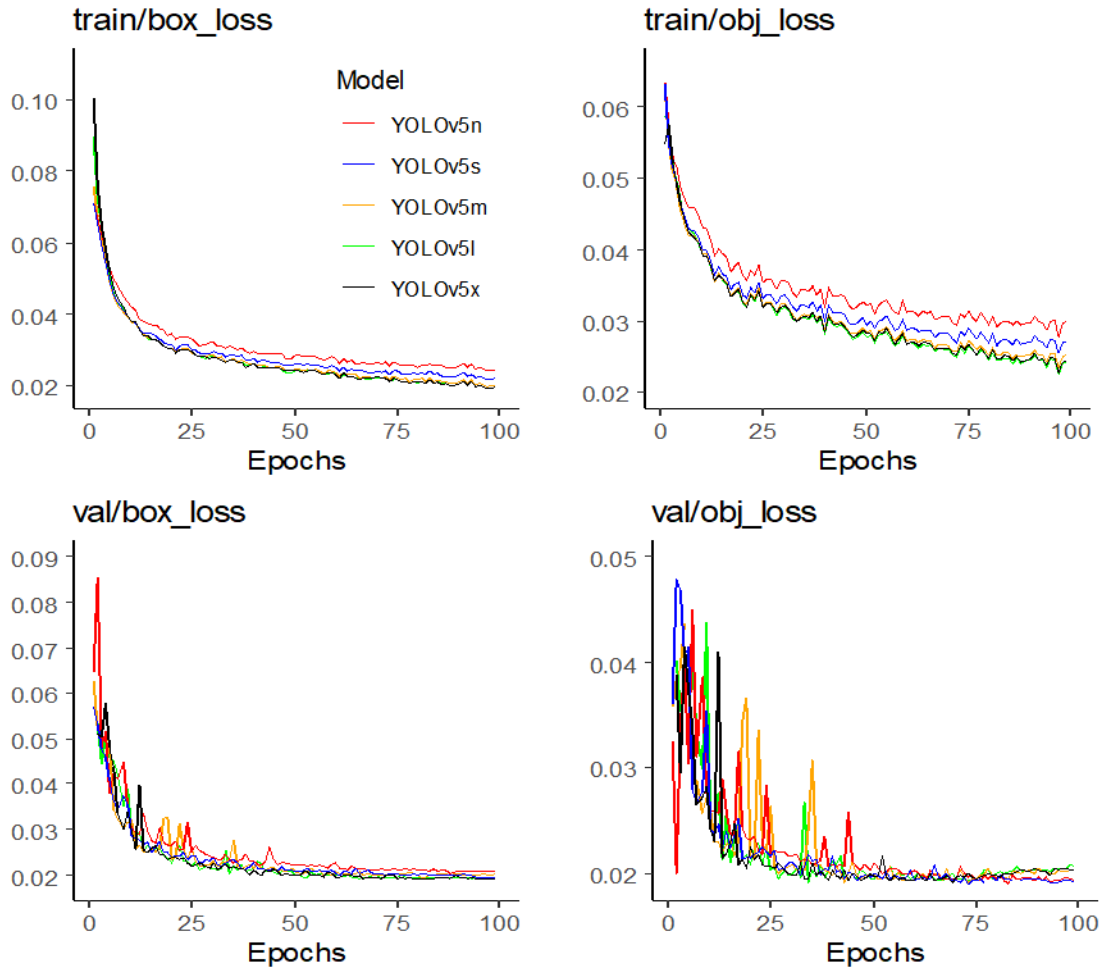

Figure 2.11: Training and Validation loss results of the YOLOv5 models.

2.3.1.5 Model computing system performances

Since the performance metrics of each model were not significantly different, each model was compared further based on computing system performance. Table 2.6 shows the computing system performance based on YOLOv5 models where different computing parameters were considered. When selecting different YOLOv5 models for FELB detection in a robot, the detector processing speed should be considered because a higher running speed or detection speed increases

the robot's performance (Li et al., 2022). Among different models, the YOLOv5s model outperforms based on higher FPS, lower training time, GPU usage, and smaller size. Previous research has shown that the YOLOv5s model saved computing costs with 75% less GPU memory and 80% less training speed (Subedi et al., 2023a). However, it depends on what kinds of object detection were considered. In this study, YOLOv5s-FELB and YOLOv5s-NFELB detection uses up to 148% less training time, up to 4.8 times less GPU usage (1.8 times higher than YOLOv5n), and up to 45% higher FPS speed. Therefore, the YOLOv5s model has superior performance for FELB detection to be considered for the detection model in a robot.

Table 2.6: Comparison table of YOLOv5 models performance in computing system use.

Computing parameter	**YOLOv5n**	**YOLOv5s**	**YOLOv5m**	**YOLOv5l**	**YOLOv5x**
FPS	51.0	53.2	42.4	33.7	29.4
Parameters	1,761,871	7,015,519	20,856,975	46,113,663	86,180,143
Layer	157	157	212	267	322
GFLOPs	4.1	15.8	47.9	107.7	203.8
Epochs (its/s)	9.84	9.57	8.65	7.85	7.84
OSS used (MB)	3.8	14.3	42.1	92.7	173.0
Training time (h)*	0.509	0.496	0.666	0.878	1.230
GPU memory (GB)	0.583	1.04	1.83	3.23	4.95

FPS-frame per second; OSS- optimizer stripped space; it/s- iteration per second; GFLOPs- Giga floating point operations per second.

2.3.2 Comparison of Different Classes Using the YOLOv5s-FELB Model

2.3.2.1 Hens FELB group size

The test result based on the FELB hen group size is shown in Table 2.7. As usual, the loss functions always have to show a decreasing tendency to increase the model performance (Figure 2.12). The model's performance increases as the group size of FELB increases, except for YOLOv5s-FELB4+. The precision, recall, and mAP@0.50 increase because the group size of FELB increases. The model performance of a single bird causes an increase in the chances of box loss, object loss, and sometimes class loss due to similar resemblances of birds' behaviors detection, like sitting, dustbathing, and resting. However, a group size greater than one bird accurately increases the detection object by splitting the images into a grid. Each grid of the cell helps to identify an object by itself (Sadykova et al., 2019). Similarly, when a hen's group size increases above four birds in a group FELB, the performance tends to decrease because of irregular FELB and grid group size.

Table 2.7: Performance of YOLOv5s model in detecting FELB group size.

Data summary	**YOLOv5s-FELB$_1$**	**YOLOv5s-FELB$_2$**	**YOLOv5s-FELB$_3$**	**YOLOv5s-FELB$_4$**	**YOLOv5s-FELB$_{4+}$**
Precision (%)	98.6	99.2	99.6	99.3	97.4
Recall (%)	96.2	100	100	100	96.0
mAP@0.50 (%)	96.6	99.5	99.5	99.5	98.8
mAP@0.50-0.95 (%)	71.6	66.2	70.5	71.6	63.3

FELB- floor egg laying behavior; NFELB- Non-floor egg laying behavior; mAP- mean average precision; FELB$_{1-4+}$ - FELB number of birds from 1 to more than 4.

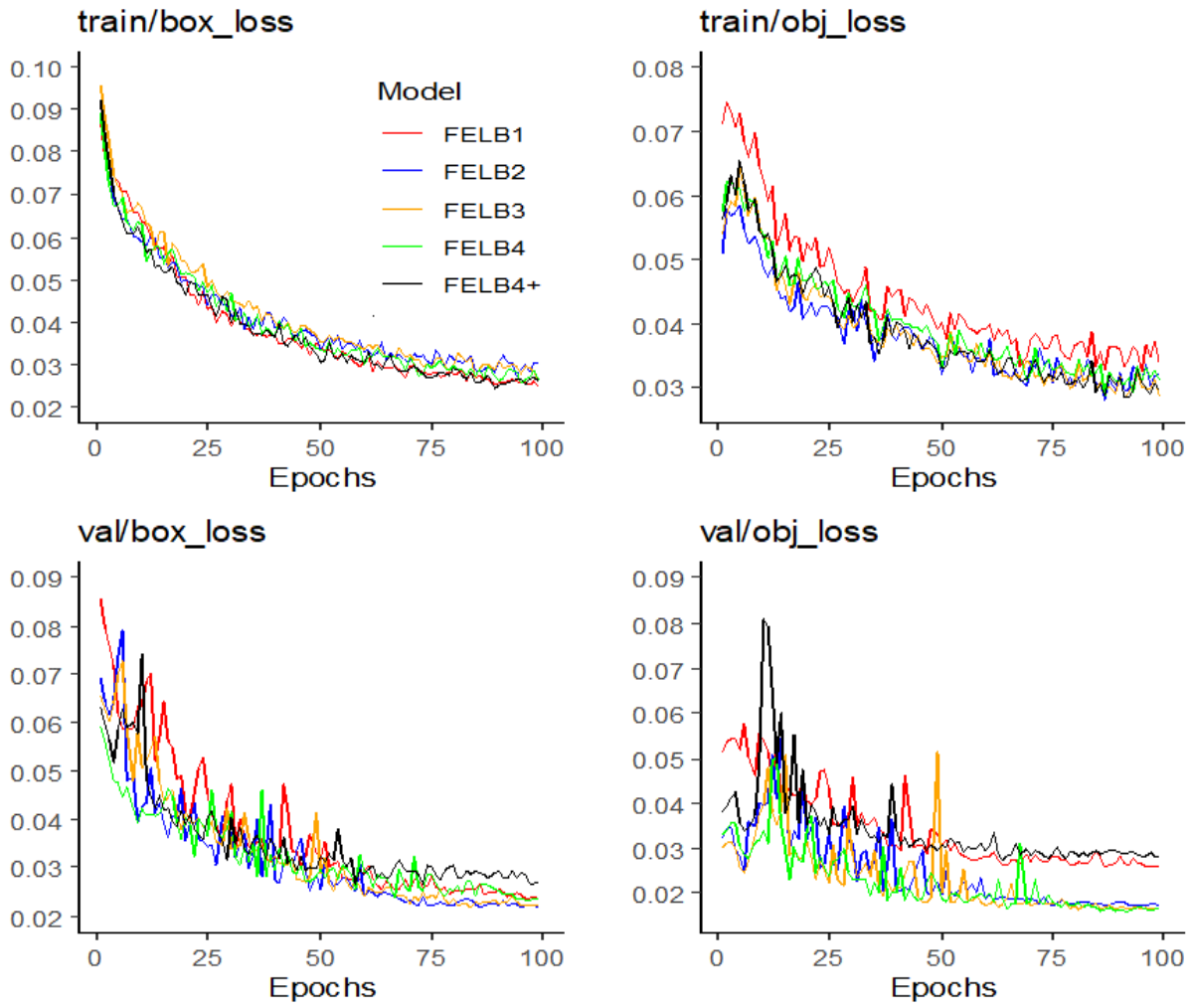

Figure 2.12: Training results of the YOLOv5s models for different hen group sizes.

The best YOLOv5s-FELB model after training and validation was used to detect the FELB behavior in unlabeled images, which were not used for validation and testing, as shown in Figure 2.13.

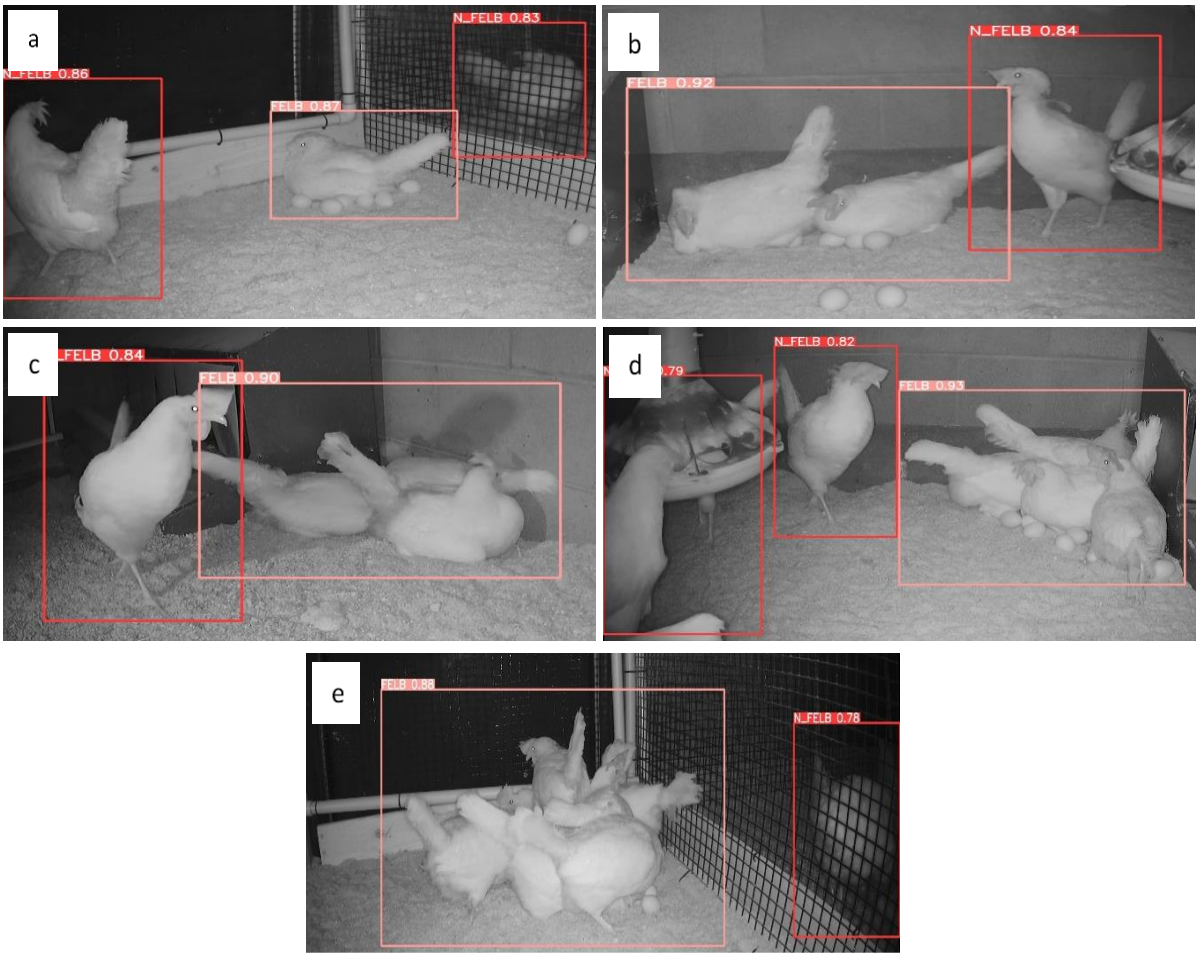

Figure 2.13: The FELB detected in collected video using the YOLOv5s model for various hen group sizes, a) $FELB_1$; b) $FELB_2$; c) $FELB_3$; d) $FELB_4$; and e) $FELB_{4+}$.

2.3.2.2 Hens FELB proportion

Detecting FELB in hens can be more challenging when observed in a group than being observed individually because when multiple hens are in the same area, visual obstructions can make it harder to accurately detect the behavior. Similarly, occlusion can still occur when observing individual hens within a group, making it more difficult to identify the behavior. After training and validating with the YOLOv5s model, group-labeled trained images show higher performance in FELB detection than individuals. The test results are given in Table 2.8, and the

detection of FELB in test data is in Figure 2.14. The detection of individual object performance decreases due to images occluded by other hens (Yang et al., 2022; Guo et al., 2021). To increase the detection performance of the individual hen, occluded objects can be restored using the ellipse fitting method (Guo et al., 2021).

Table 2.8: Performance of the YOLOv5s model in detecting FELB proportion.

Data summary	**Precision (%)**	**Recall (%)**	**mAP@0.50 (%)**	**mAP@0.50-0.95 (%)**
YOLOv5s-individual	97.6	95.5	98.3	73.0
YOLOv5s-group	99.8	98.3	99.5	75.8

mAP- mean average precision.

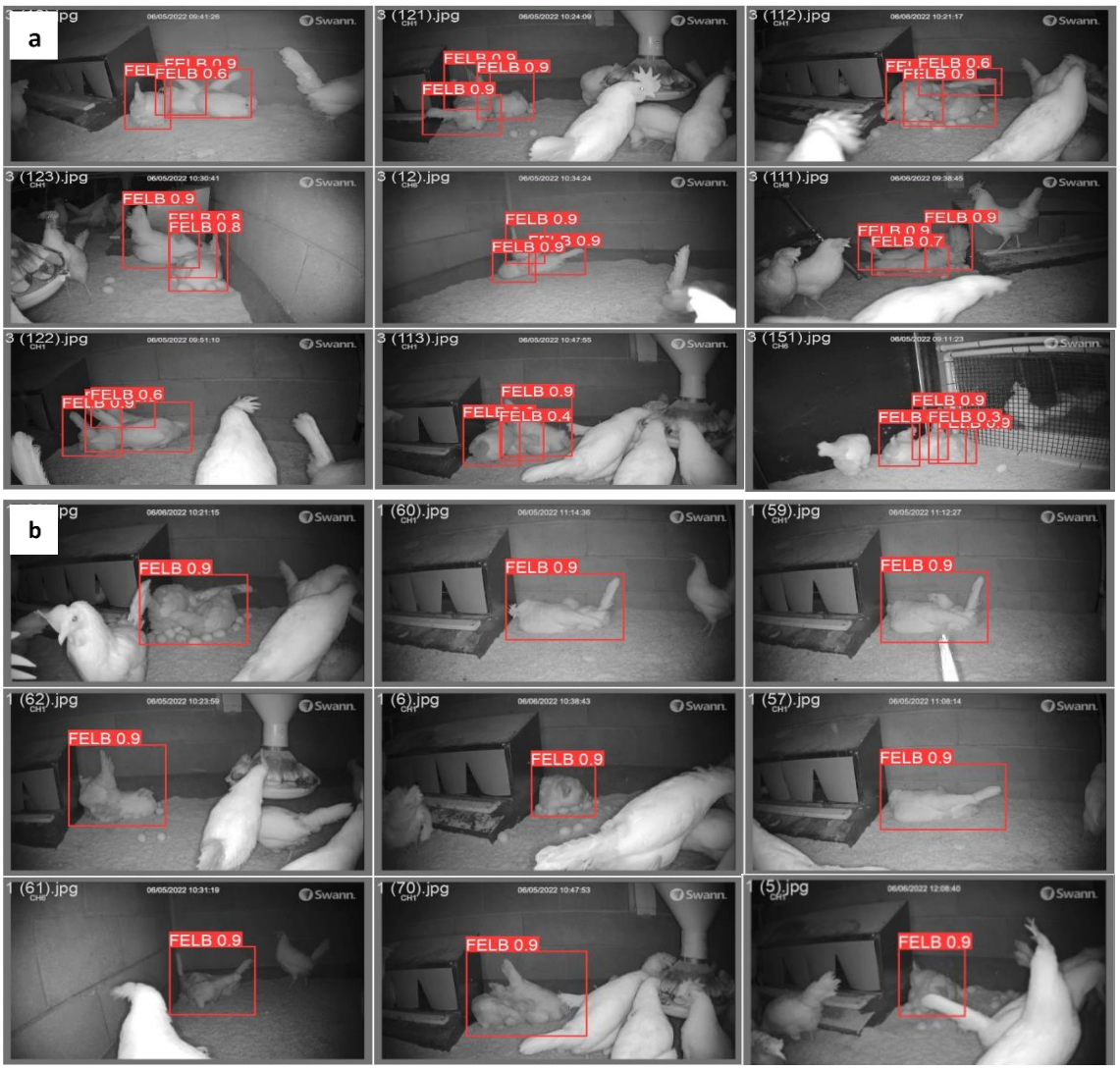

Figure 2.14: The FELB detected in test data using the YOLOv5s model for different hen proportions: a) individual hen detection and b) group hen detection.

2.3.2.3 Camera height

The previous research on floor egg detection did not show any significant effects of camera height on detecting target objects (Li et al., 2020). However, it depends on the type and size of an object (e.g., bacteria, egg, chicken, and flock) used for detection or monitoring. Current research evaluated the precision, recall, and mAP@0.50 of the optimal FELB detector (YOLOv5s) under

two cameras set at 50cm and 3m (ceiling) above the litter and found that lower camera height gave higher precision, recall, and mAP@0.50 (Table 2.9). Similarly, detected objects are shown in Figure 2.15. However, the camera adjusted in the ceiling helps provide an overview of the room area to detect where FELB was mostly observed.

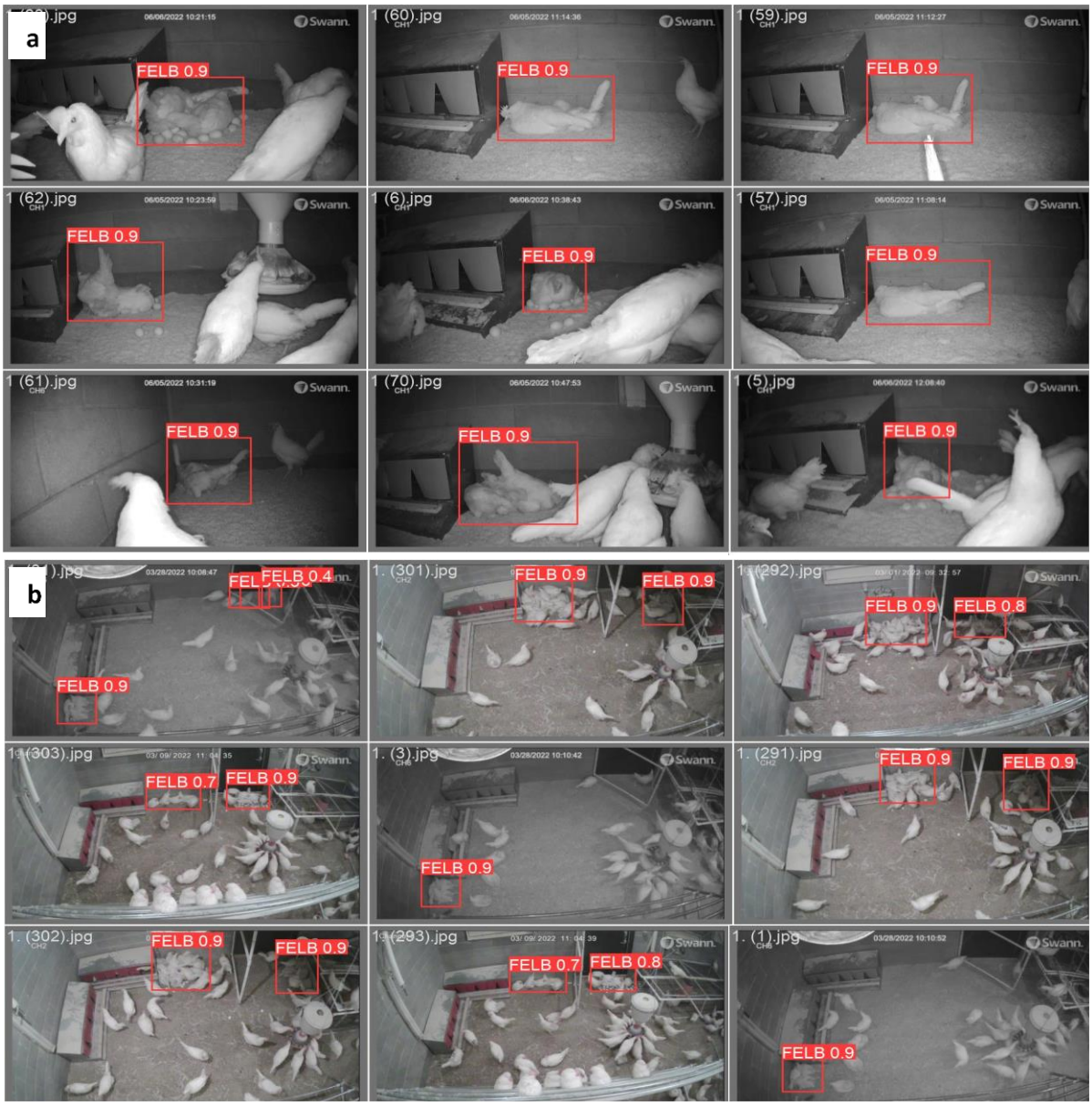

Figure 2.15: The FELB detected in test data using the YOLOv5s model for different camera settings a) height 0.5 m; and b) height 3 m from the litter floor.

2.3.2.4 Environment condition

The CF housing has the highest air pollutant-like dust particle concentration due to bird activities on the litter floor compared to conventional caged and Enriched colonies (Bist et al., 2022, 2023a; Bist and Chai, 2022). According to Yang et al. (2022), a dusty environment affects the detection performance, but if the camera is cleaned periodically, it might increase detection performance. Therefore, despite any environmental condition, if the model is trained well and the camera cleaned periodically, it might result in higher performance in detecting a targeted object. This study shows that the clean camera's test performance outperforms the dusty camera (Table 2.9). The test images after training and validation with the best YOLOv5s model for a clean and dusty environment are shown in Figure 2.16. Therefore, a clean camera and less dusty environment housing is required for the better performance of the model.

Table 2.9: Test result of YOLOv5s model based on laying hen camera height setting.

Data summary	Precision (%)	Recall (%)	mAP@0.50 (%)	mAP@0.50-0.95 (%)
YOLOv5s-height0.5m	99.8	98.3	99.5	75.8
YOLOv5s-height3m	98.7	96.8	98.4	65.5
YOLOv5s-clean	99.7	99.2	99.5	74.5
YOLOv5s-dusty	94.2	75.1	85.1	48.7

mAP- mean average precision; m- meter.

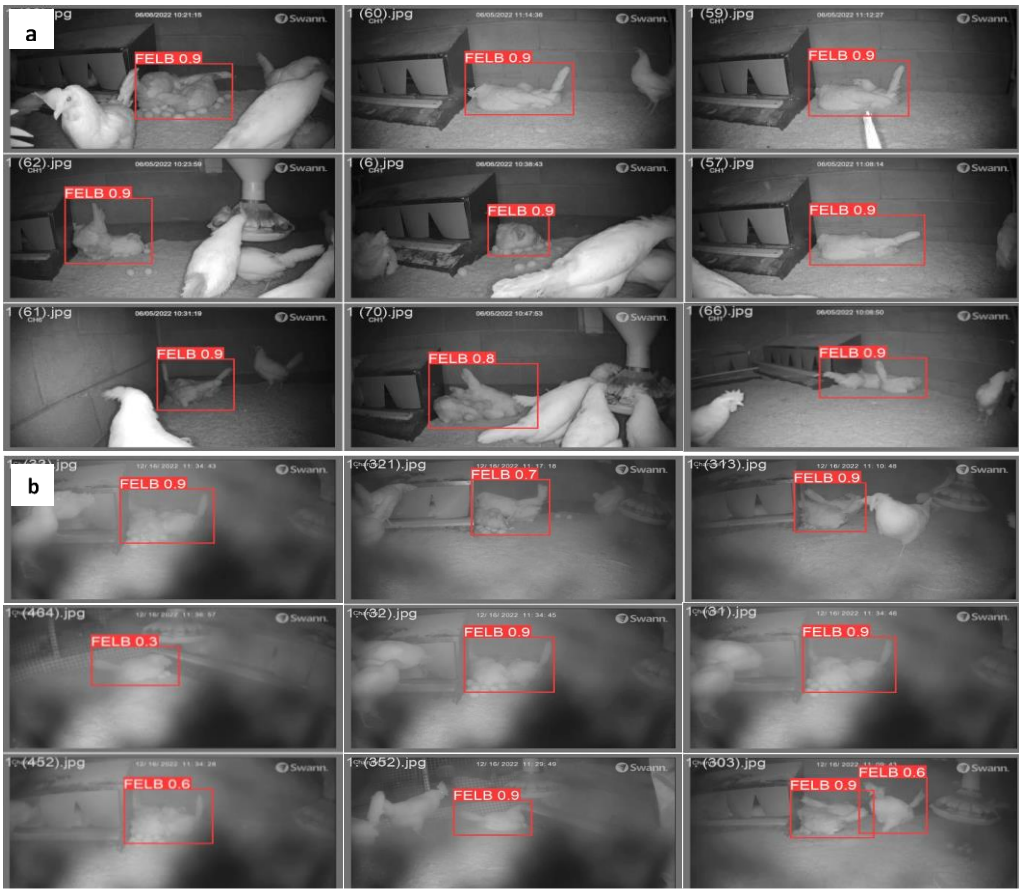

Figure 2.16: The FELB detected in test data using the YOLOv5s model for different CF rooms environment conditions a) clean and b) dusty environment.

This study was conducted in research rooms with a limited number of hens (200 hens per room). As a commercial CF house (tiered aviary system) has thousands of hens simultaneously on the floor (Chai et al., 2019), the deep learning model will be further innovated using commercial CF house data. Besides, we will integrate the YOLOv5s-FELB model detector into autonomous robots to track floor eggs lying across the CF house in the future. In addition, equipping robots with this technology will likely help farmers reduce floor eggs and associated food safety issues (e.g., bacterial egg contamination, broken eggs problem, and bird egg-eating behaviors).

2.4 CONCLUSIONS

This study trained and tested five deep-learning models based on the YOLOv5 structure and then compared them to detect floor egg-laying behaviors in four cage-free rooms in the research barn. The following conclusions were drawn from this study:

a) The YOLOv5m-FELB and YOLOv5x-FELB model detectors yielded the highest precision, recall, mAP@0.50, and F1-score in detecting floor egg-laying behaviors. However, the YOLOv5s model had a higher speed of data processing.

b) A lower camera height (e.g., 0.5 m above the floor) increased the performance of the FELB detection model compared to the ceiling camera (e.g., 3 m above the floor).

c) A dusty environment and dusty camera affect the detection accuracy; therefore, cleaning a camera is periodically recommended.

Further works include model innovation with commercial CF house data and integration of the YOLOv5s-FELB model detector into autonomous for monitoring or collecting mislaid eggs.

2.5 REFERENCES

Appleby, Michael C., Joy A. Mench, and Barry O. Hughes. Poultry behaviour and welfare. Cabi, 2004.

Bist, R. B., and L. Chai. 2022. Advanced Strategies for Mitigating Particulate Matter Generations in Poultry Houses. Applied Sciences, 12, 11323.

Bist, R. B., L. Chai, X. Yang, S. Subedi, and Y. Guo. 2022. Air Quality in Cage-free Houses during Pullets Production. In 2022 ASABE Annual International Meeting (p. 1). American Society of Agricultural and Biological Engineers.

Bist, R. B., S. Subedi, L. Chai, and X. Yang. 2023a. Ammonia Emissions, Impacts, and Mitigation Strategies for Poultry Production: A Critical Review. Journal of Environmental Management.

Bist, R.B.; Subedi, S.; Chai, L.; Regmi, P.; Ritz, C.W.; Kim, W.K.; Yang, X. 2023b. Effects of Perching on Poultry Welfare and Production: A Review. Poultry, 2, 134-157. https://doi.org/10.3390/poultry2020013

Chai, L., Xin, H, Y. Wang, J. Oliveira, K. Wang, and Y. Zhao. 2019. Mitigating Particulate Matter Generation in a Commercial Cage-Free Hen House. Transactions of the ASABE, 62, 877-886.

Chai, L., Y. Zhao, H. Xin, T. Wang, and M. L. Soupir. 2018. Mitigating airborne bacteria generations from cage-free layer litter by spraying acidic electrolysed water. Biosystems Engineering, 170, 61-71.

Cox, W. R. 2011. The problem of floor eggs. https://canadianpoultry.ca/wp-content/uploads/2020/04/breeder_floor_eggs.pdf.

Gu, Y., S. Wang, Y. Yan, S. Tang, and S. Zhao. 2022. Identification and Analysis of Emergency Behavior of Cage-Reared Laying Ducks Based on YoloV5. Agriculture, 12, 485.

Gunnarsson, S. 1999. Effect of rearing factors on the prevalence of floor eggs, cloacal cannibalism and feather pecking in commercial flocks of loose housed laying hens. British Poultry Science, 40, 12-18.

Guo, Y., Chai, L., Aggrey, S. E., Oladeinde, A., Johnson, J., & Zock, G. 2020. A machine vision-based method for monitoring broiler chicken floor distribution. Sensors, 20(11), 3179.

Guo, Y., S. E. Aggrey, A. Oladeinde, J. Johnson, G. Zock, and L. Chai. 2021. A machine vision-based method optimized for restoring broiler chicken images occluded by feeding and drinking equipment. Animals, 11, 123.

He, K., X. Zhang, S. Ren, and J. Sun. 2015. Spatial pyramid pooling in deep convolutional networks for visual recognition. IEEE transactions on pattern analysis and machine intelligence, 37, 1904-1916.

Holt, P. S., R. H. Davies, J. Dewulf, R. K. Gast, J. K. Huwe, D. R. Jones, D. Waltman, and K. R. Willian. 2011. The impact of different housing systems on egg safety and quality. Poultry Science, 90, 251-262.

Horvat, M., L. Jelecevic, and G. Gledec. 2022. A comparative study of YOLOv5 models performance for image localization and classification.

Jiang, P., D. Ergu, F. Liu, Y. Cai, and B. Ma. 2022. A Review of Yolo algorithm developments. Procedia Computer Science, 199, 1066-1073.

Jocher, G. 2020. Ultralytics/yolov5. GitHub - ultralytics/yolov5: YOLOv5 in PyTorch > ONNX > CoreML > TFLite. Accessed on 10-22-2022.

Jocher, G. 2022. https://github.com/ultralytics/yolov5/issues/6998. Accessed on 10-20-2022

Li, G., X. Hui, Y. Zhao, W. Zhai, J. L. Purswell, Z. Porter, S. Poudel, L. Jia, B. Zhang, and G. D. Chesser. 2022. Effects of ground robot manipulation on hen floor egg reduction, production performance, stress response, bone quality, and behavior. PloS One, 17, e0267568.

Li, G., Y. Xu, Y. Zhao, Q. Du, and Y. Huang. 2020. Evaluating convolutional neural networks for cage-free floor egg detection. Sensors, 20, 332.

Lin, T. Y., M. Maire, S. Belongie, J. Hays, P. Perona, D. Ramanan, P. Dollar, and C. L. Zitnick. 2014. Microsoft coco: Common objects in context. In European conference on computer vision (pp. 740-755). Springer, Cham.

Lundberg, A., and L. J. Keeling. 1999. The impact of social factors on nesting in laying hens (Gallus gallus domesticus). Applied Animal Behaviour Science, 64, 57-69.

Neethirajan, S. 2022. ChickTrack–a quantitative tracking tool for measuring chicken activity. Measurement, 191, 110819.

Octopus Robots. 2019. http://octopusrobots.com/en/home/.

Oliveira, J. L., H. Xin, L. Chai, and S. T. Millman. 2019. Effects of litter floor access and inclusion of experienced hens in aviary housing on floor eggs, litter condition, air quality, and hen welfare. Poultry Science, 98, 1664-1677.

Parisi, M. A., J. K. Northcutt, D. P. Smith, E. L. Steinberg, and P. L. Dawson. 2015. Microbiological contamination of shell eggs produced in conventional and free-range housing systems. Food Control, 47, 161-165.

Redmon, J., S. Divvala, R. Girshick, and A. Farhadi. 2016. You only look once: Unified, real-time object detection. In Proceedings of the IEEE conference on computer vision and pattern recognition (pp. 779-788).

Sadykova, D., D. Pernebayeva, M. Bagheri, and A. James. 2019. IN-YOLO: Real-time detection of outdoor high voltage insulators using UAV imaging. IEEE Transactions on Power Delivery, 35, 1599-1601.

Subedi, S., R. B. Bist, L. Chai, and X. Yang. 2023a. Tracking pecking behaviors and damages of cage-free laying hens with machine vision technologies, Computers and Electronics in Agriculture, Volume 204. https://doi.org/10.1016/j.compag.2022.107545.

Subedi, S., Bist, R., Yang, X., Chai, L., 2023b. Tracking floor eggs with machine vision in cage-free hen houses. Poultry Science, 102637. https://doi.org/10.1016/j.psj.2023.102637.

Tibot. 2019. https://www.tibot.fr/en/about-us/.

Ting, L., Z. Baijun, Z. Yongsheng, and Y. Shun. 2021. Ship detection algorithm based on improved YOLO V5. In 2021 6th International Conference on Automation, Control and Robotics Engineering (CACRE) (pp. 483-487). IEEE.

UEP (United egg producer). 2022. Retailers, restaurants continue cage-free commitments. https://unitedegg.com/retailers-restaurants-continue-cage-free-commitments/.

Vroegindeweij, B. A., S. K. Blaauw, J. M. IJsselmuiden, and E. J. Van Henten. 2018. Evaluation of the performance of PoultryBot, an autonomous mobile robotic platform for poultry houses. Biosystems Engineering, 174, 295-315.

Wang, C. Y., A. Bochkovskiy, and H. Y. M. Liao. 2022. YOLOv7: Trainable bag-of-freebies sets new state-of-the-art for real-time object detectors. arXiv preprint arXiv:2207.02696.

Wang, C. Y., H. Y. M. Liao, Y. H. Wu, P. Y. Chen, J. W. Hsieh, and I. H. Yeh. 2020. CSPNet: A new backbone that can enhance learning capability of CNN. In Proceedings of the IEEE/CVF conference on computer vision and pattern recognition workshops (pp. 390-391).

Yang, X., L. Chai, R. B. Bist, S. Subedi, Z. Wu. 2022. A Deep Learning Model for Detecting Cage-Free Hens on the Litter Floor. Animals, 12, 1983.

CHAPTER 3

PILING BEHAVIOR DETECTION IN LAYING HEN FACILITIES[2]

[2] Bist, R. B., Subedi, S., Yang, X., and Chai, L. 2023. A Novel YOLOv6 Object Detector for Monitoring Piling Behavior of Cage-Free Laying Hens. *AgriEngineering* 5 (2), 905-923. https://doi.org/10.3390/agriengineering5020056. Reprinted here with permission of the publisher.

ABSTRACT

Piling behavior (PB) is a common issue that causes negative impacts on the health, welfare, and productivity of the flock in poultry houses (e.g., cage-free layer, breeder, and broiler). When birds pile on top of each other, the weight of the birds can cause physical injuries, such as bruising or suffocation, and may even result in death. In addition, PB can cause stress and anxiety in the birds, leading to reduced immune function and increased susceptibility to disease. Piling has been reported as one of the most concerning production issues in cage-free layer houses. Several strategies (e.g., adequate space, environmental enrichments, genetic selection) have been proposed to prevent or mitigate PB in laying hens, but less scientific informations are available to control it so far. The current study aimed to develop and test the performance of a novel deep-learning model for detecting PB and evaluate its effectiveness in four CF laying hen rooms. To achieve this goal, the study utilized different versions of the YOLOv6-PB models (e.g., YOLOv6t, YOLOv6n, YOLOv6s, YOLOv6m, YOLOv6l, and YOLOv6l relu). The objectives of this study were to develop a reliable and efficient tool for detecting PB in commercial egg-laying facilities based on deep learning and to test the performance of new models in research cage-free rooms. The study used a dataset comprising 6800 images (e.g., 4760 for training, 1360 for validation, and 680 for testing). The results show that the YOLOv6m-PB models perform exceptionally well with high average recall (70.5%), mAP@0.50 (98.1%), and mAP@0.50-0.95 (63.3%) compared to other models. In addition, detection performance increases when the camera is placed close to the PB areas. Thus, the newly developed YOLOv6m-PB model demonstrated superior performance in detecting PB and huddling behaviors in the given dataset compared to other tested models.

Keywords: Egg production; Animal welfare; Behavior monitoring; Machine learning.

3.1 INTRODUCTION

Piling behavior (PB) is a common issue that can adversely affect the welfare, productivity, and overall health of the flock in any housing, including breeder, broiler, and cage-free layer facilities. Poultry piling is a phenomenon where birds densely cluster together, often resulting in birds being piled on top of one another (Campbell et al., 2016b; Winter et al., 2021). Piling one over another can result in the birds becoming trapped, which can lead to suffocation and death (Gray et al., 2020; Winter et al., 2021). In Australia, in free-range or cage-free laying hens, PB accounts for up to 40% of mortality (Rice et al., 2020). The location and timing of smothering tend to be unpredictable and may vary between farms. According to surveys, over 50% of free-range or cage-free farms in the United Kingdom (UK) reported smothering at some point in their flocks (Barrett et al., 2014). The UK egg industry is estimated to lose £6.5 million annually due to smothering caused by PB (Herbert et al., 2021). However, PB behavior has been primarily observed in loose-housed layer flocks and is a significant animal welfare and economic concern for producers and the egg-laying industry (Bright and Johnson, 2011; Barrett et al., 2014; Rayner et al., 2016; Gray et al., 2020; Winter et al., 2021).

The PB in laying hens is considered an animal welfare issue because it can negatively impact the birds' physical and psychological well-being, resulting in stress, overheating, injuries, feather pecking, and reduced mobility and natural behaviors (Gray et al., 2020; Herbert et al., 2021). Increased stress levels in birds result in reduced egg production (Gray et al., 2020), egg quality (Marder and Arad, 1989; Kang et al., 2018), and increased susceptibility to disease (Gray et al., 2020). Birds piled one over another can result in overheating, leading to heat stress, suffocation, and even increased mortality. Similarly, overcrowding causes physical injuries, such

as fractures (Gray et al., 2020). In addition, birds piled on top of each other may limit mobility, leading to muscle atrophy and other health issues (Hartcher and Jones, 2017). Piling can also prevent birds from accessing feed, water, and other resources. Sometimes, PB can also lead to feather pecking (Campbell et al., 2016a), increasing the cause of cannibalism in poultry. Piling can also reduce chickens' ability to express their natural behavior, such as foraging, dust bathing, and socializing with other birds (Campbell et al., 2016b; Winter et al., 2021). The threshold at which a pile turns into a smothering event is currently unknown (Gray et al., 2020), and understanding the biological causes of PB is necessary for effective mitigation.

The causes of PB are not well understood, and there is a lack of research in this area. However, several potential factors have been recorded. High stocking density is one of the most common factors contributing to PB (Barrett et al., 2014; Gebhardt-Henrich and Stratmann, 2016; Gray et al., 2020). Hens living in high-density environments may become stressed and develop abnormal behaviors such as piling. Besides, laying hens' nesting behavior and competition in nest use could lead to PB (Riber, 2010; Gebhardt-Henrich and Stratmann, 2016; Giersberg et al., 2019). In poultry houses, a social hierarchy can develop, with dominant birds having first access to resources such as food, water, and nest boxes, which can lead to PB as subordinate birds attempt to access these resources (Lentfer et al., 2011; Winter et al., 2021). In addition, environmental factors such as lighting, temperature, and ventilation may also influence PB (Campbell et al., 2016a; Gebhardt-Henrich and Stratmann, 2016; Winter et al., 2021). For instance, hens may pile due to low temperatures or poor ventilation. Finally, layer strains can differ in their patterns of nest use and PB, with brown hens often mislaying eggs on the floor or grids of an enclosure more often than white hybrids (Singh et al., 2009; Villanueva et al., 2017).

Therefore, different prevention strategies may be required to address the multifactorial nature of this issue.

Mitigation strategies for PB in laying hens include increasing space per bird, providing enrichment such as perches and nesting boxes, and reducing flock size (Altan et al., 2013; Gebhardt-Henrich and Stratmann, 2016; Gray et al., 2020; Winter et al., 2021). Increasing space per bird (Gray et al., 2020) and providing perches (Winter et al., 2021) reduced PB in laying hen houses. Besides, providing enrichment (e.g., toys, natural materials, and different feed types) in poultry houses encourages birds to perform natural behaviors and thus reduce stress and PB (Altan et al., 2013; Winter et al., 2021, 2022). Another way to mitigate PB is to establish a social hierarchy by providing additional resources, such as feeders and nesting boxes, to allow all birds access to the best resources. In addition, providing nest boxes for hens to lay eggs reduces PB as it fulfills their innate need for nest-building behavior (Riber, 2010). Besides adequate space, environmental enrichment, social hierarchy, and nest boxes, improved ventilation and light adjusting are important in mitigating PB. Adequate ventilation maintains a comfortable temperature and humidity level and reduces PB. Hens are photoperiodic animals, meaning their behavior is influenced by the amount and duration of light they receive (Winter et al., 2021).

Research on PB has focused on identifying potential environmental and management factors that contribute to its occurrences (Riber, 2010; Campbell et al., 2016b; Gray et al., 2020; Winter et al., 2021). However, the unpredictability and disruption caused by the presence of an observer make it challenging to conduct experiments and obtain accurate data on PB in commercial settings (Barrett et al., 2014; Rayner et al., 2016). Therefore, regularly monitoring

the flock to identify any issues contributing to PB is important for maintaining the health and well-being of the birds. PB can signify a more serious underlying issue, such as disease or poor nutrition, and should be addressed accordingly. More studies are needed to fully comprehend the reasons for PB and develop effective strategies to prevent its occurrence. Studies incorporating observational and experimental methods in commercial settings and considering the influence of genetics and individual variation in behavior can provide valuable insights into the underlying causes of PB in laying hens. The objectives of this detection study were to a) develop and test the best PB detection models; and b) compare the performance of deep learning models in research cage-free rooms.

3.2 MATERIALS AND METHODS

3.2.1 Experimental Housing and Management

This experiment follows the same housing and bird management practices as described in Chapter 2 of section 2.2.1.

3.2.2 Image and Data Collections

This study recorded the hens' behaviors using six night-vision network cameras (PRO-1080MSB, Swann Communications USA Inc.) mounted in each room, about 3 meters above the litter floor. In addition, two cameras were placed 0.5 meters above the ground floor. The data acquisition was performed daily for 24 hours and recorded in a digital video recorder (DVR-4580, Swann Communications USA Inc.). The recorded video files were stored in .avi format with a 1920 × 1080 pixels resolution and 15 frames per second sampling rate. The data acquisition took place between 46 and 50 weeks of age.

3.2.3 Image Processing

The video data was converted into individual image files in .jpg format using the Free Video to JPG Converter App version 5.0. The resulting images were filtered based on PB presence and labeled using Makesense.AI in the YOLOv5 format. This study uses image datasets of 6800 images, where 70% of the total image datasets were used for training, 20% for validation, and 10% for testing (Table 3.1). The different categories of classes used to compare in this study are illustrated in figure 3.1.

Table 3.1: Data pre-processing for PB model detection.

Class	Original dataset	Train (70 %)	Validation (20 %)	Test (10 %)
PBceiling	600	420	120	60
PBground	600	420	120	60
PBdaytime	2800	1960	560	280
PBnighttime	2800	1960	560	280
PBmodel	2800	1960	560	280

Note: PBceiling and PBground represent PB observed at camera height of 3m and 50cm, respectively, above the litter floor; PBdaytime and Pbnighttime represent PB during the light period and dark period, respectively.

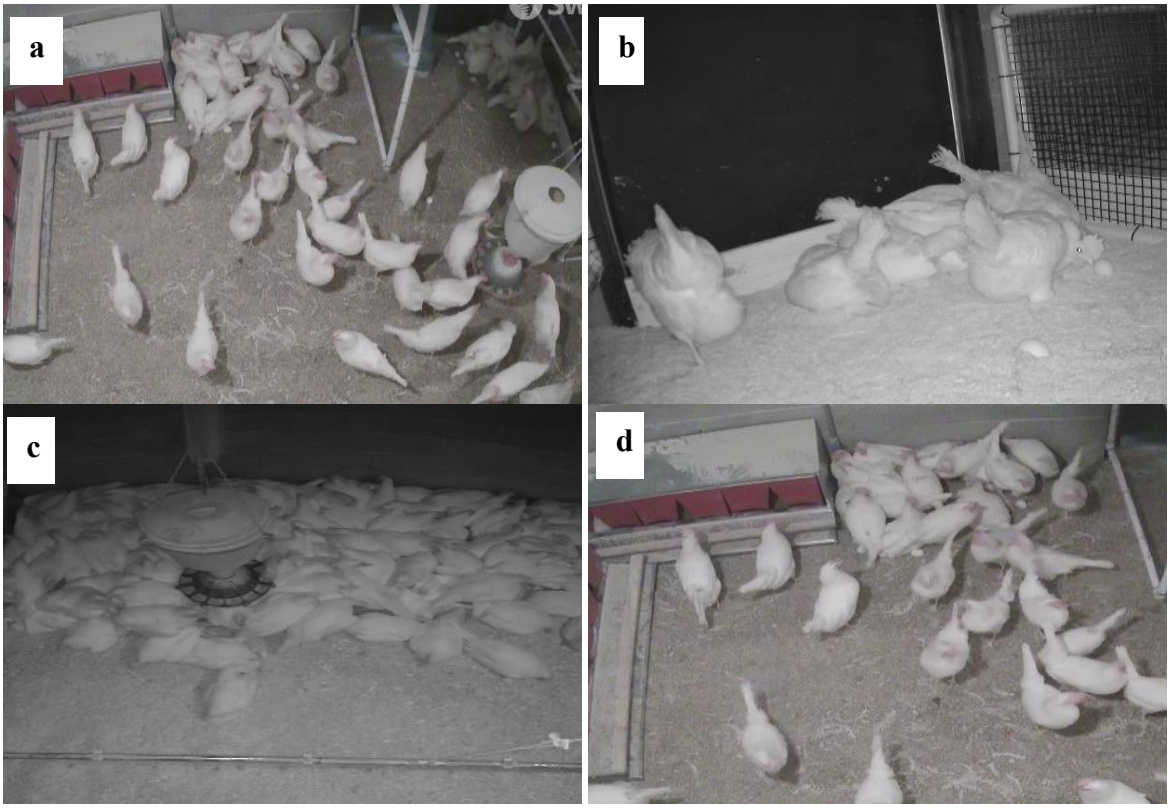

Figure 3.1: Images datasets labeled based on class a) PBceiling, b) PBground, c) PBnighttime, and d) PBdaytime. Huddling behaviors at night sometimes look like piling behaviors, but we took only piling behavior data after the light turned off.

3.2.4 YOLOv6 Network Description

YOLOv6 is the latest object detection algorithm launched and developed by Meituan in 2022 (Meituan, 2023). YOLOv6 is designed to be a single-stage object detection framework, meaning that it uses a single pass through the network to perform both object proposals and classification, which makes YOLOv6 faster and more efficient than multi-stage object detection frameworks (Horvat and Gledec, 2022). In addition, the YOLO model, like YOLOv6, is designed to be hardware efficient, which makes it suitable for industrial applications where real-time object detection is required (Li et al., 2022). Furthermore, YOLOv6 is optimized for

graphics processing units (GPUs) and can run on devices with limited computing resources, making it a popular choice for embedded systems and Internet of Things (IoT) devices. Compared to its predecessor YOLO models, YOLOv6 has improved detection accuracy and inference speed, making it a more suitable choice for object detection tasks (Meituan, 2023). In this study, different YOLOv6-PB models, i.e., YOLOv6n-PB (nano), YOLOv6t-PB (tiny), -PB (small), YOLOv6m-PB (medium), YOLOv6l-PB (large), and YOLOv6l relu-PB (large relu) were compared in PB detection. These YOLOv6-PB models differ in size and parameters. First, YOLOv6 models were compared with PBmodel image datasets (Table 3.1) and identified the best PB detection model. Later, the best model was compared with different camera settings (PBceiling & PBground) and photoperiod (PBnighttime and PBdaytime) conditions.

YOLOv6-PB is a complex neural network architecture consisting of several parts, each of which plays a specific role in object detection (Figure 3.2). Some of the main parts of YOLOv6-PB are:

3.2.4.1 Input

The pre-trained PB image datasets were fed into the model to make predictions through the input part of the YOLOv6-PB model. Input images and labels were then passed into the neural network, which usually occurs in another part of the YOLOv6-PB model. The size of the input image depends on the YOLOv6-PB architecture of the network, but it is usually expected to be a fixed size, for example, 640×640×3 pixels as the default size. In this study, a default size of the images is taken for analysis.

3.2.4.2 Backbone

The backbone extracts features from the input PB image. In YOLOv6-PB, the backbone network is typically a pre-trained Convolutional Neural Network (CNN) that has been fine-tuned for object detection. The specific architecture of the backbone network in YOLOv6-PB can vary, but it typically consists of several convolutional layers, followed by max-pooling layers, which helps to reduce the feature map's spatial dimensions. The convolutional layers detect low-level features in the PB image, such as edges and textures. Spatial pyramid pooling (SPP) helps max-pooling layers reduce the feature map's size and maintain the most important features for object detection (He et al., 2015). Similarly, The EfficientRep Backbone used in YOLOv6-PB is designed to both effectively use the computational resources of hardware such as GPUs and possess robust feature representation abilities, as compared to the CSP-Backbone utilized by YOLOv5 (Li et al., 2022).

3.2.4.3 Neck

The neck connects the backbone network to the rest of the network. It takes the PB output of the backbone network and performs additional processing to produce the final feature map used for PB object detection. In general, the purpose of the neck in YOLO-PB architectures is to provide intermediate feature maps suitable for the heads to make accurate predictions. This is often achieved through a series of convolutional, pooling, and up-sampling layers that manipulate the features from the backbone network to the desired scale and resolution for the heads. Regarding its neck design, YOLOv6-PB introduces a more efficient feature fusion network, known as the Rep-PAN Neck (Liu et al., 2018), to improve hardware utilization and the

balance between accuracy and speed. This design is based on the hardware-aware neural network architecture concept (Weng et al., 2023).

3.2.4.4 Anchor boxes

Anchor boxes are predefined bounding boxes used to represent PB objects in the image. They provide priori information about the location and size of PB objects in the image. During training, the network learns to adjust the anchor boxes to fit the PB objects in the image better.

3.2.4.5 Detection head

The detection head is responsible for predicting the PB objects in the image. It takes the output of the neck network and produces a set of class probabilities and bounding boxes for each targeted PB object in the image (Jocher, 2022). The detection head uses anchor boxes as a starting point and adjusts them to fit the PB objects in the image better. YOLOv6-PB utilizes a Decoupled Head structure, which simplifies the head design while carefully balancing the representation capabilities of the relevant operations with the computational demands on the hardware (Li et al., 2022).

3.2.4.6 Loss function

The loss function is used to train the network by measuring the difference between the predictions made by the network and the ground truth annotations. The loss function measures the error between the predicted bounding boxes and the ground truth boxes and the error between the predicted class probabilities and the ground truth class labels of PB.

$$Loss = \lambda_1 L_{cls} + \lambda_2 L_{obj} + \lambda_3 L_{loc} \qquad (i)$$

Where, L_{cls}, L_{obj}, and L_{loc} represent class loss, PB object loss, and location or bounding box loss, respectively; λ is constant for respective loss.

3.2.4.7 Post-processing

The final step in the PB object detection process is post-processing, which involves refining the predictions made by the network. This can include techniques such as filtering out low-confidence detections, rescaling the bounding boxes to the original PB image size, and drawing the final PB detections on the image. Each of these parts of YOLOv6-PB works together to perform object detection in real-time, allowing for the efficient and accurate detection of PB objects in images and videos.

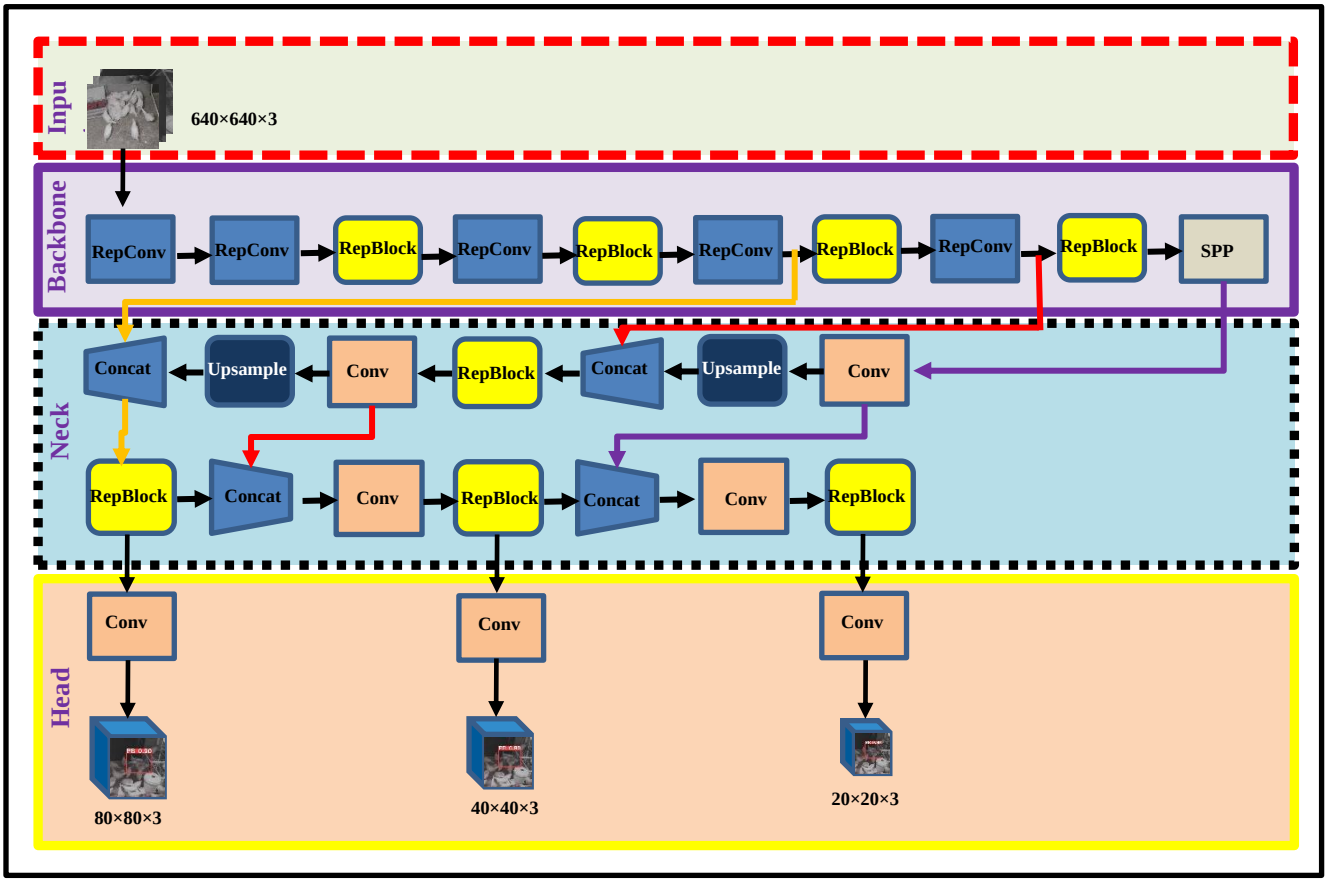

Figure 3.2: YOLOv6-PB architecture.

3.2.5 Computational Parameters

A high-performing computational configuration is used to perform PB detection. This detection study used the Oracle cloud with different configurations to train, validate, and test the image datasets (Table 3.2). The higher number of computational parameters increases the speed and detection accuracy of the model (Subedi et al., 2023a; b).

Table 3.2: Computational parameters used for the PB model evaluation.

Configuration	**Parameters**
CPU	64 core OCPU
GPU (4 counts)	4×NVIDIA® A10 (24GB)
Operating system	Ubuntu 22.10
Accelerated environment	NVIDIA CUDA
Memory	1024GB
Drive (2 counts)	7.68 TB NVMe SSD
Libraries	Torch 1.7.0, Torch-vision 0.8.1, OpenCV-python 4.1.1, NumPy 1.18.5

3.2.6 Performance Metrics

The performance of YOLOv6-PB is typically measured using several key metrics, including:

3.2.6.1 Recall

This metric measures the fraction of the total number of PB objects in an image correctly detected by the PB object detection system. It is calculated based on true positive (TP, image contains PB, so the model predicts it correctly) and false negative (FN, image contains PB but unable to detect PB) detection results obtained from the YOLOv6-MD model.

$$Recall = \frac{TP}{TP + FN} = \frac{true\ piling\ behavior\ detection}{all\ ground\ truth\ bouding\ boxed} \qquad (iii)$$

3.2.6.2 Precision

This metric measures the fraction of the total number of PB made by the PB object detection system that was correct. It is calculated by all positive detections such as TP and false positives (FP, the image does not contain PB, but the model detects PB). The formula of precision is given below.

$$Precision = \frac{TP}{TP + FP} = \frac{true\ piling\ behavior\ detection}{all\ detected\ bouding\ boxed} \qquad (iv)$$

The overall positive and negative PB detection is made clear with the help of the confusion matrix in Figure 3.3.

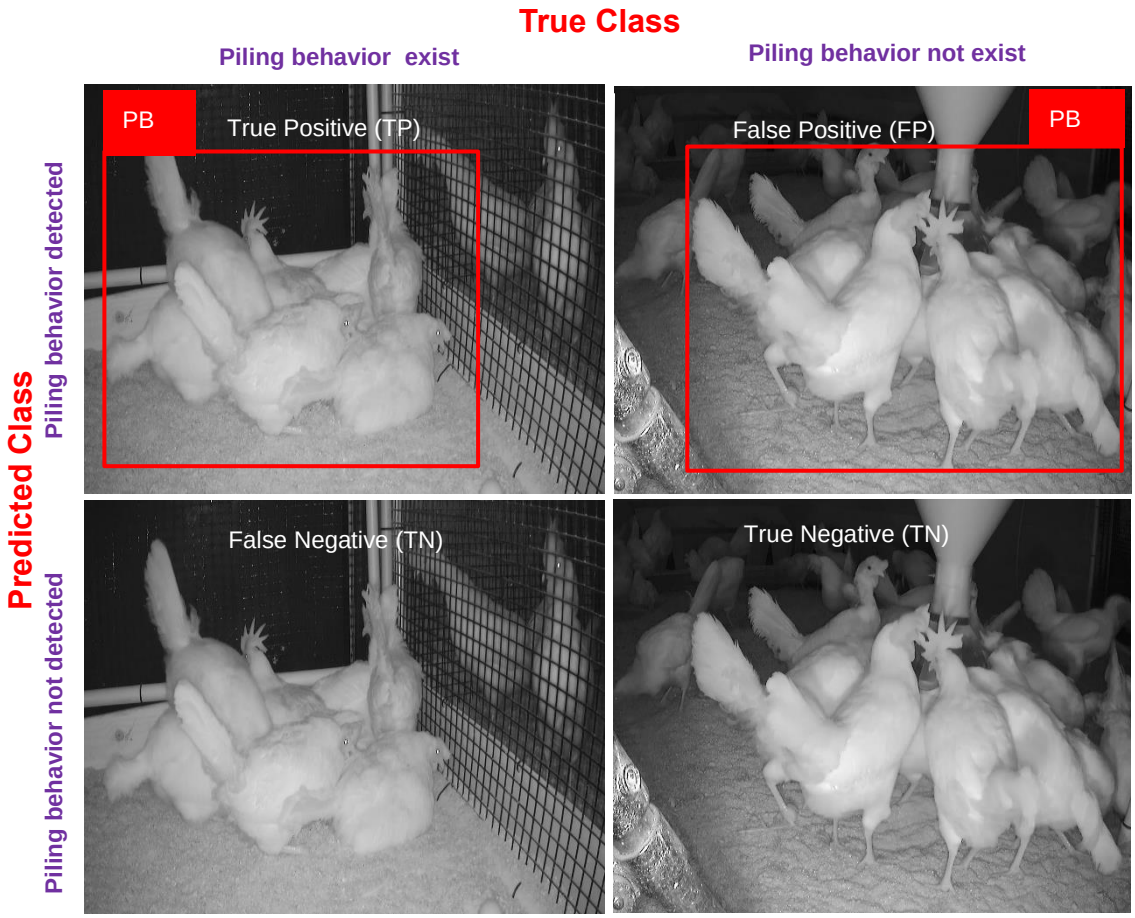

Figure 3.3: Confusion matrix for piling behavior detection used for model evaluation.

3.2.6.3 Mean average precision (mAP)

This metric measures the average precision of the PB object detection system over multiple object classes at a threshold of 0.50 (mAP@0.50) or 0.50:0.95 (mAP@0.50:0.95). The mAP is calculated as the average of the precision values for each class, considering the number of true positive PB detections and the number of false positive PB detections.

$$mAP = \frac{\sum_{i-1}^{C} APi}{C} \qquad (ii)$$

where, APi the average precision of the ith category and C represent the total number of categories.

3.2.6.4 Inference time

This metric measures the time the PB object detection system takes to process an input image and make predictions. Inference time is an important consideration for real-time object detection systems, as a fast inference time allows for faster processing of video streams and other real-time applications (Li et al., 2022).

3.3 RESULTS AND DISCUSSIONS

3.3.1 Performance Comparison of YOLOv6 Models

This study compared all YOLOv6 models to determine which model performs better in detecting PB, and the results are shown in Table 3.3 and Figure 3.4. Among all YOLOv6 models, YOLOv6m-PB performed better in terms of performance metrics such as average recall (70.5%), mAP@0.50 (98.1%), and mAP@0.50-0.95 (63.3%) compared to other models. However, YOLOv6t-PB performs lowest with 67.7% average recall, 97.3% mAP@0.50, and 60.8% mAP@0.50-0.95. Similarly, the training time increased from smaller to bigger because the bigger size YOLOv6 model consumes more time to perform and accurately detect the PB. Thus, the YOLOv6t-PB and YOLOv6n-PB perform faster to train 1960 images and validate 560 images (almost 0.71 hrs), while YOLOv6l relu-PB acts slow in training and validation (1.50 hrs) at the same time. Overall, the YOLOv6m-PB outperforms and can be used in the future to detect PB, which ultimately helps to find the actual reason for PB so that it can be reduced on time. For example, a reduction in PB might decrease floor eggs (Riber, 2010), stress (Altan et al., 2013; Winter et al., 2021, 2022), pecking behavior (Campbell et al., 2016a; Subedi et al., 2023a), and improve animal welfare.

Table 3.3: Comparison of performance of the different models with different performance metrics.

Performance metrics	**YOLOv6t - PB**	**YOLOv6n -PB**	**YOLOv6s -PB**	**YOLOv6m - PB**	**YOLOv6l - PB**	**YOLOv6 l relu- PB**
Average Recall (%)	67.7	68.5	68.9	70.5	69.2	70.2
mAP@0.50 (%)	97.3	97.7	97.9	98.1	97.6	98.1
mAP@0.50-0.95 (%)	60.8	61.4	62.3	63.3	62.3	63.0
Training time (hrs)	0.714	0.713	0.743	1.061	1.151	1.502

mAP- mean average precision; hrs- hours.

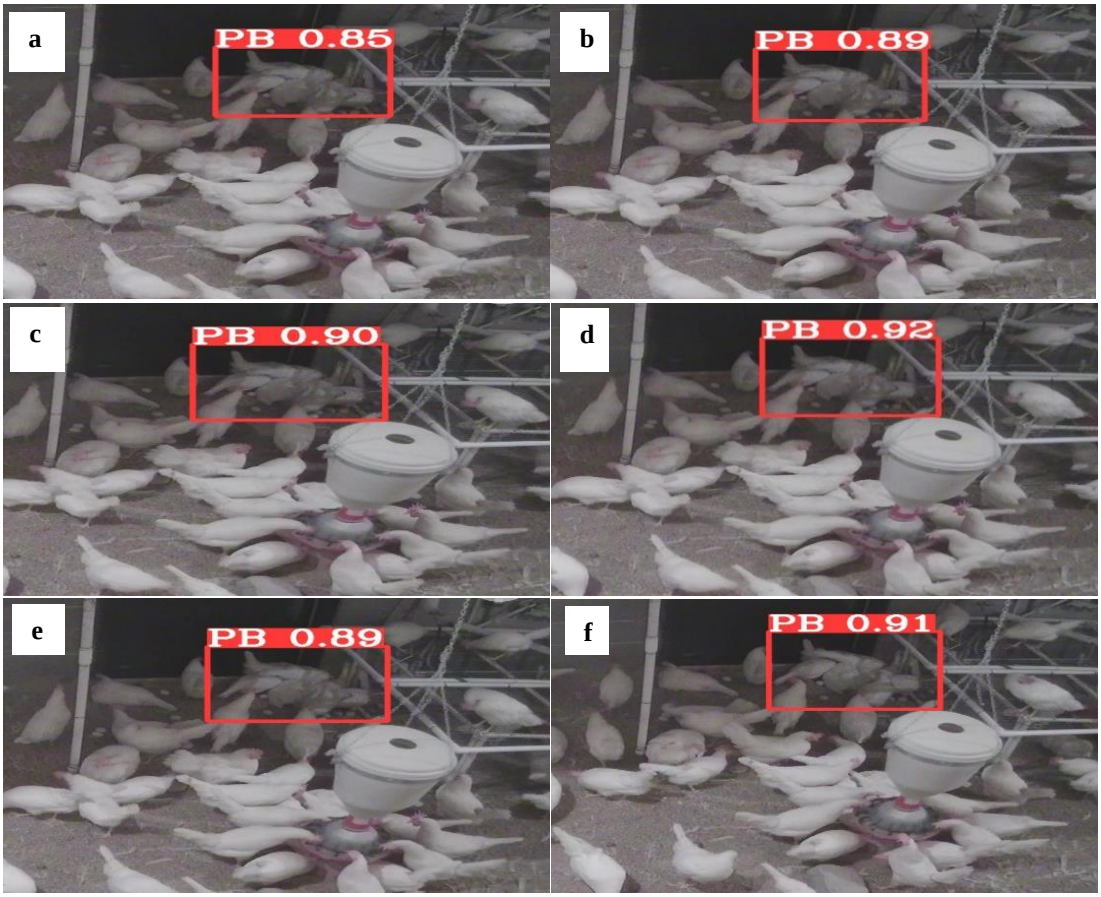

Figure 3.4: Piling behavior detection result comparison based on various models a) YOLOv6t-PB, b) YOLOv6n-PB, c) YOLOv6s-PB, d) YOLOv6m-PB, e) YOLOv6l-PB, and f) YOLOv6l relu-PB model.

3.3.2 Performance of Piling Behavior Under Different Photoperiods

Piling behavior was found mostly during nighttime and in a huge flock size for a longer time, while during the daytime, it might occur in small numbers for performing nesting behaviors. During the nighttime, hens piling one over another might cause suffocation and increase death rates (Gray et al., 2020; Winter et al., 2022). However, during the daytime, piling for nesting behavior might increase heat stress (Gray et al., 2020; Herbert et al., 2021) and directly affect animal welfare (Gray et al., 2020), egg quality (Marder and Arad, 1989; Kang et

al., 2018), and production (Gray et al., 2020). In this study, when YOLOv6m-PB was compared between nighttime and daytime, the PB detection was highest during nighttime compared to daytime (Table 3.4 & Figure 3.5). The PB was highest during nighttime because the PB flock size was found to be big in shape, which might be due to huddling together, which increased performance for PB detection (Figure 3.6). Hens show piling behaviors when the sudden light turns off, and later, hens huddle or crowd together. Therefore, our model can also detect huddling behaviors along with piling behavior. However, detection performance can be decreased during nighttime if night vision cameras are not used. That is why night vision cameras can help detect objects more clearly when the light is turned off. Statistically, if results are compared among YOLOv6 models, it will not show any significant difference between them, but in detection work, every percentage increase matters, reflecting on increasing detection accuracy. Therefore, the YOLOv6m-PB performs better, and the best model can help detect more precisely during daytime and nighttime, which eventually helps decrease PB and improve animal welfare.

Table 3.4: Comparison of piling behavior during daytime and nighttime using the YOLOv6m model.

Data summary	Average Recall (%)	mAP@0.50 (%)	mAP@0.50-0.95 (%)
YOLOv6m-nighttime	83.1	98.9	80.70
YOLOv6m-daytime	82.4	99.0	78.2

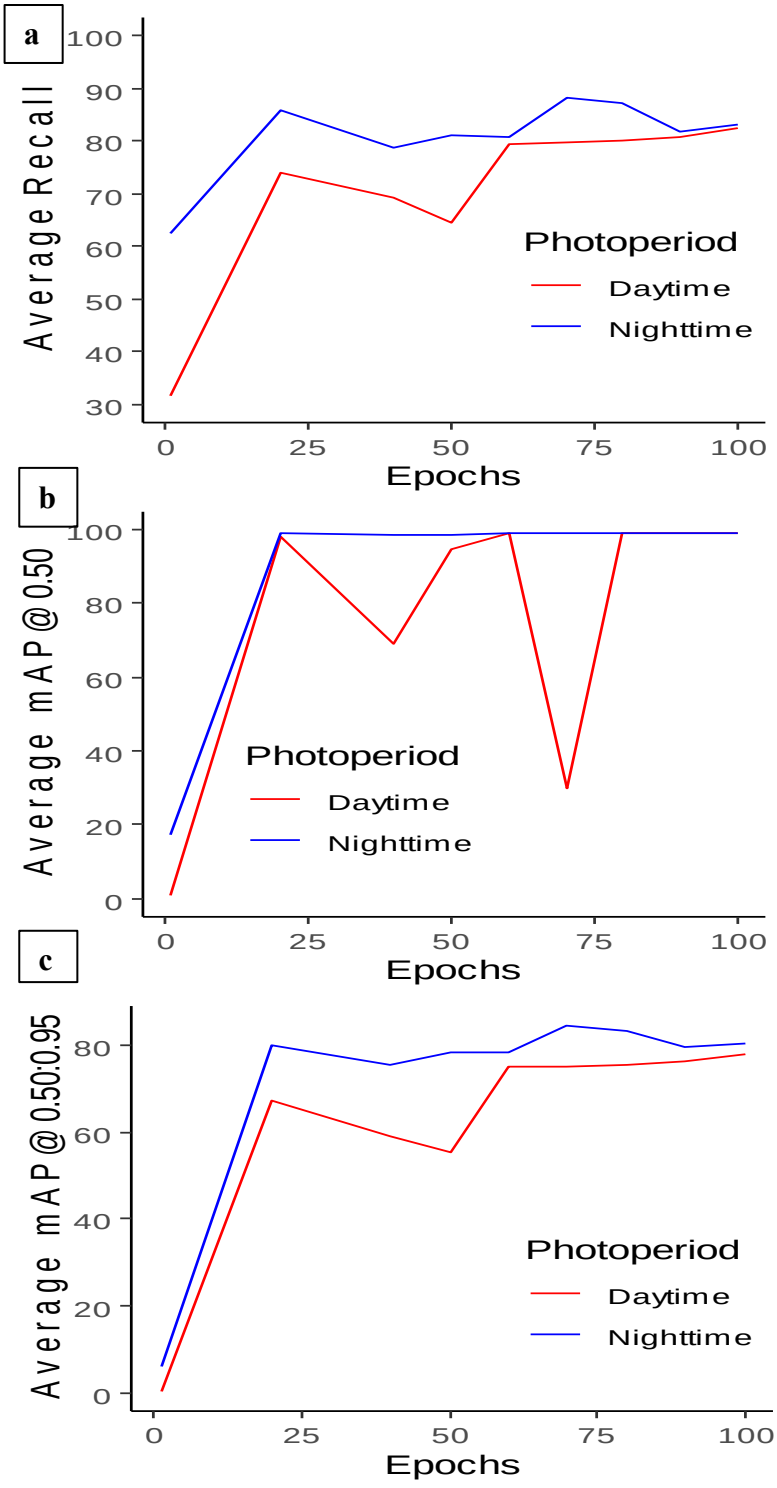

Figure 3.5: Comparison of piling behavior detection results during different photoperiods and epochs with a) average recall, b) mAP@0.50, and c) mAP@0.50-0.95.

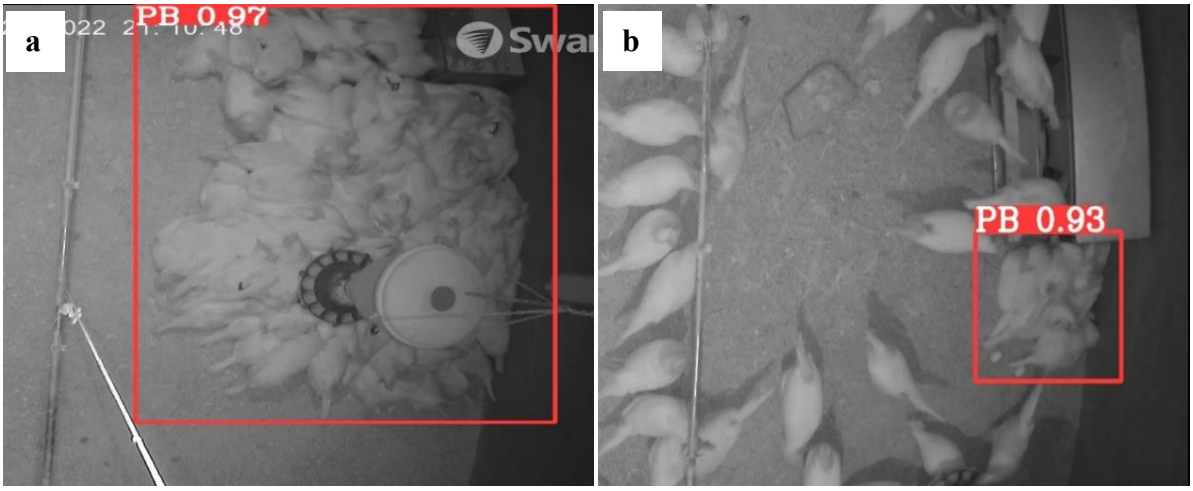

Figure 3.6: Piling behavior detection result based on different photoperiods a) nighttime (light turned off) and b) daytime (light turned on). Huddling behaviors are sometimes detected as piling behaviors.

3.3.3 Performance of Piling Behavior Under Different Camera Settings

Camera setting plays an important role in improving detection accuracy (Yang et al., 2022). The closer the camera is to target objects, the higher the detection accuracy. In this study, the mAP@0.50 was the highest for the YOLOv6m ground camera (50cm height) model because the camera gives a clear view of PB object detection (Table 3.5). However, the average recall and mAP@0.50-095 was highest for the YOLOv6m-ceiling camera model (3m height; Figure 3.7). Since the mAP@0.50 was the highest for the YOLOv6m-ground camera model, this model can be used for ground-level PB detection (Figure 3.8). A camera close to the target object can help detect an object within short parameters, but a ceiling camera can be the best option to find a whole-room overview. In the future, the ceiling camera can help with the room overview and transmit the signal of PB to the ground robot to navigate the PB area so that the robot can go to

that particular place to disturb PB. Thus, both camera heights are required to increase the PB detection model.

Table 3.5: Comparison of piling behavior under different camera settings using the YOLOv6m model.

Camera Settings	Average Recall (%)	mAP@0.50 (%)	mAP@0.75 (%)	mAP@0.50:0.95 (%)
YOLOv6l relu-ceiling	63.8	93.1	54	54.5
YOLOv6l relu-ground	66.8	96.4	56.9	57.6

Ceiling—3 m; ground—0.5 m; mAP—mean average precision.

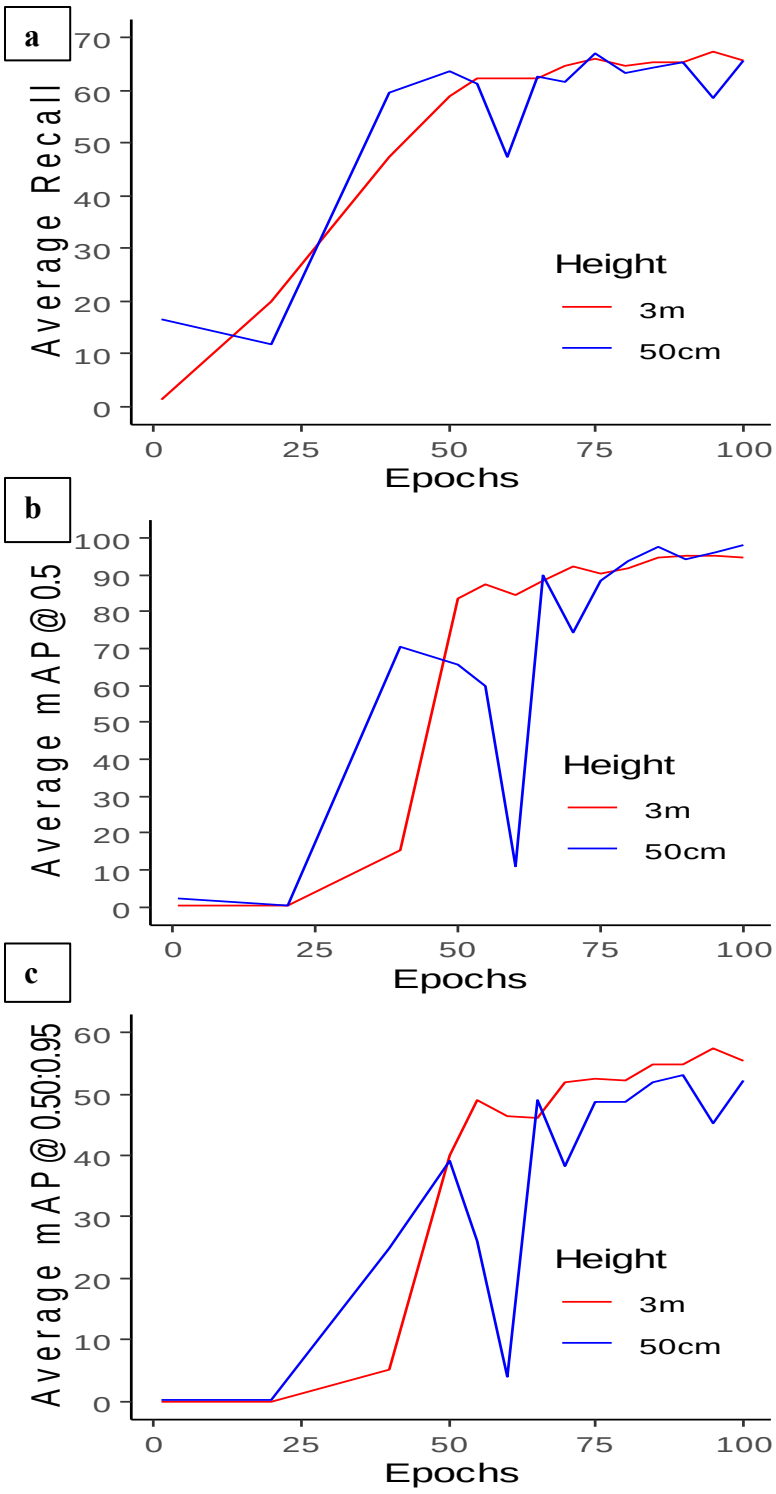

Figure 3.7: Comparison of piling behavior detection results at different camera settings and epochs with a) average recall, b) mAP@0.50, and c) mAP@0.50-0.95.

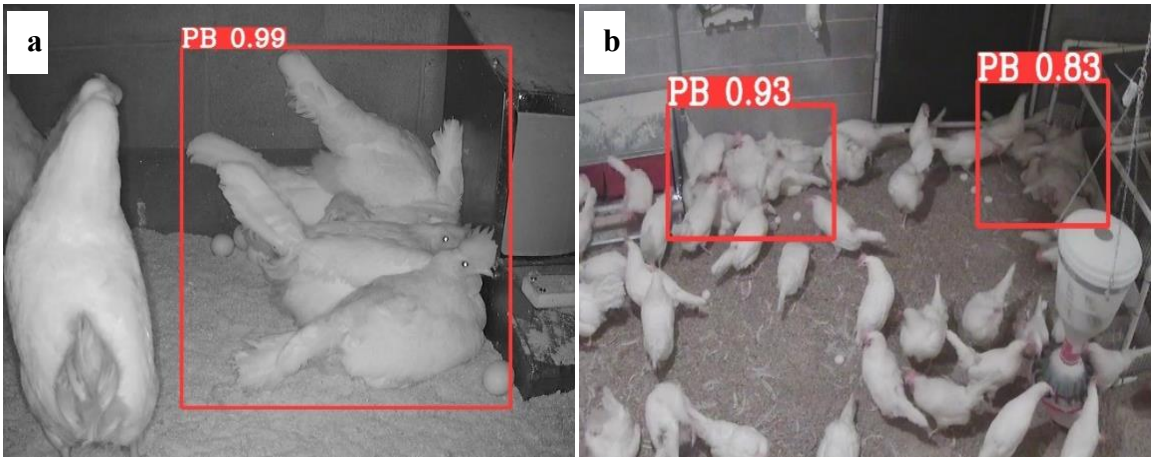

Figure 3.8: Piling behavior detection result based on different camera settings a) height 50cm (ground) and b) height 3m (ceiling).

3.4 CONCLUSION

This study tested different deep-learning models for detecting pilling behavior (PB) in research cage-free rooms. The model development used 6,800 image datasets, including bounding box annotations collected under various CF room conditions, such as photoperiods and camera settings. The results show YOLOv6m-PB model outperforms in detecting PB with higher mAP@0.50 (98.1%), mAP@0.50-0.95 (63.3%), and average recall (70.5%) compared to other models (YOLOv6n, YOLOv6t, YOLOv6s, YOLOv6l, and YOLOv6l relu). Similarly, ceiling and ground cameras are the most important in detecting PB more precisely. However, ground cameras have higher precision for detecting PB. A camera with built-in night vision technology can help increase detection accuracy. The camera placed at the ceiling showed higher precision in detecting PB, possibly due to the night vision camera and the size of the single flock. Overall, the YOLOv6m-PB model resulted in the best detection model for detecting PB. This model will be integrated into the farm's robot or computer system to decrease PB and improve animal welfare and productivity.

3.5 REFERENCES

Altan, O., C. Seremet, and H. Bayraktar. 2013. The effects of early environmental enrichment on performance, fear and physiological responses to acute stress of broiler. Archiv für Geflügelkunde 77:23–28.

Barrett, J., A. Rayner, R. Gill, T. Willings, and A. Bright. 2014. Smothering in UK free-range flocks. Part 1: incidence, location, timing and management. Veterinary Record 175:19–19.

Bist, R. B., L. Chai, X. Yang, S. Subedi, and Y. Guo. 2022. Air Quality in Cage-free Houses during Pullets Production.Page 1 in American Society of Agricultural and Biological Engineers.

Bright, A., and E. Johnson. 2011. Smothering in commercial free-range laying hens: a preliminary investigation. Animal Behaviour 119:203–209.

Campbell, D. L., G. N. Hinch, J. A. Downing, and C. Lee. 2016a. Fear and coping styles of outdoor-preferring, moderate-outdoor and indoor-preferring free-range laying hens. Applied Animal Behaviour Science 185:73–77.

Campbell, D., M. Makagon, J. Swanson, and J. Siegford. 2016b. Litter use by laying hens in a commercial aviary: dust bathing and piling. Poultry Science 95:164–175.

Gebhardt-Henrich, S. G., and A. Stratmann. 2016. What is causing smothering in laying hens? The Veterinary Record 179:250.

Giersberg, M. F., N. Kemper, and B. Spindler. 2019. Pecking and piling: The behaviour of conventional layer hybrids and dual-purpose hens in the nest. Applied Animal Behaviour Science 214:50–56.

Gray, H., R. Davies, A. Bright, A. Rayner, and L. Asher. 2020. Why do hens pile? Hypothesizing the causes and consequences. Frontiers in Veterinary Science 7:616836.

Hartcher, K. M., and B. Jones. 2017. The welfare of layer hens in cage and cage-free housing systems. World's Poultry Science Journal 73:767–782.

He, K., X. Zhang, S. Ren, and J. Sun. 2015. Spatial pyramid pooling in deep convolutional networks for visual recognition. IEEE transactions on pattern analysis and machine intelligence 37:1904–1916.

Herbert, G. T., W. D. Redfearn, E. Brass, H. A. Dalton, R. Gill, D. Brass, C. Smith, A. C. Rayner, and L. Asher. 2021. Extreme crowding in laying hens during a recurrent smothering outbreak. Veterinary Record 188:no-no.

Horvat, M., and G. Gledec. 2022. A comparative study of YOLOv5 models performance for image localization and classification.Pages 349–356 in Faculty of Organization and Informatics Varazdin.

Jocher, G. 2022. YOLOv5 (6.0/6.1) brief summary · Issue #6998 · ultralytics/yolov5. GitHub Available at https://github.com/ultralytics/yolov5/issues/6998 (verified 10 March 2023).

Kang, H., S. Park, J. Jeon, H. Kim, S. Kim, E. Hong, and C. Kim. 2018. Effect of stocking density on laying performance, egg quality and blood parameters of Hy-Line Brown laying hens in an aviary system. European Poultry Science 82.

Lentfer, T. L., S. G. Gebhardt-Henrich, E. K. Fröhlich, and E. von Borell. 2011. Influence of nest site on the behaviour of laying hens. Applied Animal Behaviour Science 135:70–77.

Li, C., L. Li, H. Jiang, K. Weng, Y. Geng, L. Li, Z. Ke, Q. Li, M. Cheng, and W. Nie. 2022. YOLOv6: A single-stage object detection framework for industrial applications. arXiv preprint arXiv:2209.02976.

Liu, S., L. Qi, H. Qin, J. Shi, and J. Jia. 2018. Path aggregation network for instance segmentation. Pages 8759–8768

Marder, J., and Z. Arad. 1989. Panting and acid-base regulation in heat stressed birds. Comparative Biochemistry and Physiology Part A: Physiology 94:395–400.

Meituan. 2023. meituan/YOLOv6. Available at https://github.com/meituan/YOLOv6 (verified 12 March 2023).

Rayner, A., R. Gill, D. Brass, T. Willings, and A. Bright. 2016. Smothering in UK free-range flocks. Part 2: investigating correlations between disease, housing and management practices. Veterinary Record 179:252–252.

Riber, A. B. 2010. Development with age of nest box use and gregarious nesting in laying hens. Applied Animal Behaviour Science 123:24–31.

Rice, M., R. Acharya, A. Fisher, P. Taylor, and P. Hemsworth. 2020. Characterising piling behaviour in Australian free-range commercial laying hens.

Singh, R., K. Cheng, and F. Silversides. 2009. Production performance and egg quality of four strains of laying hens kept in conventional cages and floor pens. Poultry Science 88:256–264.

Subedi, S., R. Bist, X. Yang, and L. Chai. 2023a. Tracking pecking behaviors and damages of cage-free laying hens with machine vision technologies. Computers and Electronics in Agriculture 204:107545.

Subedi, S., R. Bist, X. Yang, and L. Chai. 2023b. Tracking Floor Eggs with Machine Vision in Cage-free Hen Houses. Poultry Science:102637 Available at https://www.sciencedirect.com/science/article/pii/S003257912300161X (verified 10 March 2023).

Villanueva, S., A. Ali, D. Campbell, and J. Siegford. 2017. Nest use and patterns of egg laying and damage by 4 strains of laying hens in an aviary system1. Poultry Science 96:3011–3020.

Weng, K., X. Chu, X. Xu, J. Huang, and X. Wei. 2023. EfficientRep:An Efficient Repvgg-style ConvNets with Hardware-aware Neural Network Design. Available at http://arxiv.org/abs/2302.00386 (verified 10 March 2023).

Winter, J., M. J. Toscano, and A. Stratmann. 2021. Piling behaviour in Swiss layer flocks: Description and related factors. Applied Animal Behaviour Science 236:105272.

Winter, J., M. J. Toscano, and A. Stratmann. 2022. The potential of a light spot, heat area, and novel object to attract laying hens and induce piling behaviour. Animal 16:100567.

Yang, X., L. Chai, R. B. Bist, S. Subedi, and Z. Wu. 2022. A Deep Learning Model for Detecting Cage-Free Hens on the Litter Floor. Animals 12:1983.

CHAPTER 4

AUTOMATIC DETECTION OF DEAD HENS WITH DEEP LEARNING METHODS[3]

[3] Bist, R. B., Subedi, S., Yang, X., and Chai, L. 2023. Automatic Detection of Cage-Free Dead Hens with Deep Learning Methods. AgriEngineering 5 (2), 1020-1038. https://doi.org/10.3390/agriengineering5020064. Reprinted here with permission of the publisher.

ABSTRACT

Poultry farming plays a significant role in ensuring food security and economic growth in many countries, while various factors such as feeding management practices, environmental conditions, and infectious and non-infectious diseases can result in poultry mortality (dead birds). Regularly monitoring flocks with veterinary assistance at the first sign of illness or death is critical in ensuring the health and well-being of poultry and the success of poultry farming operations. However, existing monitoring is based on farm workers' inspection, which is time-consuming. Therefore, automatic early mortality detection (MD) is essential for preventing the spread of infectious diseases in poultry. This study aimed to develop, evaluate, and test the performance of different You Only Look Once (YOLO) models (YOLOv5-MD and YOLOv6-MD) in detecting mortality in poultry under various cage-free (CF) room settings, including camera height, litter condition, and feather coverage. The results show that the YOLOv5s-MD model was highly effective, with a mean average precision (mAP@0.50) of 99.5%, high frame per second (FPS) of 55.6, low graphics processing units (GPU) usage of 1.04GB, and fast processing time of 0.4 hours. Moreover, this study also evaluated the models' performance under different CF room settings, including different levels of feather coverage, litter coverage, and camera height. The YOLOv5s-MD model with 0% feathered covering achieved the best overall performance in object detection, with the highest mAP@0.50 score of 99.4% and a high precision rate of 98.4%. However, 80% litter covering resulted in a higher MD. In addition, the model achieved 100% precision and recall in detecting hen's mortality at the height of 0.5 m but struggled at higher heights (e.g., 2 m). The findings of this study indicate that YOLOv5s-MD can detect mortality in poultry more accurately than other models, and its performance can be optimized by adjusting various CF room settings. Therefore, the developed model can help

farmers to take immediate action to isolate affected birds, implement disease prevention measures, and seek veterinary assistance when necessary, reducing the impact of poultry mortality on the industry.

Keywords: Mortality, Laying hen, Cage-free housing, YOLO model, Machine learning.

4.1 INTRODUCTION

Poultry mortality refers to the death of domestic birds within a flock or population, which might occur due to various reasons which include diseases (infectious and non-infectious) (Brochu et al., 2019; Cadmus et al., 2019), management practices (Dessie and Ogle, 2001; Cadmus et al., 2019; Yerpes et al., 2020), and environmental factors (Gray et al., 2020; Yerpes et al., 2020; Ekiri et al., 2021). Among these various mortality-causing factors, the main cause of mortality is infectious diseases. Common infectious diseases that can cause high mortality rates are avian influenza, Newcastle disease, infectious bronchitis, infectious bursal disease, and coccidiosis (Ekiri et al., 2021). Infectious diseases must be diagnosed early to control disease spread across a flock and provide treatment to decrease substantial mortality rates. On the other hand, non-infectious factors like overcrowding (Gray et al., 2020), neoplasia (Brochu et al., 2019), extreme temperatures (Edwan et al., 2020), poor nutrition (Brochu et al., 2019), and poor ventilation (Edwan et al., 2020) might also contribute to mortality inside poultry housing. For example, heat stress can cause chickens to die in large numbers, especially during hot weather conditions (Saeed et al., 2019). Similarly, overcrowding can lead to stress, disease transmission, and poor air quality, resulting in high mortality rates (Gray et al., 2020). Preventing mortality requires a comprehensive approach that involves good management practices, adequate nutrition, and disease prevention and control. For example, farmers should ensure that birds have adequate

food, water, and clean house in a well-ventilated environment. It is also important to implement biosecurity measures, such as limiting access to the flock to prevent the introduction of infectious agents. Therefore, understanding the factors contributing to mortality and implementing good management practices can help reduce mortality rates and improve health and welfare.

In order to stop the spread of infectious diseases and reduce the influence of other factors that can cause mortality, early mortality detection (MD) in poultry is crucial. According to Wibisono et al. (2020), infectious diseases are the primary causes of bird mortality (Wibisono et al., 2020). Therefore, early detection of sick or dying birds can help farmers promptly isolate affected birds, implement preventive disease strategies, and seek veterinary assistance when necessary. Additionally, early MD allows farmers to minimize further losses, such as culling remaining birds to prevent the spread of disease or other risk factors. Therefore, regularly monitoring flocks and seeking veterinary assistance at the first sign of illness or death is critical in ensuring the health and well-being of poultry and the success of poultry farming operations. That is why a good MD model is required for early MD and removing dead birds from the farm.

Automatic identification of dead birds in commercial poultry production can save time and labor while providing a crucial function for autonomous mortality removal systems, which eliminates the need for manual identification and helps streamline the identification process. High-resolution thermography has been investigated as a potential method for early MD in poultry production (Blas et al., 2013). Further, MD in broilers involved extracting feathers and utilizing a pairwise approach to capturing thermal and visual spectrum images (Muvva et al.,

2018). Similarly, Zhu et al. (2009) developed a detection model based on a Support Vector Machine (SVM) and achieved 95% accuracy in identifying dead birds (Zhu et al., 2009). However, Sentas et al. (2020) found that the YOLO model performed better than the SVM model in balanced object datasets (Sentas et al., 2020). This study highlights the importance of using image analysis techniques to implement an automated system that can detect mortality early in the industry using the YOLO model.

YOLO models outperform in detecting small objects like laying hens (Yang et al., 2022; Subedi et al., 2023a) and eggs (Subedi et al., 2023b). For example, the individual hen detection with their distribution was well detected using YOLOv5 models (Yang et al., 2022). Similarly, Subedi et al. (2023) studied problematic behaviors like pecking in hens with higher accuracy (Subedi et al., 2023a). In this research, the YOLOv5 model was compared with the latest YOLOv6. The objectives of this study were to a) develop and test the performance of different deep learning models and b) evaluate the optimal YOLO model's (e.g., the YOLOv5 and YOLOv6 models) performance under different CF room settings (e.g., camera height, litter condition, and feather coverage).

4.2 MATERIALS AND METHODS

4.2.1. Experimental Design

This experiment follows the same housing and bird management practices as described in Chapter 2 of section 2.2.1.

4.2.2. Image Data Acquisition and Pre-processing

The primary data acquisition tool used in this study to record the mortality of hens was a night-vision network PRO-1080MSB camera (Swann Communications USA Inc.) with six cameras installed in each room, mounted at approximately 3 meters above the litter floor. Additionally, two cameras were placed at 0.5 meters and 1 meter above the ground floor. The video recording was performed every day for 24 hours using a digital video recorder (DVR-4580) from 50-60 weeks of age (WOA), while mortality data was collected when birds were found dead. Eight hens were found dead during that period and recorded video of those hens. The video files were saved in .avi format, with a 1920 × 1080 pixels resolution and a sampling rate of 15 frames per second (FPS). This data acquisition method provided a comprehensive and high-quality dataset for analyzing the behavior of hens, which was instrumental in drawing meaningful conclusions from the study.

The CF rooms consists of litter and feathers on the floor (Bist and Chai, 2022; Bist et al., 2022, 2023), which might affect the MD of hens. In addition, dustbathing or other hen activities might cover the dead bird fully or partially, so this research considers every scenario. To accurately represent the conditions in CF rooms, this study employed video recording to capture the dead hens in different environmental conditions with varying degrees of litter and feather coverage. This research selected three litter and feather coverage levels - 0% (no litter or feather coverage), 50% (50% of hens body covered with litters or feathers), and 80% (80% of hens body covered with litters or feathers) - as detailed in Table 4.1. The decision to not exceed 80% was motivated by the potential discrepancies between actual hen mortality and the appearance of hen images beyond that level of coverage. The resulting dataset accurately depicts the different litter

and feather coverings levels in CF rooms, enabling the deep learning model to perform effective MD detection.

Table 4.1: Experimental settings for evaluating the optimal YOLO mortality detection models.

Settings	**Parameters**	**Levels**
Camera	Height	0.5 m, 1m, 3m
Feather	Feather covering	0%, 50%, 80%
Litter	Litter covering	0%, 50%, 80%

The video data collected in this study were processed by converting them into individual images in .jpg format using the Free Video to JPG Converter App (version 5.0). The images were then labeled in YOLO format with the assistance of the image labeler website (Makesense.AI). This labeling process was essential in ensuring the images were correctly identified and classified for use in the deep learning model. Furthermore, the resulting labeled dataset was essential in developing and training the model for effective and accurate MD detection (Figure 4.1). The labeled image dataset consisting of 9000 images was divided into three sets for training, validation, and testing purposes, with approximately 70%, 20%, and 10% of the total images allocated to each set, respectively (Table 4.2). The MD_{Model} image dataset was used to compare YOLOv5s, YOLOv5m, YOLOv5x, YOLOv6s, YOLOv6m, and YOLOv6l-relu models.

Table 4.2: Labeled image datasets used for mortality detection model under various settings.

Class	Original dataset	Train (70 %)	Validation (20 %)	Test (10 %)
MD_{Litter}	3000*	2100	600	300
$MD_{Feather}$	3000*	2100	600	300
MD_{Height}	3000*	2100	600	300
MD_{Model}	2200	1540	440	220

*1000 image datasets for each level; MD- mortality detection.

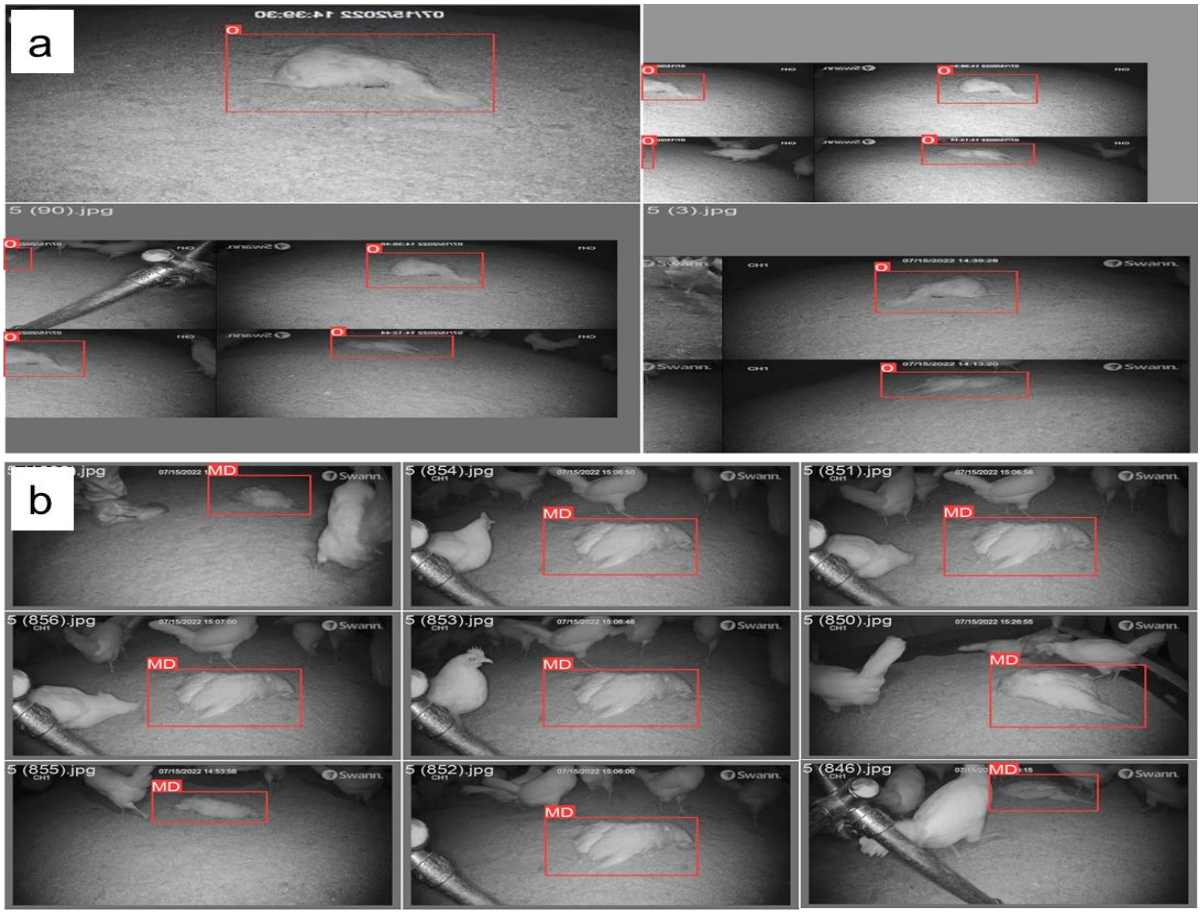

Figure 4.1: Pre-processing of mortality image data sets based on (a) training batches and (b) validation batch labels used to detect mortality hens in cage-free rooms.

"0" represents the mortality label in the image.

4.2.3. YOLO Architecture

Object detection has been an active area of research in computer vision. Among the popular algorithms in this domain, YOLO (You Only Look Once) algorithms have successfully detected objects like hens with higher accuracy and in real-time (Yang et al., 2022; Subedi et al., 2023a; b). YOLOv5 and YOLOv6 are two variants of the YOLO algorithm, each with its unique network architecture. In this study, best YOLOv5-MD (YOLOv5s-MD, YOLOv5m-MD, & YOLOv5x-MD) and YOLOv6-MD (YOLOv6s-MD, YOLOv6m-MD, & YOLOv6l-relu-MD) models were used to compare. The architecture of both the YOLO-MD models was mainly classified into three major parts: backbone, neck, and head. These YOLOv5-MD and YOLOv6-MD models differ in parameters within types. The detailed architecture of YOLOv5-MD and YOLOv6-MD used for this research is in Figure 4.2 and Figure 4.3, respectively.

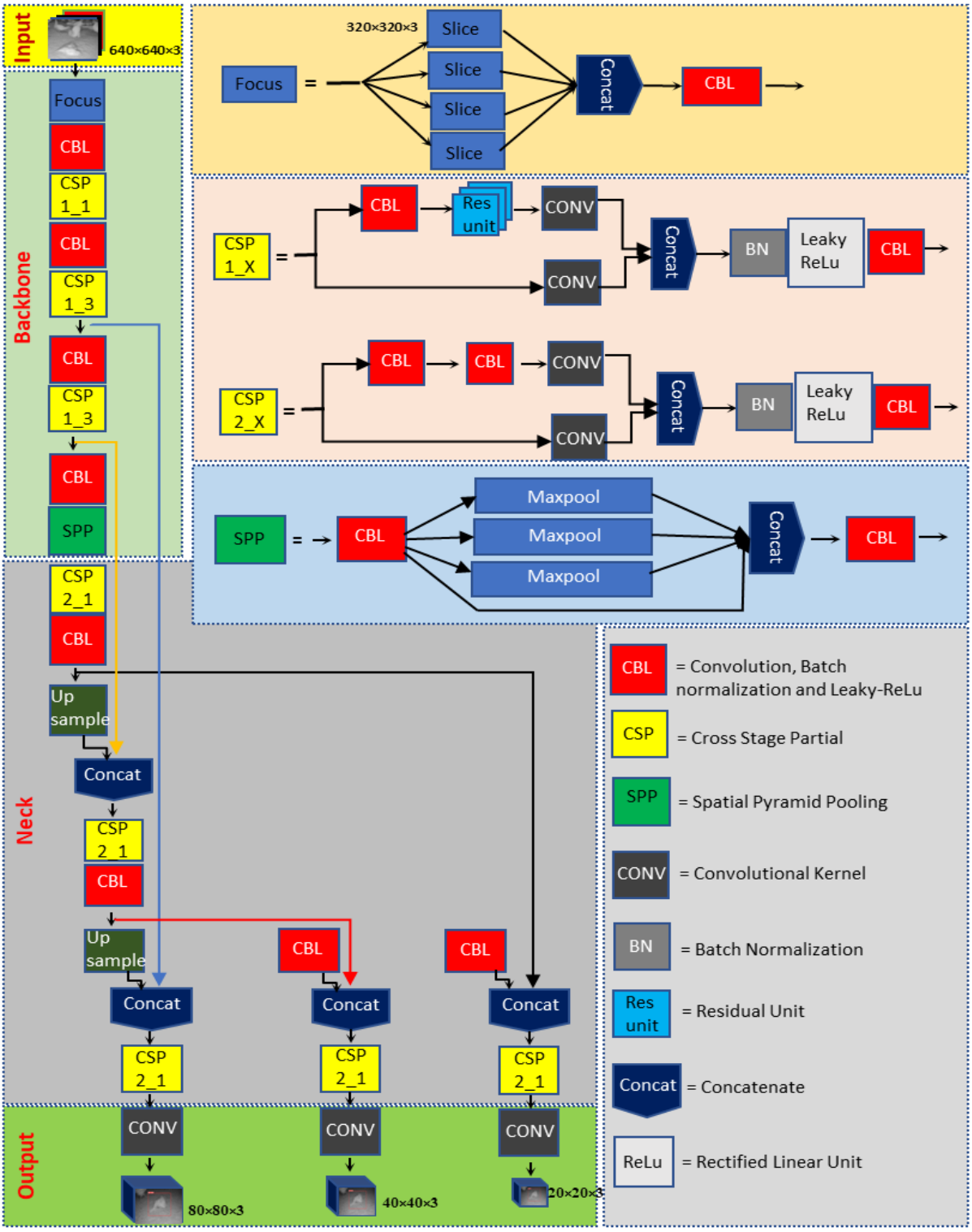

Figure 4.2: YOLOv5-MD model used in mortality detection.

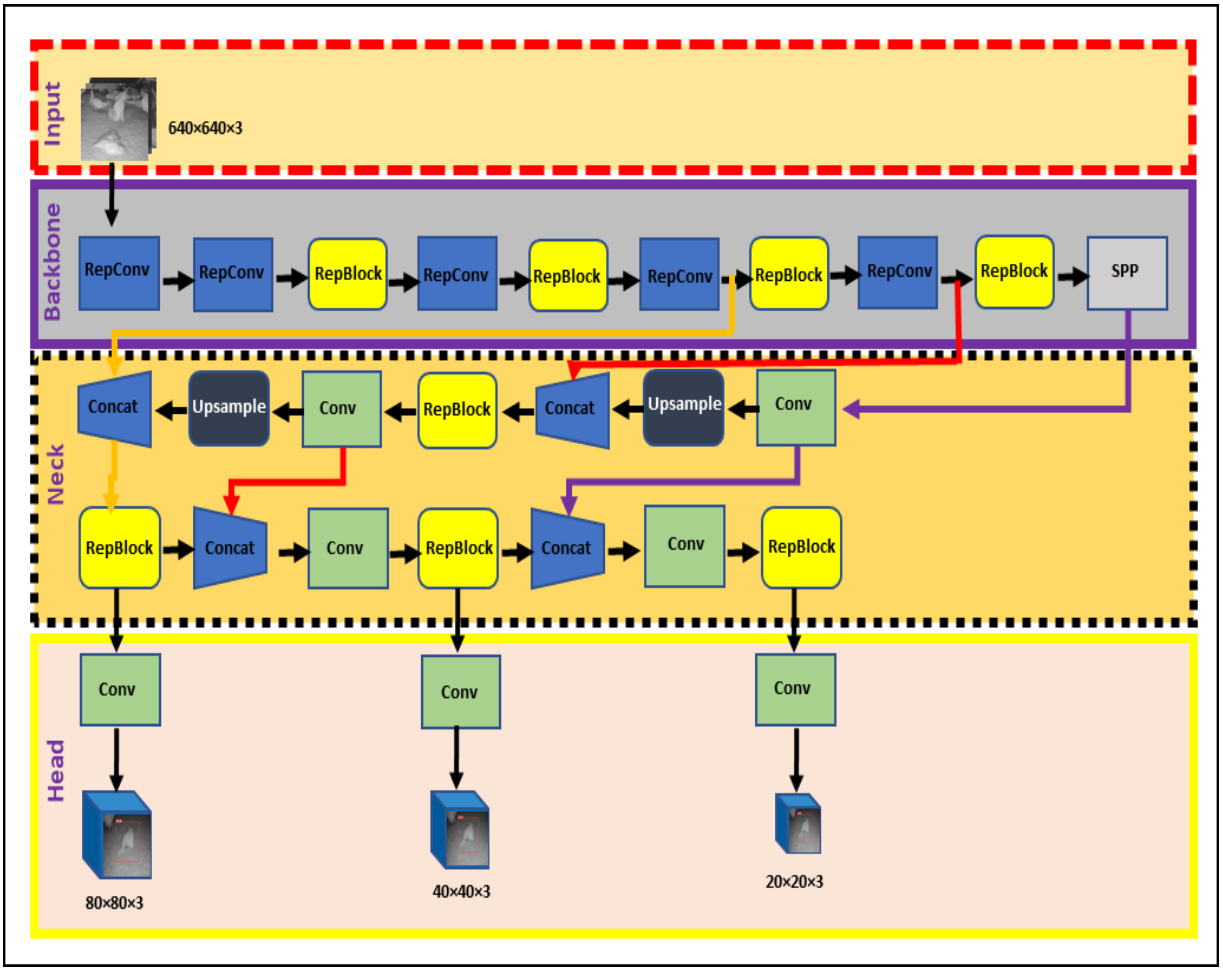

Figure 4.3: YOLOv6-MD model used in mortality detection.

4.2.3.1 Backbone

The main difference between YOLOv5 and YOLOv6 is the backbone network architecture. YOLOv5 uses a variant of the EfficientNet architecture, while YOLOv6 uses a pre-trained CNN with an EfficientRep backbone or CSP-Backbone for MD. EfficientNet is a family of neural networks designed for efficient and effective model scaling (Tan and Le, 2019). YOLOv5's backbone uses convolutional layers at different scales to perform feature extraction from labeled MD image datasets with the help of Spatial pyramid pooling (SPP), which helps it achieve good performance on object detection tasks while being lightweight and efficient (Wang

et al., 2020). On the other hand, YOLOv6's backbone network is typically a pre-trained CNN with SPP and EfficientRep architecture (He et al., 2015). SPP helps max-pooling layers reduce the feature map's size while maintaining the most important features for object detection. EfficientRep backbone is designed to both effectively use the computational resources of hardware such as GPUs and possess robust feature representation abilities compared to the CSP-Backbone utilized by YOLOv5 (Li et al., 2022). In summary, YOLOv5-MD and YOLOv6-MD use different backbone network architectures for feature extraction, affecting their efficiency and performance on object detection tasks.

4.2.3.2 Neck

The neck component is essential in YOLOv5 and YOLOv6 for connecting the backbone to the object detection head. Both YOLO-MD versions employ convolutional layers in their necks, but their specific architectures differ. YOLOv5's neck utilizes a Feature Pyramid Network (FPN) that includes a top-down and bottom-up path, which captures multi-scale objects with high accuracy (Lin et al., 2019). In contrast, YOLOv6 features a more efficient neck design known as the Rep-PAN Neck (Liu et al., 2018) that utilizes convolutional, pooling, and up-sampling layers to manipulate the backbone network's features to the desired scale and resolution for the heads. This Rep-PAN Neck design is based on hardware-aware neural network architecture concepts that balance accuracy and speed while optimizing hardware resources (Weng et al., 2023). Therefore, YOLOv5-MD and YOLOv6-MD differ in their neck designs, with YOLOv5-MD using an FPN and YOLOv6-MD utilizing a more efficient Rep-PAN Neck design.

4.2.3.3 Head

The head components in YOLOv5-MD and YOLOv6-MD are responsible for the final stage of object detection by generating predictions from the extracted features. In YOLOv5-MD, the head comprises fully connected layers and a convolutional layer that predicts the detected mortality objects' bounding boxes and class probabilities. In addition, it has three output layers: a detection layer that predicts object class probabilities, a localization layer that forecasts bounding box coordinates, and an anchoring layer that defines the prior box shapes and scales (Jocher, 2022). The YOLOv5-MD head is designed to be resource-efficient, enabling real-time object detection across a range of devices. On the other hand, YOLOv6's Decoupled Head design focuses on improving hardware utilization while maintaining high detection accuracy (Li et al., 2022). Overall, YOLOv5-MD and YOLOv6-MD have different head structures, but they aim to generate accurate and efficient object detection predictions.

4.2.4 Performance Metrics

4.2.4.1 Precision

Precision measures how many MDs the system made were correct and calculated by dividing the true positives (TP) and the sum of TP & false positives (FP).

$$\boldsymbol{Precision = \frac{TP}{TP + FP}\ or\ \frac{true\ mortality\ detection}{all\ detected\ bounding\ boxes}} \qquad (\boldsymbol{i})$$

Where TP, FP, FN, and TN represent true positive (mortality is present in the image and the model predicts it correctly), false positive (mortality is not in the image, and the model detects it), and false negative (mortality is present in the image but unable to detect it), and true negative (mortality is not present in the image and not detected by the model). In detail, visualization for evaluation metrics is mentioned in Figure 4.4.

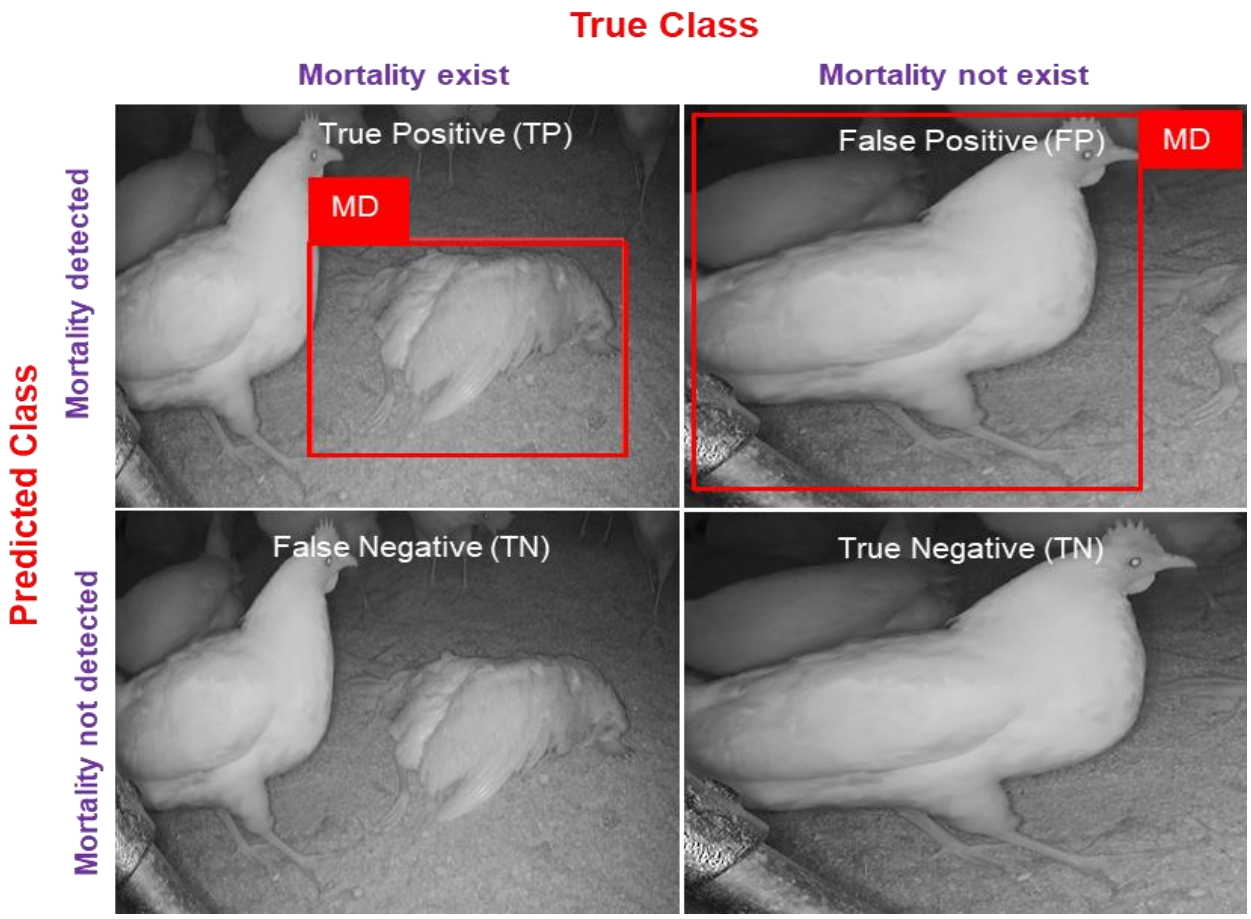

Figure 4.4: Confusion matrix for evaluating mortality detection.

4.2.4.2 Recall

Recall measures how many of the actual mortality hens in an image were correctly identified by the system. It is calculated as the ratio of TP to the sum of TP and false negatives (FN):

$$\boldsymbol{Recall = \frac{TP}{TP + FN}\ or\ \frac{true\ mortality\ detection}{all\ ground\ truth\ bounding\ boxes}} \qquad (ii)$$

4.2.4.3 Mean average precision

Mean Average Precision (mAP) is a widely used metric in object detection tasks that measures the system's overall accuracy across multiple object classes (Padilla et al., 2020). It is calculated based on the precision and recall values at a certain threshold or over a range of thresholds. The most common mAP calculation is based on the area under the precision-recall curve and is calculated as follows:

$$\boldsymbol{mAP} = \frac{\sum_{i-1}^{C} \boldsymbol{APi}}{\boldsymbol{C}} \qquad (\boldsymbol{iii})$$

where, APi is the average precision of the ith category and C represents the total number of categories of MD.

4.2.4.4 F1-score

The F1 score is a harmonic mean of precision and recall and is a widely used metric in machine learning for evaluating the performance of binary classification models (Chicco and Jurman, 2020). It combines precision and recall metrics into a single value that indicates the balance between them. The formula for the F1 score is as follows:

$$\boldsymbol{F1\ Score} = \frac{\boldsymbol{2 \times Recall \times Precision}}{\boldsymbol{Recall + Precision}} \qquad (\boldsymbol{iv})$$

In other words, the F1 score gives equal importance to precision and recall, with a higher score indicating better performance. For example, a perfect F1 score of 1.0 indicates that the model has both perfect precision and recall, while a score of 0 indicates that the model has either low precision or recall or both.

4.2.4.5 Loss function

The YOLO-MD object detection algorithm uses a custom loss function called the "YOLO Loss" to train the model. The YOLO-MD Loss combines several different loss terms that penalize the model for incorrect predictions and encourage it to make accurate predictions (Roy and Bhaduri, 2022). For example, the YOLO-MD Loss consists of the following loss terms:

Objectness loss: This loss term encourages the model to correctly predict whether a mortality object is present in a grid cell. Objectness loss (λobj) is computed between the predicted and ground truth objectness scores by the binary cross-entropy loss (Tesema and Bourennane, 2020).

Classification loss: This loss term encourages the model to correctly classify the detected mortality objects into their respective classes. Classification loss (λcls) is computed as the cross-entropy loss between the predicted class probabilities and the ground truth class labels (Tesema and Bourennane, 2020).

Regression loss: This loss term penalizes the model for incorrect predictions of the bounding box coordinates and dimensions (Tesema and Bourennane, 2020; Figure 4.5). Regression loss (λreg) is computed as the sum of the smooth L1 loss between the predicted and ground truth x and y coordinates, the smooth L1 loss between the predicted and ground truth width and height, and the focal loss between the predicted and ground truth confidence scores (Lin et al., 2019). The YOLO-MD Loss is computed as the weighted sum of the mortality objectness loss, classification loss, and regression loss. In general, the importance of each term in the loss function is determined by the user, who sets the corresponding weights accordingly. The YOLO Loss is minimized during the training process using backpropagation and gradient descent, with the goal of reducing the overall prediction error of the model (Amrani et al., 2022).

$$\boldsymbol{Loss = \lambda_1 L_{cls} + \lambda_2 L_{obj} + \lambda_3 L_{loc}} \qquad (v)$$

$$\boldsymbol{Smooth\ L1\ (x) = 0.5 * x^2\ ,\quad if\ |x| < 1} \qquad (vi)$$

$$\boldsymbol{|x| - 0.5,\qquad otherwise} \qquad (vii)$$

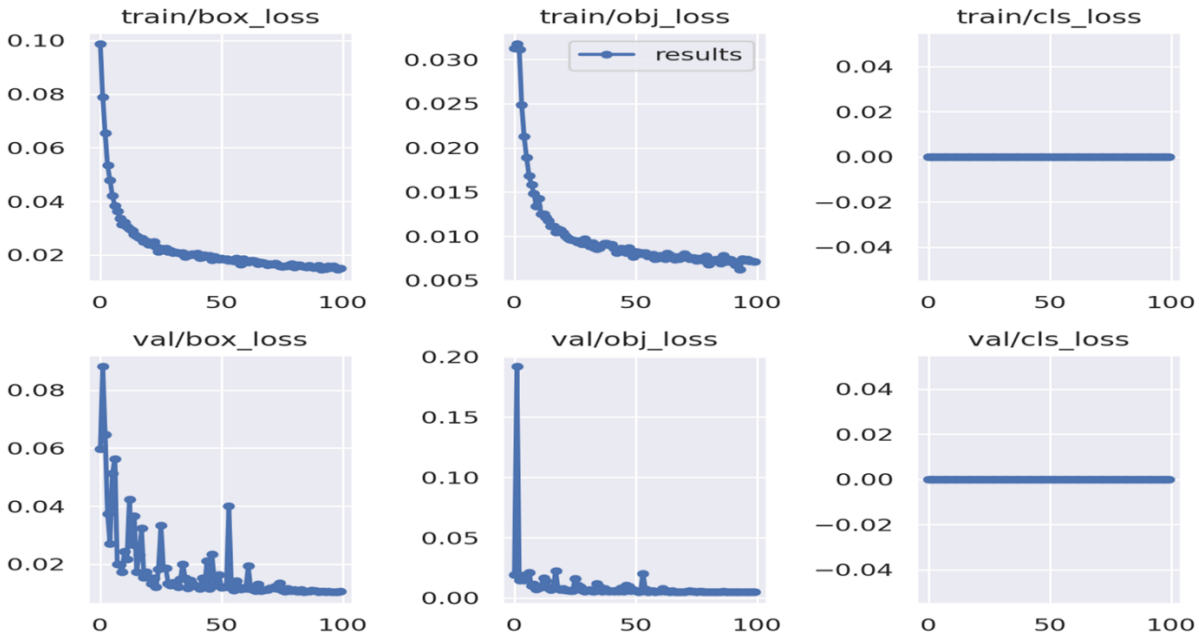

Figure 4.5: Loss function results sample for YOLO-MD model.

Where train, val, box, obj, and cls represent the training, validation, bounding box, bounding object, and class used to detect MD.

4.2.5 Computational Parameters

A high-performance computational configuration was utilized to detect mortality. The study employed various configurations on the Oracle cloud to train, validate, and test the image datasets. It has been observed that a higher number of computational parameters can enhance the

model's speed and detection accuracy. The system configuration comprises a 64-core OCPU for CPU processing and four NVIDIA® A10 GPUs, each with 24GB of memory, for GPU acceleration. The operating system employed is Ubuntu 22.10 (Kinetic Kudu), and the accelerated environment is NVIDIA CUDA. The system has ample storage capacity with 1024GB of memory and two 7.68 TB NVMe SSD drives. Torch 1.7.0, Torch-vision 0.8.1, OpenCV-python 4.1.1, and NumPy 1.18.5 were the libraries utilized in the system. Together, these components create a high-performance system capable of efficiently running deep learning models for various applications, including MD detection. In addition, The YOLO model underwent 100 epochs of training with a batch size of 16.

4.3 RESULTS AND DISCUSSIONS

4.3.1 Model Comparison

This study proposes the YOLO-MD model, which can effectively detect dead hens in the CF rooms. Table 4.3 shows the performance and results obtained from validating the proposed models' effectiveness in this experiment. When comparing different object detection models, it is important to consider various metrics such as recall, FPS, mAP, GPU usage, and time is taken (Subedi et al., 2023a). For example, YOLOv5x-MD achieved the highest recall rate of 100%, indicating that it can recall target objects in an image, while YOLOv5s-MD had a recall rate of 98.4%. On the other hand, frames per second (FPS) measures the number of frames processed by the model per second, indicating the speed at which the model can operate. YOLOv5s-MD had the highest FPS (i.e.,55.6) among the models we developed, which means faster image processing than other models, while YOLOv5x-MD had the lowest FPS (i.e.,29.6), indicating slower processing. Regarding accuracy, mAP is a common metric that measures the model's

ability to detect objects of different sizes and types (Yang et al., 2022). YOLOv5-MD models had higher mAP scores of 99.5% than YOLOv6 models at a confidence threshold of 0.5. However, at higher confidence thresholds, the mAP scores were decreased in YOLOv6 models, indicating that the models struggled to detect smaller or more complex objects. Lastly, GPU usage and time taken are important factors when selecting a model (Subedi et al., 2023a). YOLOv5x-MD required the most GPU usage of 4.95GB, while YOLOv5s-MD required the least at 1.04GB. YOLOv5s-MD also processed data in the least amount of time at 0.4 hours, while YOLOv6l_relu-MD took the longest at 1.2 hours. Thus, when selecting a model with higher performance, speed, and efficiency is crucial, and YOLOv5s-MD is the preferred option in this study. This study's findings might help researchers and producers select the best mortality detection model or choose this model for their specific object detection. In addition, they can select based on their priorities for detection performance metrics like speed, GPU usage, and efficiency.

Table 4.3: Performance metrics of different YOLO Models used for mortality detection using 2200 images in each of the six models.

Data summary	**YOLOv5 s-MD**	**YOLOv5 m-MD**	**YOLOv5 x-MD**	**YOLOv6 s-MD**	**YOLOv6 m-MD**	**YOLOv6l_ relu-MD**
Recall (%)	98.4	99.6	100.0	81.6	82.4	82.8
mAP@0.50 (%)	99.5	99.5	99.5	98.9	99.0	98.8
mAP@0.50:0.95 (%)	82.3	81.9	81.1	77.1	78.2	78.3
GPU usage (GB)	1.04	1.83	4.95	-	-	-
FPS	55.6	42.9	29.6	51.3	43.8	40.9
Time taken (hrs)	0.4	0.5	1.0	0.5	0.8	1.2

Where, GPU-graphics processing unit; GB- Gigabyte; mAP- mean average precision; FPS-frame per second; MD-mortality detection; hrs- hours.

4.3.2 Environmental Condition

The CF rooms mainly consist of litter and broken feathers from the birds (Bist and Chai, 2022; Bist et al., 2022). However, in the presence of such litter, the dead bodies of the birds can get covered or buried, making it difficult to detect them accurately. This situation can lead to the decay of hens, resulting in unpleasant odors and various other issues. Therefore, early MD is crucial to prevent such problems, especially if a bird dies due to a severe issue. Therefore, this study considers the factors of litter and feathers in detecting dead birds with deep learning models in research CF rooms.

4.3.2.1 Feathers covering

Table 4.4 summarizes the performance of YOLOv5s-MD with different feather percentages (e.g., 0%, 50%, and 80%). Precision remains relatively consistent across all three models, with recall being the highest at 100% for the 50% feather covering. The mAP and F1-score also show a slight decrease with increased feathering percentage. The mAP@0.50 score is highest for the 0% feather covering at 99.4% and decreases to 98.0% for the 80% feathered covering (Figure 4.6a). The mAP@0.50:0.95 score shows a significant decrease in performance with increased feathering, with the 0% feather covering achieving a score of 65.5%, compared to 41.6% for the 80% feather covering (Figure 4.6b). Hence, 0% feather covering resulted in higher MD rates (Figure 4.7). The mAP scores always increased with increasing epochs from 0 to 100 with batch size 16. However, there is a trade-off between feathering and overall mAP performance, with higher feathering resulting in decreased performance. Therefore, early mortality detection or proper cleaning and maintenance of CF rooms is required to increase detection.

Table 4.4: Performance of YOLOv5s model on mortality detection at different feather conditions.

Data summary	**YOLOv5s-MD 0% feather**	**YOLOv5s-MD 50% feather**	**YOLOv5s-MD 80% feather**
Precision (%)	98.4	97.4	97.5
Recall (%)	97.5	100.0	96.6
mAP@0.50 (%)	99.4	97.7	98.0
mAP@0.50:0.95 (%)	65.5	47.7	41.6
F1-score	98.0	98.0	95.0

Where, mAP- mean average precision; FPS-frame per second; MD- mortality detection; 0% feather- no feather coverage; 50% feather- feather covered up to half of the whole body of hen; 80% feather- feather covered up to 80% of the whole body of the hen.

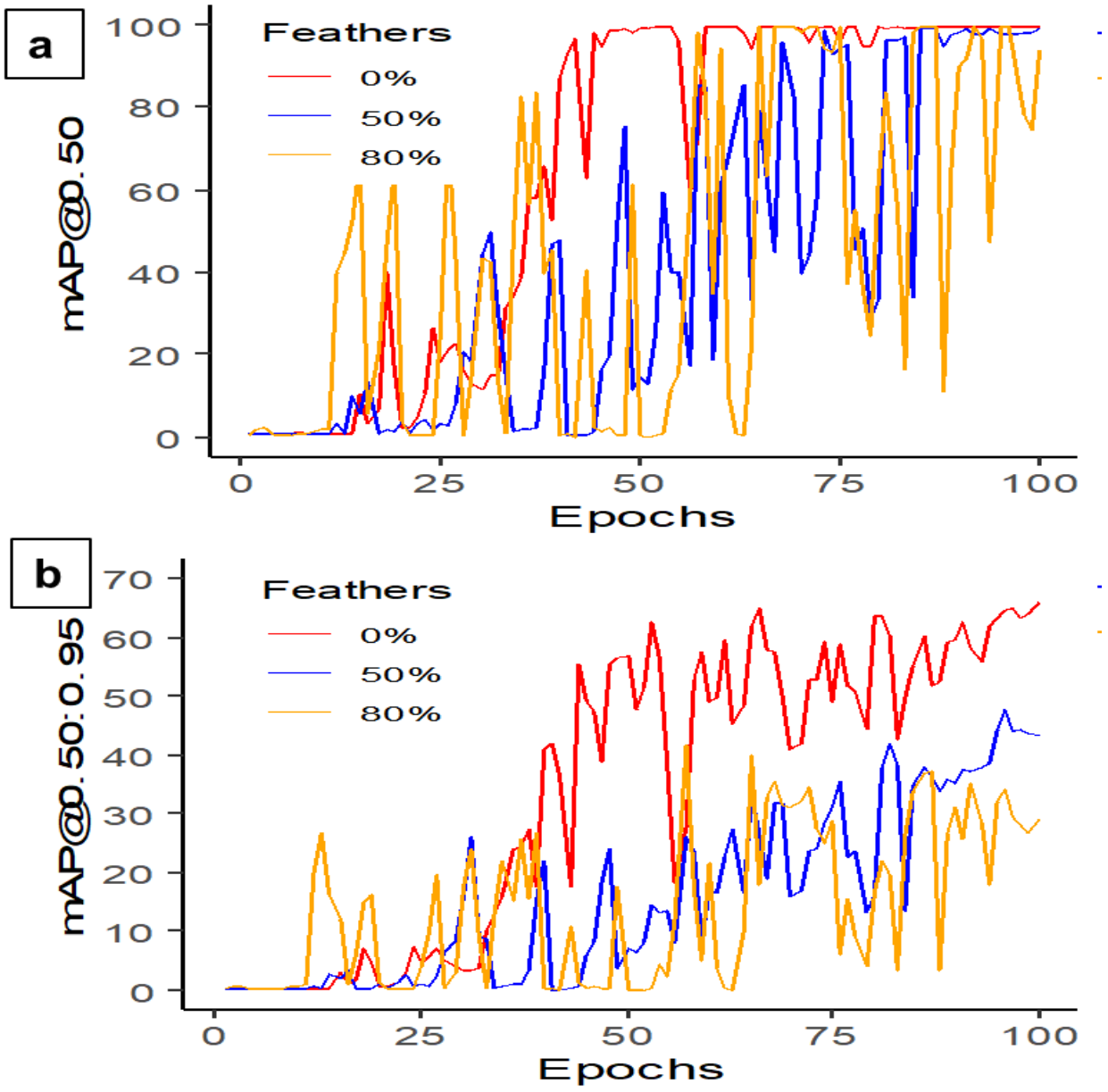

Figure 4.6: Mean average precision performance a) mAP@0.50 and b) mAP@0.50:0.95 in detecting dead hens at different percentages of feather coverages using the YOLOv5s-MD model at 100 epochs and 16 batch sizes.

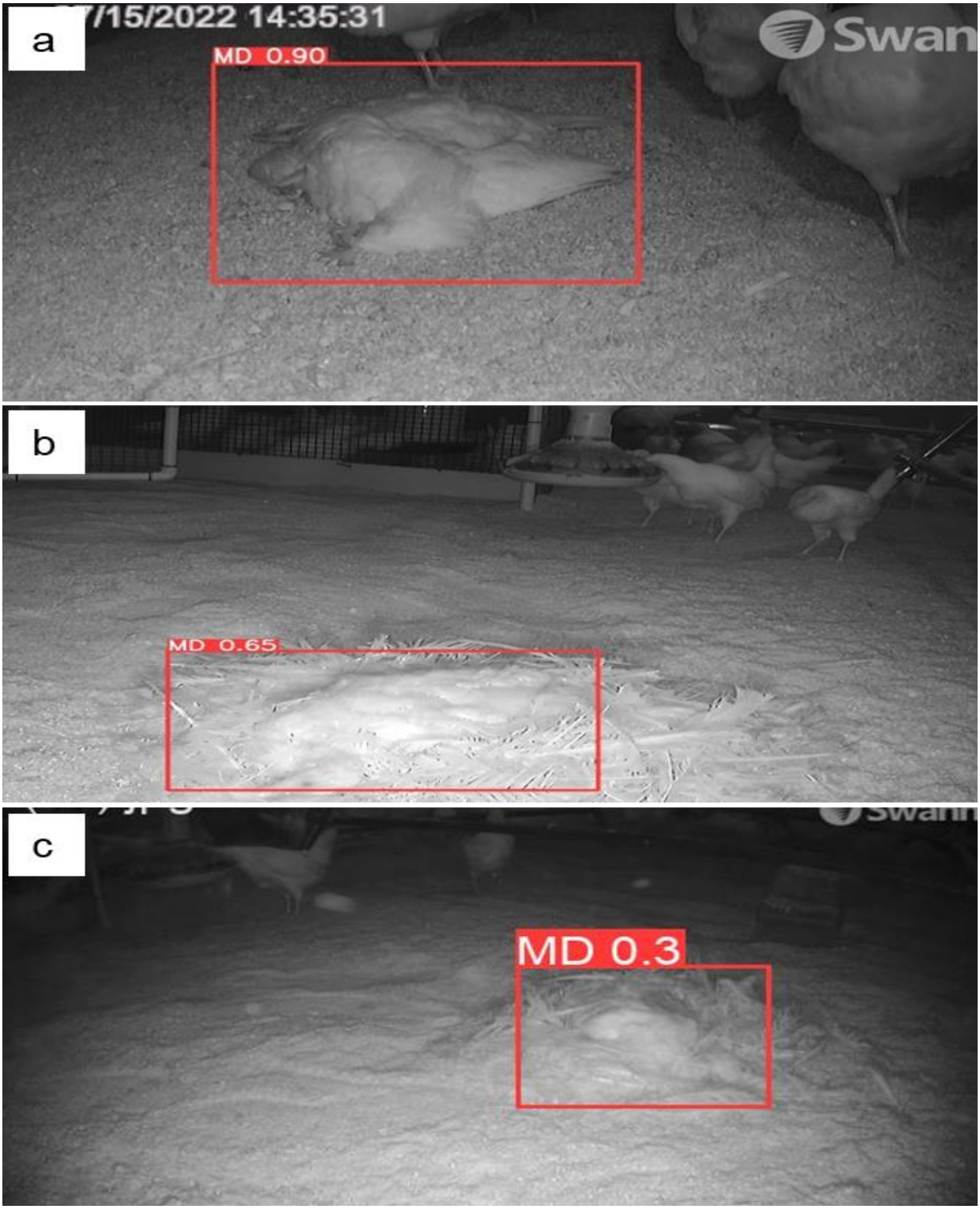

Figure 4.7: Variation of mortality detection with feather coverage: a) 0% or no feathers, b) 50% feathers, and c) 80% feathers in cage-free rooms using the YOLOv5s model in test images.

4.3.2.2 Litter

In this study, the performance of YOLOv5s-MD was evaluated on litter detection with three different levels of litter coverage in the image: 0%, 50%, and 80% (Table 4.5). The YOLOv5s-MD, with 80% litter coverage, achieved the highest precision rate of 99.9%, indicating that it can accurately detect dead hens on the litter floor from the image analysis. The model with 50% litter coverage had the lowest precision rate of 97.1%, suggesting that it struggles to accurately detect dead hens when clutter is in the image. All models achieved high recall rates of 97.5% to 100%, indicating that they can accurately recall target objects in the image. YOLOv5s-MD, with 80% litter coverage, achieved the highest mAP@0.50 (Figure 4.8a) and F1-score of 99.5 and 100%, respectively, indicating good overall detection performance. Similarly, the mAP@0.50:0.95 scores were higher for models with higher litter coverage (80%, Figure 4.8b), indicating that the model may struggle to detect smaller or more complex objects because of various behaviors like resting, sitting, and dustbathing, which might seem similar at certain points. The 80% litter coverage performs better because small hen's body parts are visible. The model for the hens with no or less litter coverage can assume the hens performing activities like dustbathing, sitting, or sleeping, which might affect the model's overall performance. Overall, the results suggest that YOLOv5s-MD can effectively detect litter-covered dead birds in images, but the level of litter coverage in the image may impact its performance (Figure 4.9).

Table 4.5: YOLOv5s model performance on mortality detection across various litter accumulation conditions.

Data summary	**YOLOv5s-MD 0% litter**	**YOLOv5s-MD 50% litter**	**YOLOv5s-MD 80% litter**
Precision (%)	98.4	97.1	99.9
Recall (%)	97.5	100.0	100.0
mAP@0.50 (%)	99.4	98.6	99.5
mAP@0.50:0.95 (%)	65.5	40.8	65.6
F1-score	98.0	99.0	100.0

Where, mAP- mean average precision; FPS-frame per second; MD- mortality detection; 0% litter- no litter coverage; 50% litter- litter covered up to half of the whole body of hen; 80% litter- litter covered up to 80% of the whole body of the hen.

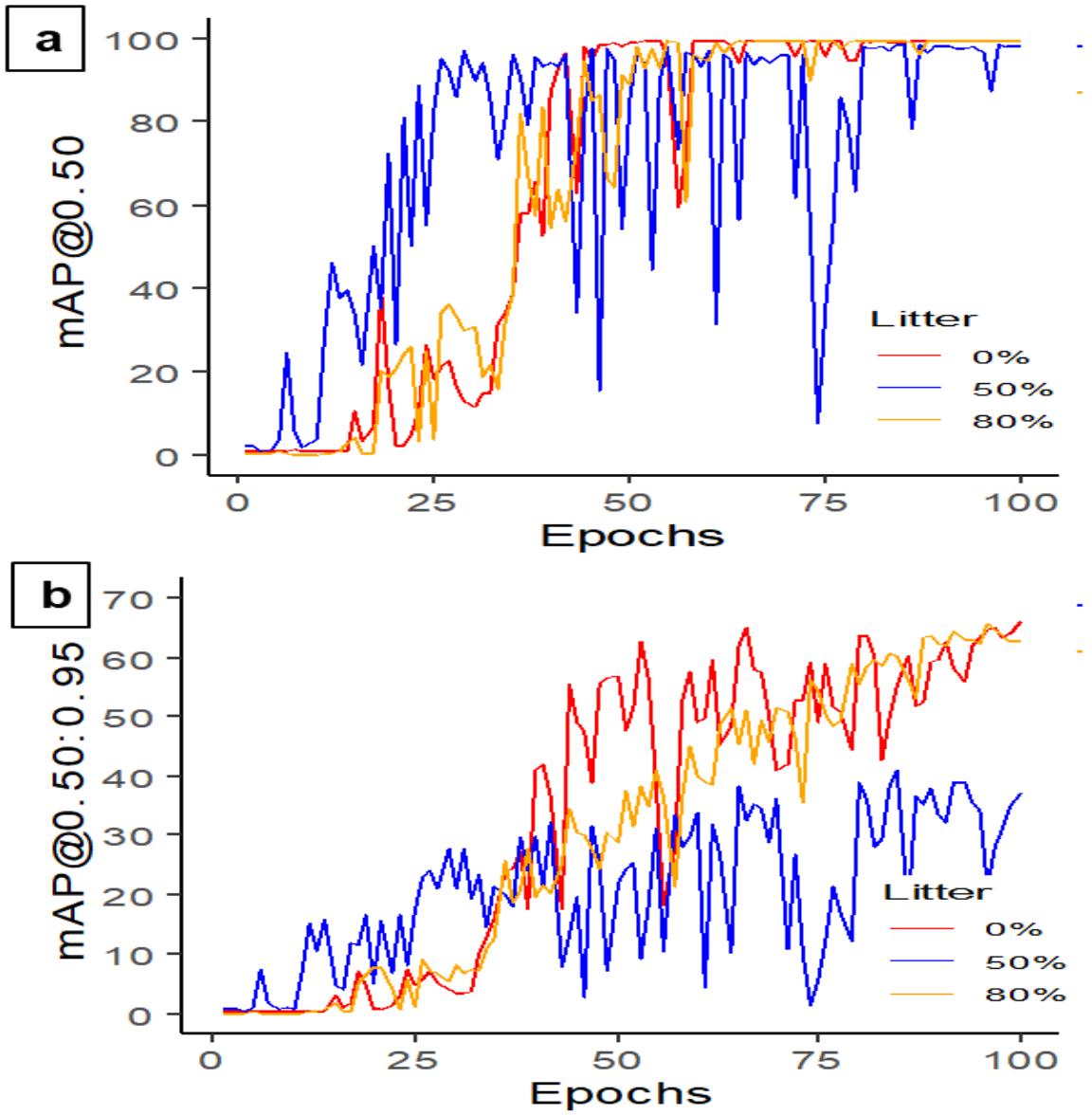

Figure 4.8: Mean average precision performance a) mAP@0.50 and b) mAP@0.50:0.95 using the YOLOv5s-MD model at 100 epochs and 16 batch sizes in detecting dead hens at different percentages of litter coverages.

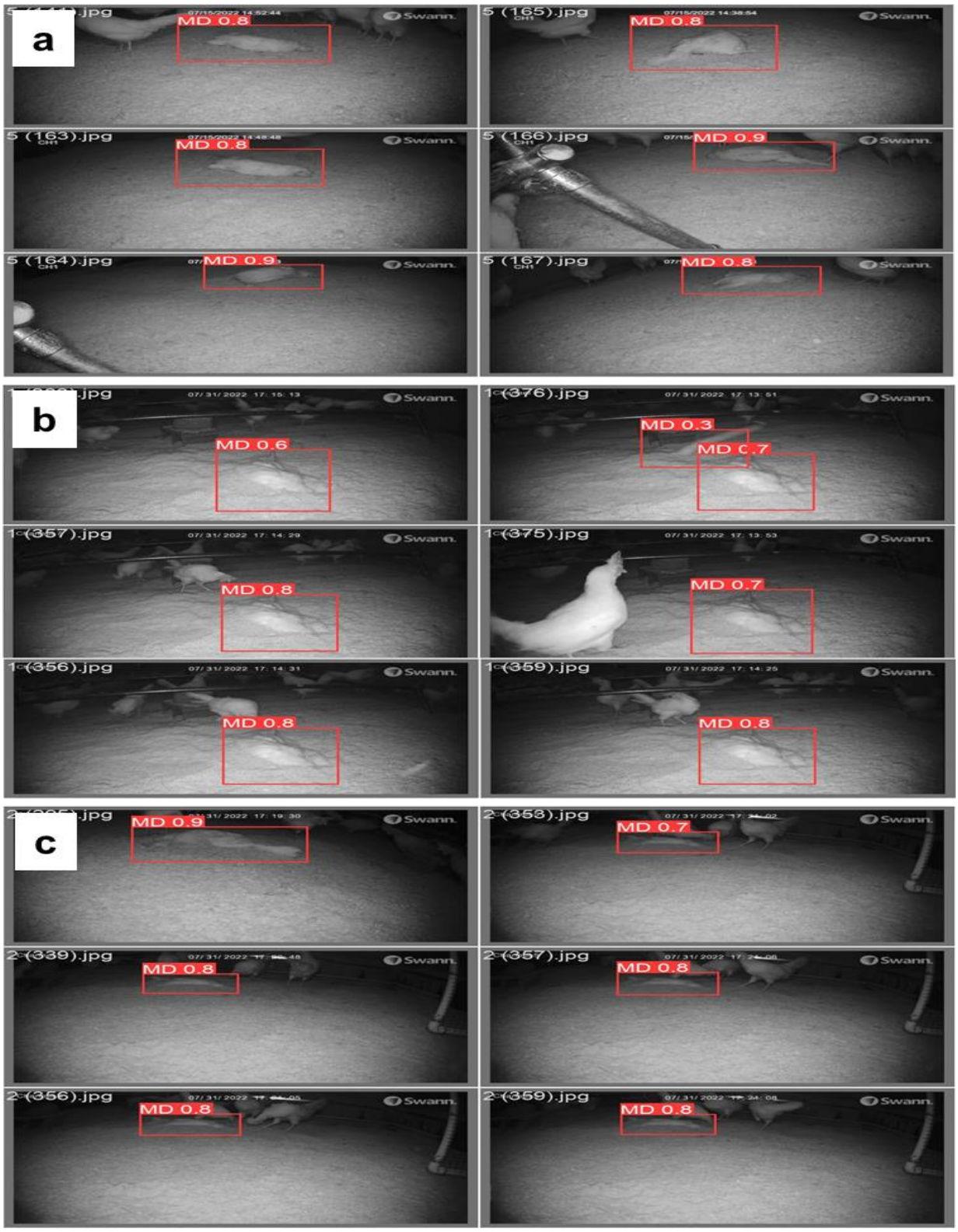

Figure 4.9: Variation of mortality detection with litter coverage: a) 0% litter or no litter, b) 50% litter, and c) 80% litter in cage-free rooms using the YOLOv5s model in test images.

4.3.3 Camera Settings

Camera height plays an important role in increasing object detection performance. When comparing the performance of YOLOv5s-MD at different camera heights from the dead hen, the model achieved the highest precision, recall, and F-1 score of 100% when detecting objects at the height of 0.5m (Table 4.6). As the camera height increased to 1m and 3m, the recall rate decreased to 99% and 94.8%, indicating that the model struggled to detect objects at higher heights. Regarding accuracy, YOLOv5s-MD achieved high mAP@0.50 across two camera heights, with the highest mAP of 99.5% obtained at the height of 0.5m and 1m (Figure 4.10a). The model's ability to detect smaller or more complex objects decreased at higher confidence thresholds, as the decreasing mAP@0.50:0.95 from 85.3% to 59.9% (Figure 4.10b). Overall, the YOLOv5s-MD model performed well across different camera heights, with the best results achieved at 0.5m (Figure 4.11). However, the model's performance deteriorated at higher camera heights, which may need to be considered in certain applications. For example, more image datasets must be labeled to increase model performance at higher heights or ceiling heights. The ceiling height camera plays a vital role in capturing a larger portion of the cage-free (CF) rooms than the ground camera. Integrating the ground's best height and ceiling height in a system can help better detect and remove dead birds from the farm.

Table 4.6: YOLOv5s model performance on mortality detection at different camera heights from the dead hen.

Data summary	**YOLOv5s-MD height 0.5m**	**YOLOv5s-MD height 1m**	**YOLOv5s-MD height 3m**
Precision (%)	100.0	99.8	99.0
Recall (%)	100.0	99.0	94.8
mAP@0.50 (%)	99.5	99.5	98.2
mAP@0.50:0.95 (%)	85.3	72.4	59.9
F1-score	100.0	99.0	97.0

Where, mAP- mean average precision; FPS-frame per second; MD- mortality detection; height 0.5, 1m, and 3m- camera height placed above the mortality hen.

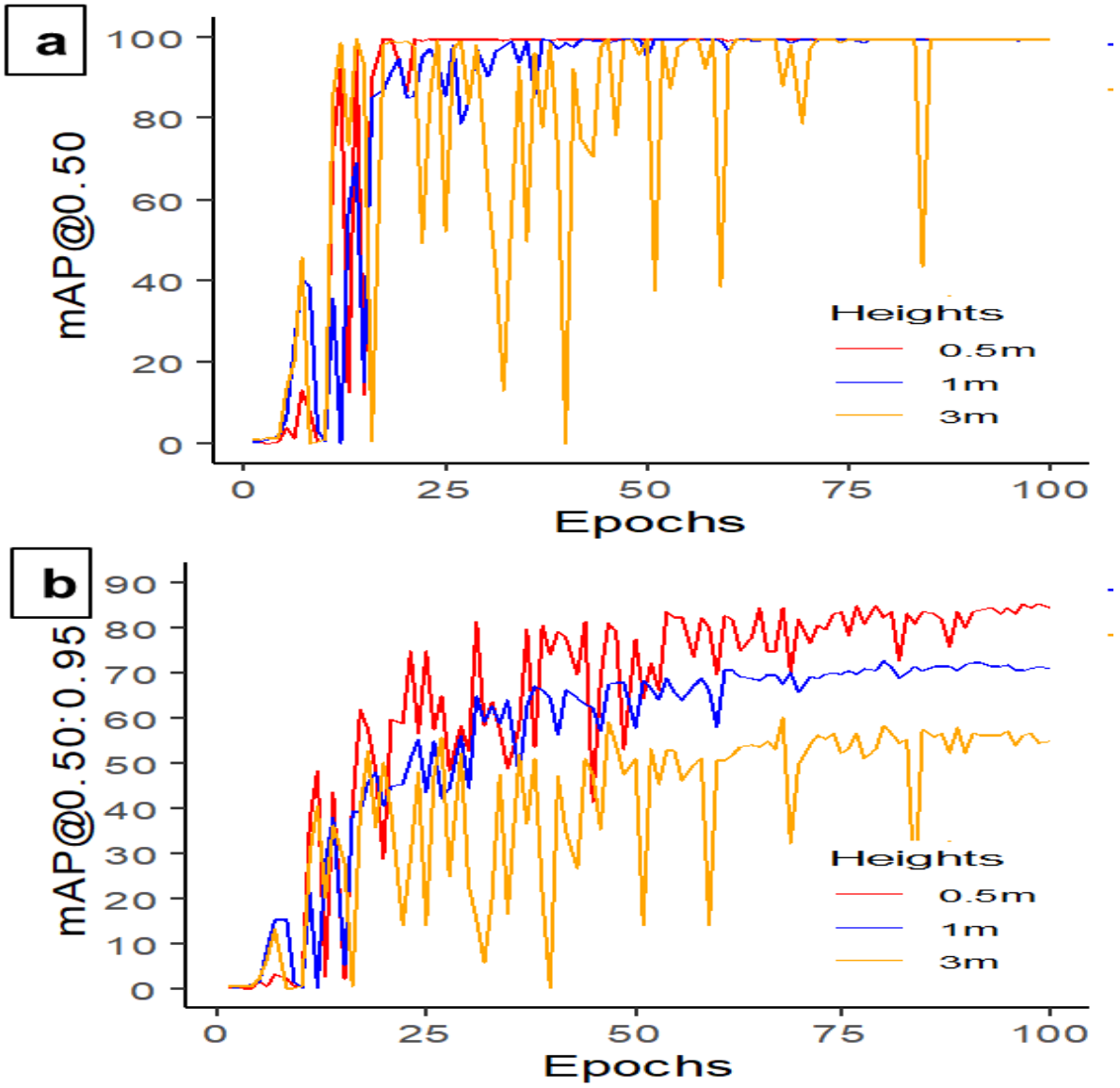

Figure 4.10: Mean average precision results a) mAP@0.50 and b)mAP@0.50:0.95 observed at different camera heights using the YOLO5s-MD model at 100 epochs and 16 batch sizes.

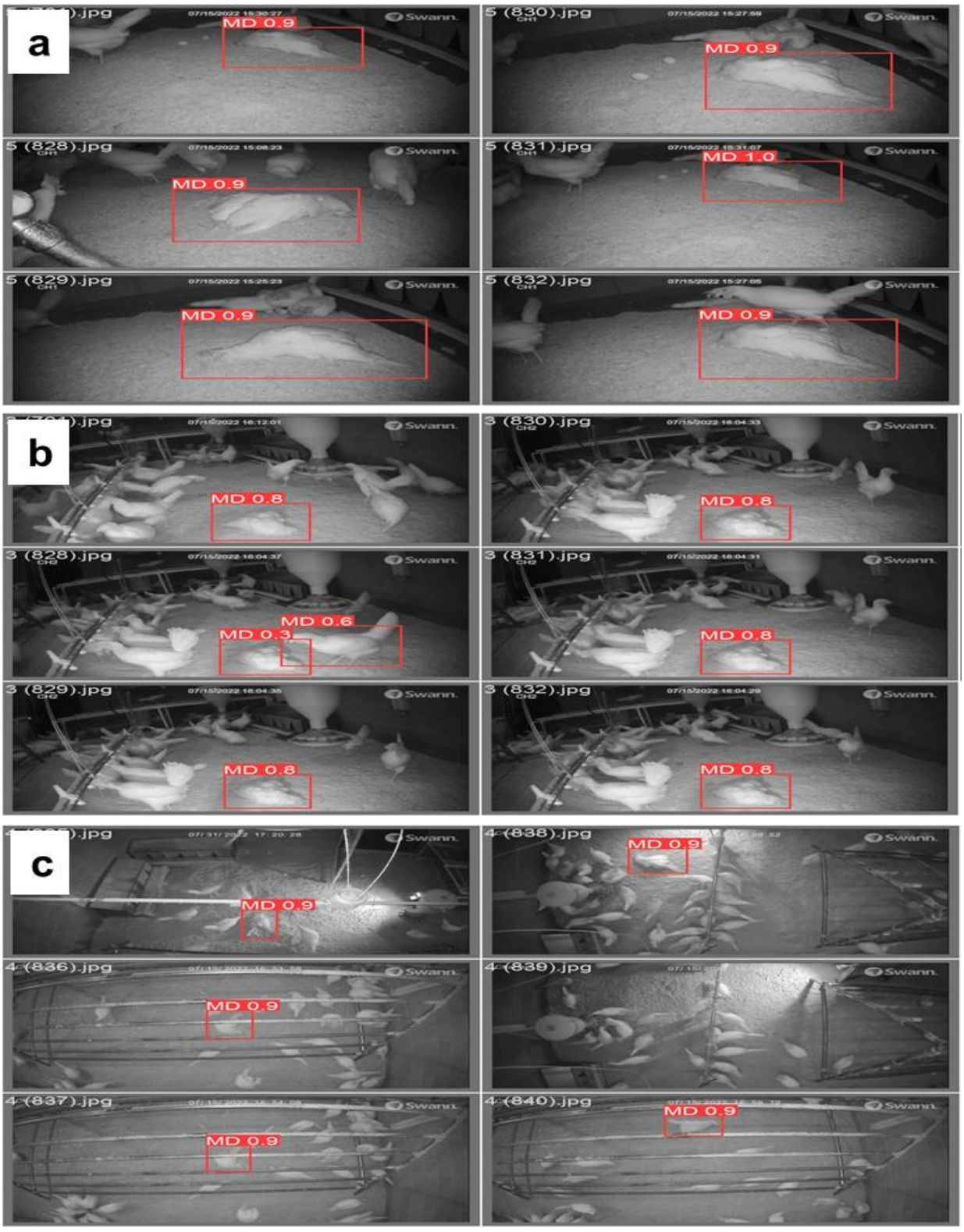

Figure 4.11: Variation of mortality detection with different camera heights (a – 0.5 m, b – 1 m, and c – 3 m) in cage-free rooms using the YOLOv5s model in test images.

The limitation of this study was the use of limited mortality image datasets, which might not fully represent the commercial CF housing variable conditions but can give an overview of those conditions. This study can be tested and implemented in commercial CF houses, where this model will be evaluated in real-world commercial CF housing setups. Furthermore, further work on larger image datasets incorporating a thermal camera and temperature & and humidity sensor can be utilized as an additional tool to improve the MD model.

4.4 CONCLUSIONS

This study developed and tested different YOLO deep learning models and identified that YOLOv5s-MD had a higher accuracy, faster processing time, and lower GPU usage than other models. In addition, the study found that the feathering percentage and litter coverage affected the model's performance, with the 0% feather covering reaching the highest mAP@0.50 and the 80% litter covering reaching the highest precision, recall, and mAP. Additionally, the model's performance varied with camera height from the target object, with the best precision, recall, and mAP achieved at 0.5m. This study provides a basis for developing a mortality scanning system in commercial CF houses.

4.5 REFERENCES

Bist, R. B., and L. Chai. 2022. Advanced Strategies for Mitigating Particulate Matter Generations in Poultry Houses. Applied Sciences 12:11323.

Bist, R. B., L. Chai, X. Yang, S. Subedi, and Y. Guo. 2022. Air Quality in Cage-free Houses during Pullets Production. Page 1 in American Society of Agricultural and Biological Engineers.

Bist, R. B., S. Subedi, L. Chai, and X. Yang. 2023. Ammonia emissions, impacts, and mitigation strategies for poultry production: A critical review. Journal of Environmental Management 328:116919.

Blas, A., B. Diezma, A. Moya, and C. Gomez-Martinez. 2013. Early detection of mortality in poultry production using high resolution thermography. VISAVET Available at https://www.visavet.es/en/early-detection-of-mortality-in-poultry-production-using-high-resolution-thermography/34=1264/ (verified 10 March 2023).

Brochu, N. M., M. T. Guerin, C. Varga, B. N. Lillie, M. L. Brash, and L. Susta. 2019. A two-year prospective study of small poultry flocks in Ontario, Canada, part 2: causes of morbidity and mortality. Journal of Veterinary Diagnostic Investigation 31:336–342.

Cadmus, K. J., A. Mete, M. Harris, D. Anderson, S. Davison, Y. Sato, J. Helm, L. Boger, J. Odani, and M. D. Ficken. 2019. Causes of mortality in backyard poultry in eight states in the United States. Journal of Veterinary Diagnostic Investigation 31:318–326.

Chicco, D., and G. Jurman. 2020. The advantages of the Matthews correlation coefficient (MCC) over F1 score and accuracy in binary classification evaluation. BMC Genomics 21:1–13.

Dessie, T., and B. Ogle. 2001. Village poultry production systems in the central highlands of Ethiopia. Tropical Animal Health and Production 33:521–537.

Edwan, E., M. A. Qassem, S. A. Al-Roos, M. Elnaggar, G. Ahmed, A. S. Ahmed, and A. Zaqout. 2020. Design and Implementation of Monitoring and Control System for a Poultry Farm. Pages 44–49 in IEEE.

Ekiri, A. B., B. Armson, K. Adebowale, I. Endacott, E. Galipo, R. Alafiatayo, D. L. Horton, A. Ogwuche, O. N. Bankole, and H. M. Galal. 2021. Evaluating disease threats to sustainable poultry production in Africa: Newcastle disease, infectious bursal disease, and avian infectious bronchitis in commercial poultry flocks in Kano and Oyo states, Nigeria. Frontiers in Veterinary Science 8:730159.

Gray, H., R. Davies, A. Bright, A. Rayner, and L. Asher. 2020. Why do hens pile? Hypothesizing the causes and consequences. Frontiers in Veterinary Science 7:616836.

He, K., X. Zhang, S. Ren, and J. Sun. 2015. Spatial pyramid pooling in deep convolutional networks for visual recognition. IEEE transactions on pattern analysis and machine intelligence 37:1904–1916.

Jocher, G. 2022. YOLOv5 (6.0/6.1) brief summary · Issue #6998 · ultralytics/yolov5. GitHub Available at https://github.com/ultralytics/yolov5/issues/6998 (verified 10 March 2023).

Li, C., L. Li, H. Jiang, K. Weng, Y. Geng, L. Li, Z. Ke, Q. Li, M. Cheng, and W. Nie. 2022. YOLOv6: A single-stage object detection framework for industrial applications. arXiv preprint arXiv:2209.02976.

Lin, Y., P. Feng, J. Guan, W. Wang, and J. Chambers. 2019. IENet: Interacting embranchment one stage anchor free detector for orientation aerial object detection. arXiv preprint arXiv:1912.00969.

Liu, S., L. Qi, H. Qin, J. Shi, and J. Jia. 2018. Path aggregation network for instance segmentation. Pages 8759–8768

Muvva, V. V., Y. Zhao, P. Parajuli, S. Zhang, T. Tabler, and J. Purswell. 2018. Automatic Identification of Broiler Mortality Using Image Processing Technology. Page 1 in American Society of Agricultural and Biological Engineers.

Padilla, R., S. L. Netto, and E. A. Da Silva. 2020. A survey on performance metrics for object-detection algorithms. Pages 237–242 in IEEE.

Roy, A. M., and J. Bhaduri. 2022. Real-time growth stage detection model for high degree of occultation using DenseNet-fused YOLOv4. Computers and Electronics in Agriculture 193:106694.

Saeed, M., G. Abbas, M. Alagawany, A. A. Kamboh, M. E. Abd El-Hack, A. F. Khafaga, and S. Chao. 2019. Heat stress management in poultry farms: A comprehensive overview. Journal of Thermal Biology 84:414–425.

Sentas, A., İ. Tashiev, F. Küçükayvaz, S. Kul, S. Eken, A. Sayar, and Y. Becerikli. 2020. Performance evaluation of support vector machine and convolutional neural network algorithms in real-time vehicle type and color classification. Evolutionary Intelligence 13:83–91.

Subedi, S., R. Bist, X. Yang, and L. Chai. 2023a. Tracking pecking behaviors and damages of cage-free laying hens with machine vision technologies. Computers and Electronics in Agriculture 204:107545.

Subedi, S., R. Bist, X. Yang, and L. Chai. 2023b. Tracking Floor Eggs with Machine Vision in Cage-free Hen Houses. Poultry Science:102637 Available at https://www.sciencedirect.com/science/article/pii/S003257912300161X (verified 10 March 2023).

Tan, M., and Q. Le. 2019. Efficientnet: Rethinking model scaling for convolutional neural networks.Pages 6105–6114 in PMLR.

Tesema, S. N., and E.-B. Bourennane. 2020. DenseYOLO: Yet Faster, Lighter and More Accurate YOLO.Pages 0534–0539 in IEEE.

Wang, C.-Y., H.-Y. M. Liao, Y.-H. Wu, P.-Y. Chen, J.-W. Hsieh, and I.-H. Yeh. 2020. CSPNet: A new backbone that can enhance learning capability of CNN. Pages 390–391

Weng, K., X. Chu, X. Xu, J. Huang, and X. Wei. 2023. EfficientRep:An Efficient Repvgg-style ConvNets with Hardware-aware Neural Network Design. Available at http://arxiv.org/abs/2302.00386 (verified 10 March 2023).

Wibisono, F. M., F. J. Wibisono, M. H. Effendi, H. Plumeriastuti, A. R. Hidayatullah, E. B. Hartadi, and E. D. Sofiana. 2020. A review of salmonellosis on poultry farms: Public health importance. Syst. Rev. Pharm 11:481–486.

Yang, X., L. Chai, R. B. Bist, S. Subedi, and Z. Wu. 2022. A Deep Learning Model for Detecting Cage-Free Hens on the Litter Floor. Animals 12:1983.

Yerpes, M., P. Llonch, and X. Manteca. 2020. Factors associated with cumulative first-week mortality in broiler chicks. Animals 10:310.

Zhu, W., C. Lu, X. Li, and L. Kong. 2009. Dead Birds Detection in Modern Chicken Farm Based on SVM. Pages 1–5 in IEEE.

CHAPTER 5

AUTOMATIC DETECTION OF HENS BUMBLEFOOT WITH COMPUTER VISION TECHNOLOGIES[4]

[4] Bist, R. B., Subedi, S., Yang, X., and Chai, L. 2024. Automatic Detection of Cage-Free Hens' Bumblefoot with Computer Vision Technologies. Submitted to *Poultry Science* Journal.

ABSTRACT

Cage-free (**CF**) housing systems are expected to be the dominant egg production system in North America and European Union countries by 2030. Within these systems, bumblefoot (a common bacterial infection and chronic inflammatory reaction) is mostly observed in hens reared on litter floors. It causes pain and stress in hens and is detrimental to their welfare. For instance, hens with bumblefoot have difficulty moving freely, thus hindering access to feeders and drinkers. However, it is technically challenging to detect hens with bumblefoot, and no automatic methods have been applied for hens' bumblefoot detection (**BFD**), especially in its early stages. This study aimed to develop and test artificial intelligence methods (i.e., deep learning models) to detect hens' bumblefoot condition in a CF environment under various settings (epochs, batch size, and camera height). The performance of three newly developed deep learning models (i.e., YOLOv5s-BFD, YOLOv5m-BFD, & YOLOv5x-BFD) were compared in detecting hens with bumblefoot of Hy-Line W-36 hens in CF environments. The result shows that the YOLOv5m-BFD model had the highest precision (93.7%), recall (84.6%), mAP@0.50 (90.9%), mAP@0.50:0.95 (51.8%), and F1-score (89.0%) compared with other models. The observed YOLOv5m-BFD model trained at 400 epochs and batch size 16 is recommended for bumblefoot detection in laying hens. This study provides a basis for developing an automatic bumblefoot detection system in commercial CF houses. This model will be modified and trained to detect the occurrence of broilers with bumblefoot in the future.

Keywords: Poultry production, Cage-free, Animal welfare, Bumblefoot, Computer vision.

5.1 INTRODUCTION

Bumblefoot (pododermatitis, footpad dermatitis, or foot rot) is the term used to describe a common bacterial infection and chronic inflammatory reaction in a bird (Shepherd and Fairchild, 2010; Stransky et al., 2016; Figure 5.1). It is clinically characterized by swelling, abrasion, hyperkeratosis, and ulceration of the digital pad, planta metatarsal region, or both (Wilcox et al., 2009; Stransky et al., 2016). Bumblefoot compromises the foot's internal tissues, including the mesoderm, tendons, and bones, leading to laminitis (inflammation and damage that affects feet and can lead to lameness), synovitis (acute to chronic systematic disease caused by *Mycoplasma synoviae* infection), osteomyelitis (an inflammatory condition leading to infection of the bone), and ultimately death if left untreated (McNamee and Smyth, 2000). In a study conducted by Wang et al. 1998, footpad lesions occurred in 38% of hens raised on dry litter and in 92% of hens raised on wet litter. Most bumblefoot cases in poultry were identified in floor housing systems instead of cage housing (Wang et al., 1998; Tauson et al., 1999; Fulton, 2019). However, the increased incidence of bumblefoot in caged laying hens is linked with pressure on the metatarsal foot pad due to perch design (Tauson, 1998) and wet or unsanitary perches (Tauson and Abrahamsson, 1996).

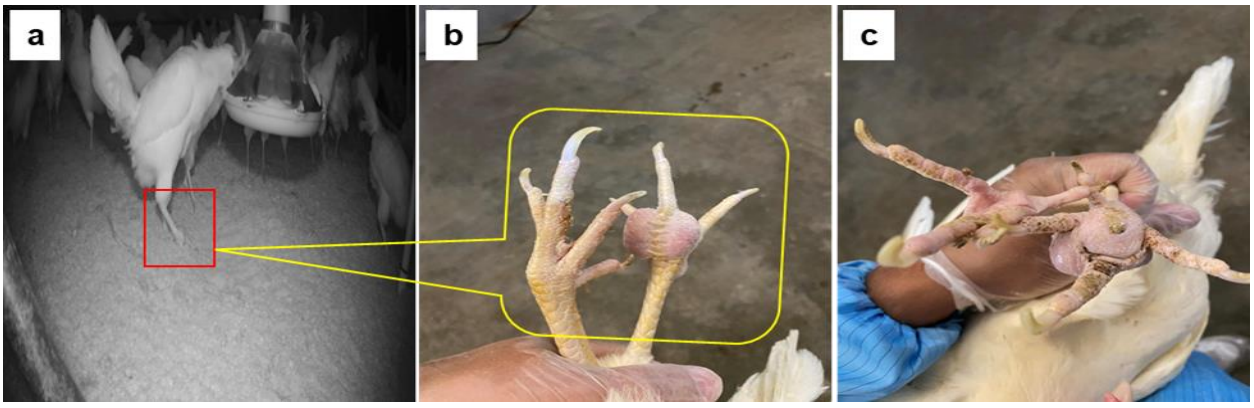

Figure 5.1: Cage-free laying hen having bumblefoot from a) side view, b) top view, and c) bottom view of the hen's foot.

There have been many predisposing factors associated with bumblefoot, including stocking density, seasonal effects, drinker design and maintenance, litter material, litter moisture content, litter depth, and litter additives in floor-housed chickens (Bilgili et al., 2009; Shepherd and Fairchild, 2010; NCC, 2018; Craven et al., 2021). Various nutritional factors, including grain source, vitamin, mineral, and amino acid supplementation, protein level, and diet density, have also been linked to pododermatitis (Nagaraj et al., 2007). In addition, the hen genetic line also significantly affects the occurrence of bumblefoot (Abrahamsson and Tauson, 1995). For example, between Lohmann Selected Leghorn (**LSL**) and Lohmann Brown, LSL hens resulted in a high bumblefoot incidence (Abrahamsson and Tauson, 1995; Abrahamsson et al., 1998). Among house types, bumblefoot was most prevalent in aviary or floor-raised hens, followed by enriched colony birds, and was almost nonexistent in conventional caged birds (Fulton, 2019). The bumblefoot issues could be significant as the egg industry is completely moving from caged to cage-free.

Most cases of bumblefoot conditions in laying hens occur at 35 weeks of age due to litter conditions and equipment (Abrahamsson et al., 1998). At the age of depopulation, approximately 62% of laying hens had keel bone damage seen in all birds with bumblefoot on both feet (Gebhardt-Henrich and Frohlich, 2015). The research suggested that hens with bumblefoot could be more prone to losing their grip on perches, potentially resulting in falls that increase the risk of keel bone damage. According to Berg (1998), the bumblefoot lesions produce pain and stress, which makes the animal reluctant to move and decreases feed consumption (De Jong et al., 2014; Chuppava et al., 2018). The decrease in feed consumption is due to impediments in walking and perching activities, which may restrict feeder and drinker access (Hester, 1994). In addition, Harms and

Simpson 1975, observed an unsteady gait in birds with bumblefoot, and Hester (1994) explained how bumblefoot results in walking with a hobbling gait. Hens with hobbling gait can be a major concern for the poultry industry regarding animal welfare (Bradshaw et al., 2002). Therefore, bumblefoot is considered painful and harms the birds' well-being (Tauson, 2002; Lay Jr et al., 2011). The bumblefoot is now used as an objective audit criterion in European and American poultry production systems (NCC, 2018). As a measure of farm well-being, the rate of bumblefoot occurrence is becoming more widely recognized (Martrenchar et al., 2002). Therefore, early detection and treatment of pathogens causing bumblefoot are needed.

Staphylococcus aureus (SA) (68%) and *Enterococcus faecalis* (14%) were the two most common bacterial species found in an examination of bacterial pathogens in egg-laying hens with bumblefoot (Heidemann Olsen et al., 2018). The SA is a gram-positive bacterium found on the skin of non-clinical animals and in large concentrations in the dust of chicken houses, feed, and gut contents (Zhu et al., 1999). Infection with SA is one of the most frequent poultry diseases in commercial layers, which decreases production efficiency and results in death rates up to 15% (Youssef et al., 2019). The SA can invade the mesoderm, proliferate, and cause inflammation when the mucosal or skin barriers are compromised due to trauma or stress. If left untreated, it will quickly go up the leg and into the body, where it could cause a fatal septicaemic infection or even cause death (Choudhury, 2019). Therefore, early diagnosis and treatment are essential for a positive prognosis and to prevent complications caused by lameness. Starting with a tiny cut on the bottom of the foot, the infection spreads through it and eventually results in a black scab. Surgery is usually required to open the scab or abscess and carefully remove all necrotic material by avoiding nerves, tendons, and blood vessels (Coles, 2007). The affected area is then treated

using a 0.1% potassium permanganate solution, and the pus is surgically removed (Choudhury, 2019). The bird received an antibiotic course as well as other supportive treatments. Topical antiseptics and oral or injected antibiotics may be used to combat the infection. A combination of surgery, local and antibiotic therapy chosen after an antibiotic sensitivity test, and proper post-operative care are effective and helpful in treating these infections. However, performing surgery-based cures in commercial laying hen facilities is hard, time-consuming, and labor-intensive. Therefore, early detection would be useful to optimize treatment to determine the prevalence of bumblefoot in the flock and determine the best course of action for prevention or correction. A potential alternative solution would be to find a detection model or technology that can detect bumblefoot with a higher detection rate. Detection early can helps producers to inform about bumblefoot rates and might give a general ideas to change environmental substrate or provide foot soaking treatment inside housing to improve foot health.

In laying hens, infrared thermal imaging technology has been extensively used to assess bumblefoot conditions (Wilcox et al., 2009; Ben Sassi et al., 2016). However, using this technology can be invasive as it may involve holding the hen several times, potentially increasing stress on laying hens. Furthermore, the stress induced in hens could be detrimental to their welfare (Lay Jr et al., 2011). Therefore, there is a need for a non-invasive real-time bumblefoot detection (**BFD**) system. Several detection algorithms are developed and widely used, but **YOLO** (You Only Look Once) has proven and outperformed in real-time detection, processing speed, and GPU usage than other models (Huang et al., 2018; Bist et al., 2023b; Subedi et al., 2023a). YOLO is a single-stage object detector that uses a single network to process image data and gives fast object recognition and positioning (Shafiee et al., 2017). Recent research has shown that the YOLOv5

model best detects small objects like chickens (Yang et al., 2022; Subedi et al., 2023a; Bist et al., 2023a) and eggs (Yang et al., 2023a; Subedi et al., 2023b) in cage-free (**CF**) housing. Similarly, abnormal behavior is hard to detect with higher precision, which is only possible with the YOLOv5 model. For example, Subedi et al. (2023a) detected the pecking behavior in CF hens and predicted it would improve animal welfare after further improvement. Overall, the YOLOv5 model is widely used to detect various objects in the poultry industry. Thus, the YOLOv5 models were used for BFD in the CF facility, where hens with different behaviors and welfare concerns have been reported (Subedi et al., 2023a; Yang et al., 2023b). The objectives of this study were to: i) develop and test a YOLOv5-BFD model as a diagnostic tool for detecting clinical bumblefoot in CF layers; ii) compare the performance of YOLOv5s-BFD, YOLOv5m-BFD, and YOLOv5x-BFD model; and iii) evaluate the performance of optimal YOLOv5-BFD model under different settings (camera heights, epochs, & batch sizes). The final model will give the best BFD model to detect bumblefoot and help to evaluate and improve animal welfare.

5.2 MATERIALS AND METHODS

5.2.1 Housing, Animal, and Data Acquisition

This experiment follows the same housing and bird management practices as described in Chapter 2 of section 2.2.1. For the BFD datasets, the two cameras were positioned 30cm and 50cm above the litter, as shown in Figure 5.2. The video was recorded from the 48-50 weeks of laying hen age with the help of a night-vision network camera (PRO-1080MSB, Swann Communications USA Inc, LA, US). The data acquisition 16 hours daily, from 5 am to 9 pm. The video obtained were recorded with the help of a Swann digital video recorder (DVR-4580, Swann Communications USA Inc, LA, US) and stored in .avi format with a picture resolution of 1920×

1080 pixels and 15 frames per second (FPS) sampling rate. Next, the videos obtained were converted into images (.jpg format) by Free Video to JPG Converter App (version 5.0). After converting videos into images, images were further selected and separated based on bumblefoot visibility, hens' positions, and leg orientation. The final image datasets obtained were labeled using the image labeler website (Makesense.AI) with one class as BFD (Figure 5.3).

Figure 5.2: Experimental CF a) laying hen rooms, b) camera setup at 30 & 50 cm above litter floor.

Figure 5.3: Training images with a labeled representation of "0" as BFD. BFD-bumblefoot detection.

A total of 2200 images were labeled as BFD datasets, 1100 from each height of 30cm and 50cm. Some of the image's datasets (30%) used various data augmentation processes (rotation, flip, brightness & contrast adjusting, color jittering, and cropping) to avoid under and overfitting problems and improve performance. The BFD_{total} datasets obtained were first compared with the three best performing YOLOv5 models (YOLOv5s, YOLOv5m, and YOLOv5x), and then the best detection model was used to compare other classes or parameters for this study (Table 5.1). First, images were trained, validated, and test in the ratio of 7:2:1. The BFD_{total} datasets were trained and compared at 100 epochs and batch size 16. Later, the BFD by height dataset was trained based on the best epoch and batch size obtained from the epoch and batch size comparison.

Table 5.1: Data pre-processing for model detection.

Class[a]	Original dataset	Train (70 %)	Validation (20 %)	Test (10 %)
BFD_{total}	2200	1540	440	220
$BFD_{batch4\text{-}32}^{*}$	2200	1540	440	220
$BFD_{epoch50\text{-}400}^{\#}$	2200	1540	440	220
$BFD_{height30cm}$	1100	770	220	110
$BFD_{height50cm}$	1100	770	220	110

[*]batch sizes of 4, 8, 16, and 32 trained each with 2200 datasets; [#]epochs of 50, 100, 200, and 400 trained each with 2200 datasets; BFD-bumblefoot detection; BFD_{total} consist of images at different heights (30cm and 50cm), standing position, and walking distances.

5.2.2 Proposed YOLOv5 Model

Many versions of the YOLO series for object detection have been released; YOLOv5 is the fifth YOLO series version, released in 2020 (Jocher, 2022). As it is a single-stage detector instead of a double-stage detector like RCNN, the YOLOv5 model is a faster and more real-time detector model used today (Yang et al., 2022; Subedi et al., 2023a). The architecture of the YOLOv5 model for the proposed method is shown in Figure 5.4. The YOLOv5-BFD model is mainly composed of Input, backbone as extracting features, neck as a combined structure of a feature pyramid network (FPN) (Lin et al., 2017), and path aggregation network (PANet) (Liu et al., 2018) and head as output or prediction of BFD.

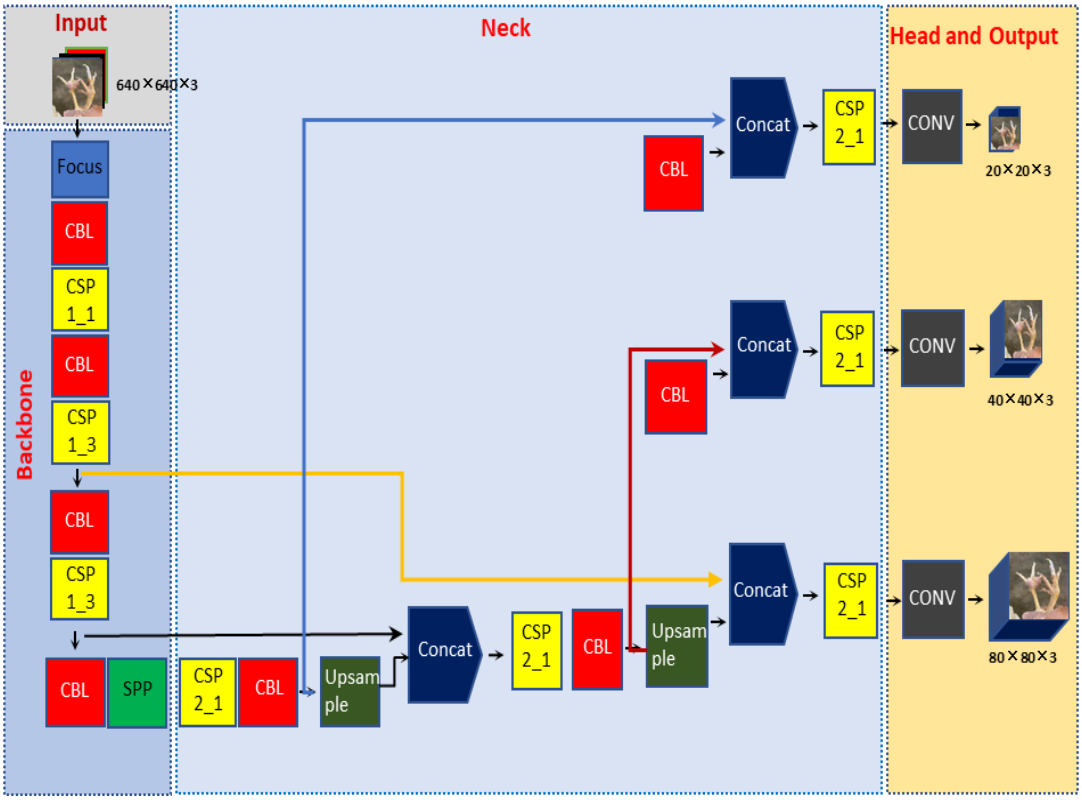

Figure 5.4: Architecture of YOLOv5 model used in bumblefoot detection.

CBL- convolution, batch normalization, and leaky-ReLu; CSP- cross stage partial; SPP- spatial pyramid pooling; CONV- convolutional kernel; BN- batch normalization; Res- residual; ReLu- rectified linear unit; Concat- concatenate.

5.2.2.1 Inputs

The input part of the YOLOv5-BFD model enriches the BFD dataset with mosaic data augmentation, which helps decrease the hardware device requirement and lower computational cost (Wang et al., 2020). This mosaic data augmentation is the same as in the YOLOv4 model but performs better for small object detection (Yao et al., 2021). However, decreasing the original BFD dataset size to smaller might deteriorate the model's overall BFD performance. All the labeled BFD images that are input later changed into the default image size of 640×640×3 and further

sliced into four slices (320×320×12) by the Focus when it reaches the backbone for extracting features (Figure 5.5).

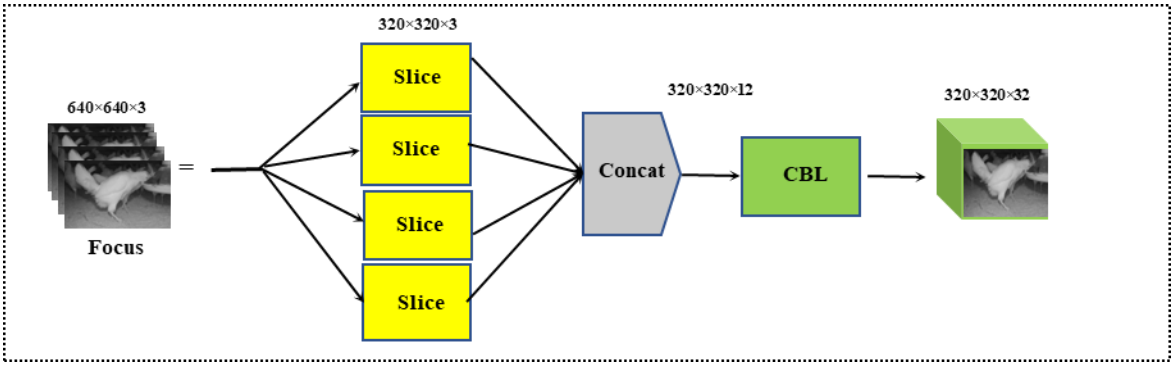

Figure 5.5: Structure of Focus module used in bumblefoot detection.

CBL- convolution, batch normalization, and leaky-ReLu; Concat- concatenate.

5.2.2.2 Backbone

In the YOLOv5-BFD backbone (Figure 5.6), Focus reduces parameters, layers, FLOPs, and CUDA memory usage while increasing forward and backward speed and minimizing the impact on mAP (Jocher, 2021). The Cross-Stage-Partial-connections (**CSP**) module extracts features via the CSPDarkner53 (Bochkovskiy et al., 2020). The CSPDarker53 helps to achieve high and improved processing speed and superior detection accuracy (Wang et al., 2020). Furthermore, the backbone network's receptive field is efficiently increased by using the SPP to Concat feature maps from various kernel sizes together as an output, separating important context features (He et al., 2015).

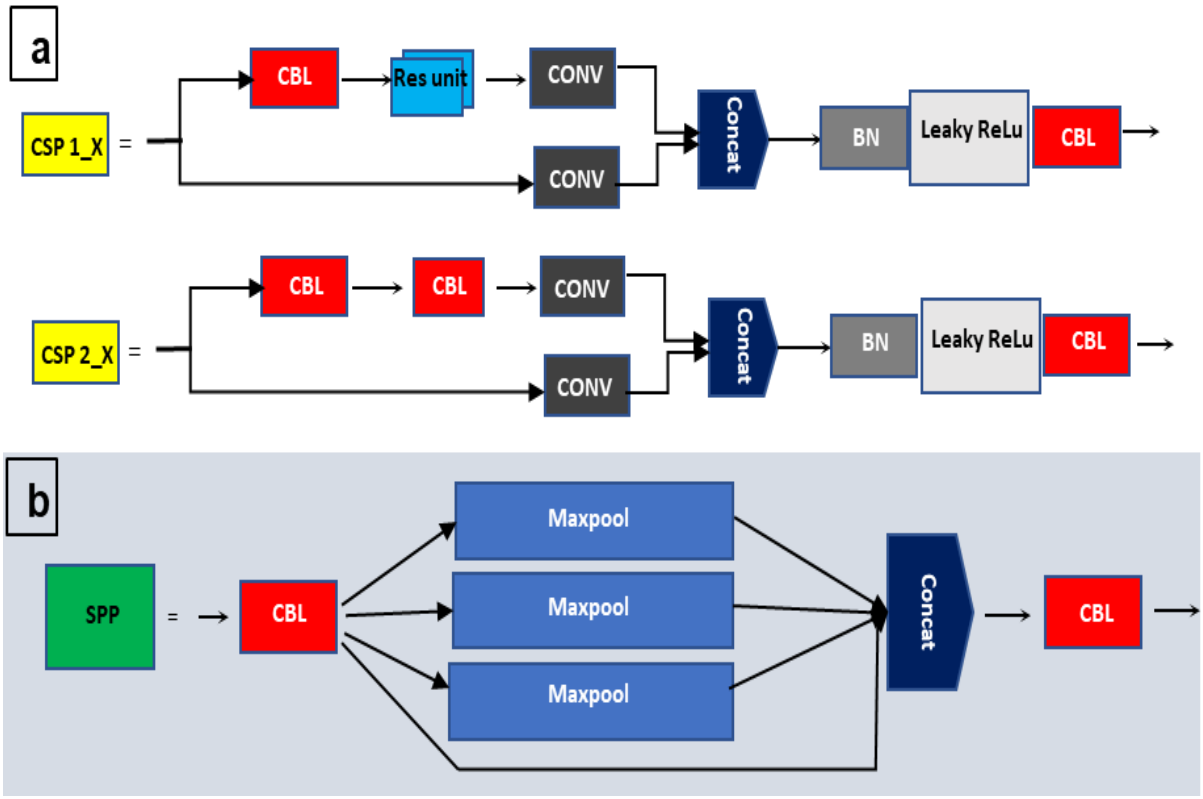

Figure 5.6: The structure of a) CSP and b) SPP module used in YOLOv5-BFD.

CSP- cross-stage partial; CBL- convolution, batch normalization, and leaky-ReLu; CONV- convolutional kernel; Concat- concatenate; BN- batch normalization; SPP- spatial pyramid pooling.

5.2.2.3 Neck

In YOLOv5-BFD neck, FPN and PANet aggregate the image feature, which benefits the bumblefoot object in generalizing or identifying the same bumblefoot objects in different sizes and scales. The FPN and PANet use an effective multi-scale feature fusion matrix that generates feature pyramids and enhances BFD model detection of different object sizes and scales (Yao et al., 2021). In addition, the FPN module enhances the bottom-up path, improving the low-level feature propagation of the BFD model.

5.2.2.4 Head

The head of YOLOv5-BFD uses the same head structure used in YOLOv3 and YOLOv4. The head consists of three convolution layers and helps in the multi-scale prediction of a BFD object. These convolution layers predict the BFD object classes, bounding box locations (x, y, height, width), and the scores (Jocher, 2022).

5.2.3 Loss Function

The loss function in the YOLOv5-BFD model uses binary cross entropy to compute objectness loss and class loss; as a result, YOLOv5-BFD gives three outputs of bounding boxes, objectness scores, and detected object classes. First, the loss is calculated by the following equation:

$$Loss = \lambda_1 L_{cls} + \lambda_2 L_{obj} + \lambda_3 L_{loc} \qquad (i)$$

5.2.4 Network Training Parameters

The YOLOv5-BFD model for the BFD was obtained from the GitHub repository developed by Ultralytics in 2020 (Jocher, 2021). The three YOLOv5-BFD types (YOLOv5s-BFD, YOLOv5m-BFD, and YOLOv5x-BFD) were compared in this study. Each YOLOv5-BFD model differs based on size, layers, parameters, gradients, and GLOPs (Table 5.2).

Table 5.2: Training datasets based on the YOLOv5-BFD model parameters.

Model	YOLOv5s	YOLOv5m	YOLOv5x
Type	Small	Medium	XLarge
Layers	214	291	445
Parameters	7,025,023	20,875,359	86,224,543
Gradients	7,025,023	20,875,359	86,224,543
GFLOPs	16.0	48.2	204.6

BFD-Bumblefoot detection; GFLOPs-Giga floating point operations per second

The experimental computing configuration was prepared before the BFD model detector was developed for model evaluation (Table 5.3). For training BFD datasets, the Oracle cloud computing system (Oracle America, Austin, Texas) was used for data analysis.

Table 5.3: Experimental computing configuration used for the YOLOv5-BFD model evaluation.

Configuration	Computing parameter
GPU (4 counts)	4×NVIDIA® A10 (24GB)
CPU	64 core OCPU
Memory (RAM)	1024GB
Drive (2 counts)	7.68 TB NVMe SSD
Operating system	Ubuntu 22.10 (Kinetic Kudu)
Accelerated environment	NVIDIA CUDA
Libraries	NumPy 1.18.5, Torch-vision 0.8.1, OpenCV-python 4.1.1, Torch 1.7.0.

5.2.5 Performance Evaluation

This study uses precision, recall, mean average precision (**mAP**), and F1-score to evaluate the performance of the YOLOv5-BFD model. All the parameters are calculated based on true positive (**TP**; bumblefoot present in the image and model accurately detect it), true negative (**TN**; bumblefoot is neither present nor detected by the model in the image), false positive (**FP**; bumblefoot is not present in the image while model detect it), and false negative (**FN**; bumblefoot present in the image but cannot detected by the model) value obtained from the BFD model (Figure 5.7).

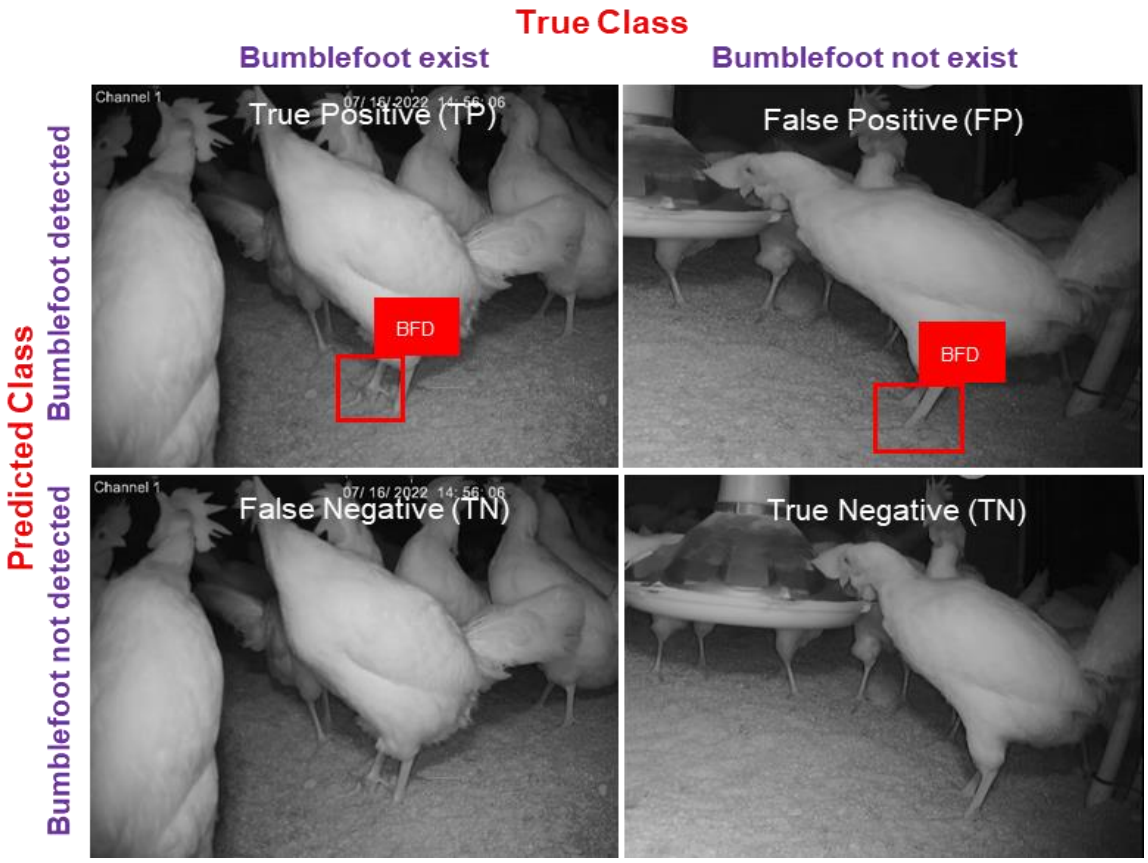

Figure 5.7: Confusion matrix for bumblefoot detection model. BFD-bumblefoot detection.

(a) Precision represents the proportion of the number of correct bounding box predictions in BFD objects from the BFD datasets.

$$Precision = \frac{TP}{TP + FP} = \frac{true\ bumblefoot\ detection}{all\ detected\ bounding\ boxes} \qquad (ii)$$

(b) Recall indicates the proportion of the number of correct BFD predictions or true bounding box measures correctly predicted from all samples from the BFD datasets.

$$Recall = \frac{TP}{TP + FN} = \frac{true\ bumblefoot\ detection}{all\ ground\ truth\ bounding\ boxes} \qquad (iii)$$

(c) The F1-score is the weighted average or harmonic mean of precision and recall obtained from evaluating the BFD model.

$$F1\ Score = \frac{2 \times Recall \times Precision}{Recall + Precision} \qquad (iv)$$

(d) The mAP is the mean average precision metric that helps evaluate the BFD model. The mAP is measured at the intersection over a union (IoU) threshold of 0.50 (mAP@0.50) or 0.5:0.95 (mAP@0.5:0.95).

$$mAP = \frac{\sum_{i=1}^{C} APi}{C} \qquad (v)$$

Where, APi represents the average precision of the *i*th BFD category and C indicates the total number of BFD categories.

5.3 RESULTS AND DISCUSSION

5.3.1 Comparative Analysis of Different YOLOv5 Models

5.3.1.1 Experimental results

The comparison of YOLOv5-BFD models on test data is shown in Table 5.4. From Table 5.4, we can see that the precision, recall, precision-recall (PR), mAP@0.50, mAP@0.50:95, and F1-score of the YOLOv5m-BFD model were 93.7%, 84.6%, 90.9%, 90.9%, 51.8%, and 89.0%, respectively, which was higher than that of YOLOv5s-BFD and YOLOv5x-BFD model (Table 5.4). The YOLOv5x-BFD model showed the lowest test detection result. However, many studies have shown that the YOLOv5s model has higher performance in detecting a smaller object (Yang et al., 2022; Subedi et al., 2023a; b), but the overall performance of the YOLOv5m-BFD model (Figure 5.8) is the best among tested models and can be used to detect BFD in the poultry housing.

Table 5.4: Test result of YOLOv5-BFD model based on CF laying hen condition.

Data summary	YOLOv5s-BFD	YOLOv5m-BFD	YOLOv5x-BFD
Precision (%)	91.5	93.7	92.5
Recall (%)	81.8	84.6	72.7
PR (%)	88.4	90.9	84.0
mAP@0.50 (%)	88.6	90.9	84.0
mAP@0.50:0.95 (%)	49.8	51.8	47.3
F1-score (%)	86.0	89.0	81.0

CF-Cage free; BFD-Bumblefoot detection; PR- precision-recall; mAP- mean average precision.

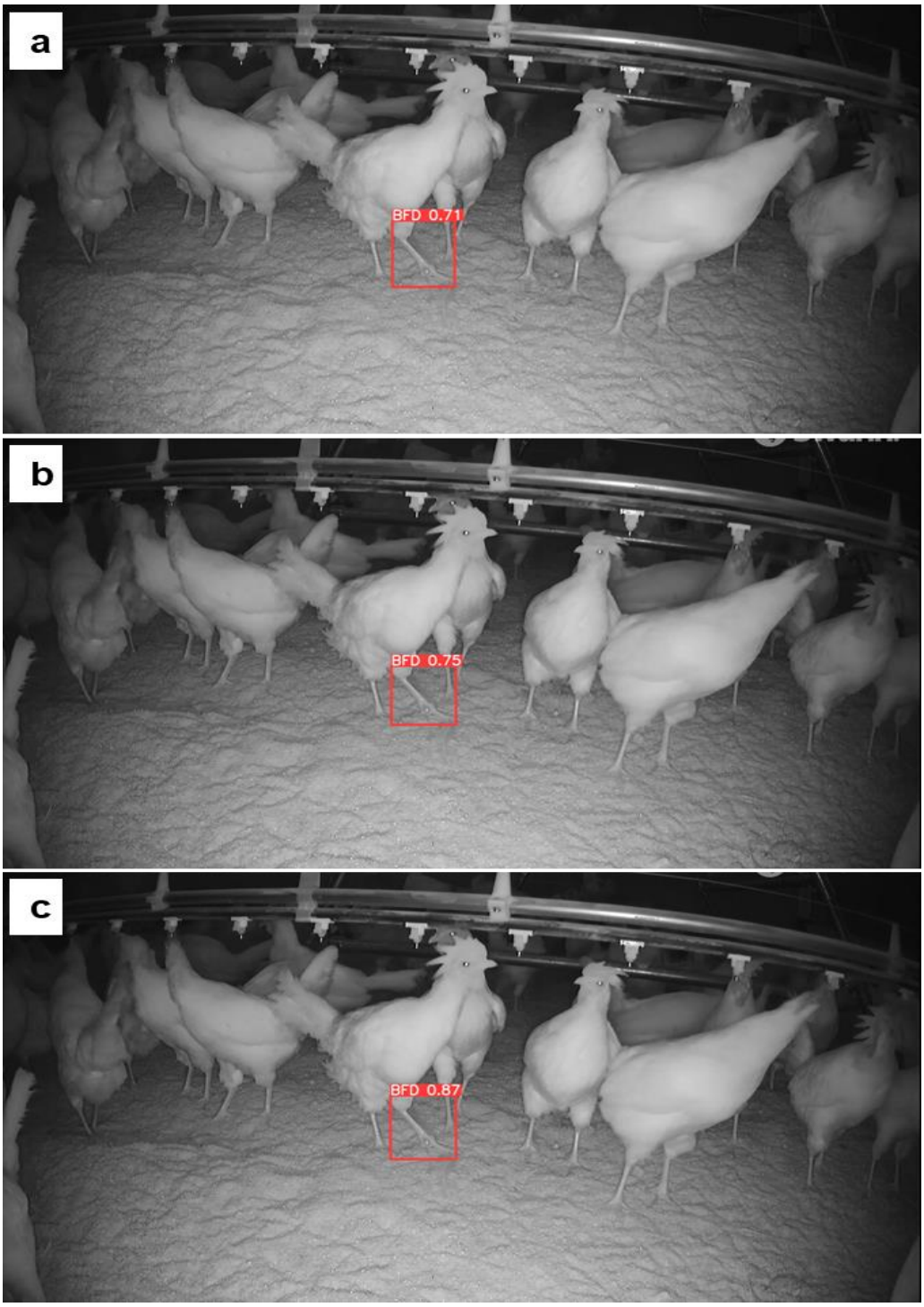

Figure 5.8: The bumblefoot detection results of a) YOLOv5x-BFD, b) YOLOv5s-BFD, and c) YOLOv5m-BFD. BFD-bumblefoot detection.

5.3.1.1.1 Model performance curves

From Figure 5.9, the precision, recall, mAP@0.50, and mAP@0.50:0.95 increased with the epoch, meaning more image training improves the detection performance. For example, the precision score was 0.0019, 0.0020, and 0.0013 during the initial stage of training at one epoch, reaching 0.900, 0.949, and 0.858 at 100 epochs for the YOLOv5s, YOLOv5m, and YOLOv5x, respectively. Similarly, the recall value at one epoch was 0.483, 0.509, and 0.320, while 0.817, 0.760, and 0.646 at 100 epochs for the YOLOv5s, YOLOv5m, and YOLOv5x, respectively. Overall, performance metrics for YOLOv5m perform better than other models from the beginning to the end of the training.

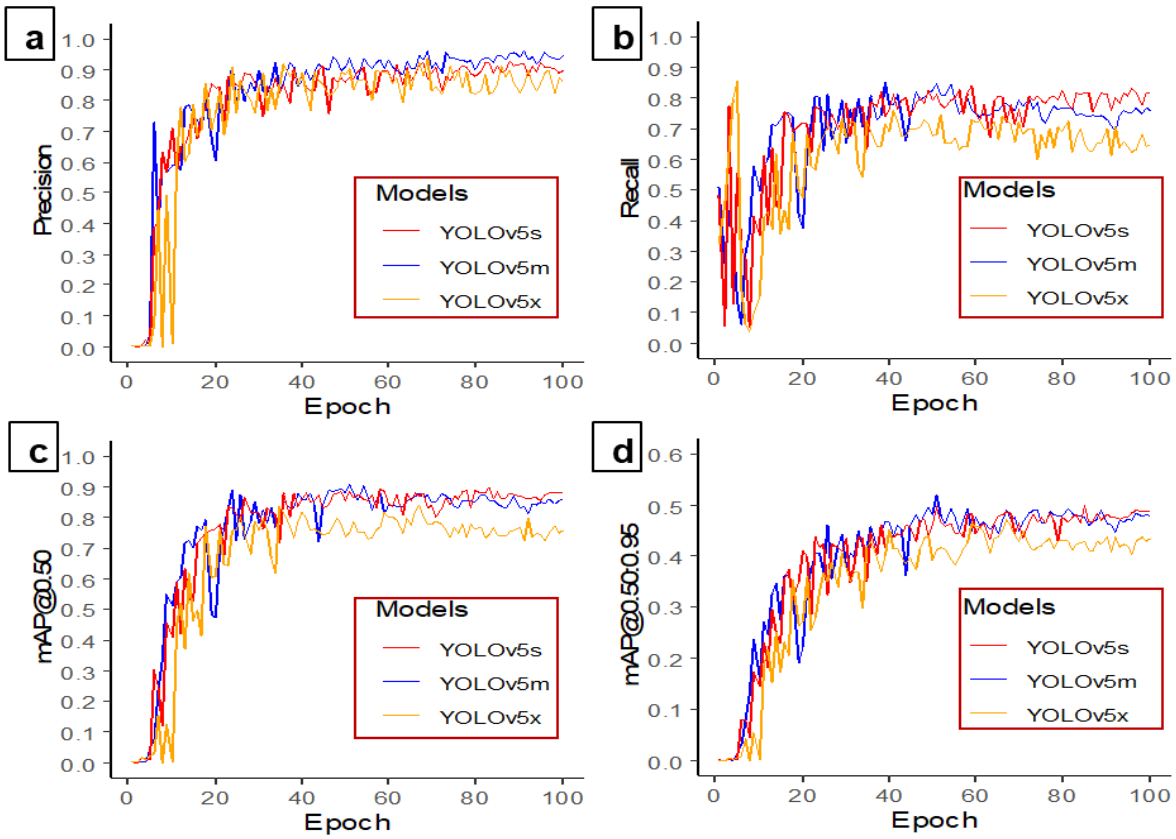

Figure 5.9: Performance metrics a) Precision, b) Recall, c) mAP@0.50, and d) mAP@0.50:0.95 comparison of different YOLOv5-BFD models.

The PR curve for the YOLOv5-BFD models is shown in Figure 5.10. The PR curves visualize how the model detects the positive classes. Among YOLOv5s-BFD, YOLOv5m-BFD, and YOLOv5x-BFD, PR curves seem higher for the YOLOv5m-BFD model of 90.9% at mAP@0.5 and lowest for YOLOv5x-BFD of 84.0% at mAP@0.50:0.95. Similarly, the F1-confidence curve for each model is given in Figure 5.10. The F1 scores give the model's performance evaluation and the combined information on the precision and recall of a model. The F1-confidence curves show that the F1-score was highest for the YOLOv5m-BFD model at 89.0% at 0.312 confidence level and lowest for the YOLOv5x-BFD model at 81.0% at 0.424 confidence level. The higher the value of PR and F1-confidence curves, the better the model performance. Thus, the YOLOv5m-BFD model outperforms in both PR and F1-confidence scores.

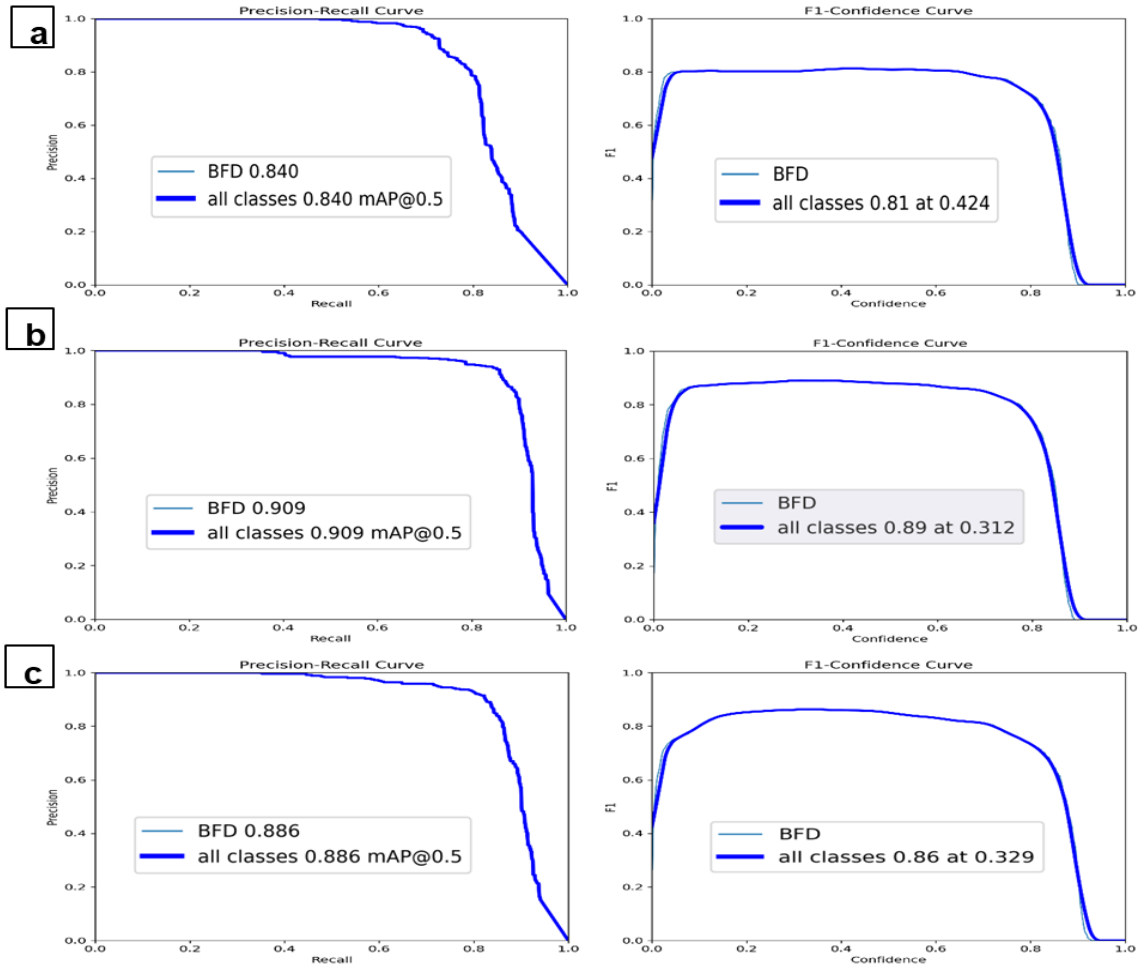

Figure 5.10: Graph showing performance comparison, PR-curves, and F1-confidence curve obtained after training with a) YOLOv5x-BFD, b) YOLOv5m-BFD, and c) YOLOv5s-BFD.

BFD- bumblefoot detection; PR- precision-recall.

In this study, the confusion matrix offers insights into the performance of various YOLOv5-BFD models (Figure 5.11**)**. Among these models, YOLOv5m-BFD stands out as the most balanced, achieving an impressive 86% accuracy in detecting BFD cases. Following closely behind, YOLOv5s-BFD exhibits an 84% accuracy rate in BFD detection. On the other hand, YOLOv5x-BFD, while still effective, demonstrates a somewhat lower positive detection rate at

74%. These findings provide valuable guidance for selecting and enhancing models for bumblefoot detection, with YOLOv5m-BFD emerging as a strong candidate.

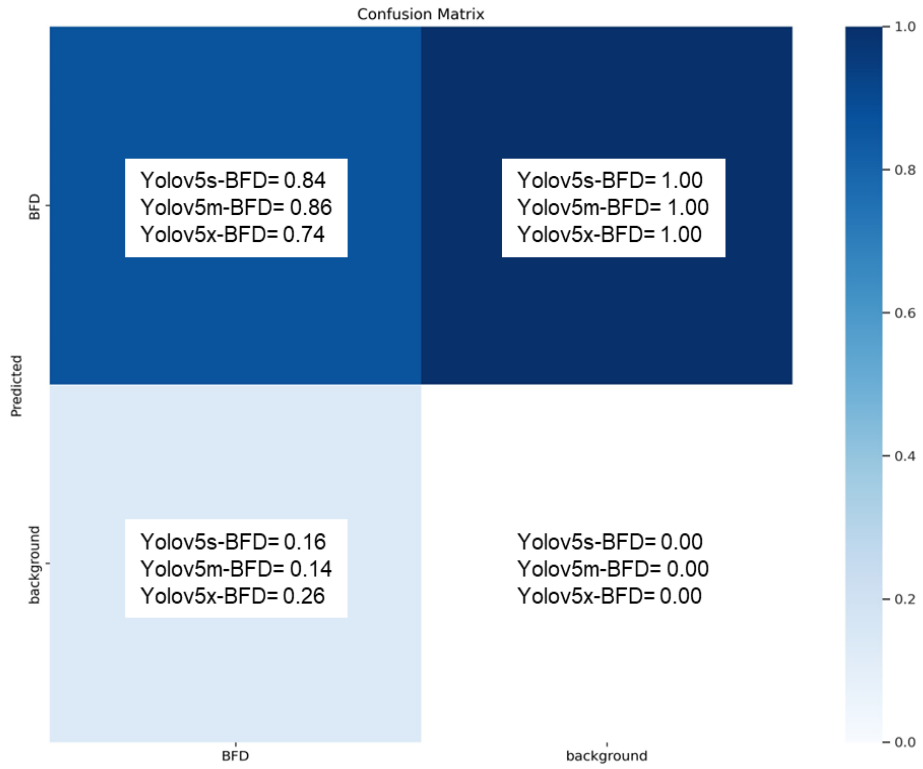

Figure 5.11: Comparison of YOLOv5-BFD models using confusion matrix.

5.3.1.1.2 Performances in data training and validation

Figure 5.12 shows each model's training and validation loss when each model was run at 100 epochs and 16 batch sizes. The training and validation loss function helps to determine and evaluate the model's performance. From Figure 5.12, the Val box loss, Val object loss, train box loss, and train object loss values decreased as the number of epochs increased. It is obvious that, in order to improve the model, the various losses should be minimized. However, the Val box loss

and Val object loss seem to be the highest in the YOLOv5x-BFD model, so this model was not a good fit for BFD.

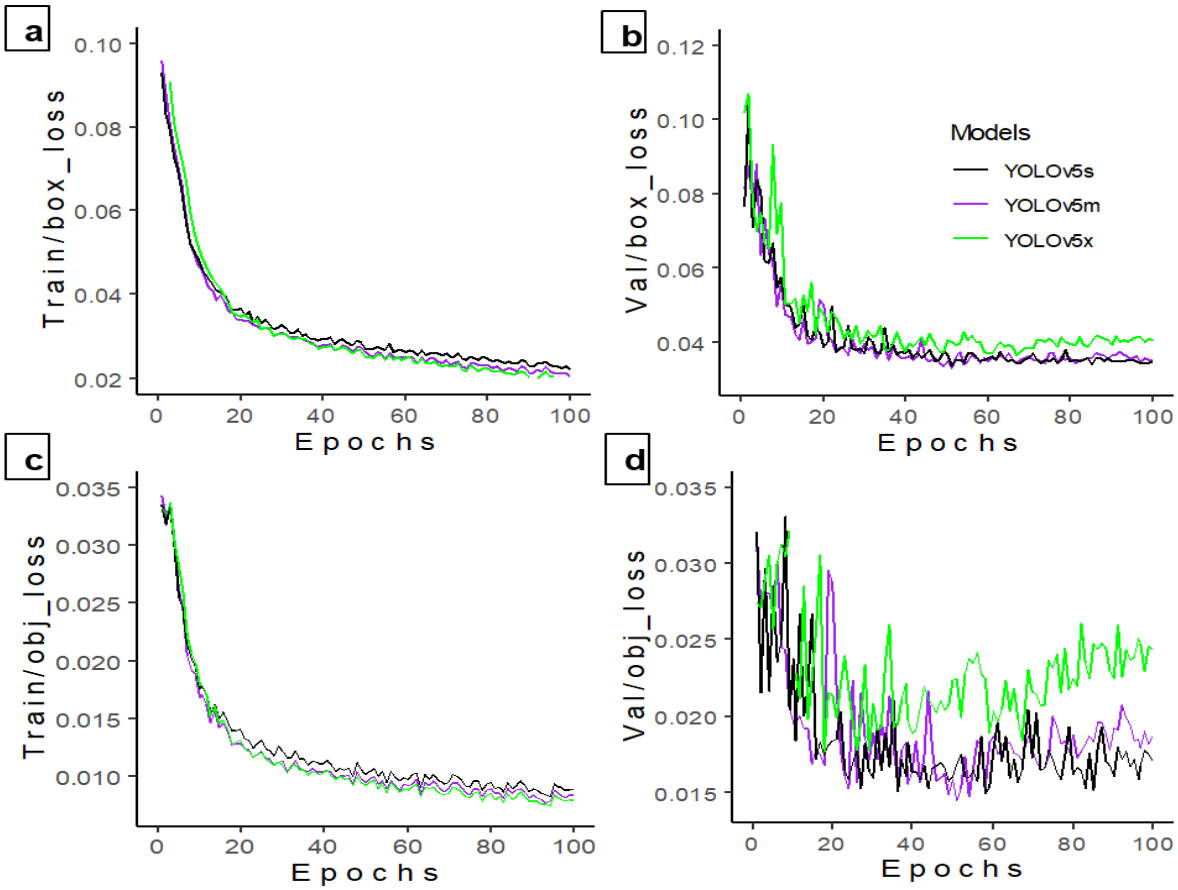

Figure 5.12: Training and validation result from a) Train/box_loss, b) Val/box_loss, c) Train/obj_losss, and d) Val/obj_loss of different YOLOv5 models.

Train- training; Val- validation; obj- object.

5.3.1.1.3 Model computing network performance

From Table 5.5, the model computing network performance for different YOLOv5 models was used, and performance was evaluated. When comparing different models, the computing parameters play an important role in speed, time consumption, and GPU usage. Higher speed and FPS image processing with lower training time and GPU usage are recommended for better

performance and productivity. When comparing all the computing parameters, YOLOv5s performs better by giving up to 26.2 FPS imaging processing speed, up to 145.0% higher training time, and up to 4.8 times less GPU usage. Therefore, the YOLOv5s outperforms in computing speed, whereas YOLOv5x shows poor computing performance.

Table 5.5: Comparison of the YOLOv5 model's performance in computing network performance.

Computing network	**YOLOv5s**	**YOLOv5m**	**YOLOv5x**
FPS	55.3	42.6	29.1
Parameters	7,012,822	20,852,934	86,173,414
Layer	157	212	322
GFLOPs	15.8	47.9	203.8
Epochs (its/s)	11.95	10.57	10.02
OSS used (MB)	14.3	42.1	173.0
Training time (hrs)*	0.420	0.535	1.029
GPU memory (GB)	1.04	1.83	4.95

FPS-frame per second; GFLOPs- Giga floating point operations per second; OSS- optimizer stripped space; it/s- iteration per second; hrs- hours; GB-gigabyte; MB-megabyte.

Overall, after comparing the performance metrics and computing parameters used, the YOLOv5m-BFD model performs better and higher in terms of performance metrics (precision, recall, mAP@0.50, and mAP@0.50:0.95) while performing a little slow in computing speed (27.4% higher training time) and GPU usage (1.8 times high) than YOLOv5s-BFD model. Sometimes, computing speed and GPU usage can be considered less if performance metrics are higher and best at target object detection.

5.3.2 Comparison Results of Different Classes using the YOLOv5m Model

Deep learning often overlooks batch sizes and epochs (Lee et al., 2019). However, it has a significant effect on network performance. The model's performance can be improved by adjusting the number of epochs and batch size. Larger batch sizes and lower epochs can lower the model's validation performance of the model so the right batch size and epochs should be chosen to enhance performance. However, batch size and epochs depend more on the object detection type and model.

5.3.2.1 Batch sizes

The results of different batch sizes and their effects on YOLOv5m-BFD model performance are shown in Table 5.6. As batch size increases, the precision increases while recall value decreases after batch size 8, which ultimately decreases mAP@0.50 and other performance metrics. For example, the batch size of 4 showed lower precision (89.2%), while the batch size 32 resulted in 94.4% precision. If we look at the recall, mAP@0.50, mAP@0.50:0.95, and F1-score decreased while increasing the batch size, but the performance metrics were higher for batch sizes 8 and 16, while the lowest was for batch size 32. The model's generalization ability appears to have deteriorated because of the large batch size (Lee et al., 2019). Therefore, Batch size 16 is recommended for enhancing model accuracy.

Table 5.6: Performance comparison of the YOLOv5-BFD model at different batch sizes.

Data summary*	Precision (%)	Recall (%)	mAP@0.50 (%)	mAP@ 0.50:0.95 (%)	F1-score	Training time (h)	GPU memory (GB)
BFD_{batch4}	89.2	79.8	85.5	48.9	84.0	0.932	1.27
BFD_{batch8}	89.7	86.9	90.1	52.4	88.0	0.498	1.34
$BFD_{batch16}$	93.7	84.6	90.9	51.8	89.0	0.535	1.83
$BFD_{batch32}$	94.4	75.2	85.2	48.7	84.0	0.204	3.38

*run at 100 epochs; BFD-Bumblefoot detection; mAP- mean average precision; GB-gigabytes.

Similarly, training time increases, and GPU usage decreases as batch size increases (Abri et al., 2019). Therefore, a larger batch size can help lower the GPU usage cost per epoch (Lee et al., 2019). For example, the training time for batch size 4 is higher because it takes a smaller number of images for training at one time (4 images at one time), but for batch size 32, training time decreases because it uses 32 images of total images at once for processing and it will be quick to finish training. In the case of GPU usage, the higher the number of images used for training, the higher the GPU usage. GPU usage was found to be highest for batch size 32 and lowest for batch size 4. Overall, based on the evaluation of performance, computing speed, and GPU usage, batch size 16 outperformed (Figure 5.13).

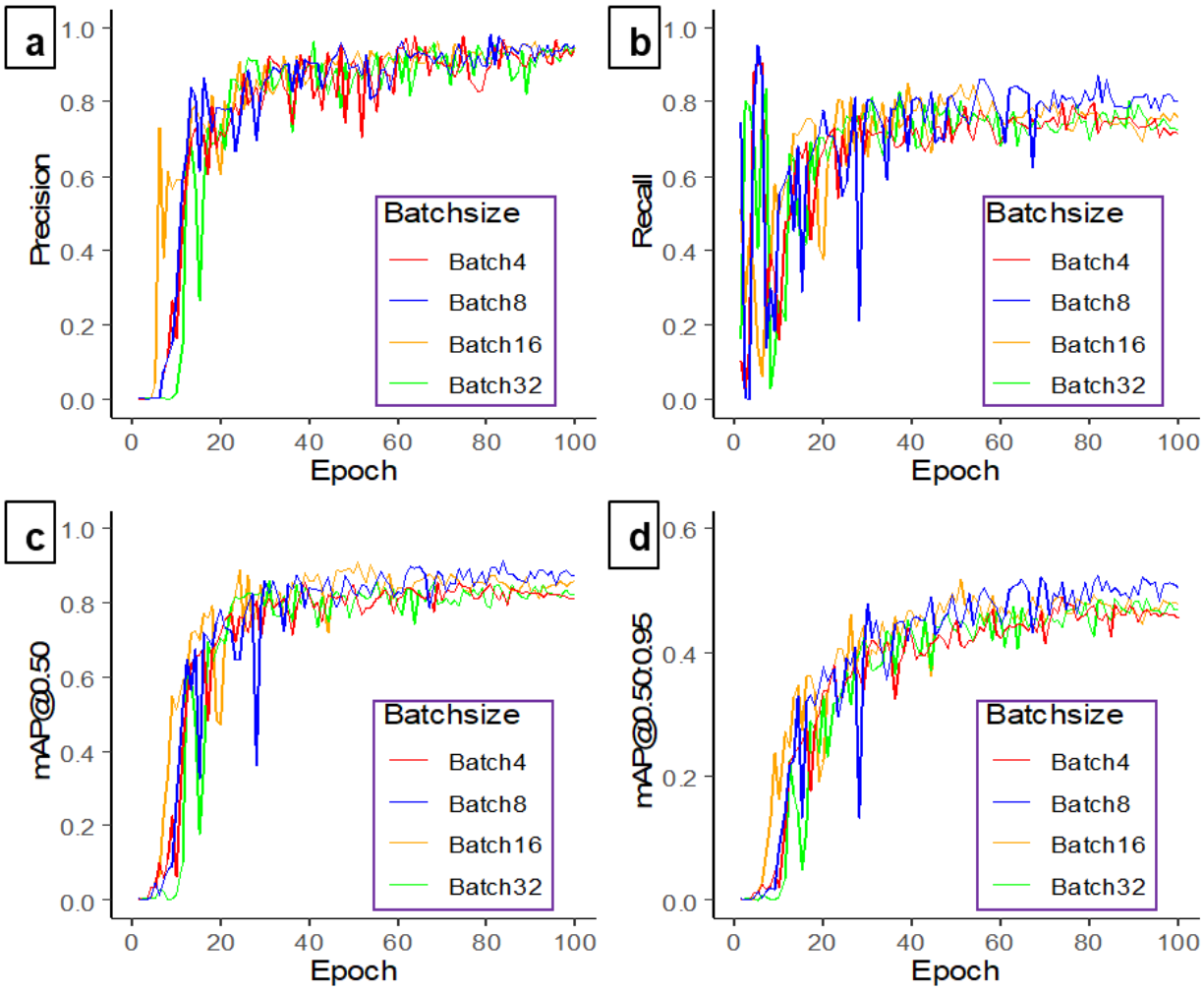

Figure 5.13: Performance metrics a) Precision, b) Recall, c) mAP@0.50, and d) mAP@0.50:0.95 of YOLOv5m-BFD model at different batch sizes.

5.3.2.2 Epochs

Table 5.7 shows the comparative results of the YOLOv5m model at different epochs in detecting hens' bumblefoot. In terms of precision, as the epochs number increases, the precision, mAP@0.50:0.95, and F1-score increases. For example, the YOLOv5m-BFD model of epoch 400 resulted in higher precision, mAP@0.50:0.95, and F1-score up to 10.7%, 36.9%, and 7%, respectively. However, the YOLOv5m-BFD model was stopped at 304 epochs because no

improvement was observed in the last 100 epochs; the best epoch was observed at 204. Therefore, there was a chance to consider 200 epochs, but the YOLOv5m-BFD model ran at 200 epochs and stopped at 192 epochs because no improvement was observed in the last 100 epochs; the best epoch was observed at 92. Although the model stopped before the set epochs, the model trained with epoch 400 should be considered for future detection model training because of better detection results. According to Lee et al. (2019), a larger epoch size slows the model training speed, which, in turn, achieves lower validation accuracy. However, we found the highest validation results with more training time consumption. It appears that longer training durations lead to improved accuracy in the result. The overall performance metrics were comparatively highest at epoch 400, as seen in Figure 5.14.

Table 5.7: Performance comparison of the YOLOv5m-BFD model at different epochs.

Data summary*	**Precision (%)**	**Recall (%)**	**mAP@0.50 (%)**	**mAP@ 0.50:0.95 (%)**	**F1-score**	**Training time (h)**	**GPU memory (GB)**
$BFD_{epoch50}$	88.0	76.0	82.2	46.6	82.0	0.258	1.34
$BFD_{epoch100}$	89.7	86.9	90.1	52.4	88.0	0.498	1.34
$BFD_{epoch200}$	94.9	77.2	90.6	51.7	85.0	0.919	1.34
$BFD_{epoch400}$	98.7	80.8	89.2	83.5	89.0	1.471	1.34

*run at batch size 16; BFD-Bumblefoot detection; mAP- mean average precision; GB-gigabytes.

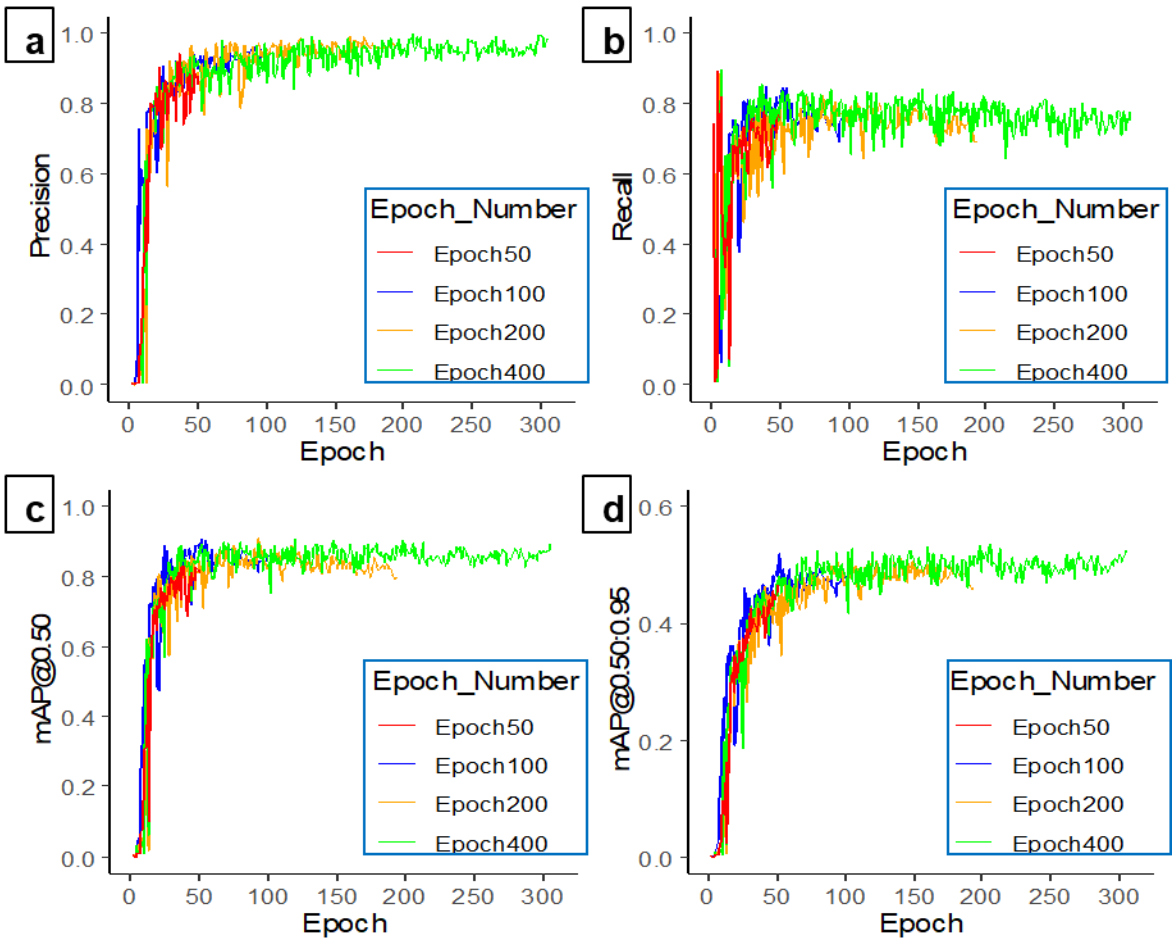

Figure 5.14: Performance metrics a) Precision, b) Recall, c) mAP@0.50, and d) mAP@0.50:0.95 of YOLOv5m-BFD model at different epochs.

5.3.2.3 Camera settings

The camera's height affects the model detection and depends on the objects used. For example, Li et al. (2020) used cameras at various heights to detect floor eggs but found no significant difference in accuracy. However, in Table 5.8, camera height showed a huge difference in precision, recall, mAP@0.50, mAP@0.50:0.95, and F1-score for the detection model. Camera height at 30cm resulted in 12.6%, 22.3%, 19.6%, 12.6%, and 17% higher precision, recall, mAP@0.50, mAP@0.50:0.95, and F1-score, respectively, than height at 50cm. Camera height

might differ in the accuracy of detecting objects based on object conditions, whether objects are moving, fixed, or of variable shape and size. Thus, the camera height of 30cm best performs for BFD and can be seen in Figures 5.15 and 5.16.

Table 5.8: Performance comparison of the YOLOv5-BFD model for different heights.

Data summary*	**Precision (%)**	**Recall (%)**	**mAP@0.50 (%)**	**mAP@ 0.50:0.95 (%)**	**F1-score**	**Training time (h)**
$BFD_{height30cm}$	89.7	86.9	90.1	52.4	88.0	0.497
$BFD_{height50cm}$	77.1	64.6	70.5	39.8	71.0	0.506

*run at batch size 16, epoch 100; BFD-Bumblefoot detection; mAP- mean average precision.

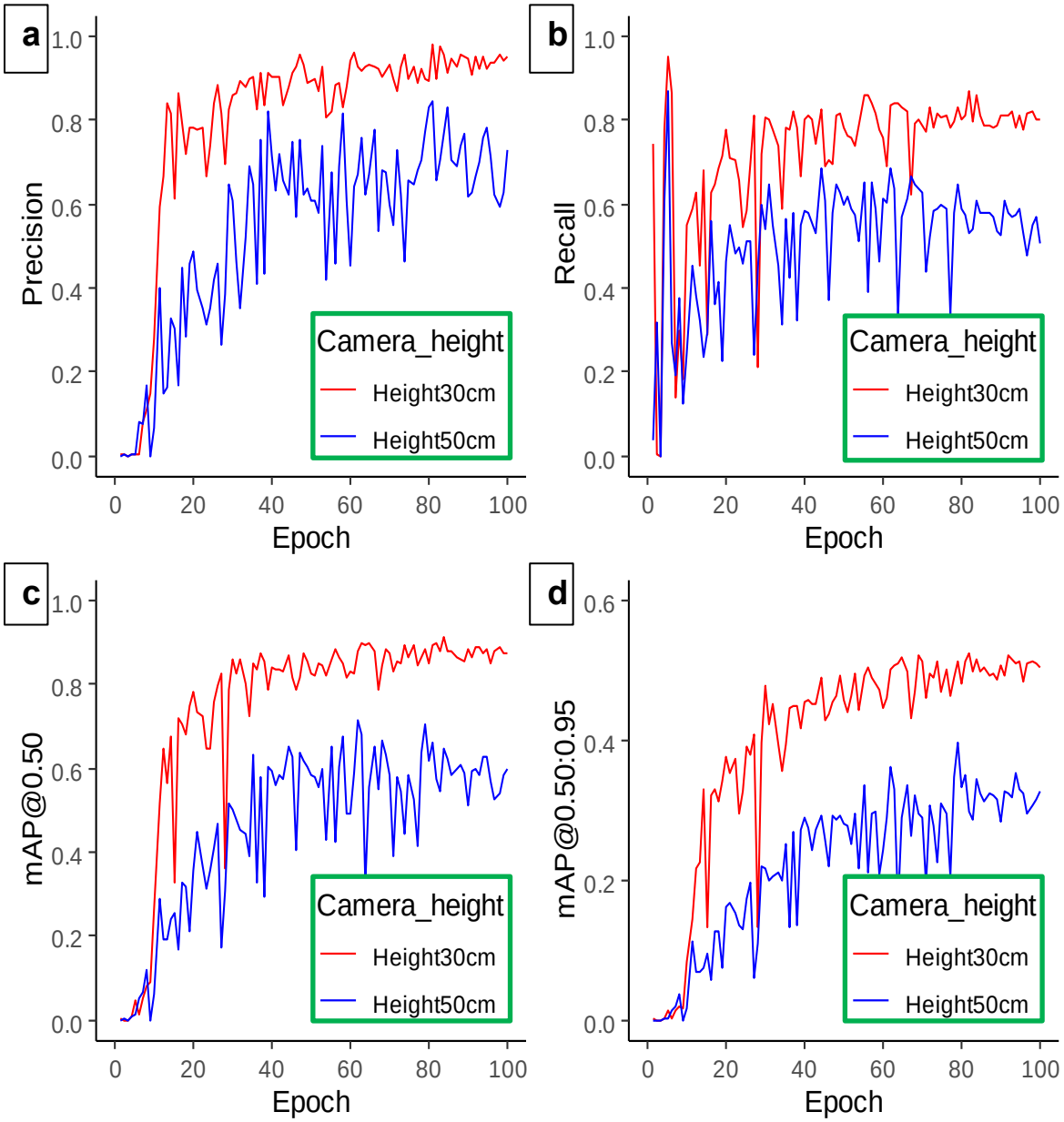

Figure 5.15: Performance metrics a) Precision, b) Recall, c) mAP@0.50, and d) mAP@0.50:0.95 of YOLOv5m-BFD model at a different height.

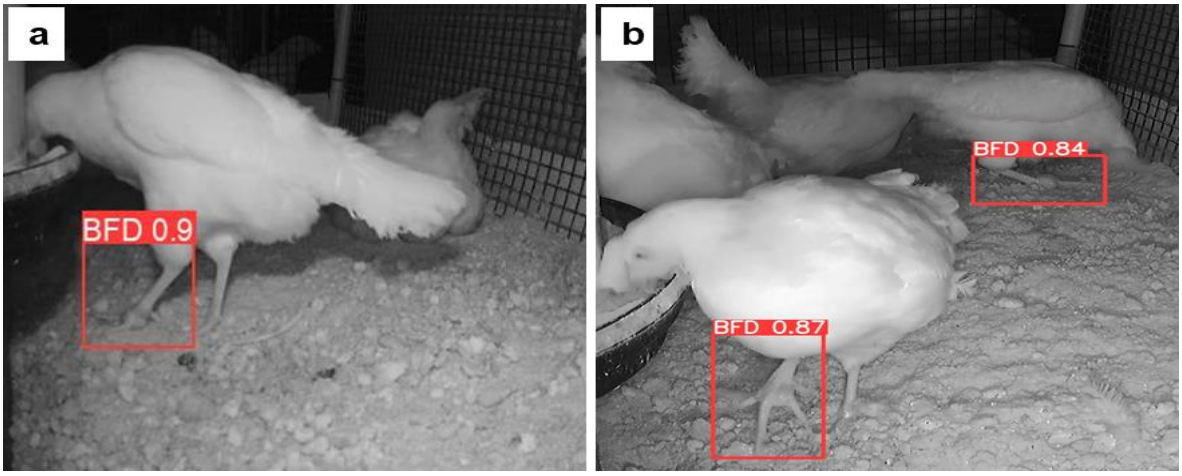

Figure 5.16: YOLOv5m detection results of bumblefoot at the camera: a) height of 30 cm and b) height of 50 cm. BFD- bumblefoot detection.

Since bumblefoot is small and found in digital pads, plantar metatarsal, or both, it is very hard to detect when a hen is far from the camera. As camera height increases, the distance from the targeted object increases, thus increasing train box loss, train object loss, Val object loss, and Val box loss (Figure 5.17). As a result of BFD at the height of 50cm, the Val box loss and Val object loss were the highest, which resulted in the lowest detection performance.

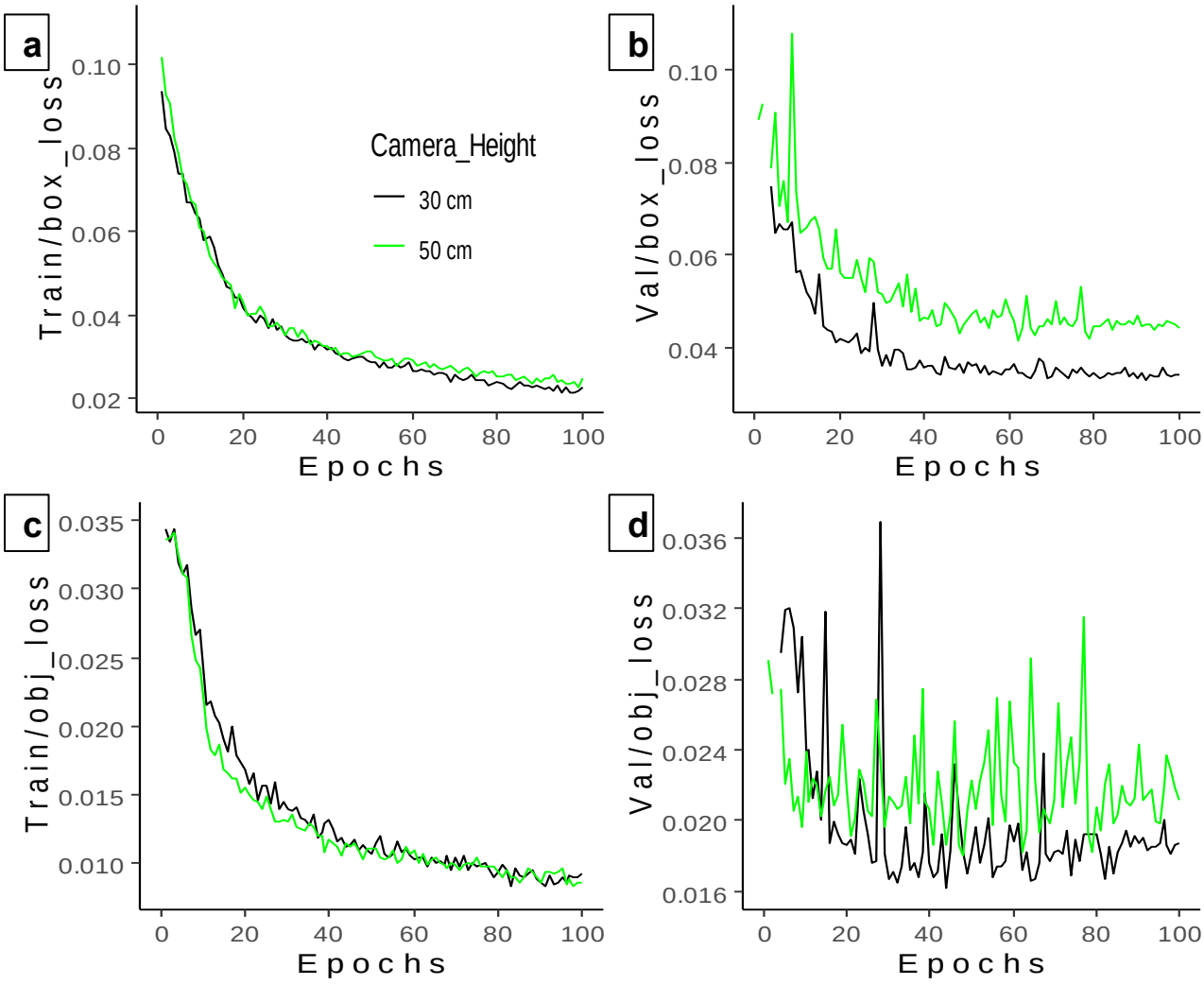

Figure 5.17: Training and validation results a) train/box loss, b) val/box loss, c) train/object loss, and d) val/object loss of the YOLOv5m-BFD models at different camera heights.

BFD- bumblefoot detection; Train- training; Val- validation; obj- object.

5.3.3 Limitations and Future Directions

The YOLOv5 model assists in accurately identifying bumblefoot conditions in laying hens, yet it has notable limitations. Firstly, detection becomes challenging when birds are densely packed together, as the occlusion of bumblefoot by neighboring hens impedes accurate detection. Secondly, environmental factors such as higher dust concentrations in cage-free housing can

obscure camera lenses, necessitating regular cleaning. Thirdly, the study's experimental setup with fewer hens per room than commercial housing may pose challenges in scaling up detection for larger groups of hens. To address these limitations, continual testing, data collection, and model training with commercial hen images are essential for enhancing detection accuracy.

Furthermore, the presence of manure on litter floors can obscure bumblefoot conditions or artificially enlarge foot sizes, reducing detection accuracy. Despite these limitations, the research offers an innovative solution for early detection of footpad conditions, providing producers with timely alerts to address worsening conditions. Future improvements entail training the model on large commercial datasets and considering various environmental scenarios affecting footpad health. Additionally, future iterations aim to detect bumblefoot and identify factors contributing to its occurrence. Ultimately, achieving near-perfect accuracy in bumblefoot detection across different hen types (white, brown, broilers) will enhance user-friendliness for producers, who can install cameras and connect to the system for real-time monitoring. Regular updates to the model or software will ensure continual improvement in accuracy. Early detection of bumblefoot conditions enables prompt intervention, improving footpad health and overall animal welfare.

5.4 CONCLUSIONS

The YOLOv5m-BFD model demonstrated superior performance in bumblefoot detection compared to other models. In addition, the model trained with batch size 16 and epochs 400 resulted in higher detection results. Similarly, a lower camera height (30 cm) for capturing closer imaging of chicken feet is recommended for future bumblefoot detection. The success of this model establishes a foundation for the development of a ground robot for bumblefoot scanning in

CF houses, with future plans to extend its application to commercial broiler and layer housing. Early bumblefoot detection facilitated by this technology holds promise for improving animal welfare and overall farm productivity by early detection.

5.5 REFERENCES

Abrahamsson, P., O. Fossum, and R. Tauson. 1998. Health of Laying Hens in an Aviary System over Five Batches of Birds. Acta Vet Scand 39:367–379. Available at https://doi.org/10.1186/BF03547785 (verified 4 April 2024).

Abrahamsson, P., and R. Tauson. 1995. Aviary systems and conventional cages for laying hens: Effects on production, egg quality, health and bird location in three hybrids. Acta Agriculturae Scandinavica A-Animal Sciences 45:191–203.

Abri, F., S. Siami-Namini, M. A. Khanghah, F. M. Soltani, and A. S. Namin. 2019. Can machine/deep learning classifiers detect zero-day malware with high accuracy? Pages 3252–3259 in IEEE.

Ben Sassi, N., X. Averós, and I. Estevez. 2016. Technology and poultry welfare. Animals 6:62. https://doi.org/10.3390/ani6100062.

Berg, L. 1998. Foot-pad dermatitis in broilers and turkeys. Acta Univ. Agric. Sueciae Vet, 36, 7-43. Available at https://pub.epsilon.slu.se/1514/1/Lotta_Berg_Avhandling.pdf.

Bilgili, S., J. Hess, J. Blake, K. Macklin, B. Saenmahayak, and J. Sibley. 2009. Influence of bedding material on footpad dermatitis in broiler chickens. Journal of Applied Poultry Research 18:583–589.

Bist, R. B., S. Subedi, X. Yang, and L. Chai. 2023a. Automatic Detection of Cage-Free Dead Hens with Deep Learning Methods. AgriEngineering 5:1020–1038 Available at https://www.mdpi.com/2624-7402/5/2/64 (verified 29 August 2023).

Bist, R. B., X. Yang, S. Subedi, and L. Chai. 2023b. Mislaying behavior detection in cage-free hens with deep learning technologies. Poultry Science 102:102729.

Bochkovskiy, A., C.-Y. Wang, and H.-Y. M. Liao. 2020. Yolov4: Optimal speed and accuracy of object detection. arXiv preprint arXiv:2004.10934.

Bradshaw, R., R. Kirkden, and D. Broom. 2002. A review of the aetiology and pathology of leg weakness in broilers in relation to welfare. Avian and poultry biology reviews 13:45–104.

Choudhury, D. 2019. Management of Bumble Foot in Duck. Int. J. Curr. Microbiol. App. Sci 8:12–15. Available at https://www.researchgate.net/profile/Dimpi-Choudhury-2/publication/362909440_Management_of_Bumble_Foot_in_Duck/links/630716ff1ddd44702108b8f5/Management-of-Bumble-Foot-in-Duck.pdf.

Chuppava, B., C. Visscher, and J. Kamphues. 2018. Effect of different flooring designs on the performance and foot pad health in broilers and turkeys. Animals 8:70. https://doi.org/10.3390/ani8050070.

Coles, B. H. 2007. Essentials of Avian Medicine and Surgery. 1st ed. Wiley. John Wiley & Sons, ISBN 978-1-4051-5755-1.

Craven, M., E. De Haas, D. Van Grembergen, T. Boswell, J. Guy, F. Tuyttens, and T. Smulders. 2021. Does footpad dermatitis induce a chronic negative welfare state in laying hens? In 54th Congress of the International Society for Applied Ethology (ISAE2021) (pp. 255-255).

De Jong, I. C., H. Gunnink, and J. Van Harn. 2014. Wet litter not only induces footpad dermatitis but also reduces overall welfare, technical performance, and carcass yield in broiler chickens. Journal of Applied Poultry Research 23:51–58.

Fulton, R. M. 2019. Health of commercial egg laying chickens in different housing systems. Avian diseases 63:420–426. https://doi.org/10.1637/11942-080618-Reg.1.

Gebhardt-Henrich, S. G., and E. K. Frohlich. 2015. Early onset of laying and bumblefoot favor keel bone fractures. Animals 5:1192–1206. https://doi.org/10.3390/ani5040406.

Harms, R. H., and C. Simpson. 1975. Biotin deficiency as a possible cause of swelling and ulceration of foot pads. Poultry Science 54:1711–1713. https://doi.org/10.3382/ps.0541711.

He, K., X. Zhang, S. Ren, and J. Sun. 2015. Spatial pyramid pooling in deep convolutional networks for visual recognition. IEEE transactions on pattern analysis and machine intelligence 37:1904–1916. https://doi.org/10.1109/TPAMI.2015.2389824.

Heidemann Olsen, R., H. Christensen, S. Kabell, and M. Bisgaard. 2018. Characterization of prevalent bacterial pathogens associated with pododermatitis in table egg layers. Avian Pathology 47:281–285.

Hester, P. 1994. The role of environment and management on leg abnormalities in meat-type fowl. Poultry Science 73:904–915.

Huang, R., J. Pedoeem, and C. Chen. 2018. YOLO-LITE: a real-time object detection algorithm optimized for non-GPU computers.Pages 2503–2510 in IEEE.

Jocher, G. 2021. YOLOv5 Focus() Layer · ultralytics yolov5 · Discussion #3181. GitHub Available at https://github.com/ultralytics/yolov5/discussions/3181 (verified 15 March 2023).

Jocher, G. 2022. YOLOv5 (6.0/6.1) brief summary · Issue #6998 · ultralytics/yolov5. GitHub Available at https://github.com/ultralytics/yolov5/issues/6998 (verified 10 March 2023).

Lay Jr, D., R. Fulton, P. Hester, D. Karcher, J. Kjaer, J. A. Mench, B. Mullens, R. C. Newberry, C. J. Nicol, and N. P. O'Sullivan. 2011. Hen welfare in different housing systems. Poultry science 90:278–294.

Lee, S., Q. Kang, S. Madireddy, P. Balaprakash, A. Agrawal, A. Choudhary, R. Archibald, and W. Liao. 2019. Improving scalability of parallel CNN training by adjusting mini-batch size at run-time.Pages 830–839 in IEEE.

Li, G., Y. Xu, Y. Zhao, Q. Du, and Y. Huang. 2020. Evaluating convolutional neural networks for cage-free floor egg detection. Sensors 20:332.

Lin, T.-Y., P. Dollár, R. Girshick, K. He, B. Hariharan, and S. Belongie. 2017. Feature pyramid networks for object detection.Pages 2117–2125

Liu, S., L. Qi, H. Qin, J. Shi, and J. Jia. 2018. Path aggregation network for instance segmentation.Pages 8759–8768

Martrenchar, A., E. Boilletot, D. Huonnic, and F. Pol. 2002. Risk factors for foot-pad dermatitis in chicken and turkey broilers in France. Preventive Veterinary Medicine 52:213–226.

McNamee, P. T., and J. A. Smyth. 2000. Bacterial chondronecrosis with osteomyelitis ('femoral head necrosis') of broiler chickens: a review. Avian Pathology 29:477–495.

Nagaraj, M., C. Wilson, J. Hess, and S. Bilgili. 2007. Effect of high-protein and all-vegetable diets on the incidence and severity of pododermatitis in broiler chickens. Journal of applied poultry research 16:304–312.

NCC. 2018. National chicken council animal welfare guidelines and audit checklist for broilers. Available at https://www.nationalchickencouncil.org/wp-content/uploads/2018/07/NCC-Animal-Welfare-Guidelines_Broilers_July2018.pdf.

Shafiee, M. J., B. Chywl, F. Li, and A. Wong. 2017. Fast YOLO: A fast you only look once system for real-time embedded object detection in video. arXiv preprint arXiv:1709.05943.

Shepherd, E., and B. Fairchild. 2010. Footpad dermatitis in poultry. Poultry science 89:2043–2051.

Stransky, O., R. Blum, W. Brown, D. Kruse, and P. Stone. 2016. Bumble Foot: A Rare Presentation of a Fusobacterium varium Infection of the Heel Pad in a Healthy Female. The Journal of Foot and Ankle Surgery 55:1087–1090.

Subedi, S., R. Bist, X. Yang, and L. Chai. 2023a. Tracking pecking behaviors and damages of cage-free laying hens with machine vision technologies. Computers and Electronics in Agriculture 204:107545.

Subedi, S., R. Bist, X. Yang, and L. Chai. 2023b. Tracking Floor Eggs with Machine Vision in Cage-free Hen Houses. Poultry Science:102637 Available at https://www.sciencedirect.com/science/article/pii/S003257912300161X (verified 10 March 2023).

Tauson, R. 1998. Health and production in improved cage designs. Poultry Science 77:1820–1827.

Tauson, R. 2002. Furnished cages and aviaries: production and health. World's Poultry Science Journal 58:49–63 Available at https://www.tandfonline.com/doi/full/10.1079/WPS20020007 (verified 4 April 2024).

Tauson, R., and P. Abrahamsson. 1996. Foot and keel bone disorders in laying hens: Effects of artificial perch material and hybrid. Acta Agriculturae Scandinavica A-Animal Sciences 46:239–246.

Tauson, R., A. Wahlström, and P. Abrahamsson. 1999. Effect of two floor housing systems and cages on health, production, and fear response in layers. Journal of Applied Poultry Research 8:152–159.

Wang, G., C. Ekstrand, and J. Svedberg. 1998. Wet litter and perches as risk factors for the development of foot pad dermatitis in floor-housed hens. British Poultry Science 39:191–197.

Wang, C.-Y., H.-Y. M. Liao, Y.-H. Wu, P.-Y. Chen, J.-W. Hsieh, and I.-H. Yeh. 2020. CSPNet: A new backbone that can enhance learning capability of CNN.Pages 390–391

Wilcox, C. S., J. Patterson, and H. W. Cheng. 2009. Use of thermography to screen for subclinical bumblefoot in poultry. Poult Sci 88:1176–1180.

Yang, X., R. B. Bist, S. Subedi, and L. Chai. 2023a. A Computer Vision-Based Automatic System for Egg Grading and Defect Detection. Animals 13:2354.

Yang, X., R. Bist, S. Subedi, Z. Wu, T. Liu, and L. Chai. 2023b. An automatic classifier for monitoring applied behaviors of cage-free laying hens with deep learning. Engineering Applications of Artificial Intelligence 123:106377 Available at https://www.sciencedirect.com/science/article/pii/S0952197623005614 (verified 29 August 2023).

Yang, X., L. Chai, R. B. Bist, S. Subedi, and Z. Wu. 2022. A Deep Learning Model for Detecting Cage-Free Hens on the Litter Floor. Animals 12:1983.

Yao, J., J. Qi, J. Zhang, H. Shao, J. Yang, and X. Li. 2021. A real-time detection algorithm for Kiwifruit defects based on YOLOv5. Electronics 10:1711.

Youssef, F., A. Soliman, G. Ibrahim, and H. Saleh. 2019. Advanced bacteriological studies on bumblefoot infections in broiler chicken with some clinicopathological alteration. Vetry Sci Rech 1:1–9.

Zhu, X. Y., C. C. Wu, and P. Y. Hester. 1999. Induction of the delayed footpad and wattle reaction to killed Staphylococcus aureus in chickens. Poultry science 78:346–352.

CHAPTER 6

AUTOMATIC FOOTPAD DERMATITIS SCORING IN CHICKENS WITH MACHINE VISION METHODS[5]

[5] Bist, R. B., Subedi, S., Yang, X., Li, G., and Chai, L. 2024. Automatic Footpad Dermatitis Scoring in Poultry using Machine Learning Models. *Under-Review.*

ABSTRACT

Footpad dermatitis (FPD) can negatively influence hen production, welfare, and health. However, there is currently no tool for automatic FPD scoring. The objective of this study was to develop and optimize deep learning models to automatically score hen FPD on a 0-2 scale, with higher scores indicating poorer footpad conditions. 700 Hy-Line W-36 hens were raised in four cage-free rooms integrated with Electrostatic Particle Ionization and various bedding materials. A GoPro camera with an upward lens was placed inside a transparent box. Individual laying hens were placed on the top surface of the box to acquire RGB images. In addition, a thermal camera was used to record RGB and thermal images of footpads, and the images were manually scored to assess footpad conditions. Preprocessing techniques (e.g., filtration, separation, and augmentation) were deployed to enhance dataset quality and size. Moreover, five YOLOv8 models (YOLOv8n, YOLOv8s, YOLOv8m, YOLOv8l, and YOLOv8x) were comparatively evaluated for predicting FPD scores. The results show that the YOLOv8l outperformed other models, with higher recall (96.6%), mAP@0.50 (97.0%), and F1-score (95.0%). Additionally, the YOLOv8l-FPD model exhibited a high mAP@0.50 for score 0 (98.0%), score 1 (95.0%), and score 2 (97.9%) and F1-score (95.0%) for all FPD scores. Notably, using thermal images could result in faster convergence of model training and slightly better FPD score prediction performance than RGB images. The proposed technique can be useful for non-invasive automatic FPD scoring and further improve automation levels and animal welfare in the egg industry.

Keywords: Poultry house; Footpad scoring; Animal welfare; Machine learning, YOLOv8

6.1 INTRODUCTION

The global demand for food is increasing due to a growing population, and the egg industry plays a vital role by providing affordable, nutritious, and safe daily protein for humans. To meet the increasing demand, the number of laying hens increased from 308 million in 2022 to 322 million in 2023, with daily egg consumption projected to be 277 to 289 eggs per person in the USA (Statista, 2023; UEP, 2023). In addition, the egg industry is transitioning to cage-free (CF) systems due to public demand and welfare concerns (UEP, 2023; USDA, 2020), and CF production proportion is projected to reach 66% by 2026 (UEP, 2023). These CF housings pose several animal welfare concerns in the egg industry, among which footpad dermatitis (FPD) is a major concern (AMER, 2020; Kaukonen et al., 2016; Shepherd and Fairchild, 2010; Wilcox et al., 2009).

FPD, also known as pododermatitis, is a widespread condition affecting laying hens (Berg, 2004, 1998; Stransky et al., 2016). It is characterized by the development of inflammatory lesions, ulcers, and necrotic tissue on the plantar surface of the hens' feet (Berg, 2004; Shepherd and Fairchild, 2010; Stransky et al., 2016; Wilcox et al., 2009). FPD condition is often influenced by a combination of environmental factors, including litter quality (Bilgili et al., 2009; Dozier et al., 2005; NCC, 2018), litter depth (Ekstrand et al., 1997; Meluzzi et al., 2008), floor conditions (Fulton, 2019; Heerkens et al., 2016), stocking density (Dozier et al., 2005; Sorensen et al., 2000; Zhang et al., 2011), drinker design and management (Ekstrand et al., 1997); and intrinsic factors like genetics (Allain et al., 2009; Chavez and Kratzer, 1972; Kjaer et al., 2006), nutrition (Eichner et al., 2007; Nagaraj et al., 2007), and overall health. FPD lesions can cause pain and discomfort in affected birds impacting their perching, walking, and access to

food and water resources (Chuppava, 2018; De Jong et al., 2014; Hester, 1994). Such challenges could further lead to reduced body weight, decreased egg production, and heightened veterinary expenditures.

Various solutions have been researched to address FPD, including improving litter quality (Bilgili et al., 2009; Martland, 1985, 1984; Shepherd and Fairchild, 2010), optimizing housing conditions to reduce overcrowding (Dozier et al., 2005; Fulton, 2019; Sorensen et al., 2000; Zhang et al., 2011), and developing specialized diets to enhance the hens' overall health and resilience (Eichner et al., 2007; Nagaraj et al., 2007). Tackling FPD directly impacts the welfare of laying hens, ensuring that they can exhibit their natural behaviors and reduce pain during their lifespans while improving industry viability and productivity. Early FPD assessment can also help with timely intervention and reinforce consumer confidence in buying welfare-labeled products. The gold standard manual FPD assessment could be time-consuming and laborious and needs skilled welfare assessors, which could be limited due to labor shortages in farm work. Computer vision for data collection and machine learning for data analysis offer an alternative efficient solution for FPD scoring, which can overcome the abovementioned manual assessment drawbacks.

In recent years, the YOLO (You Only Look Once) family models have gained significant prominence due to their exceptional speed and accuracy in object detection tasks (Bist et al., 2023a, 2023c; Guo et al., 2023; Li et al., 2023; Sorbelli et al., 2023; Subedi et al., 2023a; Yan et al., 2021; Yang et al., 2022; X. Yang et al., 2023a). Previous studies have explored the applicability of YOLO models in CF housing with highest accuracy in bird monitoring (Chen et

al., 2023; Guo et al., 2023; Hong et al., 2019; Yang et al., 2022; X. Yang et al., 2023a) and detection of piling behavior (Bist et al., 2023a), mislaying behavior (Bist et al., 2023c), pecking behavior (Subedi et al., 2023a), mortality (Bist et al., 2023b; Muvva et al., 2018), and floor eggs (Subedi et al., 2023b; X. Yang et al., 2023b). Built on the similar YOLO family model architecture, the recent YOLO model, YOLOv8, was improved by incorporating improvements in backbone design, feature fusion mechanisms, and training strategies (Jocher et al., 2023b). However, the model's accuracy and efficiency remained unclear when predicting FPD scores. This research aimed to develop and optimize YOLOv8 models to detect and score the FPD automatically.

6.2 MATERIALS AND METHODS

6.2.1 Experimental Housing and Management

This experiment follows the same housing and bird management practices as described in Chapter 2 of section 2.2.1. Each rooms were provided with 175 Hy-line W-36 laying hens, totaling 700 hens for four rooms. The study collected RGB video data with a GoPro camera (GoPro, Inc., San Mateo, California, USA) over a week when the hens were 85 weeks of age.

6.2.2 Treatments and Experimental Groups

The study integrated two treatments: a) the combined Electrostatic Particle Ionization (EPI) system (EPIAir, Columbia, MO, USA) and bedding material (BM) treatment, and b) control rooms without the EPI+BM intervention. Within each room, a top-dressing of wood chips (Beta Chips, Northeastern Products Corp., Warrensburg, NY, USA) was supplemented to 6 cm-deep litter when laying hens were 82 weeks of age, accounting for 20% of the initial litter

depth. The EPI systems, each measuring 11 m in length, were positioned 2.44 m above the litter floor and operated continuously. This study utilized four rooms for FPD scoring, with two as treatment rooms (EPI+BM rooms) and the other two as control rooms. The research involved capturing videos of footpad conditions randomly recorded across all four rooms.

6.2.3 Footpad Dermatitis Assessment

Forty hens (>20% of the total hen counts per room) were randomly selected from each room after four weeks of treatment to initiate the video recording process for FPD assessment. The FPD scoring was based on guidelines outlined by the previous papers (AAAP, 2022; GAP, 2020) (Table 6.1). Before video recording was started, a trained Ph.D. student conducted the FPD scoring on randomly selected hens and assigned scores ranging from 0 (indicating normal footpad condition) to 2 (indicating severe dermatitis condition). Manual FPD scoring was done to find the footpad condition before starting the recording.

Table 6.1: Evaluating footpad scoring in different footpad conditions.

FPD score	Footpad condition	Figures
Score 0	➢ Normal color. ➢ No lesions. ➢ No discoloration or slight area. ➢ Old scars or no scarring.	
Score 1	➢ Mild and/or superficial lesions. ➢ Footpad discoloration. ➢ Dark papillae without ulceration. ➢ Lesion(s) covering less than $^1/_2$ of footpad.	
Score 2	➢ Severe lesions with ulceration and significant damage. ➢ Dark papillae with ulceration. ➢ Abscesses and/ or swollen footpad. ➢ Lesion(s) covering more than $^1/_2$ of footpad.	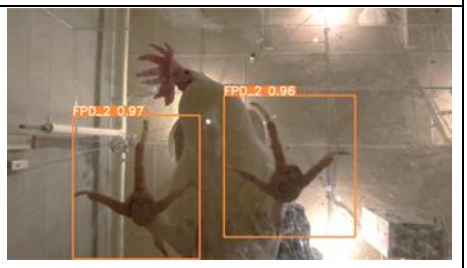

The figure in the table showcases rectangular bounding boxes corresponding to various footpad dermatitis (FPD) scores detected by a model, along with their associated confidence scores.

6.2.4 Footpad Condition Image Data Acquisition

Two GoPro Hero11 Black cameras (GoPro, Inc., San Mateo, California, USA) were utilized for this purpose within treatment and control rooms, with each 2-hour daily recording session per room managed to account for the GoPro's battery limitations. The cameras were positioned in a transparent acrylic display box (Academy Sport, Houston, Texas, USA) to ensure consistent data collection, measuring 0.3 m long × 0.2 m wide × 0.2 m high (Figure 6.1a). The transparent display box was used to record a clear picture of FPD conditions and prevent damage to the camera caused by laying hens. A 7-day video recording (total 56 hours) was started to monitor FPD following manual FPD scoring. Initially, we randomly selected hens for a two-day training phase, where they were trained to stand and sit over a glass box, with video recordings taken. Following the training and two days of video recording, we left the box with a GoPro camera on for the remaining five days and observed hens standing and sitting on it. The recorded video data was analyzed to identify and score FPD condition.

Similarly, the specialized thermal image system was employed to accurately capture FPD thermal images of footpads, as depicted in Figure 6.1b. Utilizing a professional thermal imager (FLIR T540, FLIR Systems, Wilsonville, Oregon, USA) equipped with an adjustable lens (14°–24°), thermal images of the hens were meticulously acquired. The camera was positioned at 0.6 meters above the targeted bird's footpad to ensure the utmost image quality. The process of recording image datasets using the thermal camera commenced before and after the initiation of GoPro recording by holding the bird's two legs with trained personnel. During the thermal imaging, 400 randomly selected hens (constituting over 50% of the flock) were consistently employed to gather the requisite thermal image data. Furthermore, the FLIR Thermal Studio

software was adeptly utilized to extract the RGB images to benchmark predictive accuracy. This streamlined approach created dual datasets for each measured bird: the RGB and thermal datasets. In this research, both RGB and thermal images generated from the thermal camera were meticulously labeled and analyzed to discern differences in detection based on image types.

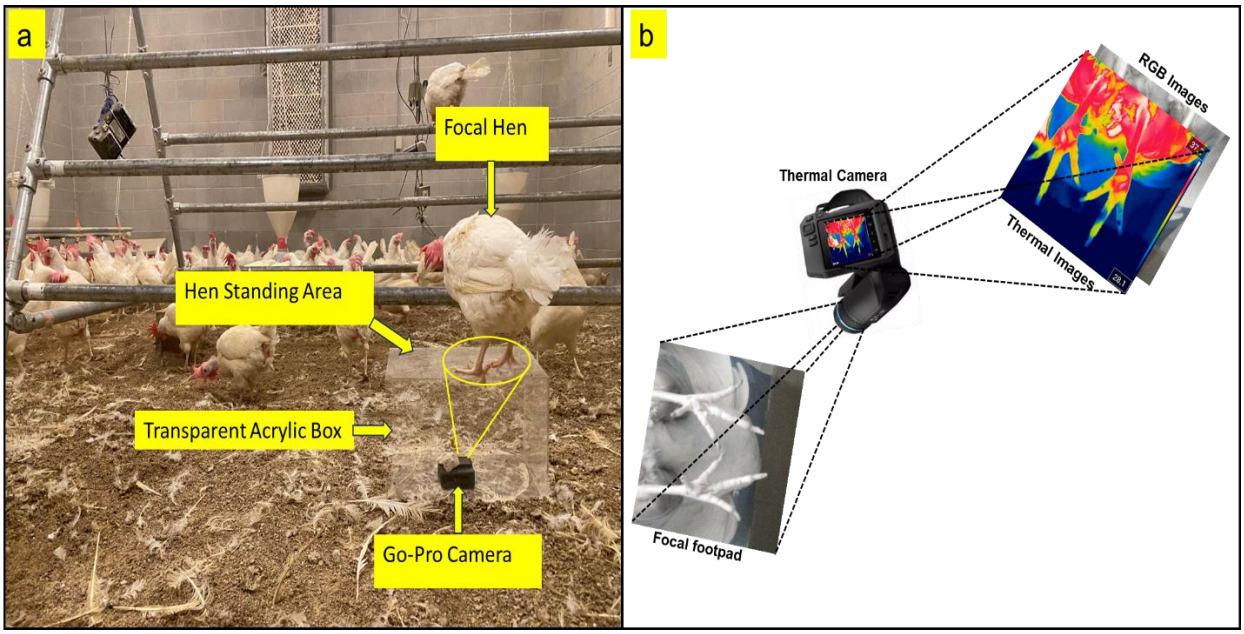

Figure 6.1: Footpad dermatitis conditions recording set up in cage-free hen rooms using a) GoPro camera and b) Thermal camera.

6.2.5 Image Labeling and Data Preprocessing

The video datasets captured by the GoPro camera were converted into image files (.jpg) via the Free Video to JPG Converter App (version 5.0) at a sampling rate of 15 frames per second (FPS). Following this, the obtained image datasets were subjected to manual filtration, separation, and a data augmentation process encompassing rotation, cropping, resizing, scaling, horizontal and vertical flipping, and color jittering. These augmentation techniques enhanced the dataset's diversity and robustness, driven by the need to observe FPD within the images.

Subsequently, a collection of 3,150 images was separated for the FPD_{all} category, while an additional 1,800 images were extracted from the thermal camera, encompassing both thermal and RGB images (Table 6.2). These selected images were subsequently divided into train (70%), validation (20%), and testing (10%) sets. This comprehensive approach ensures a representative and diverse dataset for training, validating, and testing the models.

Table 6.2: Data preprocessing for YOLOv8-FPD model detection.

Class[a]	Original dataset	Train (70%)	Validation (20%)	Test (10%)
FPD_{all}	3150	2205	630	315
FPD_{RGB}	900	630	180	90
$FPD_{Thermal}$	900	630	180	90

FPD_{all} consists of all kinds of images, including augmented images, which were recorded without holding hens and used to compare each YOLOv8 model. In addition, FPD_{all} did not contain images produced by thermal cameras.

[a]Each class or experimental setting was run for 300 Epochs with a batch size of 16.

The training and validation datasets were labeled by an experienced researcher trained by a prior researcher with expertise in machine learning and data annotation utilizing the image labeling platform (Makesense.AI). The labeled data were then stored in the YOLO format. Manual labeling was executed for these images by enclosing the targeted FPD instances scored as FPD 0, FPD 1, or FPD 2 with rectangular bounding boxes. The detailed sequence of data collection, labeling, preprocessing, training, validation, testing, and inference was outlined in the previous research (Bist et al., 2023c).

6.2.6 Experimental Setup for Model Evaluation

The five YOLOv8 models were acquired from the GitHub repository created by Ultralytics (Jocher et al., 2023a). These models, namely YOLOv8n, YOLOv8s, YOLOv8m, YOLOv8l, and YOLOv8x, had been pre-trained using the Common Objects in Context (COCO) datasets and were adaptable for customization according to specific object detection requirements through training with target object datasets. The experimental configurations for the FPD detector development are outlined in Table 6.3. The labeled and unlabeled image and video datasets underwent Oracle Cloud (Oracle Corporation, Austin, TX, USA) analysis. This approach systematically assesses the models' performance under different settings.

Table 6.3: Experimental configurations employed for model development.

Configuration	**Parameters**
CPU	128 core OCPU
Memory (RAM)	2048GB
Drive (2 counts)	7.68 TB NVMe SSD
GPU (4 counts)	4×NVIDIA® A10 (24GB)
Operating system	Ubuntu 22.10 (Kinetic Kudu)
Accelerated environment	NVIDIA CUDA
Libraries	OpenCV-python 4.1.1, Torch 1.7.0, NumPy 1.18.5, Torch-vision 0.8.1
Cloud image	Oracle Linux 8
Network bandwidth	100 Gbps

CPU-Central processing unit; GPU- Graphics processing unit; RAM- Random access memory; OCPU- Oracle-based CPU; Gbps- Gigabits per second.

6.2.7 Machine Learning Models

In this study, the YOLOv8 model was extracted from GitHub Ultralytics (Jocher et al., 2023a), which can be publicly accessed at https://github.com/ultralytics/ultralytics. Ultralytics introduced this model in January 2023, and the visionary company also developed the YOLO series model (Jocher et al., 2023b; Figure 6.2). The advancement in the YOLOv8 architecture was accompanied by the introducing an array of meticulously scaled versions (Jocher et al., 2023a; King, 2023). It was a testament to YOLOv8's versatility that it gracefully accommodated an expansive array of vision tasks, ranging from object detection, segmentation, and pose estimation to tracking and classification (Jocher et al., 2023a). Delving further into YOLOv8's neural underpinnings, it is sculpted around a convolutional neural network architecture, prominently demarcated into two pivotal realms: the steadfast backbone and the visionary head (Jocher et al., 2023b). The CSPDarknet53 architecture forms the reimagined backbone, boasting 53 convolutional layers interwoven with cross-stage partial connections that ensure a seamless information flow. YOLOv8, built on a shared foundation with YOLOv5, strategically enhances its core architecture by introducing the C2f module (previously CSPLayer). This module replaces the traditional YOLO neck, featuring a Cross-Stage Partial Bottleneck with two Convolutions. This innovation harmonizes high-level features and context, significantly improving object detection precision. The head of YOLOv8 employs multiple convolutional layers transitioning into fully connected layers, which are vital for predicting bounding boxes, abjectness scores, and class probabilities. A remarkable addition is integrating a self-attention mechanism within the network's head. This mechanism captures spatial dependencies in feature maps, enhancing YOLOv8's ability to discern contextual relationships crucial for precise object

detection. This model's advanced features and capabilities made it a valuable choice for this research.

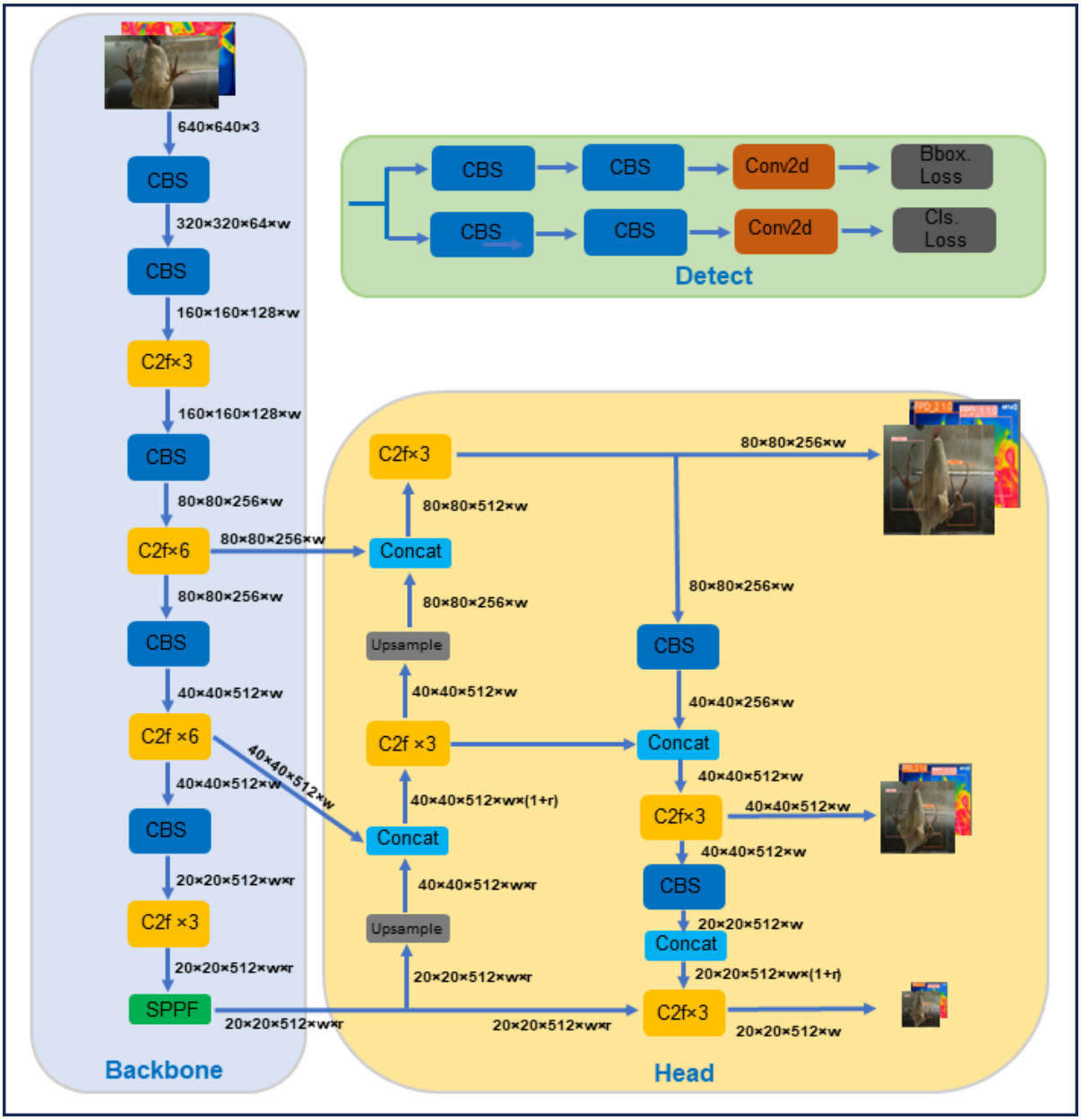

Figure 6.2: Architecture of the YOLOv8 model for FPD scoring and detection.

C2f- Cross-Stage Partial Bottleneck with two Convolutions; CBS- composed of convolution (Conv2d), batch normalization, and SiLu activation functions; SPPF- adopted Spatial Pyramid Pooling (SPP) fast with less FLOPs.

6.2.8 Model Evaluation Metrics

Python (version 3.10.6) was used to conduct descriptive statistics and comprehensive statistical analyses during the model evaluation phase. Crucial metrics such as precision, recall, F1 score, and mAP (mean average precision) were computed to test the model's performance. The definitions with formulas guiding these calculations were as follows:

6.2.8.1 Precision

Precision delineates the accuracy of the bounding box predictions in correspondence with the dataset.

$$Precision = \frac{TP}{TP + FP} \times 100\% = \frac{true\ FPD\ detection\ or\ scored}{all\ detected\ bounding\ boxes} \qquad (i)$$

where, TP, FP, and FN denote true positive, false positive, and false negative values, respectively.

6.2.8.2 Recall

Recall indicates the ability of the model to accurately predict true bounding box measurements within the dataset.

$$Recall = \frac{TP}{TP + FN} \times 100\% = \frac{true\ FPD\ detection\ or\ scored}{all\ ground\ truth\ bounding\ boxes} \qquad (ii)$$

6.2.8.3 F1 score

The F1 score, a crucial metric in object detection, encapsulates a weighted average or harmonic mean of both precision and recall (Equation iii). The highest F1 score signifies improved detector performance. Object detection is highly accurate without negative outcomes when F1 score = 100%.

$$F1\ Score = \frac{2 \times Recall \times Precision}{Recall + Precision} \times 100\% \qquad (iii)$$

6.2.8.4 Mean average precision (mAP)

The mAP serves as a pivotal evaluation metric. It gauges the model's detection capabilities, employing an intersection over union (*IoU*) threshold of 0.5 (mAP@0.50) or a wider range of 0.5 to 0.95 (mAP@0.50:0.95).

$$mAP = \frac{\sum_{i-1}^{C} APi}{C} \qquad (iv)$$

Within this equation, AP_i signifies the average precision of the i^{th} category, and C represents the total number of categories.

$$IoU = \frac{Area\ of\ Overlap\ between\ bounding\ boxes}{Area\ of\ Union\ between\ bounding\ boxes} = \qquad (v)$$

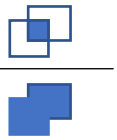

6.2.8.5 Loss function

The YOLOv8-FPD object-detection algorithm employs a custom loss function referred to as the "YOLO Loss" during its training and validation process (Figure 6.3). This loss function integrates various terms to penalize incorrect predictions and promote accuracy. The YOLOv8-FPD Loss is a weighted combination of objectness loss, classification loss, and DFL (Distribution Focal Loss), with the significance of each term determined by user-set weights. Through backpropagation and gradient descent during training, the YOLO Loss is minimized to reduce overall prediction errors, thereby enhancing the model's performance (Bist et al., 2023c). The regression Loss in YOLOv8 combined the CIoU (Complete Intersection over Union) loss

with DFL (Lou et al., 2023). DFL approached box position modeling through a general distribution, emphasizing proximity to object locations.

$$DFL_{s_i,s_{i+1}} = -\big((y_{i+1} - y)\log(s_i) + (y - y_i)\log(S_{i+1})\big) \qquad (vi)$$

Where Si denotes sigmoid network output, yi and yi+1 represent interval orders, and y is a label.

YOLOv8 employs an Anchor-Free over Anchor-Based approach and introduces dynamic TaskAlignedAssigner for matching. It computes Anchor-level alignment using equation (vii);

$$t = s^{\alpha} \times u^{\beta} \qquad (vii)$$

Where, classification score (s), IoU value (u), and weight hyperparameters (α and β).

It selects top m anchors per instance as positives and trains through the loss function. These upgrades led to YOLOv8's 11.4% mAP@0.50:0.95 gain over YOLOv5 over Pascal VOC2007 datasets, establishing it as one of the most accurate detectors (Lou et al., 2023).

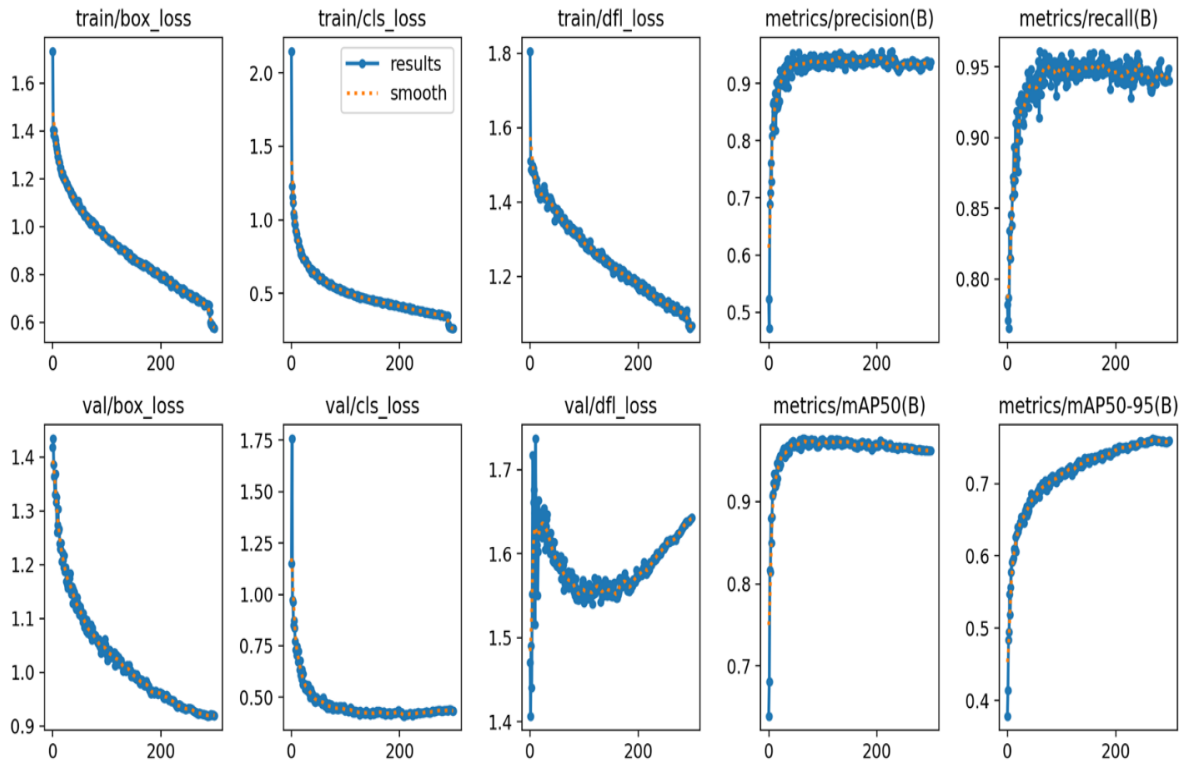

Figure 6.3: Performance metrics results sample for YOLOv8-FPD model.

Where train, val, box, obj, cls, dfl, and mAP represent the training, validation, bounding box, bounding object, class classification, distribution focal loss, and mean average precision used to detect and score FPD.

6.2.9 Statistical Analysis

The statistical analysis of the FPD scoring research encompassed a randomized arrangement involving four CF floor-raised rooms, with two rooms designated as control and the remaining two as treatment groups. These treatment groups incorporated EPI+BM over four weeks. FPD scoring was manually recorded at the end of 3 weeks from the start of the EPI+BM research using a sample size of 40 hens per room (total 160 hens) to gain an overview of FPD cases in each room to start video recording later. The assessment of FPD involved logistic regression analysis using RStudio 4.1.0.

6.3 RESULTS AND DISCUSSION

6.3.1 Footpad Dermatitis Condition

The study investigated the influence of EPI+BM treatment on FPD scoring in laying hens and compared it to a control group. However, the study's findings revealed no significant difference in FPD scoring between the control and EPI+BM treatment groups (ChiSquare P = 0.36). This outcome implies that introducing new bedding did not result in an observable distinction in footpad condition, which could be attributed to lower litter moisture content (<12%) and the possibility that the hens were too old to adapt to the changes in their environment in a short period. Lower moisture content is linked to a reduced FPD incidence (Bilgili et al., 2009; Martland, 1984; Shepherd and Fairchild, 2010). Since the litter was dry in all rooms, the occurrence of FPD remained similar in both treatment and control rooms. The distribution of FPD scores, categorized as levels 0, 1, and 2, approximately ranged from 28% to 36%, 46% to 48%, and 18% to 25%, respectively, as illustrated in Figure 6.4. In comparison to our study, it was observed in a previous study that there was a higher occurrence of severe FPD cases, reaching over 13%, particularly in conditions of dry litter with a moisture content of 17% (Wang et al., 1998). This disparity could likely be attributed to their study's significantly higher litter moisture content. Additionally, their investigation found that birds had a 92% incidence of severe FPD when raised in wet litter environments exceeding 55%. Thus, this study provides a better FPD analysis outcome, offering a comprehensive overview of the FPD conditions in each room designated for video recording.

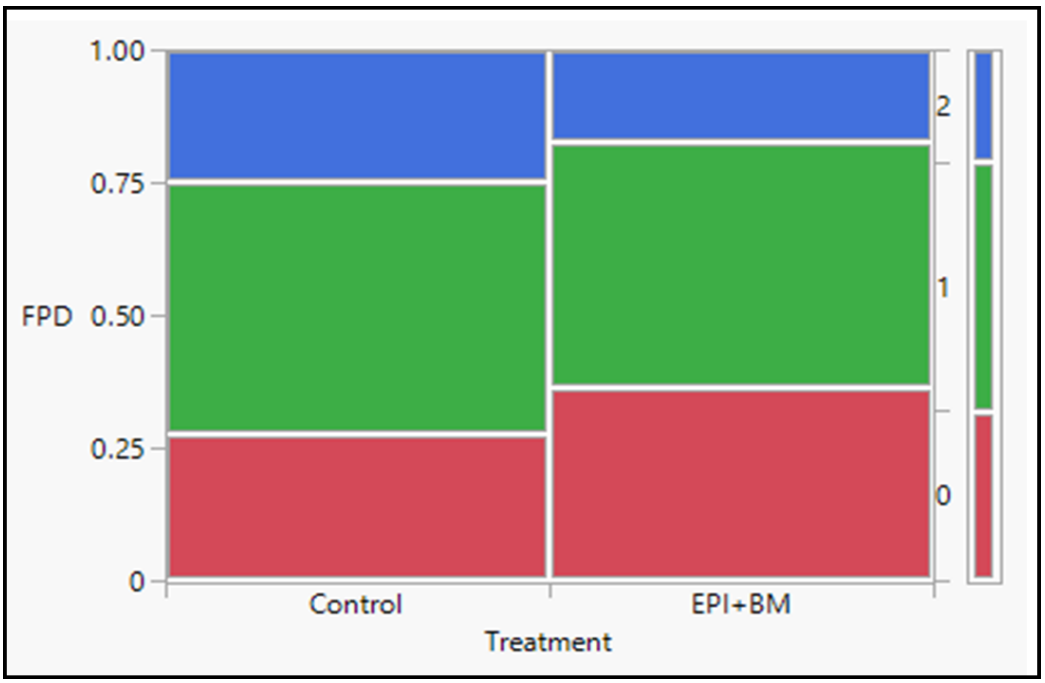

Figure 6.4: Mosaic plot of FPD scoring.

FPD- footpad dermatitis; EPI- Electrostatic Particle Ionization; BM-Bedding materials; the numbers 0, 1, 2 represent FPD score from 0 (indicating normal footpad condition) to 2 (indicating severe FPD condition).

6.3.2 Comparative Analysis of YOLOv8-FPD Models

6.3.2.1 Performance metrics comparison

Table 6.4 comprehensively evaluates diverse YOLOv8 model variations in their efficacy for detecting FPD, scoring them individually across various performance metrics. This meticulous assessment encompasses precision, recall, and mAP at distinct confidence thresholds and the F1-score (Table 6.4). This comprehensive analysis gives us a deep understanding of each model's performance and enables a nuanced comparison across various dimensions. Examining the outcomes, it is evident that the YOLOv8l-FPD model emerges with higher performance among the studied variants but with little variations among performance metrics. A closer analysis of its results reveals a remarkable recall of 96.6% and an impressive recall of 96.3% for

class FPD 0, indicating its proficiency in precise identifications. The model's mAP@0.50 score of 98.0% for FPD 0 further underscores its ability to localize FPD instances with a high confidence score. The overall mAP@0.50 (97.0%) in our study surpassed the results of the prior research, which employed the YOLOv8 model for small object detection and reported a mAP@0.50 in the range of 18-83% (Lou et al., 2023). However, another study that also utilized the YOLOv8 model achieved the lowest Map@0.50 at 47%, which was 50% lower than our result (Wang et al., 2023). The lower Map in that study may be attributed to the targeted object's greater height relative to the camera's location. Consequently, factors such as camera height and image quality can significantly impact detection accuracy (Corregidor-Castro et al., 2021; Gadhwal et al., 2023). Additionally, our study consistently achieved high-performance levels for both FPD 1 and FPD 2 classes, underscoring the model's effectiveness across the entire spectrum of FPD categories. These individual metrics collaborate to yield an impressive overall F1 score of 95.0%.

Table 6.4: Performance metrics results of different YOLOv8 models for footpad dermatitis scoring.

Models	FPD scores	Precision (%)	Recall (%)	mAP@0.50 (%)	mAP@0.50-0.95 (%)	F1-score (%)
YOLOv8n-FPD	0	93.7	96.3	97.9	78.7	94.0
	1	89.9	93.3	95.7	72.6	
	2	95.3	96.4	97.7	69.0	
	Overall	93.0	95.3	97.1	73.4	
YOLOv8s-FPD	0	94.7	93.7	97.4	84.4	94.0
	1	90.3	92.1	94.8	73.4	
	2	95.6	95.4	97.4	70.4	
	Overall	93.5	93.7	96.5	76.1	
YOLOv8m-FPD	0	97.9	93.5	97.6	86.8	95.0
	1	91.7	93.1	94.8	74.0	
	2	96.6	95.2	97.2	70.6	
	Overall	95.4	93.9	96.5	77.1	
YOLOv8l-FPD	0	93.6	96.3	98.0	88.7	95.0
	1	90.1	95.6	95.0	74.8	
	2	94.6	97.9	97.9	72.5	
	Overall	92.8	96.6	97.0	78.7	
YOLOv8x-FPD	0	98.0	91.5	97.2	88.7	94.0
	1	92.3	89.8	94.2	74.2	
	2	96.7	95.0	97.5	72.3	

	Overall	95.7	92.1	96.3	78.4	

Where FPD-Footpad dermatitis; mAP-mean average precision; the score 0, 1, 2 represents FPD score from 0 (indicating normal footpad condition) to 2 (indicating severe FPD condition).

When contextualizing these results within the context of other model variations, such as YOLOv8n-FPD and YOLOv8s-FPD, it becomes apparent that the YOLOv8l-FPD model maintains higher performance results with increasing epochs (Figure 6.5). While YOLOv8n-FPD and YOLOv8s-FPD exhibit comparable precision and recall for class FPD 0, the former lags behind with a mAP@0.50 score of 97.9%, compared to the latter's 97.4%. This difference suggests that YOLOv8s-FPD excels in localizing FPD instances with higher confidence. However, the YOLOv8l-FPD model surpasses both variations across the board, showcasing slightly higher recall, mAP, and F1-score metrics. The YOLOv8l-FPD variant maintains superiority when analyzing the overall performance landscape. With an impressive collective F1-score of 95.0%, effectively balancing precision and recall dynamics, this model accurately detects FPD instances across varying confidence thresholds. The higher the F1 score, the better the performance of the classifier and models will be (Bist et al., 2023c; Hand et al., 2021). These observations underscore the YOLOv8l-FPD model's ascendancy as a strong candidate for precise and dependable FPD detection, illustrating its potential to positively impact poultry management strategies.

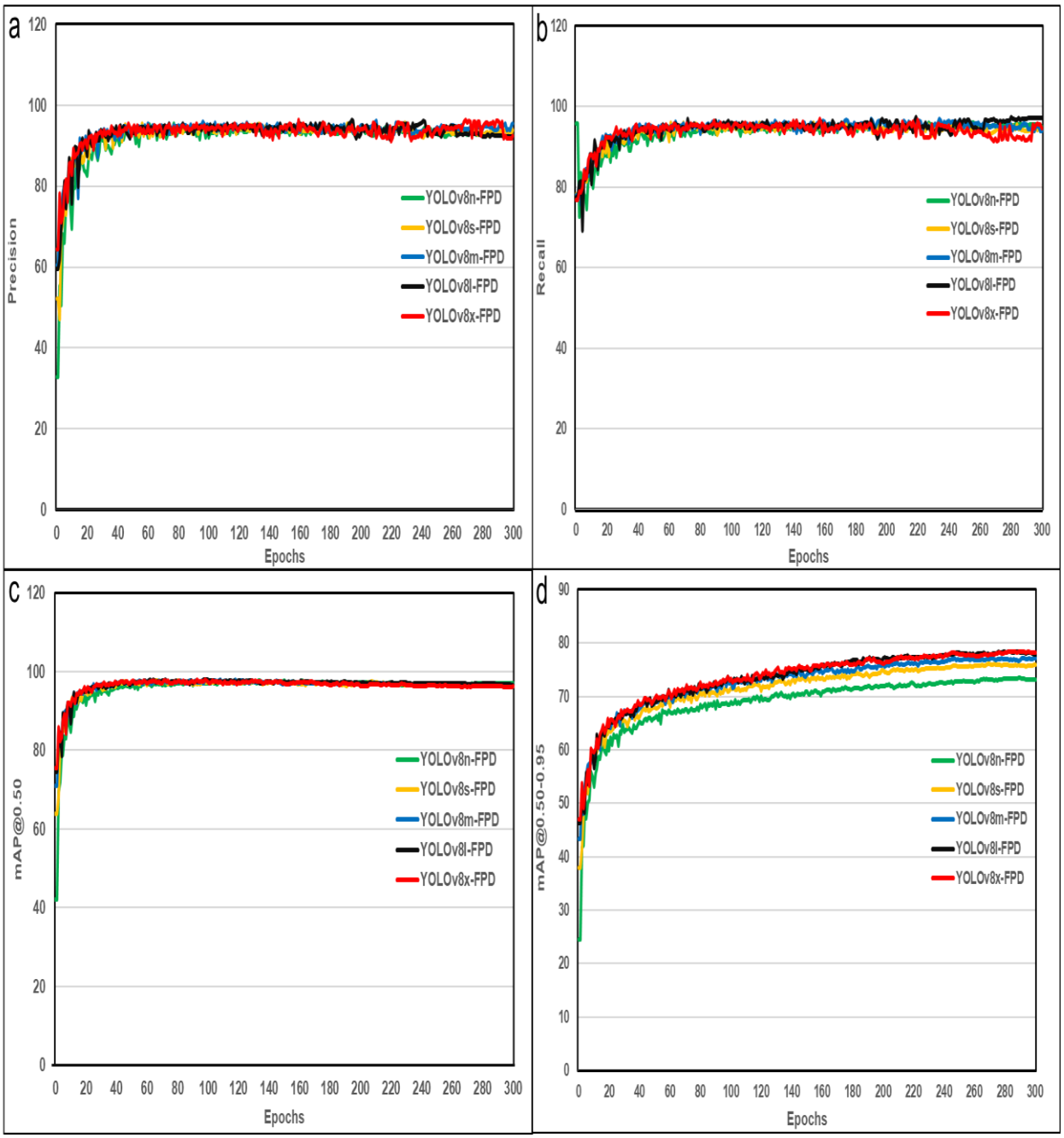

Figure 6.5: Comparative analysis results of footpad dermatitis detection performance across various YOLOv8 models.

FPD-Footpad dermatitis; mAP-mean average precision; the score 0, 1, 2 represents FPD score from 0 (indicating normal footpad condition) to 2 (indicating severe FPD condition).

Similarly, from the tested images, comprehensive analysis reaffirms the remarkable performance of the "YOLOv8l-FPD" model in effectively identifying FPD instances (Figure 6.6). The model's higher recall and mAP scores collectively underscore its proficiency in recognizing FPD instances across diverse scenarios. Each incremental improvement in performance metrics was important in reducing false detections by the model (Anowar and Sadaoui, 2021; Bist et al., 2023c; Yuan et al., 2016). Therefore, every marginal disparity holds significance within the context of the detection model. These findings substantiate the model's potential as a valuable tool for expediting timely and accurate FPD detection, thereby enhancing the efficiency of poultry management practices.

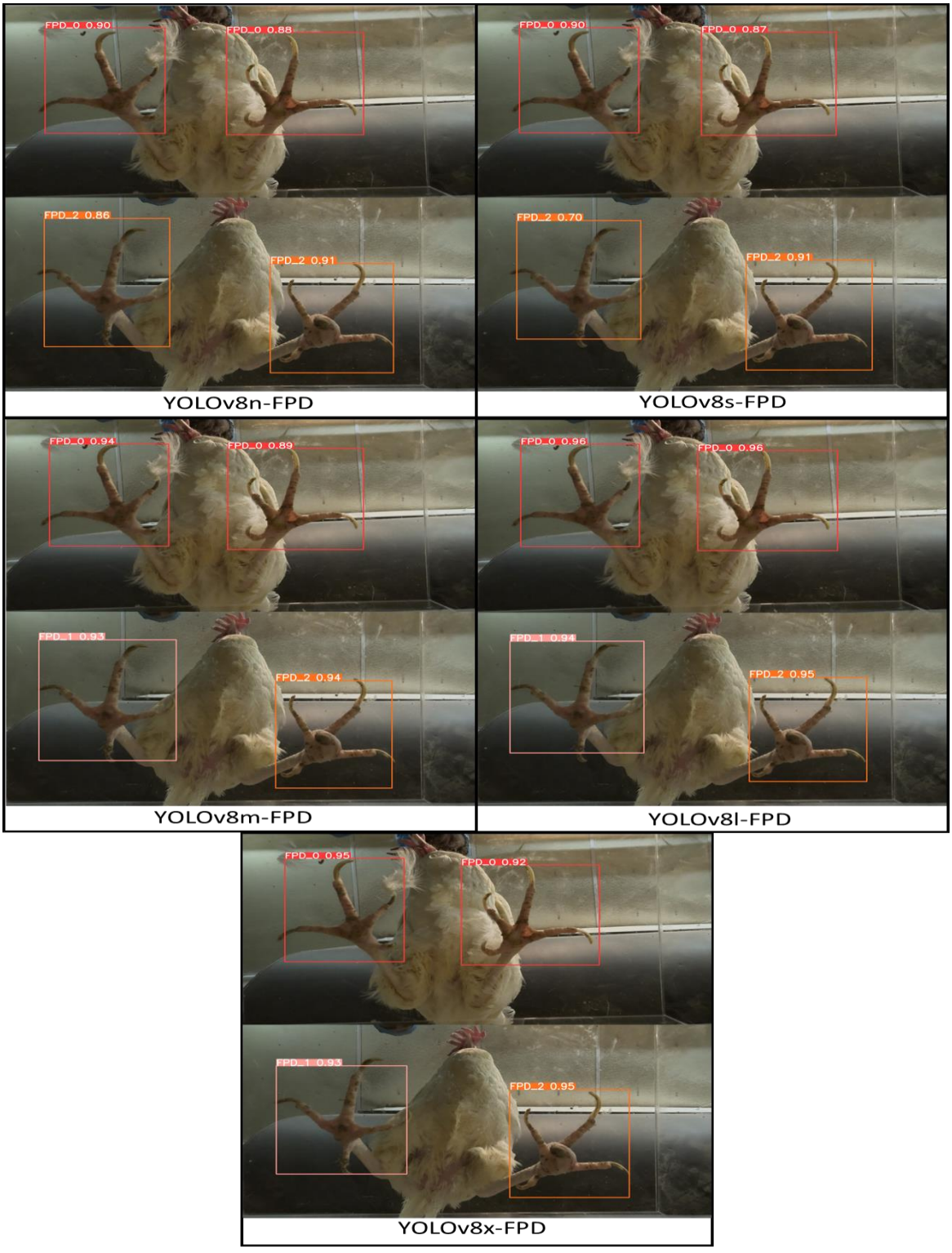

Figure 6.6: Comparison of detected footpad dermatitis score across various YOLOv8 models.

The comprehensive evaluation of the F1-confidence curve for the YOLOv8 models across all classes (FPD 0, FPD 1, and FPD 2) is depicted in Figure 6.7. The results underscore the strong performance exhibited by all YOLOv8 models in accurately classifying FPD instances across varying severity levels. Notably, the F1-scores for FPD 0, FPD 1, and FPD 2 consistently maintained high values for each model, with YOLOv8n-FPD, YOLOv8s-FPD, YOLOv8m-FPD, YOLOv8l-FPD, and YOLOv8x-FPD achieving F1-scores of 0.94, 0.94, 0.95, 0.95, and 0.94, respectively. This remarkable performance highlights the YOLOv8 models' adeptness at striking a fine balance between precision and recall across different FPD severity levels. The outstanding performance of the YOLOv8l-FPD and YOLOv8m-FPD models is of particular significance, boasting a high F1-score of 0.95 for all classes. The higher the F1 score, the better the model's performance (Bist et al., 2023c; Li, 2018). The consistent excellence in F1 scores observed across the various YOLOv8 models serves as a testament to the architecture's robustness and efficacy in accurately classifying FPD instances. Additionally, the notable prowess of the YOLOv8l-FPD model suggests its proficiency in achieving a meticulously calibrated equilibrium between precision and recall, ultimately contributing to heightened accuracy in FPD detection. This performance distinction of the YOLOv8l-FPD model carries substantial implications, emphasizing its potential to reliably and precisely identify FPD cases, thereby holding the promise of advancing poultry health management strategies.

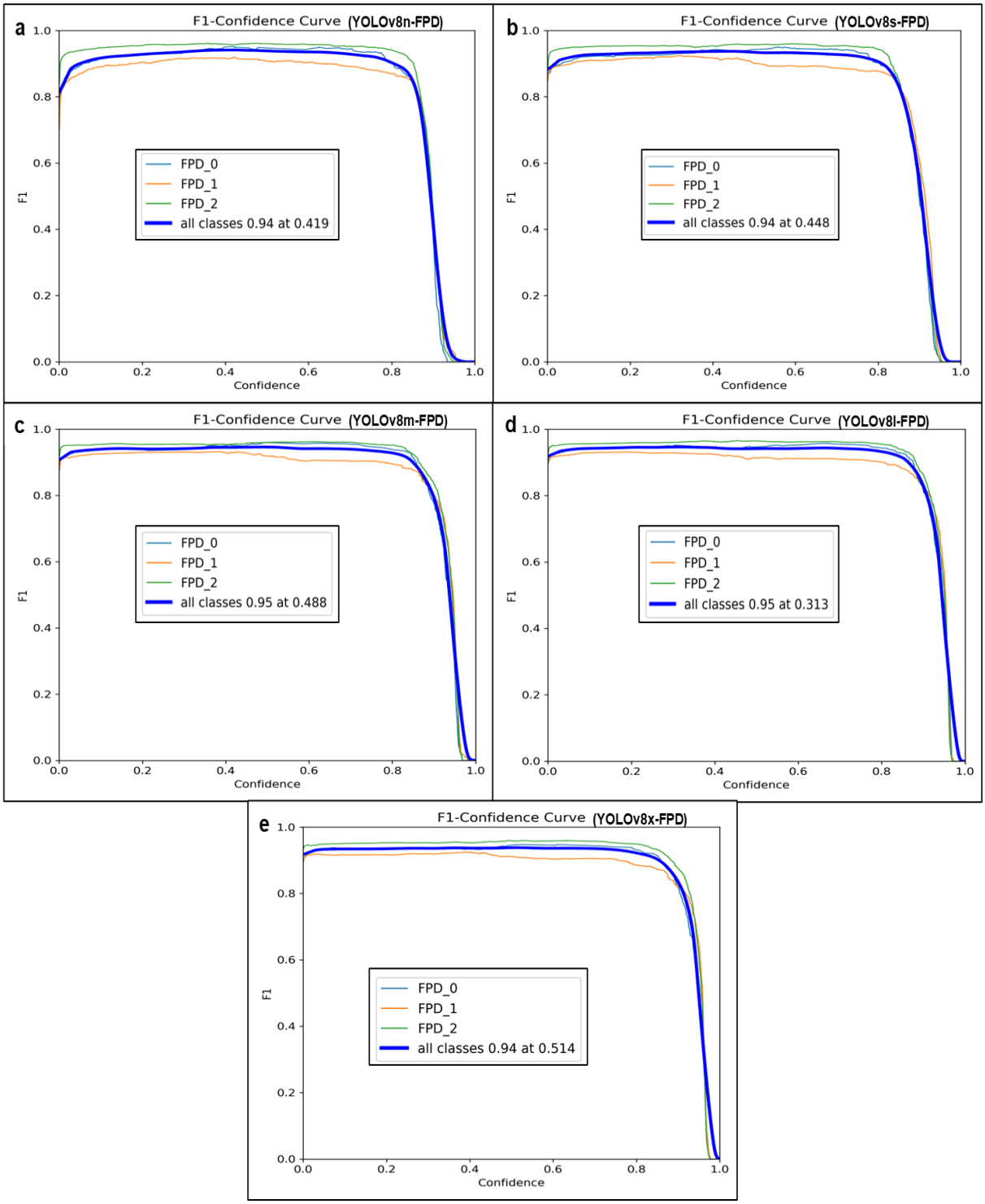

Figure 6.7: F1-confidence curve analysis among a) YOLOv8n-FPD, b) YOLOv8s-FPD, c) YOLOv8m-FPD, d) YOLOv8l-FPD, and e) YOLOv8x-FPD models.

6.3.2.2 Confusion matrix analysis

The validation dataset's confusion matrix encompassed 630 hens' FPD score datasets, totaling 1260 footpads with all FPD classes (Figure 6.8a). The YOLOv8l-FPD models exhibited the highest True Positive values with 234 FPD 0, 358 FPD 1, and 542 FPD 2 detections (surpassed only by YOLOv8x-FPD's 543 FPD 2 detections). Conversely, the lowest True Positive values were recorded at 226 FPD 0 by YOLOv8x-FPD, 344 FPD 1 by YOLOv8n-FPD, and 536 FPD 2 by YOLOv8n-FPD and YOLOv8m-FPD. A more insightful view is provided by Figure 6.8b, presenting the confusion matrix in normalized form with the percentage of accurate predictions. The higher the true positive counts, the better the model detects and identifies positive instances from the datasets (S. Yang et al., 2023). The highest true positive rates were achieved by the YOLOv8l-FPD model for FPD 0 (0.95), YOLOv8l-FPD and YOLOv8m-FPD models for FPD 1 (0.92), and YOLOv8x-FPD for FPD 2 (0.97), followed closely by the YOLOv8l model. These results underscore the YOLOv8 models' adeptness in accurately detecting different FPD severity levels, with the YOLOv8l-FPD model consistently demonstrating strong performance. This proficiency has substantial implications for efficient poultry health monitoring and underscores the potential of YOLOv8l-FPD models in precise FPD scoring and detection applications.

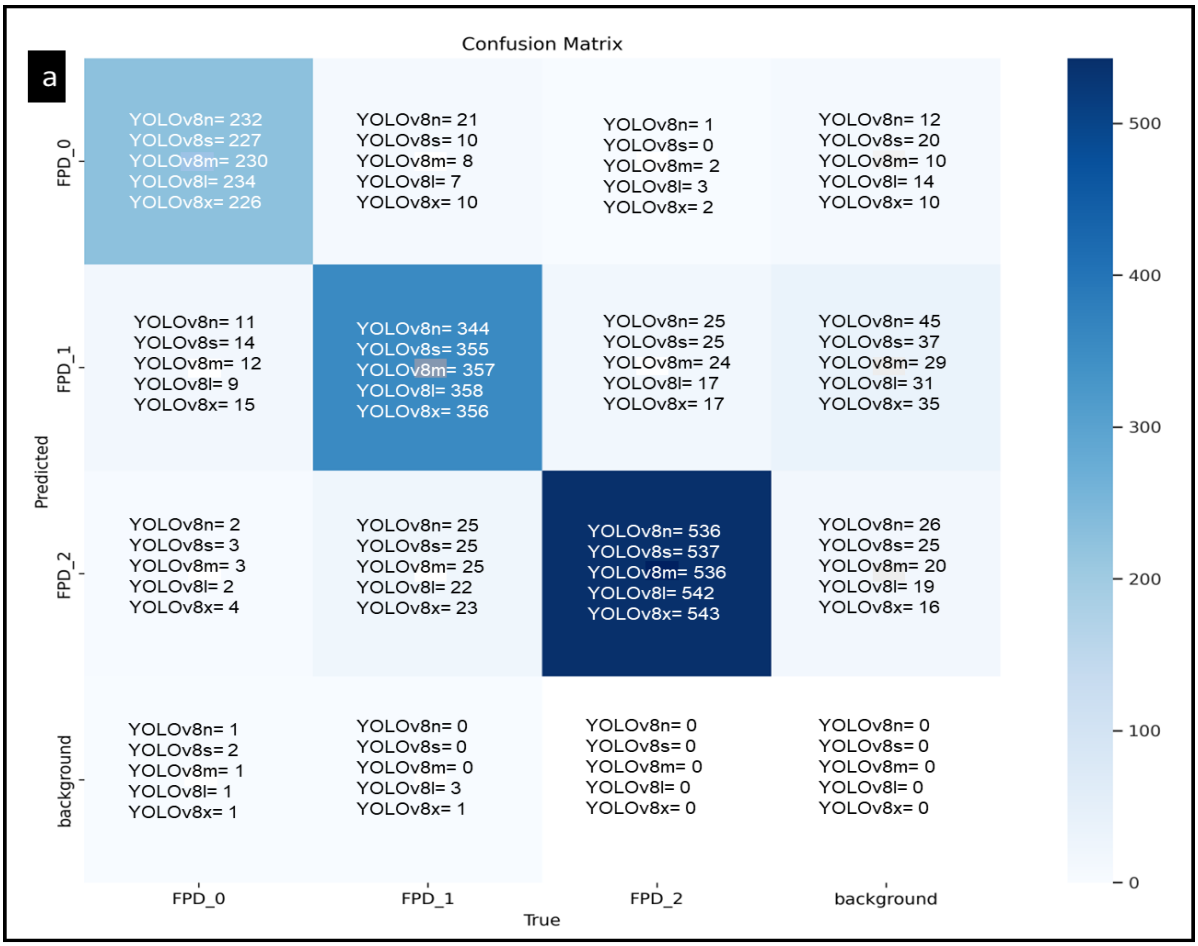

Figure 6.8: Comparative performance results of YOLOv8 models based on FPD scoring a) confusion matrix of footpad scoring in counts and b) normalized confusion matrix in percentage.

6.3.2.3 Training and validation loss functions

The training and validation processes exhibited a rapid decrease in the loss function as the model was trained over 300 epochs, as shown in Figure 6.9. The increase in epochs leads to a decrease in the loss function as the machine learning model iteratively adjusts its parameters to better fit the training data and improve its predictive accuracy (Bist et al., 2023c; Subedi et al., 2023a). The "mAP@0.5: 0.95" value signifies the average mAP across these thresholds, providing an insightful evaluation of detection accuracy. Notably, a lower box and classification

loss correspond to higher accuracy in correctly detecting and scoring FPD instances. Among the YOLOv8-FPD models, the YOLOv8x-FPD model demonstrated the lowest Train/Box_loss, Train/Cls_Loss, and Val/Box_Loss, closely followed by the YOLOv8l-FPD model. However, a slightly different trend was observed for Val/Cls_Loss, where the YOLOv8l-FPD model exhibited the lowest value, albeit marginally distinct from the other models.

On the contrary, the YOLOv8n-FPD model displayed the highest values for Train/Box_loss, Train/Cls_Loss, Val/Box_Loss, and Val/Cls_Loss, indicating relatively poorer performance than other models. These observations shed light on different models' varying efficacy and ability to learn and generalize FPD detection patterns. These insights into the loss function dynamics provide a deeper understanding of model training and validation, offering valuable guidance for model selection and refinement in FPD detection. This disparity in loss values can be attributed to various intricacies inherent to the training process. As the model undergoes training, it familiarizes itself with the dataset, learning the intricate patterns and features associated with FPD scoring and detection. The Train/Box_loss and Train/Cls_Loss metrics quantify the discrepancies between the model's predictions and actual classifications as the model iteratively refines its parameters to minimize these discrepancies.

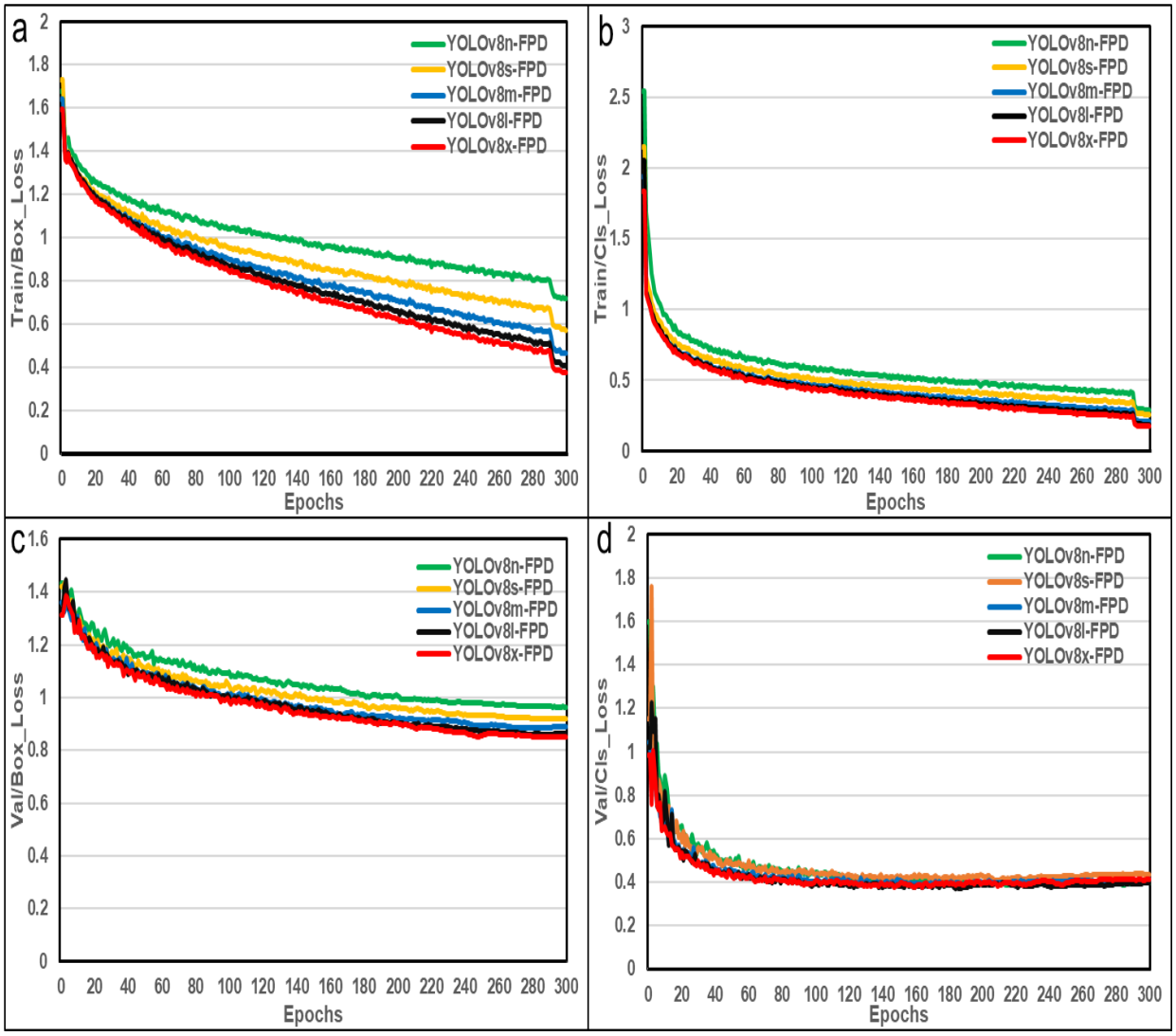

Figure 6.9: Comparison of a) Train/Box_Loss, b) Train/Cls_Loss, c) Val/Box_Loss, and d) Val/Cls_Loss across various YOLOv8 models.

However, during validation, when the model confronts new and previously unseen data (as reflected in Val/Box_Loss and Val/Cls_Loss), its performance may not be as strong as during training (Figure 6.10). This phenomenon, termed overfitting, signifies that the model has become excessively specialized in fitting the training data and may struggle to generalize effectively to novel data (Geron, 2022). Consequently, the validation loss values might be higher, indicating a

relatively weaker performance on unseen data instances. The discernible contrast between Training and Validation loss values underscores the significance of maintaining a harmonious equilibrium between model complexity and generalization. To enhance the model's ability to generalize to new data, potential strategies include implementing regularization techniques like dropout or weight regularization, as well as fine-tuning hyperparameters such as learning rate or model architecture (Ba and Frey, 2013; Merity et al., 2017). In essence, this observation emphasizes the dynamic nature of model training and the crucial role of meticulous parameter adjustments to achieve optimal outcomes in FPD detection.

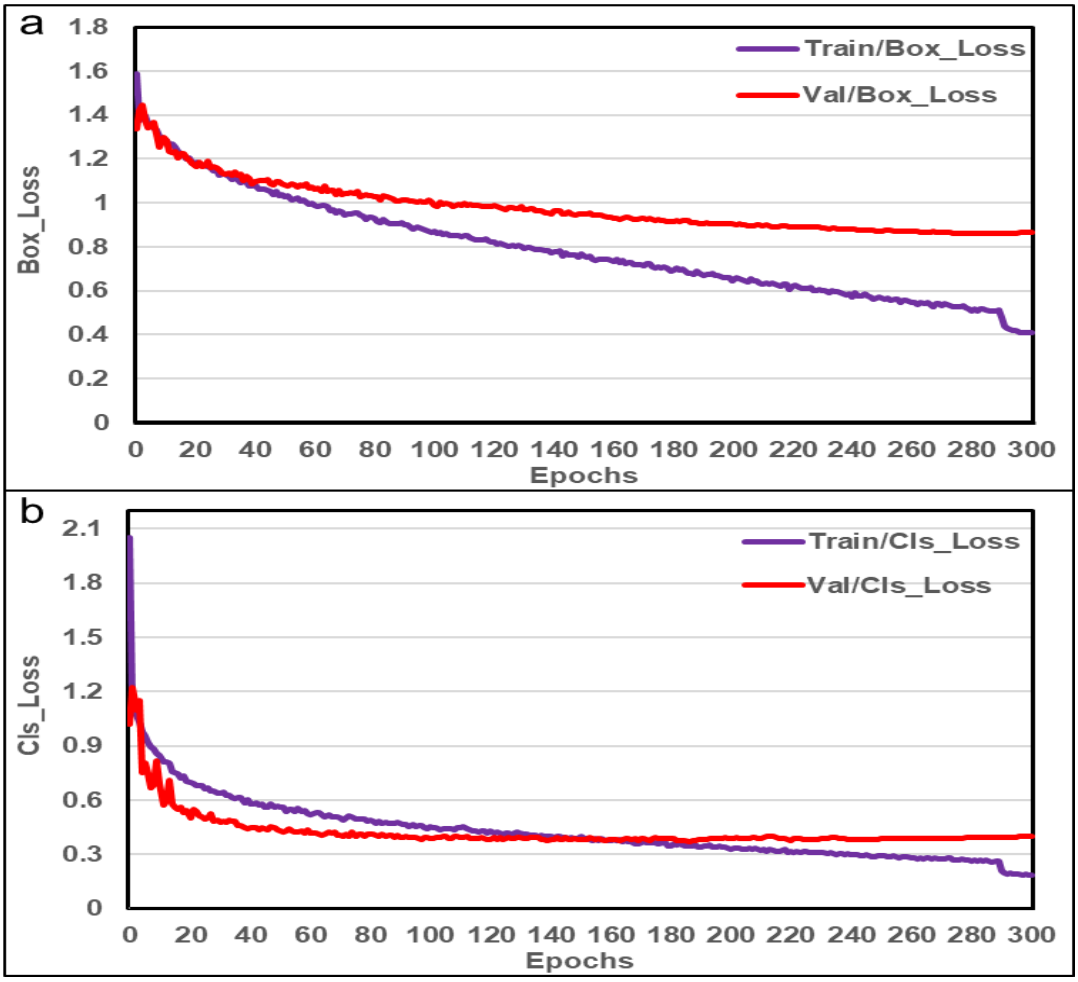

Figure 6.10: Comparative analysis of a) box loss and b) classification loss of training and validation for YOLOv8l model.

6.3.2.4 Comparison based on training time and GPU usage

The results of the YOLOv8 model comparisons, involving training time (in hours) and GPU usage (in GB), are outlined in Figure 6.11. When assessing the discrepancies between the lowest and highest values, it becomes evident that the YOLOv8n-FPD model displays the smallest variation with 0.478 hours and 11.47 GB for training time and GPU usage, respectively. On the contrary, the YOLOv8x-FPD model presents the highest training time and GPU usage. This reflects how YOLOv8 sizes increase training time and GPU usage due to augmented layers, parameters, gradients, and GFLOPs (Dumitriu et al., 2023; Jocher et al., 2023a). Training time and GPU usage play another important role because fast training with less cost is essential (Subedi et al., 2023a, 2023b). Less training time allows developers and researchers to achieve faster results and make faster model development decisions (Majumder et al., 2018). On the other hand, less GPU usage may extend the personal computer lifespan as personal computers run at the maximal capacity for FPD prediction. These findings emphasize how model complexity impacts training duration and GPU resource utilization. While models like YOLOv8x-FPD with advanced capabilities necessitate more training time and GPU resources, simpler models like YOLOv8n-FPD offer more efficient alternatives. Researchers and practitioners should consider these insights when selecting models, including the highest performance metrics, accounting for computational limitations and performance requirements. This comparative analysis provides valuable guidance for model selection in practical applications.

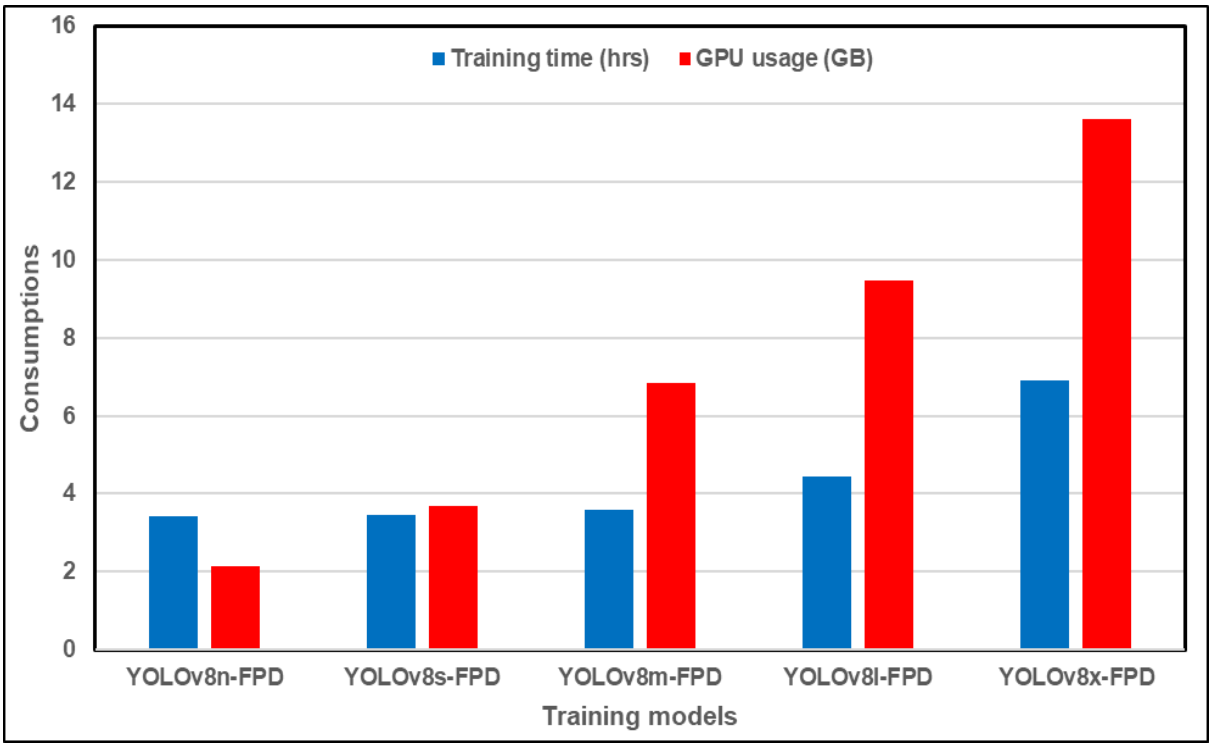

Figure 6.11: Comparison of training time (hrs) and GPU usage (GB) among various YOLOv8 models.

6.3.3 Comparison FPD Detection Under Different Image Settings

6.3.3.1 Performance metrics comparison

Exhibiting remarkable performance metrics within the YOLOv8-FPD model category, the YOLOv8l-FPD model was selected to conduct a comparative analysis between thermal and RGB FPD assessments in this study. The assessment includes critical metrics such as precision, recall, mAP at varying thresholds, and the F1-score. Table 6.5 provides a comprehensive overview of the YOLOv8l-FPD model's performance metrics detecting FPD across thermal and RGB images. For the YOLOv8l-FPD$_{RGB}$, it attains an impressive precision of 99.9%, complete recall at 100%, and high mAP values, notably mAP@0.50 (99.5%) and mAP@0.50-0.95 (99.3%). The F1 score for this class is flawless 100%, highlighting the model's harmonious

balance between precision and recall. Equally noteworthy results are observed for classes 1 and 2. Overall, the model consistently excels in detecting FPD in RGB images.

Table 6.5: Performance metrics comparison for footpad dermatitis detection under different camera image settings using YOLOv8l-FPD models.

Models	FPD scores	Precision (%)	Recall (%)	mAP@0.50 (%)	mAP@0.50:0.95 (%)	F1-score (%)
YOLOv8l-FPD_{RGB}	0	99.9	100	99.5	99.3	100
	1	99.9	100	99.5	99.5	
	2	99.9	100	99.5	99.5	
	Overall	99.9	100	99.5	99.4	
YOLOv8l-$FPD_{Thermal}$	0	99.9	100	99.5	99.5	100
	1	100	100	99.5	99.5	
	2	99.9	100	99.5	99.5	
	Overall	99.9	100	99.5	99.5	

FPD-Footpad dermatitis; mAP-mean average precision; the score 0, 1, 2 represents FPD score from 0 (indicating normal footpad condition) to 2 (indicating severe FPD condition).

Similarly, the YOLOv8l-$FPD_{Thermal}$ model achieved an impressive precision of 99.9%, complete recall, and elevated mAP values – mAP@0.50 (99.5%) and mAP@0.50-0.95 (99.5%). The F1 score for this class remains a perfect 100%. Although a slight precision variation is observed for class 1, the overall performance for classes 1 and 2 remains consistently robust. This further underscores the model's proficiency in detecting FPD across thermal images. In conclusion, among thermal and RGB images, the YOLOv8l-FPD model did not show much

difference in performance with image type. However, YOLOv8l-FPD detection for thermal images was comparatively higher and more accurate for FPD detection. Previous research papers consistently indicate higher detection accuracy with thermal cameras than with RGB images (Corregidor-Castro et al., 2021; Grbovic et al., 2019; Lee et al., 2021). Nonetheless, our model achieved higher object detection accuracy than these studies, which could be attributed to the proximity of our images to the camera.

Upon conducting a comprehensive comparison based on key performance metrics such as precision, recall, mAP@0.50, and mAP@0.50-0.95 (Figure 6.12), noteworthy insights emerged. The analysis unveiled that most performance metrics exhibited their highest values for the YOLOv8l-$FPD_{Thermal}$ model until the 260th epoch (except mAP@0.50 up to 180 epochs). However, beyond this point, the YOLOv8l-$FPD_{Thermal}$ and YOLOv8l-FPD_{RGB} models demonstrated converging performance trends. Specifically, the Precision, Recall, mAP@0.50, and mAP@0.50-0.95 metrics for the YOLOv8l-$FPD_{Thermal}$ model remarkably reached 100% after 100 epochs, 100 epochs, 90 epochs, and 220 epochs, respectively. In parallel, the YOLOv8l-FPD_{RGB} model achieved these same metrics at 180, 190, 160, and 260 epochs. It is noteworthy that the mAP@0.50 metric witnessed a distinct trend. Initially, the YOLOv8l-$FPD_{Thermal}$ model exhibited a superior mAP@0.50 value until the 180th epoch, which showcased comparable performance with the YOLOv8l-FPD_{RGB} model. Overall, the YOLOv8l-$FPD_{Thermal}$ model comparably demonstrated higher performance metrics throughout most of the training process. This implies that utilizing thermal images for training yields enhanced accuracy in detecting and scoring FPD (Figure 6.13). From inception, the slightly higher performance of the YOLOv8l-FPDThermal model underscores the intrinsic advantages of thermal imagery in fostering more accurate and reliable FPD detection. This study did not observe a significant disparity in

detection performance when utilizing a thermal camera. In contrast, prior research reported a substantial improvement in detection accuracy when employing thermal images compared to RGB images (Corregidor-Castro et al., 2021). This insight holds promising implications for refining poultry health monitoring protocols and underscores the pivotal role of thermal imaging in bolstering the precision and effectiveness of FPD detection methodologies.

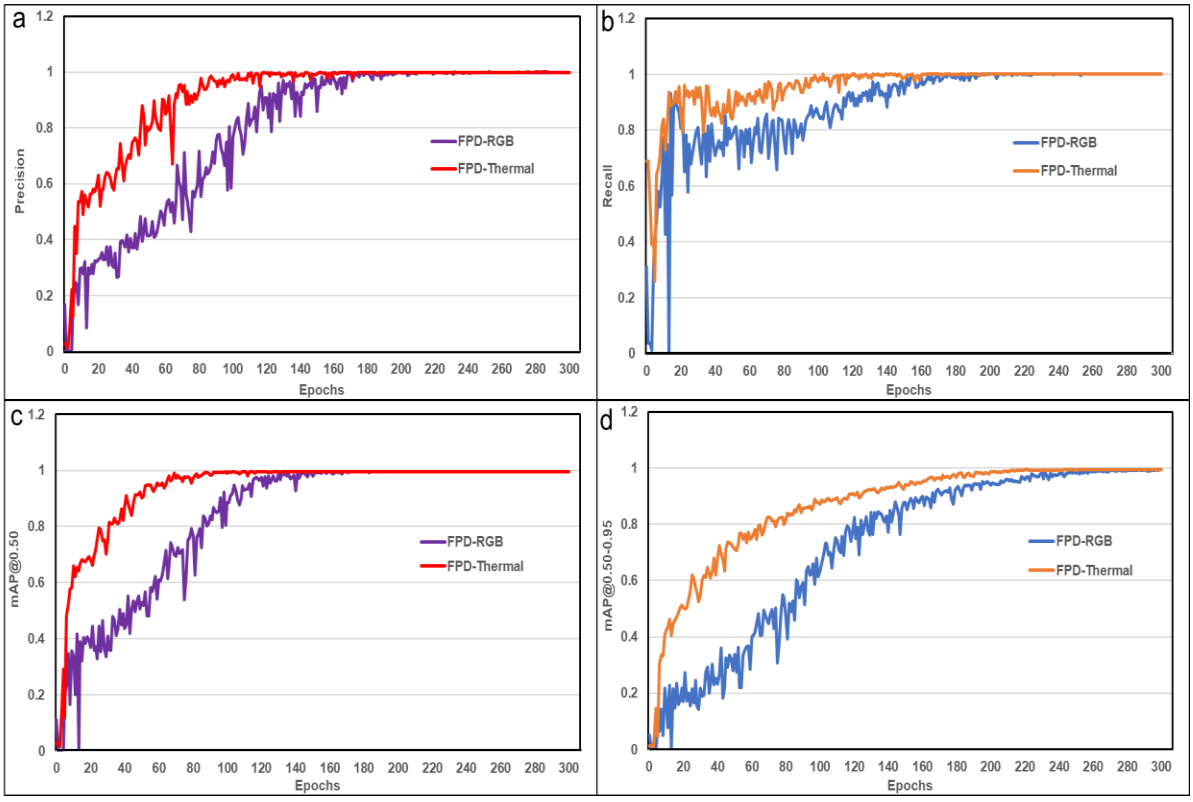

Figure 6.12: Comparison of performance metrics a) Precision, b) Recall, c) mAP@0.50, and mAP@0.50-0.95 for footpad dermatitis detection under RGB and thermal image conditions.

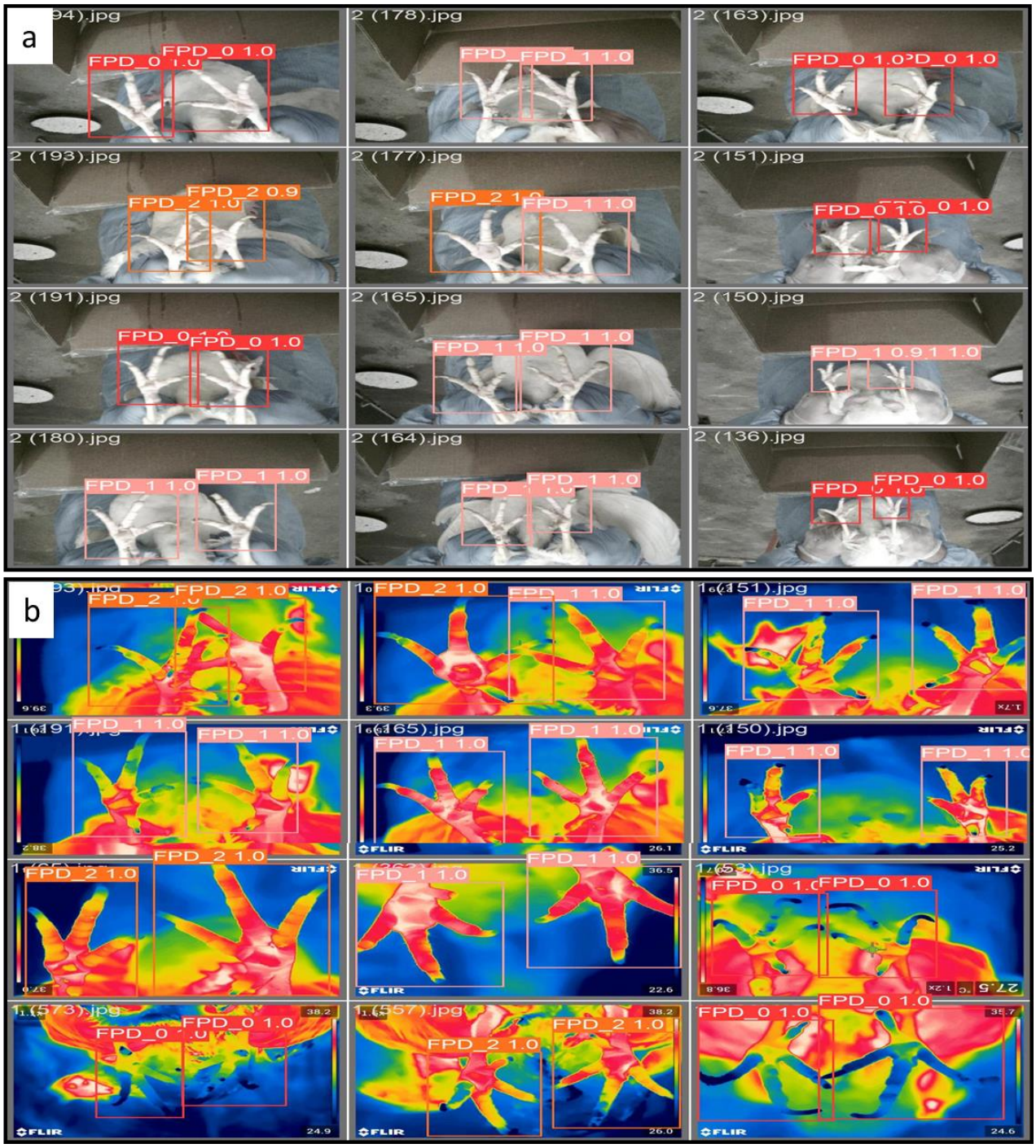

Figure 6.13: The FPD score detected in test image datasets using the YOLOv8l model for a) RGB images and b) thermal images.

The F1-Confidence curve analysis revealed that both the YOLOv8l-FPD_{RGB} and YOLOv8l-$FPD_{Thermal}$ models achieved a perfect F1 score of 1.00 for all classes (FPD 0, FPD 1, and FPD 2) at confidence levels of 0.881 and 0.933, respectively (Figure 6.14). This remarkable outcome underscores both models' high accuracy and reliability in classifying FPD instances across different severity levels. The attainment of a perfect F1 score suggests that the models effectively balance precision and recall, which is particularly valuable for a robust object detection system (Hand et al., 2021; Li, 2018). The perfect F1-Confidence curve results hold promising implications for poultry health monitoring, as they signify the potential of these models to reliably detect and classify FPD cases across different severity levels, contributing to the overall welfare of poultry populations and supporting more efficient management practices.

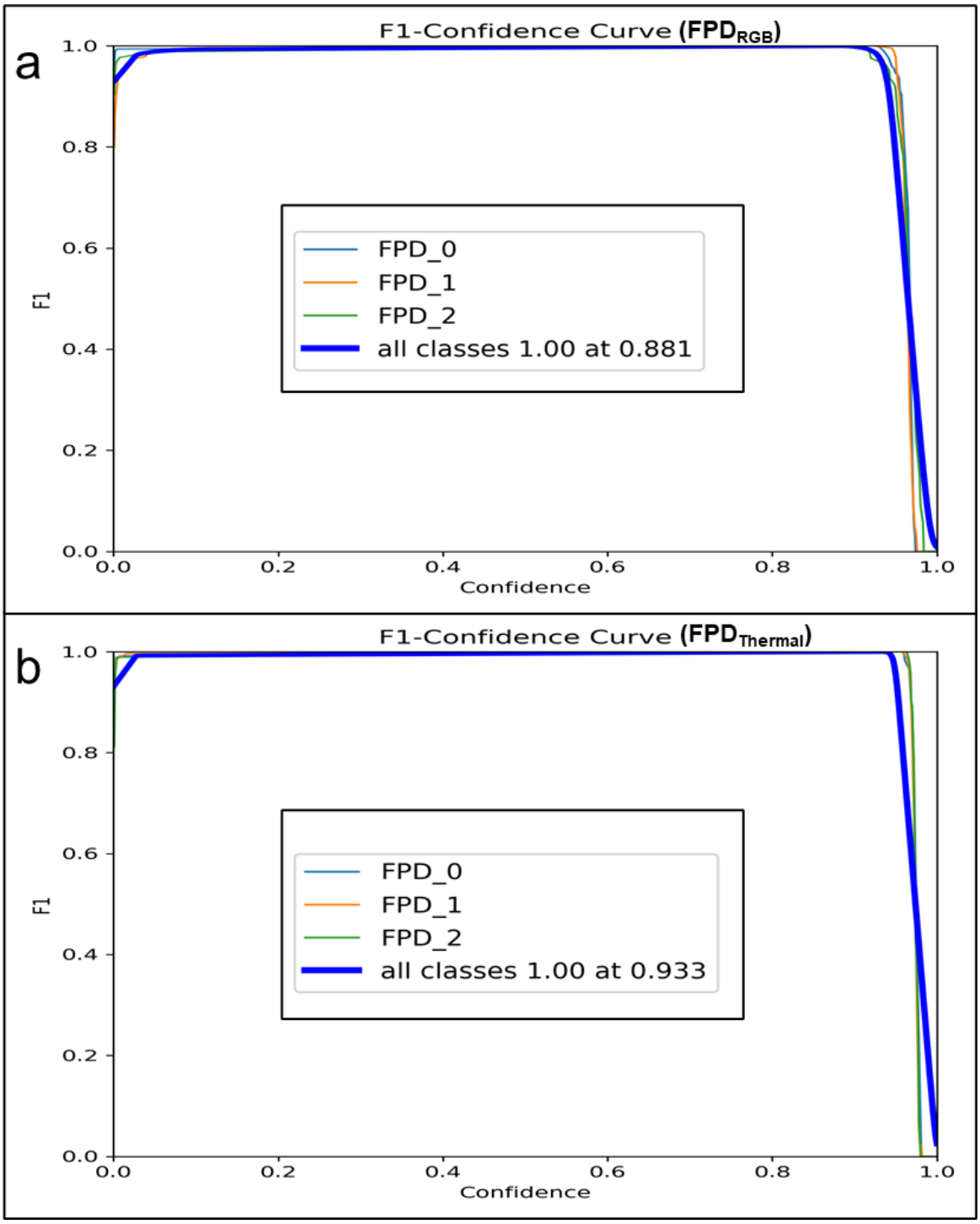

Figure 6.14: F1-Confidence curve analysis for footpad dermatitis detection results under RGB and thermal images.

6.3.3.2 Confusion matrix comparison

The confusion matrix is a crucial tool for evaluating the performance of the YOLOv8l-FPD_{RGB} and YOLOv8l-$FPD_{Thermal}$ models by dissecting their predictive outcomes into four components: TP, TN, FP, and FN. In this study, the TP value for both models were consistently 1.00, signifying instances where the classifier accurately predicted the presence of FPD and the actual class was indeed positive (i.e., the image contained FPD and was correctly scored as such) (Figure 6.15). On the other hand, the TN value for both models were 0, which corresponds to situations where the models correctly predicted the absence of FPD (i.e., no FPD detected), and the actual class was also negative (i.e., the images did not contain FPD).

Furthermore, the analysis revealed that both models achieved a perfect prediction and detection accuracy for FPD scores across all levels (FPD 0, FPD 1, and FPD 2), with an accuracy of 1.00 (100%). These results underscore the models' ability to consistently identify and classify images containing varying degrees of FPD. The detailed examination of the confusion matrix provides valuable insights into the models' performance and alignment with the ground truth data. This information has important implications for assessing the reliability and accuracy of the models in FPD detection tasks, ultimately contributing to informed decision-making in poultry management strategies.

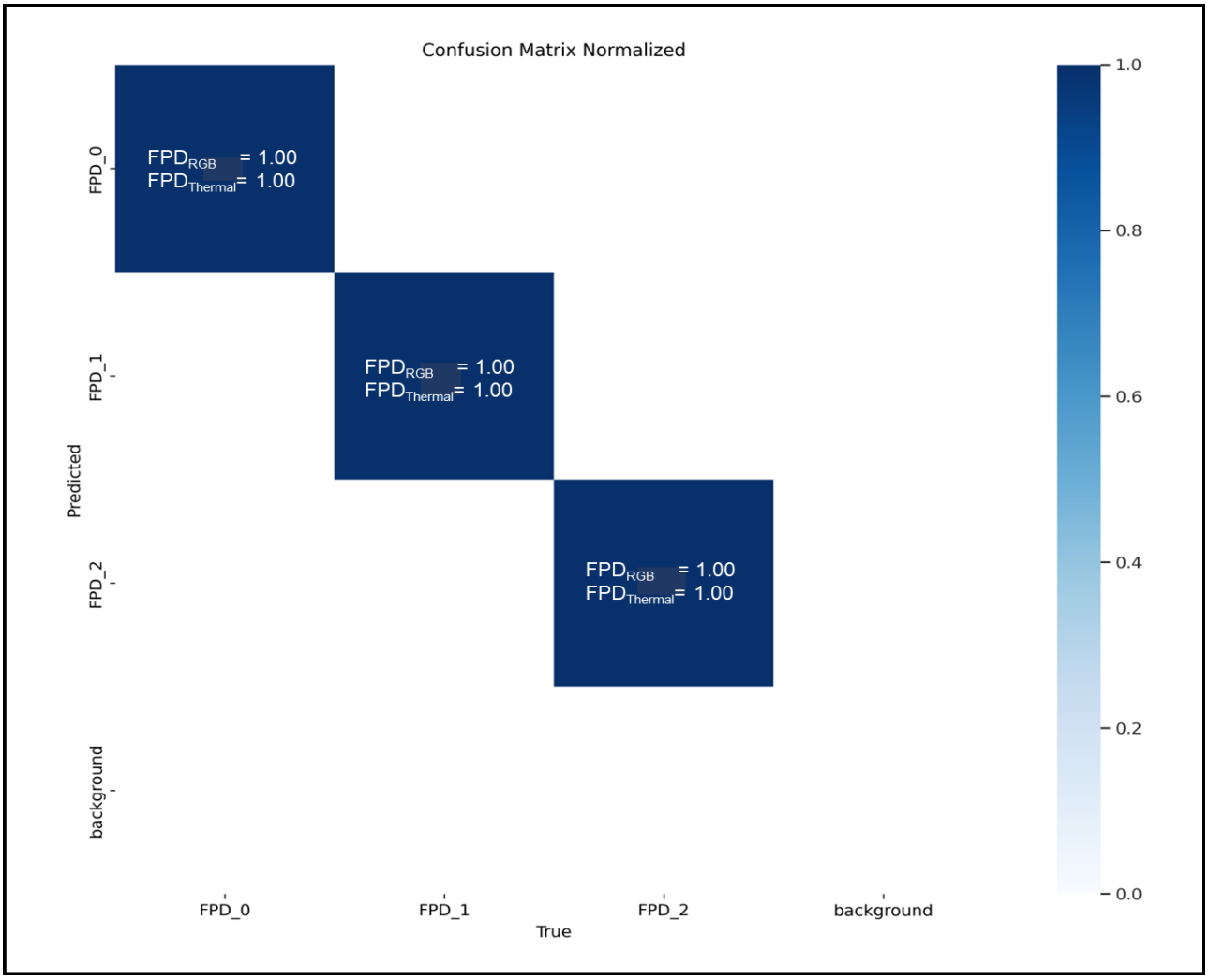

Figure 6.15: Confusion matrix comparison of footpad dermatitis detection results between RGB and thermal images.

6.3.3.3 Training and validation loss functions

During the comparative analysis of the Train/Box_Loss, Train/Cls_Loss, Val/Box_Loss, and Val/Cls_Loss functions between the YOLOv8l-FPD$_{Thermal}$ and YOLOv8l-FPD$_{RGB}$ labeled datasets, a consistent trend emerged (Figure 6.16). Each loss metric exhibited a discernible reduction with the progression of epochs. Notably, the YOLOv8l-FPD$_{Thermal}$ model consistently demonstrated lower loss values than the YOLOv8l-FPD$_{RGB}$ model. This pattern of diminishing

loss values with increasing epochs holds significant implications for the performance and accuracy of the model in detecting and scoring the designated FPD objects. The trend observed in the decreasing loss values as epochs advanced aligns with the principles of successful model training (Bist et al., 2023c; Subedi et al., 2023a). Lower loss values signify a closer alignment between the model's predictions and the ground truth labels, indicating enhanced convergence and learning (Carion et al., 2020). The consistent advantage of the YOLOv8l-$FPD_{Thermal}$ model over the YOLOv8l-FPD_{RGB} model implies that thermal images contribute to a more effective and accurate learning process. The inherently distinct information carried by thermal images gives the model a superior foundation for object detection, as evidenced by the consistently lower loss values. Ultimately, the correlation between lower loss values and improved model performance underscores the viability of thermal imaging in bolstering the model's ability to accurately detect and score FPD objects. This insight affirms the efficacy of thermal imaging in enhancing the robustness and precision of FPD detection, which holds the potential to elevate the overall welfare and health monitoring of the poultry population.

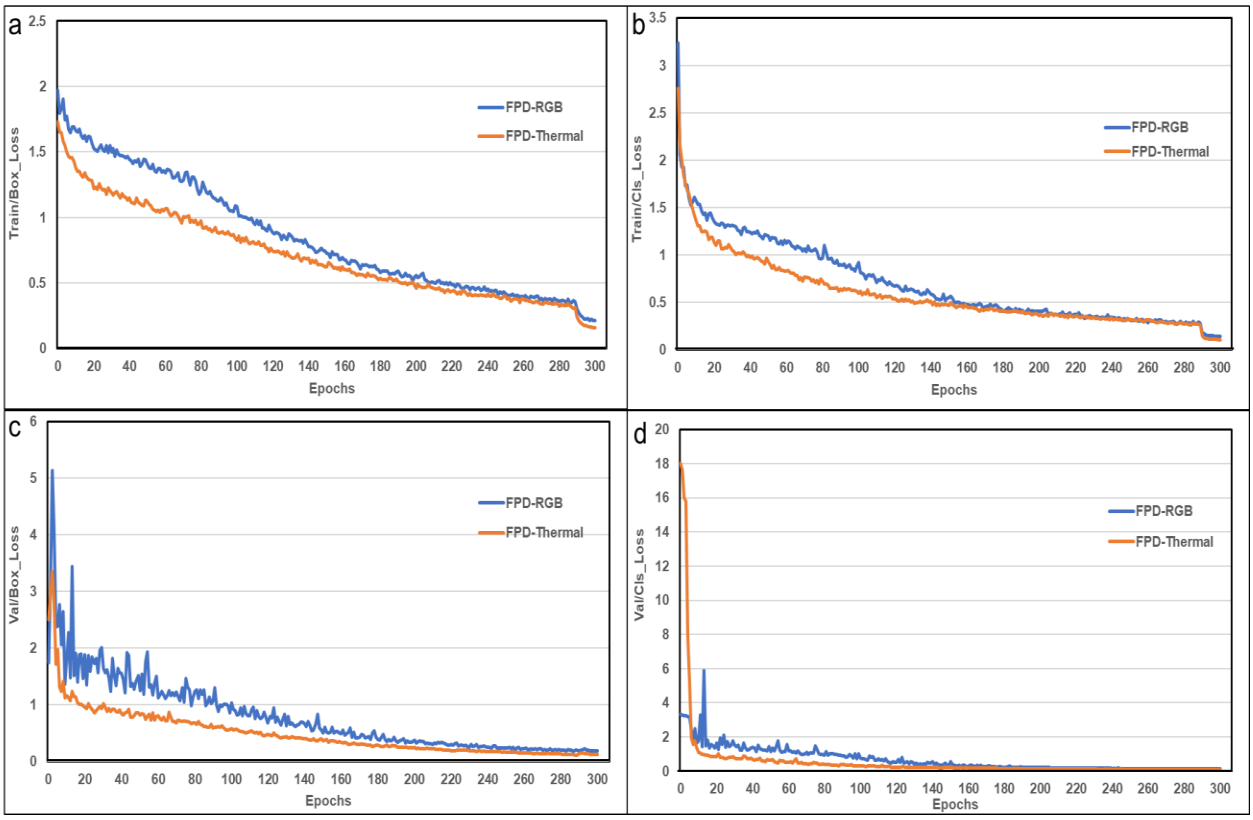

Figure 6.16: Comparison of box and classification loss for training and validation under RGB and thermal image conditions.

6.3.4 Limitations in FPD Scoring and Detecting

The YOLOv8 model performs well in accurately detecting and scoring FPD; however, several factors can impact the detection accuracy. One primary concern found was the presence of manure on a bird's footpad (Figure 6.17a), which can potentially trigger false detections. Instances, where a bird with an FPD score of 0 is inaccurately identified as FPD 1 due to manure on its foot (as shown in Figure 6.17a and Figure 6.17b), underscore the challenge of ensuring accuracy in such scenarios. Furthermore, introducing fresh manure onto the footpad could notably undermine the precision of FPD detection. Similarly, manure and litter on bird legs (as depicted in Figure 6.17c) can also lead to misleading detections. Addressing this issue

necessitates exploring alternative, more precise methodologies or omitting datasets affected by this confounding variable. Additionally, the impact of manure extends to the imaging box's transparency, requiring regular cleaning to uphold optimal image quality. Within this context, ensuring appropriate lighting conditions within the imaging box is essential to capture clear images of the footpad. Light obstruction caused by chickens or other objects can contribute to false positives and negatives in FPD detection (Figure 6.17d).

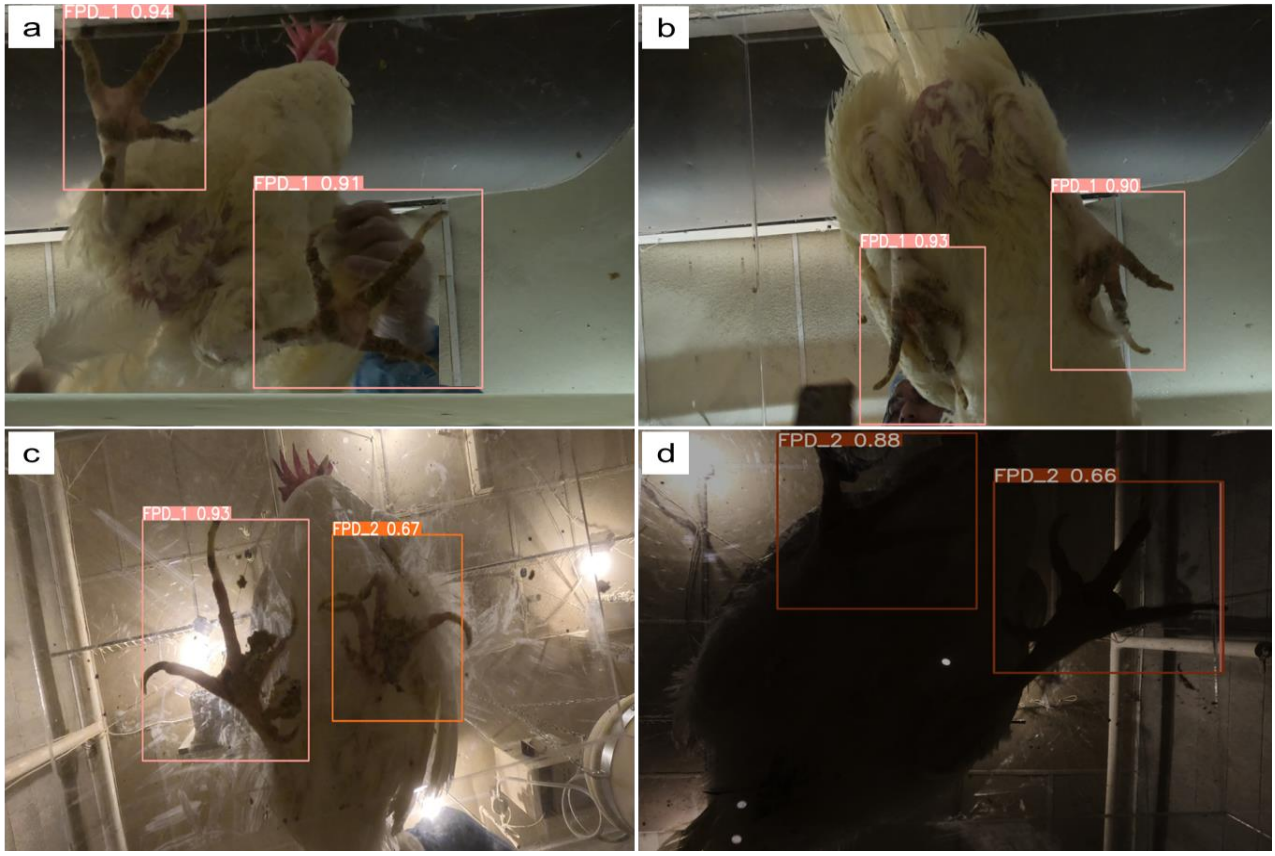

Figure 6.17: FPD detection accuracy limiting factors: a) partially covered footpad with wet manure, b) fully covered footpad with wet manure, c) footpad with litter on box, and d) improper lighting.

Furthermore, the inherent characteristics of the imaging box introduce a set of limitations. The potential slipperiness or discomfort experienced by the hens within the box can influence their posture and movements, consequently affecting detection accuracy. To mitigate this, incorporating supportive elements or adjustments to enhance the comfort and stability of the hens during the imaging process is advisable. The CF environment (higher dust level) introduces yet another complexity (Bist et al., 2023d; Shepherd et al., 2015; Zhao et al., 2015). Regularly cleaning the transparent imaging box is imperative to uphold image quality and prevent dust accumulation from obstructing the camera's view. Likewise, a previous study noted that cameras placed in rooms needed periodic cleaning to improve video quality (Bist et al., 2023c; Yang et al., 2022). Neglecting this maintenance could lower image quality and impact detection accuracy. Additionally, in our study, it is crucial to have a tightly sealed box to prevent dust from getting inside and to ensure the camera functions properly.

6.3.5 Future direction for FPD scoring and detection

In the future, researchers can explore innovative imaging techniques and technologies designed to address factors such as the presence of manure, variations in lighting, and different environmental conditions. This could significantly enhance the accuracy of FPD scoring and detection. Exploring the implementation of automated cleaning mechanisms for the imaging box holds promise for sustaining image quality over time. Moreover, integrating AI-driven algorithms to counteract false detections resulting from environmental factors could further refine FPD detection accuracy in challenging scenarios. Collaboration with poultry health experts could facilitate the practical integration of models into health management strategies, leveraging their expertise for real-world impact. Delving into long-term performance

assessments under diverse conditions and poultry populations would bolster the validation of model applicability. Additionally, exploring thermal imaging technologies could amplify the efficiency of FPD detection. Enhancing model interpretability, diversifying datasets, and investigating real-time detection systems and human-AI collaboration could collectively contribute to the pragmatic utility of the research. These future directions collectively hold the potential to revolutionize FPD detection methodologies and their integration into poultry management practices.

6.4 CONCLUSIONS

This study presents a comprehensive FPD scoring and detection analysis, including valuable insights and performance metrics of different YOLOv8 models. Despite the challenges posed by variables like the presence of manure and environmental factors, the YOLOv8l-FPD model performed better in accurately detecting and scoring FPD conditions. The YOLOv8l-FPD model resulted in higher recall, mAP, and F1 scores across varying image settings, and scoring detection underscores its proficiency and reliability. Notably, there was a subtle difference in detection accuracy between RGB and thermal images, with thermal images exhibiting a slightly higher level of accuracy. This finding underscores the potential advantages of thermal imaging for FPD detection and highlights the importance of considering the specific imaging modality when implementing poultry health management systems. However, challenges such as frequent, transparent box cleaning, battery changing, manure interference, and lighting conditions emphasize the need for future study and improvement. The study emphasizes the potential of YOLOv8 models to revolutionize poultry health management, guiding the way for more effective FPD detection and ultimately enhancing poultry welfare.

6.5 REFERENCES

AAAP, 2022. Broiler footpad condition scoring guide. URL 2022_Broiler foot condition scoring guide_approved.pub (memberclicks.net) (accessed 8.23.23).

Allain, V., Mirabito, L., Arnould, C., Colas, M., Le Bouquin, S., Lupo, C., Michel, V., 2009. Skin lesions in broiler chickens measured at the slaughterhouse: relationships between lesions and between their prevalence and rearing factors. British Poultry Science 50, 407–417.

AMER, M.M., 2020. Footpad dermatitis (FPD) in chickens. The Korean Journal of Food & Health Convergence 6, 11–16.

Anowar, F., Sadaoui, S., 2021. Incremental learning framework for real-world fraud detection environment. Computational Intelligence 37, 635–656.

Ba, J., Frey, B., 2013. Adaptive dropout for training deep neural networks. Advances in neural information processing systems 26.

Berg, C., 2004. Pododermatitis and hock burn in broiler chickens., in: Measuring and Auditing Broiler Welfare. CABI publishing Wallingford UK, pp. 37–49.

Berg, L., 1998. Foot-pad dermatitis in broilers and turkeys.

Bilgili, S., Hess, J., Blake, J., Macklin, K., Saenmahayak, B., Sibley, J., 2009. Influence of bedding material on footpad dermatitis in broiler chickens. Journal of Applied Poultry Research 18, 583–589.

Bist, R.B., Subedi, S., Yang, X., Chai, L., 2023a. A Novel YOLOv6 Object Detector for Monitoring Piling Behavior of Cage-Free Laying Hens. AgriEngineering 5, 905–923.

Bist, R.B., Subedi, S., Yang, X., Chai, L., 2023b. Automatic Detection of Cage-Free Dead Hens with Deep Learning Methods. AgriEngineering 5, 1020–1038. https://doi.org/10.3390/agriengineering5020064

Bist, R.B., Yang, X., Subedi, S., Chai, L., 2023c. Mislaying behavior detection in cage-free hens with deep learning technologies. Poultry Science 102729.

Bist, R.B., Yang, X., Subedi, S., Sharma, M.K., Singh, A.K., Ritz, C.W., Kim, W.K., Chai, L., 2023d. Temporal Variations of Air Quality in Cage-Free Experimental Pullet Houses. Poultry 2, 320–333.

Carion, N., Massa, F., Synnaeve, G., Usunier, N., Kirillov, A., Zagoruyko, S., 2020. End-to-end object detection with transformers. Presented at the European conference on computer vision, Springer, pp. 213–229.

Chavez, E., Kratzer, F., 1972. Prevention of foot pad dermatitis in poults with methionine. Poultry Science 51, 1545–1548.

Chen, X., Pu, Hongli, He, Y., Lai, M., Zhang, D., Chen, J., Pu, Haibo, 2023. An Efficient Method for Monitoring Birds Based on Object Detection and Multi-Object Tracking Networks. Animals 13, 1713.

Chuppava, B., 2018. Effects of different flooring designs on the performance and foot pad health and on the development of antimicrobial resistance in commensal Escherichia coli in broiler and turkey production.

Corregidor-Castro, A., Holm, T.E., Bregnballe, T., 2021. Counting breeding gulls with unmanned aerial vehicles: camera quality and flying height affects precision of a semi-automatic counting method. Ornis Fennica 98, 33–45.

De Jong, I.C., Gunnink, H., Van Harn, J., 2014. Wet litter not only induces footpad dermatitis but also reduces overall welfare, technical performance, and carcass yield in broiler chickens. Journal of Applied Poultry Research 23, 51–58.

Dozier 3rd, W., Thaxton, J., Branton, S., Morgan, G., Miles, D., Roush, W., Lott, B., Vizzier-Thaxton, Y., 2005. Stocking density effects on growth performance and processing yields of heavy broilers. Poultry Science 84, 1332–1338.

Dumitriu, A., Tatui, F., Miron, F., Ionescu, R.T., Timofte, R., 2023. Rip Current Segmentation: A Novel Benchmark and YOLOv8 Baseline Results. Presented at the Proceedings of the IEEE/CVF Conference on Computer Vision and Pattern Recognition, pp. 1261–1271.

Eichner, G., Vieira, S., Torres, C., Coneglian, J., Freitas, D., Oyarzabal, O., 2007. Litter moisture and footpad dermatitis as affected by diets formulated on an all-vegetable basis or having the inclusion of poultry by-product. Journal of Applied Poultry Research 16, 344–350.

Ekstrand, C., Algers, B., Svedberg, J., 1997. Rearing conditions and foot-pad dermatitis in Swedish broiler chickens. Preventive Veterinary Medicine 31, 167–174.

Fulton, R.M., 2019. Health of commercial egg laying chickens in different housing systems. Avian Diseases 63, 420–426.

Gadhwal, M., Sharda, A., Sangha, H.S., Van der Merwe, D., 2023. Spatial corn canopy temperature extraction: How focal length and sUAS flying altitude influence thermal infrared sensing accuracy. Computers and Electronics in Agriculture 209, 107812.

GAP, 2020. Chicken-v3.2-FPD-Assessment-on-farm-record-template.pdf [WWW Document]. URL https://globalanimalpartnership.org/wp-content/uploads/2020/05/Chicken-v3.2-FPD-Assessment-on-farm-record-template.pdf (accessed 11.4.23).

Geron, A., 2022. Hands-on machine learning with Scikit-Learn, Keras, and TensorFlow. O'Reilly Media, Inc.

Grbovic, Z., Panic, M., Marko, O., Brdar, S., Crnojevic, V., 2019. Wheat ear detection in RGB and thermal images using deep neural networks. Environments 11, 13.

Guo, Y., Regmi, P., Ding, Y., Bist, R.B., Chai, L., 2023. Automatic detection of brown hens in cage-free houses with deep learning methods. Poultry Science 102, 102784.

Hand, D.J., Christen, P., Kirielle, N., 2021. F*: an interpretable transformation of the F-measure. Machine Learning 110, 451–456.

Heerkens, J., Delezie, E., Rodenburg, T.B., Kempen, I., Zoons, J., Ampe, B., Tuyttens, F., 2016. Risk factors associated with keel bone and foot pad disorders in laying hens housed in aviary systems. Poultry Science 95, 482–488.

Hester, P., 1994. The role of environment and management on leg abnormalities in meat-type fowl. Poultry Science 73, 904–915.

Hong, S.-J., Han, Y., Kim, S.-Y., Lee, A.-Y., Kim, G., 2019. Application of deep-learning methods to bird detection using unmanned aerial vehicle imagery. Sensors 19, 1651.

Hy-Line, 2020. 36 COM ENG.pdf [WWW Document]. URL https://www.hyline.com/filesimages/Hy-Line-Products/Hy-Line-Product-PDFs/W-36/36%20COM%20ENG.pdf (accessed 9.10.22).

Jocher, G., Chaurasia, A., Qiu, J., 2023a. Ultralytics.

Jocher, G., Waxmann, S., Chaurasia, A., Q, L., 2023b. Ultralytics YOLOv8 Docs [WWW Document]. URL https://docs.ultralytics.com/ (accessed 8.26.23).

Kaukonen, E., Norring, M., Valros, A., 2016. Effect of litter quality on foot pad dermatitis, hock burns and breast blisters in broiler breeders during the production period. Avian Pathology 45, 667–673.

King, R., 2023. Brief summary of YOLOv8 model structure · Issue #189 · ultralytics/ultralytics [WWW Document]. GitHub. URL https://github.com/ultralytics/ultralytics/issues/189 (accessed 8.28.23).

Kjaer, J., Su, G., Nielsen, B., Sørensen, P., 2006. Foot pad dermatitis and hock burn in broiler chickens and degree of inheritance. Poultry Science 85, 1342–1348.

Lee, S., Song, Y., Kil, S.-H., 2021. Feasibility analyses of real-time detection of wildlife using UAV-derived thermal and RGB images. Remote Sensing 13, 2169.

Li, Q., Shao, Z., Zhou, W., Su, Q., Wang, Q., 2023. MobileOne-YOLO: Improving the YOLOv7 network for the detection of unfertilized duck eggs and early duck embryo development - a novel approach. Computers and Electronics in Agriculture 214, 108316. https://doi.org/10.1016/j.compag.2023.108316

Li, Y., 2018. Performance Evaluation of Machine Learning Methods for Breast Cancer Prediction. ACM 7, 212. https://doi.org/10.11648/j.acm.20180704.15

Lou, H., Duan, X., Guo, J., Liu, H., Gu, J., Bi, L., Chen, H., 2023. DC-YOLOv8: Small-Size Object Detection Algorithm Based on Camera Sensor. Electronics 12, 2323. https://doi.org/10.3390/electronics12102323

Majumder, S., Balaji, N., Brey, K., Fu, W., Menzies, T., 2018. 500+ times faster than deep learning: A case study exploring faster methods for text mining stackoverflow. Presented at the Proceedings of the 15th International Conference on Mining Software Repositories, pp. 554–563.

Martland, M., 1985. Ulcerative dermatitis dm broiler chickens: The effects of wet litter. Avian Pathology 14, 353–364.

Martland, M., 1984. Wet litter as a cause of plantar pododermatitis, leading to foot ulceration and lameness in fattening turkeys. Avian Pathology 13, 241–252.

Meluzzi, A., Fabbri, C., Folegatti, E., Sirri, F., 2008. Effect of less intensive rearing conditions on litter characteristics, growth performance, carcase injuries and meat quality of broilers. British Poultry Science 49, 509–515.

Merity, S., Keskar, N.S., Socher, R., 2017. Regularizing and optimizing LSTM language models. arXiv preprint arXiv:1708.02182.

Muvva, V.V., Zhao, Y., Parajuli, P., Zhang, S., Tabler, T., Purswell, J., 2018. Automatic Identification of Broiler Mortality Using Image Processing Technology. Presented at the 10th International Livestock Environment Symposium (ILES X), American Society of Agricultural and Biological Engineers, p. 1.

Nagaraj, M., Wilson, C., Hess, J., Bilgili, S., 2007. Effect of high-protein and all-vegetable diets on the incidence and severity of pododermatitis in broiler chickens. Journal of Applied Poultry Research 16, 304–312.

NCC, 2018. National chicken council animal welfare guidelines and audit checklist for broilers.

Shepherd, E., Fairchild, B., 2010. Footpad dermatitis in poultry. Poultry Science 89, 2043–2051.

Shepherd, T.A., Zhao, Y., Li, H., Stinn, J.P., Hayes, M.D., Xin, H., 2015. Environmental assessment of three egg production systems—Part II. Ammonia, greenhouse gas, and particulate matter emissions. Poultry Science 94, 534–543.

Sorbelli, F.B., Palazzetti, L., Pinotti, C.M., 2023. YOLO-based detection of Halyomorpha halys in orchards using RGB cameras and drones. Computers and Electronics in Agriculture 213, 108228. https://doi.org/10.1016/j.compag.2023.108228

Sorensen, P., Su, G., Kestin, S., 2000. Effects of age and stocking density on leg weakness in broiler chickens. Poultry Science 79, 864–870.

Statista, 2023. Per capita consumption of eggs in the U.S. 2023 [WWW Document]. Statista. URL https://www.statista.com/statistics/183678/per-capita-consumption-of-eggs-in-the-us-since-2000/ (accessed 11.2.23).

Stransky, O., Blum, R., Brown, W., Kruse, D., Stone, P., 2016. Bumble Foot: A Rare Presentation of a Fusobacterium varium Infection of the Heel Pad in a Healthy Female. The Journal of Foot and Ankle Surgery 55, 1087–1090.

Subedi, S., Bist, R., Yang, X., Chai, L., 2023a. Tracking pecking behaviors and damages of cage-free laying hens with machine vision technologies. Computers and Electronics in Agriculture 204, 107545.

Subedi, S., Bist, R., Yang, X., Chai, L., 2023b. Tracking Floor Eggs with Machine Vision in Cage-free Hen Houses. Poultry Science 102637. https://doi.org/10.1016/j.psj.2023.102637

UEP, 2023. Facts & Stats. United Egg Producers. URL https://unitedegg.com/facts-stats/ (accessed 11.2.23).

USDA, 2020. Poultry Production Systems and Well-being: Sustainability for Tomorrow - University of California, Davis. USDA NIFA. URL https://portal.nifa.usda.gov/web/crisprojectpages/1013484-poultry-production-systems-and-well-being-sustainability-for-tomorrow.html (accessed 11.2.23).

Wang, G., Chen, Y., An, P., Hong, H., Hu, J., Huang, T., 2023. UAV-YOLOv8: A Small-Object-Detection Model Based on Improved YOLOv8 for UAV Aerial Photography Scenarios. Sensors 23, 7190.

Wang, G., Ekstrand, C., Svedberg, J., 1998. Wet litter and perches as risk factors for the development of foot pad dermatitis in floor-housed hens. British Poultry Science 39, 191–197.

Wilcox, C.S., Patterson, J., Cheng, H.W., 2009. Use of thermography to screen for subclinical bumblefoot in poultry. Poult Sci 88, 1176–1180. https://doi.org/10.3382/ps.2008-00446

Yan, B., Fan, P., Lei, X., Liu, Z., Yang, F., 2021. A real-time apple targets detection method for picking robot based on improved YOLOv5. Remote Sensing 13, 1619.

Yang, S., Wang, W., Gao, S., Deng, Z., 2023. Strawberry ripeness detection based on YOLOv8 algorithm fused with LW-Swin Transformer. Computers and Electronics in Agriculture 215, 108360. https://doi.org/10.1016/j.compag.2023.108360

Yang, X., Bist, R., Subedi, S., Chai, L., 2023a. A deep learning method for monitoring spatial distribution of cage-free hens. Artificial Intelligence in Agriculture.

Yang, X., Bist, R.B., Subedi, S., Chai, L., 2023b. A Computer Vision-Based Automatic System for Egg Grading and Defect Detection. Animals 13, 2354.

Yang, X., Chai, L., Bist, R.B., Subedi, S., Wu, Z., 2022. A Deep Learning Model for Detecting Cage-Free Hens on the Litter Floor. Animals 12, 1983.

Yuan, Y., Xiong, Z., Wang, Q., 2016. An incremental framework for video-based traffic sign detection, tracking, and recognition. IEEE Transactions on Intelligent Transportation Systems 18, 1918–1929.

Zhang, H.-F., Jiao, H.-C., Song, Z.-G., Hai, L., 2011. Effect of alum-amended litter and stocking density on ammonia release and footpad and hock dermatitis of broilers. Agricultural Sciences in China 10, 777–785.

Zhao, Y., Shepherd, T.A., Li, H., Xin, H., 2015. Environmental assessment of three egg production systems–Part I: Monitoring system and indoor air quality. Poultry Science 94, 518–533.

CHAPTER 7

EFFECTIVENESS OF ELECTROSTATIC PARTICLE IONIZATION WITH VARYING HEIGHTS AND DURATIONS IN REDUCING PARTICULATE MATTER[6]

[6] Bist, R. B., Yang, X., Subedi, S., and Chai, L. 2024. Effectiveness of Electrostatic Particle Ionization in Reducing Particulate Matter in Cage-Free Hen Houses with Varying Heights and Durations. Under-Review.

ABSTRACT

The poultry industry is shifting towards more sustainable and ethical practices, including adopting cage-free (CF) housing to enhance hen welfare. However, ensuring optimal indoor air quality, particularly concerning particulate matter (PM), remains challenging in CF environments. This study explores the effectiveness of Electrostatic Particle Ionization (EPI) technology in mitigating PM in CF hen rooms while considering the height at which the technology is placed and the duration of the electric supply. The primary objectives are to analyze the impact of EPI in reducing PM and investigate its power consumption correlation with electric supply duration. The study was conducted at UGA research farm with four identical rooms housing 720 Hy-line W-36 laying hens. The study utilized a Latin Square Design (LSD) method in two experiments to assess the impact of EPI height and electric supply durations on PM levels and electricity consumption. Experiment 1 tested four EPI heights: H1 (5ft or 1.52m), H2 (6ft or 1.83m), H3 (7ft or 2.13m), and H4 (8ft or 2.44m), while Experiment 2 examined four electric supply durations: D1 (Control), D2 (8 hours), D3 (16 hours), and D4 (24 hours) through 32 feet corona pipes. Particulate matter levels were measured twice a week at three different locations within each rooms, and statistical analysis was conducted using ANOVA with a significance level of ≤ 0.05. The study found no significant differences in PM concentrations among different heights within the EPI system ($P > 0.05$). However, the duration of EPI system operation had significant effects on PM_1, $PM_{2.5}$, and PM_4 concentrations ($P < 0.05$). The results show that there were significant differences between EPI duration treatments. Longer EPI durations resulted in significant reductions: D3 - 37.6% for PM_1, 30.4% for $PM_{2.5}$, 39.7% for PM_4, 40.2% for $PM_{10,}$ and 41.1% for TSP; D4- 36.6% for PM_1, 24.9% for $PM_{2.5}$, 38.6% for PM_4, 36.3% for PM_{10}, and 37.9% for TSP compared with D1. However, there was no significant

difference between D3 and D4. Therefore, D3 treatment can be the best choice and reduce 8 hours electricity every day which may offer a more energy-efficient approach while maintaining effective PM reduction. Further research is needed to optimize PM reduction strategies, considering factors such as animal activities, to improve air quality and environmental protection in CF hen environments.

Keywords: Cage-free, Air pollutant concentration, Mitigation strategy, Electrostatic-ionization technology.

7.1 INTRODUCTION

The poultry industry is transforming towards more sustainable and ethical practices, driven by consumer demand for ethically sourced products and heightened concerns about animal welfare (USDA, 2016; UEP, 2017; Mintus, 2021; Bist et al., 2022). Cage-free (CF) housing systems have emerged as a promising alternative to caged housing environments for laying hens, offering hens the freedom to roam, perch, and engage in natural behaviors, leading to improved welfare and potentially enhanced egg production. Despite the numerous benefits, adopting CF systems introduces new challenges, particularly in ensuring optimal indoor air quality (e.g., particulate matters) within hen houses (Chai et al., 2018; Bist and Chai, 2022; Bist et al., 2023a; b).

The accumulation of particulate matter (PM) constitutes a significant concern in CF environments, encompassing various airborne pollutants such as dust, feathers, and dander (Qi et al., 1992; Cambra-López et al., 2011; Ahaduzzaman et al., 2021; Bist and Chai, 2022). These particles can adversely affect the respiratory health of hens, leading to respiratory issues, reduced

productivity, and compromised well-being (Cambra-López et al., 2010; Michiels et al., 2015; Zhao et al., 2016; EPA, 2022a; EPA, 2022b). Moreover, PM poses health risks to farmworkers (Donham, 2000; Radon et al., 2001; Bist and Chai, 2022; EPA, 2022a), contributes to environmental pollution (WHO, 2021; EPA, 2022a), and may affect the safety and quality of egg products, ultimately impacting consumer trust. Addressing this pressing concern requires innovative air quality management solutions that effectively reduce PM emissions while maintaining a conducive and healthy indoor environment for the hens. Researchers and practitioners have explored various technologies to mitigate PM in poultry facilities, each with varying levels of efficacy. These measures include oil and water spraying (Almuhanna, 2007; Aarnink et al., 2011; Winkel et al., 2016a; Chai et al., 2017), scrubbers (Zhao et al., 2011), air filtration (Demmers et al., 2010; Mostafa and Buescher, 2011; Winkel et al., 2015), manure management (Nimmermark et al., 2009; Shepherd et al., 2015), and electrostatic particle ionization (EPI; Mitchell et al., 2004; Ritz et al., 2006; Mitchell and Baumgartner, 2007; Jerez et al., 2013).

Oil spraying systems with handheld spraying lances have shown the capability to remove up to 94% of $PM_{2.5}$ and 82% of PM_{10} (Winkel et al., 2016b). However, the mixture of oil and PM is trapped on floors, walls, and cages, necessitating frequent house cleaning to prevent worker hazards. Acidic electrolyzed water spraying systems have demonstrated up to 89% removal efficiencies for total PM in CF poultry facilities (Chai et al., 2017). Wet scrubbers with packed-bed configurations exhibit high removal efficiencies of up to 90% for $PM_{2.5}$ and 93% for PM_{10} (Zhao et al., 2011), but they tend to become easily clogged, require significant water usage, and raise concerns about shifting the pollution problem from air to liquid waste. Filtration is a

commonly used technique, effectively removing up to 60% of fine dust in poultry layer facilities (Ogink et al., 2009). However, this method is susceptible to frequent clogging and particle resuspension.

Among the emerging technologies, electrostatic charging system has garnered attention as a potential solution to reduce airborne particles in various experimental and commercial settings (Veenhuizen and Bundy, 1990; Mitchell and Waltman, 2003; Mitchell et al., 2004; Ritz et al., 2006; Mitchell and Baumgartner, 2007; Cambra-López et al., 2009; Jerez et al., 2013; Winkel et al., 2016b). Electrostatic particle ionization systems utilize electrostatic charges to attract and neutralize airborne particles, providing a promising avenue for mitigating PM in CF henhouses. Studies have reported significant PM reductions in broiler houses, with electrostatic charging systems achieving up to 43% reduction in PM levels (Ritz et al., 2006). Research in other broiler houses demonstrated a reduction of 36% for PM_{10} and 10% for $PM_{2.5}$ using an electrostatic charging system (Cambra-López et al., 2009). Furthermore, specific studies have evaluated the effectiveness of electrostatic charging systems in hatching cabinets, with reductions in dust levels ranging from 77% to 79% (Mitchell and Waltman, 2003). In another recent study, a prototype electrostatic precipitator effectively reduced $PM_{2.5}$ and PM_{10} levels by up to 97.8% and 99.0%, respectively, under different weather and ventilation conditions (Knight et al., 2021).

Despite these promising findings, the application of EPI in CF hen houses remains relatively unexplored, necessitating comprehensive research to evaluate its efficacy and practical implementation. The success of EPI technology in this specific context is influenced

significantly by crucial factors such as the facility's layout and the height at which the electric supply is situated above the litter floor. However, the efficacy of EPI technology with respect to height in CF hen houses has yet to be fully explored. Ritz et al. (2006) recommend placing the EPI technology closer to the litter floor where dust is generated. In this study, the goal is to evaluate the effectiveness of EPI technology in reducing PM in CF hen rooms while considering the height at which the technology is placed. Similarly, several studies used 24 hours of electric supply (Mitchell et al., 2004; Ritz et al., 2006; Cambra-López et al., 2009). However, it is worth questioning whether running the system 24 hours a day is necessary, especially when the birds show no activity during the dark period. Thus, the hypothesis is that the reduction in PM concentration significantly depends on the duration of the electricity supply and the height at which EPI technology is placed. Hence, the primary objectives of this research paper are:

a) To conduct a thorough analysis of the impact of EPI in mitigating PM, with a particular emphasis on the influence of varying electric supply durations or heights.

b) To investigate the power consumption of the EPI system and its correlation with the duration of the electric supply.

The findings of this study aim to provide practical insights that can guide poultry farmers and industry stakeholders in developing effective air quality management strategies, ultimately fostering improved animal welfare, increased egg production, and sustainable practices in the poultry industry. This research can potentially drive significant advancements toward a more responsible and ethical approach to egg production by addressing the crucial challenge of maintaining optimal indoor air quality in CF environments.

7.2 MATERIALS AND METHODS

7.2.1 Ethical Approval

Before commencing the study, all procedures were approved by the Institutional Animal Care and Use Committee at the University of Georgia (AUP#: A2020 08-014-A3).

7.2.2 Experimental Setup

This experiment follows the same housing and bird management practices as described in Chapter 2 of section 2.2.1. In addition, the EPI system was hung from the ceiling and connected to the EPI device (EPIAir, Columbia, MO, USA) for particle ionization (Figure 7.1b).

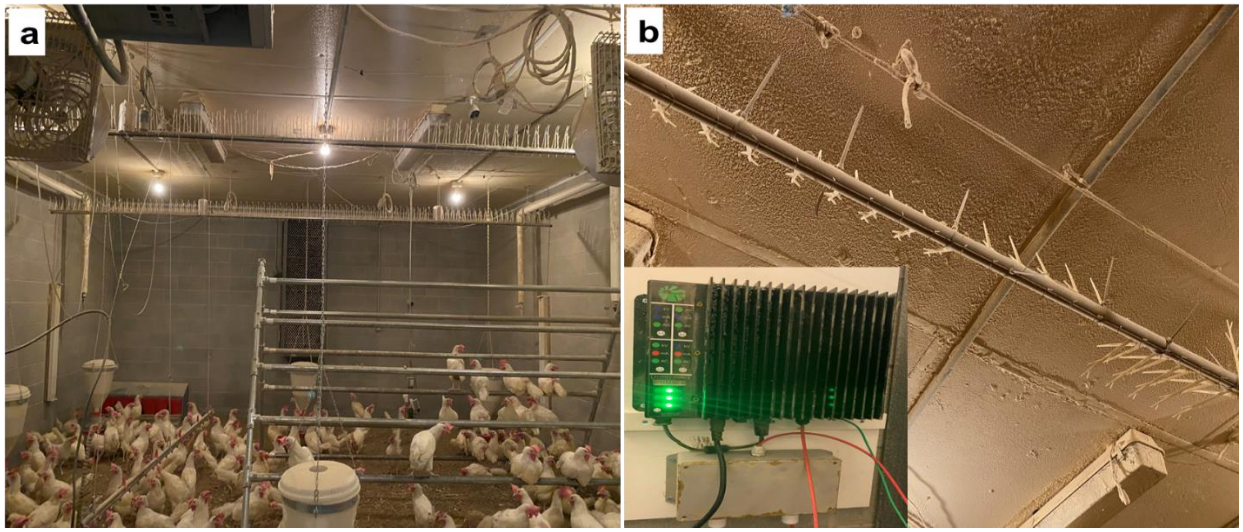

Figure 7.1: a) Experimental cage-free hen room with b) Electrostatic particle ionization system.

7.2.2.1 Experiment 1

Experiment 1 utilized the Latin Square Design (LSD) method to conduct the study, considering the limited availability of rooms (Table 7.1). The available rooms were provided with four distinct height treatments of EPI: 5 feet (H1 = 1.5 m), 6 feet (H2 = 1.8 m), 7 feet (H3 =

2.1 m), and 8 feet (H4 = 2.4 m) above the litter floor. These heights were selected based on suggestions from previous studies, including 7ft (Ritz et al., 2006) and 8ft (Mitchell et al., 2004; Cambra-López et al., 2009), and additional heights of 5ft and 6ft, closer to the average human height, were also included. The lower heights were recommended by Ritz et al. (2006) for increased dust reduction efficiency. However, the 9ft EPI height was not used due to the presence of different equipment in the experimental rooms, and heights below 5ft were avoided to prevent harm to the hens as they tend to jump and fly around. To adjust the EPI height, a manual winch was installed, allowing caretakers to raise or lower the system safely when entering the room to avoid accidents. Each trial duration lasted one week, with continuous operation. To ensure the hens did not sit on the corona pipe, bird-repellent spikes were thoughtfully placed above it. For minimizing electric shocks on nearby objects, the EPI system was carefully positioned 1 foot (0.3m) away from the walls and 8 feet (2.4 m) away from each other. The configuration involved two rows of 18 feet (5.5m) long corona pipes, resulting in a total length of 36 feet (11m) for the entire EPI system.

Table 7.1: Experimental LSD setup for EPI heights among four CF hen experimental rooms.

Trial/WOA	Room 1	Room 2	Room 3	Room 4
1 (68)	H1	H2	H4	H3
2 (69)	H4	H3	H1	H2
3 (70)	H2	H4	H3	H1
4 (71)	H3	H1	H2	H4

Where, LSD- Latin Square Design; EPI- electrostatic particle ionization; CF- cage-free; WOA- weeks of age; H1= 5ft (1.5m), H2= 6ft (1.8m), H3= 7ft (2.1m), and H4= 8ft (2.4m) high above the litter.

7.2.2.2 Experiment 2

Experiment 2 employed the LSD, dividing the rooms into four different treatments: Control (D1), 8 hours (D2), 16 hours (D3), and 24 hours (D4) of EPI operation (Table 7.2). These durations were selected based on several studies that used a 24-hour electric supply (Mitchell et al., 2004; Ritz et al., 2006; Cambra-López et al., 2009). However, considering that laying hen housing provided a 16-hour light period, it is worth questioning whether running the system 24 hours a day is necessary, especially when the birds show no activity during the dark period (8 hours). Moreover, the inclusion of an 8-hour duration treatment was based on the half-light period time to assess whether using 8 hours can yield similar PM reduction compared to other treatments. Each trial lasted one week, and an EPI system was placed 8 feet from each other to accommodate existing equipment in the rooms. Bird-repellent spikes were also thoughtfully placed above the corona pipe to prevent hens from sitting on it. The EPI system was positioned 1 foot (0.3m) away from the ceiling and walls to avoid electric field effects on nearby objects, using two rows of 18 feet (5.5m) long corona pipes totaling 36 feet (11m) in length.

Table 7.2: Experimental setup for EPI duration electric supply in four CF hen experimental rooms using LSD.

Trial/WOA	Room 1	Room 2	Room 3	Room 4
1 (73)	D1	D2	D4	D3
2 (74)	D4	D3	D1	D2
3 (75)	D2	D4	D3	D1
4 (76)	D3	D1	D2	D4

Where, LSD- Latin Square Design; EPI- electrostatic particle ionization; CF- cage-free; WOA- weeks of age; D1= control (0 hour of electric supply), D2= 8 hours of electric supply, D3= 16 hours of electric supply, and D4= 24 hours of electric supply.

7.2.3 Working Mechanism of EPI

Electrostatic Particle Ionization technology offers a revolutionary approach to improving air quality by releasing negative ions into the surrounding atmosphere. These negative ions play a critical role in charging and surrounding airborne particles, causing them to be attracted to grounded or positively charged surfaces. As a result, the charged particles either adhere to surfaces or settle on the ground, leading to noticeably cleaner and safer air to breathe. EPI systems comprise essential components, such as a 2.0 mA power supply, a corona pipe with a sharp point, insulators, and a high-voltage direct current of -30 KV with a current limit of 2 mA or lower for enhanced safety (EPIAir, 2023). This cost-effective technology operates with power consumption comparable to a 100-watt light bulb and can connect to standard electrical services. EPI systems emit an impressive volume of up to a thousand trillion negative ions into the air every second, effectively saturating airborne particles and inducing charge shifts. This process causes PM to adhere to surfaces or descend to the ground, improving air cleanliness. Designed specifically for agriculture, EPI technology creates a protective barrier in the airspace, safeguarding animals and workers from various airborne contaminants. Treating airspace with negative ions naturally attracts and polarizes airborne particles, facilitating their bonding and adhesion to surfaces they encounter. Furthermore, EPI technology triggers essential air chemistry reactions that help reduce the presence of noxious gases, ensuring a healthier and more pleasant indoor environment.

7.2.4 Electricity Consumption by EPI

The research focused on examining the power consumption of the EPI system and its correlation with the duration of the electric supply used. The study aimed to understand how the duration of the electric supply influences the EPI system's power consumption in this specific context. In Experiment 1, the length and duration of EPI systems were the same, resulting in no difference in electric consumption. However, the duration of the EPI system is critical information that holds significance for poultry producers, as it facilitates the selection of an appropriate EPI duration that balances effectiveness in mitigating airborne pollutants with energy expenditure. To achieve this objective, a digital power monitor meter (Zhengzhou Paiji Technology, China) was utilized for each treatment room to measure electricity consumption accurately. The digital power monitor meter operated at a voltage of 120V, a frequency of 60Hz, and an operating current of up to 15A, providing real-time data on the power consumption of the EPI system. The power consumption analysis was carried out at the end of the study to assess the power requirements and efficiency of the EPI system under various configurations. By monitoring the electricity usage in kilowatt-hours (KWh), valuable insights were obtained regarding the relationship between the duration of the electric supply and the energy consumed by the EPI system. These findings play a crucial role in assisting poultry producers in making informed decisions, enabling them to optimize the air quality management in their facilities while ensuring energy conservation and sustainable poultry production practices.

7.2.5 Environment Parameter Measurements

Temperature and humidity measurements were conducted inside and outside each room using Onset HOBO data loggers (HOBO MX1101, Onset, Bourne, MA, USA), programmed to collect data every 10 minutes throughout 24 hours. Inside sensors were positioned 1.2 m above the floor, while outside sensors were placed 1.8 m above the ground. Daily temperature and relative humidity data checks were performed through a phone to ensure a comfortable environment for the birds.

The moisture content of the litter (LMC) influences the levels of air pollutants within poultry housing (Bist et al., 2022, 2023b; Carr et al., 1990). To assess the LMC of the litter in the rooms, 100g samples were collected weekly from four random locations within each room and placed into Ziplock bags as mentioned in Yang et al., 2022. These samples were then transported to a laboratory for analysis. The collected samples were thoroughly mixed in the laboratory, and two separate 10g samples were extracted from each bag. One sample was used for testing, while the other was used as a validation sample. The samples were weighed and then heated in a THELCO Laboratory oven (Precision Scientific; Chicago, IL, USA) at 105 °C for 24 hours (Corkery et al., 2013). Following the heating process, the final litter weights were recorded after cooling in the desiccator. The litter moisture content was calculated using Equation (1), which compares the initial wet litter weight (LWW) to the final dry litter weight (LDW). This calculation enables the determination of the percentage of moisture present in the litter samples, providing essential insights into the litter's condition and potential impact on air quality within the poultry facility.

$$LMC\ (\%) = \frac{LWW - LDW}{LWW} \times 100 \qquad (1)$$

7.2.6 Particulate Matter Measurement

In this study, PM levels were systematically monitored twice a week using an optical PM sensor, specifically the DustTrak DRX Aerosol Monitor 8533 (TSI Incorporated in Shoreview, MN, USA). The PM sensor was capable of measuring various sizes of PM, including PM_1, $PM_{2.5}$, PM_4, PM_{10}, and TSP (Total Suspended Particulates), allowing for a comprehensive assessment of airborne pollutants. The measurements were taken at three locations inside each room, strategically chosen to represent different activity areas and potential particle concentrations. These locations included positions near the perch, between the feeder and drinker, and near the exhaust ventilation. The light turned on at 05:00 and turned off at 21:00, providing a 16-hour light period. For Experiment 1, we collected the PM data twice a week and only once during the sampling day at three different locations. For Experiment 2, we collected the PM data twice a week and four times during the sampling day and at three different locations (1 hour before and after the first 8 hours of the light period, 1 hour before and after the 16 hours of the light period, which also included the dark period PM data).

Specific protocols were strictly followed before each measurement to ensure the accuracy and reliability of the data collected. The PM sensor was carefully positioned at a consistent height of 36 cm above the floor and covered with a plastic cover to prevent dust buildup or external interference that might compromise the readings. Furthermore, to maintain precise calibration and data integrity, the PM sensor underwent manufacturer calibration before the research commenced, and regular maintenance was upheld throughout the study. This maintenance routine involved periodic cleaning and filter replacement every two weeks. The first 30 seconds (out of 120 seconds) of each reading were excluded from the data analysis process to

avoid potential interference from sensor relocation within the rooms during the initial measurement moments. By adhering to these rigorous procedures, the research team ensured that the collected PM measurements provided accurate and reliable insights into the indoor air quality of the laying hen facility.

7.2.7 Statistical Analysis

In this research, four cage-free rooms were arranged in an LSD manner, with room and trial serving as blocking factors, and four different EPI heights (H1, H2, H3, and H4) or electric supply durations (D1, D2, D3, and D4) considered as treatments. Statistical analyses were performed using R-studio (version 4.1.0) to assess the impact of varying heights or electric supply durations on PM levels, litter moisture content (LMC), and electricity consumption within the laying hen facility. ANOVA was employed to analyze the PM, LMC, and electricity consumption data collected from each room, followed by LSMeans Tukey HSD method to determine significant differences between the treatments. Differences were considered significant at a *P*-value of ≤ 0.05. The study aimed to gain insights into the effectiveness of EPI technology in mitigating airborne pollutants and maintaining optimal litter conditions, providing valuable information for enhancing indoor air quality and overall well-being in the laying hen environment.

$$\boldsymbol{Y_{ijl} = \mu + \alpha_i + \beta_j + \gamma_l + \varepsilon_{ijl}} \quad (2)$$

Where: i=1,.., K; j=1,.., K, l=1,.., K; K represents the Latin letter for treatment in the $(i,j)^{th}$ cell of the Latin Square; Y_{ijk} represents the LMC, PM, or electricity consumption corresponding to K^{th} Latin letter in the $(i,j)^{th}$ cell; μ is the overall mean of the LMC, PM, or electricity consumption; α_i is the effect of i^{th} Rooms; β_j is the effect of j^{th} Trials or WOA; γ_l is the effect of l^{th} EPI heights or electric supply duration; and ε_{ijk} represents the random error term corresponding to K^{th} Latin letter in the $(i,j)^{th}$ cell.

7.3 RESULTS AND DISCUSSION

7.3.1 Experiment 1

7.3.1.1 Environment parameters

The study compared the influence of different EPI height treatments (H1, H2, H3, and H4) on temperature, RH, and the LMC (Table 7.3). The study observed slight variations in temperature among the different treatments. The average values ranged from 21.82 °C for H2 to 23.19 °C for H1. The differences observed could be attributed to various factors, including the heat generated by the different treatments. Similarly, the study identified slight differences in RH levels among the various treatments. The average RH values ranged from 43.94% for H2 to 47.64% for H1. As with temperature, these differences in RH, although relatively small, can impact certain experiments or processes sensitive to humidity variations.

Contrary to the observed variations in temperature and RH, the study found no significant differences in LMC among the treatments (P=0.946), and percentages ranged from 10.05% to 10.36% across all treatments. These LMC is less than previous research reported in CF aviary housing (Oliveira et al., 2019). One possible explanation for the consistent LMC values across treatments could be the environmentally controlled housing (Corkery et al., 2013; Bist and Chai, 2022; Yang et al., 2022) and the same length of EPI system used. The housing system's ability to regulate temperature and RH precisely may contribute to the stable LMC observed in the study. Controlled housing minimizes external factors that could otherwise influence humidity levels, ensuring a reliable and reproducible experimental environment.

Table 7.3: Environmental parameters in CF hen rooms with varying EPI heights.

Parameters	H1	H2	H3	H4
Temperature (°C)	23.19 ± 1.52	21.82 ± 1.15	22.54 ± 1.46	22.88 ± 1.39
RH (%)	47.64 ± 10.39	43.94 ± 10.99	45.11 ± 10.83	44.08 ± 9.05
LMC (%)	10.05 ± 0.81	10.30 ± 0.89	10.15 ± 1.28	10.36 ± 0.51

Where, EPI- electrostatic particle ionization; CF- cage-free; RH- relative humidity; LMC- litter moisture content; H1= 5ft (1.5m), H2= 6ft (1.8m), H3= 7ft (2.1m), and H4= 8ft (2.4m) high above the litter.

7.3.1.2 PM concentration

The study's results showed no statistically significant differences in PM concentrations among different heights within the EPI system, indicating that the treatments (H1, H2, H3, and H4) did not cause substantial variations in PM levels (Table 7.4). The controlled parameters, including an equal corona pipe length and uniform discharge of charged particles, likely ensured consistent exposure and interaction of air pollutants with the EPI system, leading to a relatively uniform neutralization of PM throughout the treatment (Figure 7.2). As a result, the treatments consistently reduced PM_1, $PM_{2.5}$, PM_4, PM_{10}, and TSP levels, regardless of the height of implementation. However, it is crucial to acknowledge the study's limited scope, focusing on specific treatments within the EPI system. Further investigations are needed to comprehensively understand PM dynamics and potential PM mitigation strategies.

Table 7.4: Effect of EPI heights on PM concentrations (mg m^{-3}) in CF hen rooms.

Treatments	PM_1	$PM_{2.5}$	PM_4	PM_{10}	TSP
H1	1.71 ± 0.36	1.79 ± 0.34	1.98 ± 0.37	3.50 ± 0.72	9.12 ± 1.73
H2	2.14 ± 0.57	2.22 ± 0.59	2.46 ± 0.64	4.31 ± 1.11	11.20 ± 2.93
H3	2.28 ± 0.48	2.37 ± 0.49	2.61 ± 0.55	4.56 ± 0.95	12.10 ± 2.33
H4	1.91 ± 0.52	1.98 ± 0.53	2.19 ± 0.60	3.82 ± 1.11	10.00 ± 2.92
***P*-value**	0.2530	0.2664	0.2845	0.3080	0.2976

Where, EPI- electrostatic particle ionization; CF- cage-free; H1= 5ft (1.5m), H2= 6ft (1.8m), H3= 7ft (2.1m), and H4= 8ft (2.4m) high above the litter. PM- particulate matter; PM_1- PM with a diameter of ≤1 micrometer, $PM_{2.5}$- PM with a diameter of ≤2.5 micrometers, PM_4- PM with a diameter of ≤4 micrometers, PM_{10}- PM with a diameter of ≤10 micrometers, TSP- Total Suspended Particles.

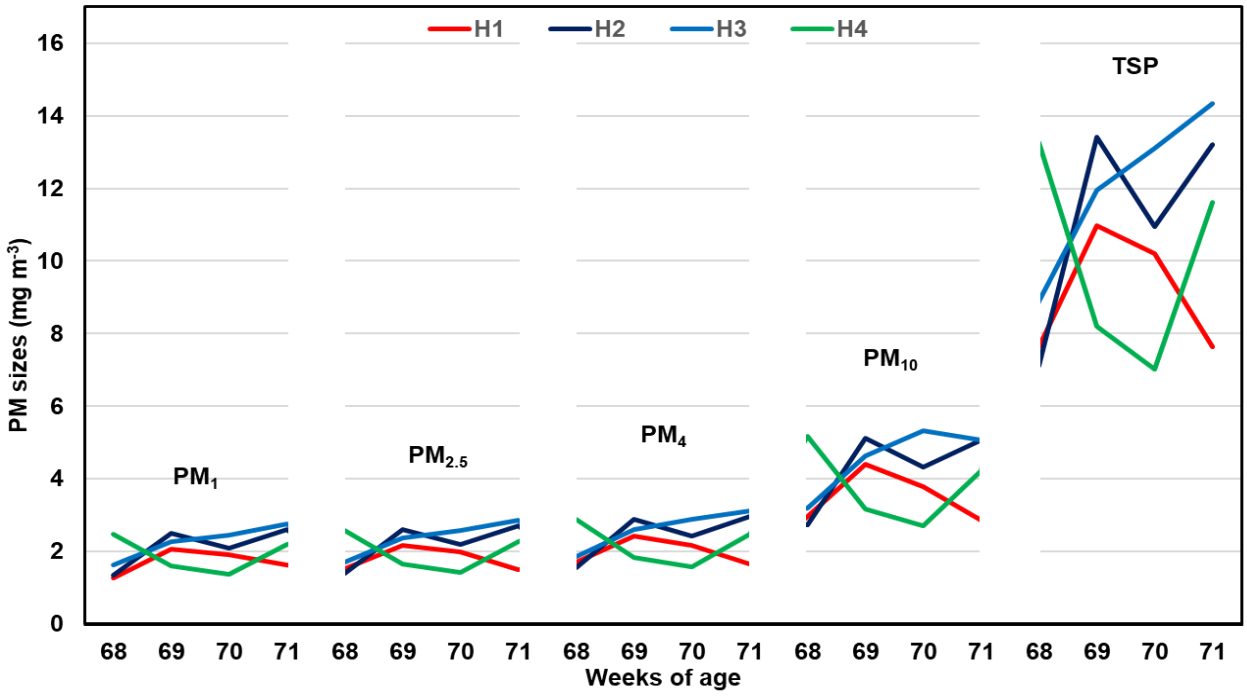

Figure 7.2: Influence of EPI heights on PM concentrations in CF rooms with varying hen's weeks of age.

Where, EPI- electrostatic particle ionization; CF- cage-free; H1= 5ft (1.5m), H2= 6ft (1.8m), H3= 7ft (2.1m), and H4= 8ft (2.4m) high above the litter. PM- particulate matter; PM_1- PM with a diameter of ≤1 micrometer, $PM_{2.5}$- PM with a diameter of ≤2.5 micrometers, PM_4 - PM with a diameter of ≤4 micrometers, PM_{10} - PM with a diameter of ≤10 micrometers, TSP - Total Suspended Particles.

7.3.2 Experiment 2

7.3.2.1 Environment parameters

The study compared temperature, RH, and the LMC of different EPI duration treatments (D1, D2, D3, and D4). The rooms exhibited similar temperatures across all treatments, with average values ranging from 22.54 to 23.24 °C (Table 7.5). Additionally, the RH levels in the rooms were consistent, showing average values between 43.58% and 48.10%. These findings suggest that the environmentally controlled housing significantly provided consistent temperature and humidity levels throughout the study period (Corkery et al., 2013; Bist and Chai, 2022), irrespective of the treatment applied.

Furthermore, the study found consistent LMC values across all treatments, with average percentages ranging from 10.55% to 11.12%. The absence of statistically significant differences in LMC among the treatments (P=0.731) further supports the notion that the housing system maintained a stable and uniform moisture content within the EPI system. Thus, it highlights the housing system's robust performance in controlling and stabilizing humidity levels, resulting in a constant and optimal LMC across the different treatments. Overall, the study's results demonstrate that similar environmentally controlled housing tended to yield similar temperature and RH levels (Verma et al., 2014; Bist and Chai, 2022; Yang et al., 2022) with comparable LMC percentages, providing valuable insights into the importance of environmentally controlled

research housing systems in offering reliable and reproducible experimental conditions. This benefit might contributes to research endeavors that demand a consistent and stable environment.

Table 7.5: Environmental parameters in CF hen rooms with varying EPI duration.

Parameters	D1	D2	D3	D4
Temperature (°C)	23.24 ± 1.26	22.71 ± 1.38	23.23 ± 1.25	22.54 ± 1.40
RH (%)	43.58 ± 12.33	47.66 ± 10.04	44.87 ± 11.79	48.10 ± 12.10
LMC (%)	11.00 ± 1.04	10.89 ± 0.89	10.55 ± 1.46	11.12 ± 1.80

Where, EPI- electrostatic particle ionization; CF- cage-free; RH- relative humidity; LMC- litter moisture content; D1= control (0 hour), D2= 8 hours, D3= 16 hours, and D4= 24 hours electric supply into EPI corona pipes.

7.3.2.2 PM concentration

The study aimed to investigate the impact of different durations of the EPI system operation on PM concentrations, specifically focusing on PM_1, $PM_{2.5}$, PM_4, PM_{10}, and TSP. The results revealed significant differences in PM concentrations among the various durations for PM_1, $PM_{2.5}$, and PM_4 (*P*-values: 0.0103, 0.0074, and 0.0473, respectively), while PM_{10} and TSP did not show statistically significant variations at the 5% significance level (Table 7.6; Figure 7.3). In the Control treatment (D1), the average concentrations of PM_1, $PM_{2.5}$, PM_4, PM_{10}, and TSP were measured as 2.98 ± 0.49 mg/m³, 2.83 ± 0.39 mg/m³, 3.63 ± 1.1 mg/m³, 6.59 ± 2.25 mg/m³, and 16.80 ± 5.59 mg/m³, respectively. Comparing the other treatments (D2, D3, and D4) to D1, percentage reductions were calculated using the differences in PM levels. The 8-hour duration treatment (D2) showed reductions of 17.8% for PM_1, 11.0% for $PM_{2.5}$, 23.1% for PM_4, 23.7% for PM_{10}, and 22.7% for TSP. With a 16-hour duration (D3), the reductions significantly

increased to 37.6% for PM_1, 30.4% for $PM_{2.5}$, 39.7% for PM_4, 40.2% for PM_{10}, and 41.1% for TSP. The 24-hour duration treatment (D4) resulted in percentage reductions of 36.6% for PM_1, 24.9% for $PM_{2.5}$, 38.6% for PM_4, 36.3% for PM_{10}, and 37.9% for TSP compared to the Control. These findings suggest that extending the EPI system operation duration can lead to more substantial reductions in PM_1, $PM_{2.5}$, and PM_4 concentrations, which is essential for effective air quality management and environmental protection efforts. However, further investigation is needed to better understand the factors influencing PM_{10} and TSP concentrations and optimize PM reduction strategies.

Although PM_{10} and TSP did not show statistically significant variations among treatments at the 5% significance level, they exhibited a trend toward reducing PM concentrations. However, at a 10% significance level, these treatments significantly reduced PM concentrations, highlighting the importance of a prolonged duration of operation for enhanced PM reduction. Longer durations may lead to a higher release of charged particles, resulting in more effective PM neutralization. Interestingly, there was no significant difference between D1 and D2, as well as among D2, D3, and D4. The lack of difference between D3 and D4 could be attributed to the absence of hen activities during the dark period. As the activities of hens were limited during the dark period, this could have contributed to the similarity in PM concentration between D3 and D4. Therefore, the EPI duration of D3 seems to be a promising duration requirement with minimum electricity consumption in mitigating PM. However, further research is needed to explore additional variables and external factors, including the impact on animal activities and behaviors.

Table 7.6: Effect of EPI duration treatments on PM concentrations (mg m^{-3}) in CF hen rooms.

Treatments	PM_1	$PM_{2.5}$	PM_4	PM_{10}	TSP
D1	2.98 ± 0.49^{a}	2.83 ± 0.39^{a}	3.63 ± 1.1^{a}	6.59 ± 2.25	16.8 ± 5.59
D2	2.45 ± 0.35^{ab}	2.52 ± 0.21^{ab}	2.79 ± 0.24^{ab}	5.03 ± 0.49	12.98 ± 1.12
D3	1.86 ± 0.18^{b}	1.97 ± 0.24^{b}	2.19 ± 0.27^{b}	3.94 ± 0.54	9.89 ± 1.36
D4	1.89 ± 0.12^{b}	2.12 ± 0.28^{b}	2.23 ± 0.23^{b}	4.20 ± 0.80	10.43 ± 1.90
***P*-value**	0.0103	0.0074	0.0473	0.0738	0.0535

Where, EPI- electrostatic particle ionization; CF- cage-free; RH- relative humidity; LMC- litter moisture content; D1= control (0 hour), D2= 8 hours, D3= 16 hours, and D4= 24 hours electric supply into EPI corona pipes; PM- particulate matter; PM_1 - PM with a diameter of ≤1 micrometer, $PM_{2.5}$- PM with a diameter of ≤2.5 micrometers, PM_4 - PM with a diameter of ≤4 micrometers, PM_{10} - PM with a diameter of ≤10 micrometers, TSP - Total Suspended Particles.

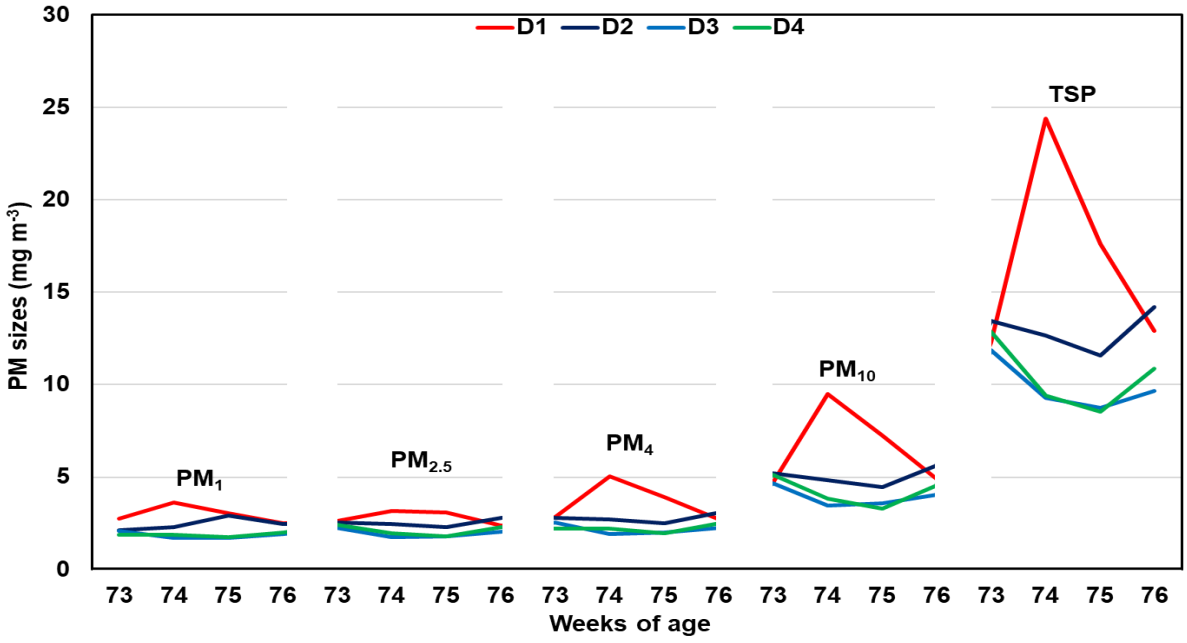

Figure 7.3: Impact of EPI duration treatments on PM concentrations in CF rooms with varying hen's weeks of age.

Where, EPI- electrostatic particle ionization; CF- cage-free; RH- relative humidity; LMC- litter moisture content; D1= control (0 hour), D2= 8 hours, D3= 16 hours, and D4= 24 hours electric supply into EPI corona pipes; PM- particulate matter; PM_1- PM with a diameter of ≤1 micrometer, $PM_{2.5}$- PM with a diameter of ≤2.5 micrometers, PM_4 - PM with a diameter of ≤4 micrometers, PM_{10} - PM with a diameter of ≤10 micrometers, TSP - Total Suspended Particles.

7.3.2.3 Electricity consumption

The study's results demonstrated significant variations in the electric consumption of the EPI system based on its operation duration (P<0.001). The system consumed 3.79 ± 0.25 Kwh for 8 hours, 7.58 ± 0.58 Kwh for 16 hours, and the highest energy consumption of 11.37 ± 0.48 Kwh for 24 hours throughout the EPI treatment. The findings underscore the direct correlation between operation duration and energy consumption, with longer durations requiring more energy to sustain the treatment process. As decision-makers evaluate the optimal operation duration for the EPI system, it becomes crucial to carefully weigh the balance between achieving effective PM reduction and the associated increase in energy consumption. Therefore, the D3 treatment results in appropriate treatment to reduce similar PM reduction with significantly less electric consumption than D4. The EPI system has demonstrated effective PM reduction capabilities, and the study highlights the importance of evaluating its energy consumption to ensure overall cost-effectiveness. Achieving a balance between desired PM reduction and energy conservation measures will be pivotal for implementing the EPI system on a larger scale and maximizing its benefits in improving air quality and promoting environmental protection.

7.4 CONCLUSIONS

The study's results demonstrated that the EPI system consistently reduced PM concentrations within CF hen environments, irrespective of the height at which it was implemented. This finding indicates that the EPI system's performance remained stable and uniform, providing effective PM reduction across all tested heights. On the other hand, the duration of EPI system operation significantly influenced PM_1, $PM_{2.5}$, and PM_4 concentrations, with longer durations leading to more substantial reductions. While PM_{10} and TSP did not show statistically significant variations, trends suggested a reduction in PM concentrations with extended operation. Therefore, employing the EPI system for a prolonged period is essential for achieving enhanced overall PM reduction.

Despite the benefits of 24-hour EPI system usage, the study highlighted that continuous electric supply did not show significant differences compared to using the EPI system for 16 hours. This observation presents an important practical implication concerning energy consumption. Opting for 16-hour EPI system operation during daylight can lead to significant energy cost savings without compromising the system's effectiveness in reducing PM. Considering the need for sustainable practices, this insight can guide decision-makers in the poultry industry to strike a balance between achieving effective PM reduction and managing energy consumption. Nevertheless, the study acknowledges the scope limitations and suggests further research to explore additional factors, such as the impact of animal activities on PM dynamics within the EPI system. By gaining a more comprehensive understanding of PM generation and neutralization in relation to hen activities, researchers can optimize PM reduction strategies and contribute to improved air quality and environmental protection in CF hen houses.

7.5 REFERENCES

Aarnink, A., J. van Harn, T. Van Hattum, Y. Zhao, and N. Ogink. 2011. Dust reduction in broiler houses by spraying rapeseed oil. Transactions of the ASABE 54:1479–1489.

Ahaduzzaman, M., L. Milan, C. L. Morton, P. F. Gerber, and S. W. Walkden-Brown. 2021. Characterization of poultry house dust using chemometrics and scanning electron microscopy imaging. Poultry Science 100:101188.

Almuhanna, E. A. 2007. Dust control in livestock buildings with electrostatically-charged water spray. Kansas State University, UMI Number: 3259316.

Bist, R. B., and L. Chai. 2022. Advanced Strategies for Mitigating Particulate Matter Generations in Poultry Houses. Applied Sciences 12:11323.

Bist, R. B., L. Chai, X. Yang, S. Subedi, and Y. Guo. 2022. Air Quality in Cage-free Houses during Pullets Production. Page 1 in American Society of Agricultural and Biological Engineers, 2200925.

Bist, R. B., S. Subedi, L. Chai, and X. Yang. 2023a. Ammonia emissions, impacts, and mitigation strategies for poultry production: A critical review. Journal of Environmental Management 328:116919.

Bist, R. B., X. Yang, S. Subedi, M. K. Sharma, A. K. Singh, C. W. Ritz, W. K. Kim, and L. Chai. 2023b. Temporal Variations of Air Quality in Cage-Free Experimental Pullet Houses. Poultry 2:320–333.

Cambra-López, M., A. J. Aarnink, Y. Zhao, S. Calvet, and A. G. Torres. 2010. Airborne particulate matter from livestock production systems: A review of an air pollution problem. Environmental Pollution 158:1–17.

Cambra-López, M., T. Hermosilla, H. T. Lai, A. J. A. Aarnink, and N. Ogink. 2011. Particulate matter emitted from poultry and pig houses: source identification and quantification. Transactions of the ASABE 54:629–642.

Cambra-López, M., A. Winkel, J. Van Harn, N. Ogink, and A. Aarnink. 2009. Ionization for reducing particulate matter emissions from poultry houses. Transactions of the ASABE 52:1757–1771.

Chai, L., H. Xin, Y. Zhao, T. Wang, M. Soupir, and K. Liu. 2018. Mitigating ammonia and PM generation of cage-free henhouse litter with solid additive and liquid spray. Transactions of the ASABE 61:287–294.

Chai, L., Y. Zhao, H. Xin, T. Wang, A. Atilgan, M. Soupir, and K. Liu. 2017. Reduction of particulate matter and ammonia by spraying acidic electrolyzed water onto litter of aviary hen houses: a lab-scale study. Transactions of the ASABE 60:497–506.

Corkery, G., S. Ward, M. C. Kenny, and P. Hemmingway. 2013. of Submission: Monitoring Environmental Parameters in Poultry Production Facilities.

Demmers, T., A. Saponja, R. Thomas, G. Phillips, A. McDonald, S. Stagg, A. Bowry, and E. Nemitz. 2010. Dust and ammonia emissions from UK poultry houses.

Donham, K. 2000. Occupational health hazards and recommended exposure limits for workers in poultry buildings.Pages 92–109 in National Poultry Waste Management Symposium Committee.

EPA, O. 2022a. Health and Environmental Effects of Particulate Matter (PM). Available at https://www.epa.gov/pm-pollution/health-and-environmental-effects-particulate-matter-pm (verified 15 June 2023).

EPA, O. 2022b. Particulate Matter (PM) Basics. Available at https://www.epa.gov/pm-pollution/particulate-matter-pm-basics (verified 30 September 2022).

EPIAir. 2023. FAQ's about EPI Air System | Agricultural Dust Reduction. EPI AIR Available at https://epiair.com/faqs/ (verified 15 June 2023).

Jerez, S. B., S. Mukhtar, W. Faulkner, K. D. Casey, M. S. Borhan, and R. A. Smith. 2013. Evaluation of electrostatic particle ionization and BioCurtain^{TM} technologies to reduce air pollutants from broiler houses. Applied Engineering in Agriculture 29:975–984.

Knight, R. M., L. Zhao, and H. Zhu. 2021. Modelling and optimisation of a wire-plate ESP for mitigation of poultry PM emission using COMSOL. Biosystems Engineering 211:35–49.

Michiels, A., S. Piepers, T. Ulens, N. Van Ransbeeck, R. D. P. Sacristán, A. Sierens, F. Haesebrouck, P. Demeyer, and D. Maes. 2015. Impact of particulate matter and ammonia on average daily weight gain, mortality and lung lesions in pigs. Preventive Veterinary Medicine 121:99–107.

Mintus, C. 2021. More States in the United States to Switch to Cage-Free Eggs. Available at https://www.thepoultrysite.com/news/2021/06/more-states-in-the-united-states-to-switch-to-cage-free-eggs (verified 1 April 2023).

Mitchell, B. W., and J. W. Baumgartner. 2007. Electrostatic Space Charge System for reducing dust in poultry production houses and the hatchery.Pages 23–24 in International Conference How to improve air quality. Citeseer.

Mitchell, B., L. Richardson, J. Wilson, and C. Hofacre. 2004. Application of an electrostatic space charge system for dust, ammonia, and pathogen reduction in a broiler breeder house. Applied Engineering in Agriculture 20:87.

Mitchell, B. W., and W. D. Waltman. 2003. Reducing Airborne Pathogens and Dust in Commercial Hatching Cabinets with an Electrostatic Space Charge System. avdi 47:247–253 Available at https://bioone.org/journals/avian-diseases/volume-47/issue-2/0005-2086_2003_047_0247_RAPADI_2.0.CO_2/Reducing-Airborne-Pathogens-and-Dust-in-Commercial-Hatching-Cabinets-with/10.1637/0005-2086(2003)047[0247:RAPADI]2.0.CO;2.full (verified 15 June 2023).

Mostafa, E., and W. Buescher. 2011. Indoor air quality improvement from particle matters for laying hen poultry houses. Biosystems Engineering 109:22–36.

Nimmermark, S., V. Lund, G. Gustafsson, and W. Eduard. 2009. Ammonia, dust and bacteria in welfare-oriented systems for laying hens. Annals of Agricultural and Environmental Medicine 16:103–113.

Ogink, N. W., R. W. Melse, and J. Mosquera. 2009. Multi-pollutant and one-stage scrubbers for removal of ammonia, odor, and particulate matter from animal house exhaust air.Page 37 in American Society of Agricultural and Biological Engineers.

Oliveira, J. L., H. Xin., L. Chai., and S. T. Millman. 2019. Effects of litter floor access and inclusion of experienced hens in aviary housing on floor eggs, litter condition, air quality, and hen welfare. Poultry Science, 98(4), 1664-1677.

Qi, R., H. Manbeck, and R. Maghirang. 1992. Dust net generation rate in a poultry layer house. Transactions of the ASAE 35:1639–1645.

Radon, K., C. Weber, M. Iversen, B. Danuser, S. Pedersen, and D. Nowak. 2001. Exposure assessment and lung function in pig and poultry farmers. Occupational and Environmental Medicine 58:405–410.

Ritz, C., B. Mitchell, B. Fairchild, M. Czarick III, and J. Worley. 2006. Improving in-house air quality in broiler production facilities using an electrostatic space charge system. Journal of Applied Poultry Research 15:333–340.

Shepherd, T. A., Y. Zhao, H. Li, J. P. Stinn, M. D. Hayes, and H. Xin. 2015. Environmental assessment of three egg production systems—Part II. Ammonia, greenhouse gas, and particulate matter emissions. Poultry Science 94:534–543.

UEP. 2017. CF-UEP-Guidelines_17-3.pdf. Available at https://uepcertified.com/wp-content/uploads/2021/08/CF-UEP-Guidelines_17-3.pdf (verified 18 August 2022).

USDA. 2016. USDA Graded Cage-Free Eggs: All They're Cracked Up To Be. Available at https://www.usda.gov/media/blog/2016/09/13/usda-graded-cage-free-eggs-all-theyre-cracked-be (verified 11 May 2023).

Veenhuizen, M., and D. Bundy. 1990. Electrostatic precipitation dust removal system for swine housing. Paper-American Society of Agricultural Engineers.

Verma, K. K., V. Singh, S. L. Gupta, J. Yadav, and A. K. Verma. 2014. Environmentally Controlled House-In Poultry Production. Poultry Line 1:29–32.

WHO, (World Health Organization). 2021. Ambient (outdoor) air pollution. Available at https://www.who.int/news-room/fact-sheets/detail/ambient-(outdoor)-air-quality-and-health (verified 30 September 2022).

Winkel, A., J. Mosquera, A. J. Aarnink, P. W. G. Koerkamp, and N. W. Ogink. 2016a. Evaluation of oil spraying systems and air ionisation systems for abatement of particulate matter emission in commercial poultry houses. Biosystems Engineering 150:104–122.

Winkel, A., J. Mosquera, A. J. Aarnink, P. W. G. Koerkamp, and N. W. Ogink. 2016b. Evaluation of oil spraying systems and air ionisation systems for abatement of particulate matter emission in commercial poultry houses. Biosystems Engineering 150:104–122.

Winkel, A., J. Mosquera, P. W. G. Koerkamp, N. W. Ogink, and A. J. Aarnink. 2015. Emissions of particulate matter from animal houses in the Netherlands. Atmospheric Environment 111:202–212.

Yang, X., L. Chai, R. B. Bist, S. Subedi, and Y. Guo. 2022. Variation of litter quality in cage-free houses during pullet production.Page 1 in American Society of Agricultural and Biological Engineers.

Zhao, Y., A. Aarnink, M. De Jong, N. Ogink, and P. G. Koerkamp. 2011. Effectiveness of multi-stage scrubbers in reducing emissions of air pollutants from pig houses. Transactions of the ASABE 54:285–293.

Zhao, Y., D. Zhao, H. Ma, K. Liu, A. Atilgan, and H. Xin. 2016. Environmental assessment of three egg production systems–Part III: Airborne bacteria concentrations and emissions. Poultry Science 95:1473–1481.

CHAPTER 8

ELECTROSTATIC PARTICLE IONIZATION FOR SUPPRESSING AIR POLLUTANTS[7]

[7] Bist, R. B., Yang, X., Subedi, S., Ritz, C. W., Kim, W. K., and Chai, L. 2024. Electrostatic particle ionization for suppressing air pollutants in cage-free layer facilities. *Poultry Science*, https://doi.org/10.1016/j.psj.2024.103494. Reprinted here with permission of the publisher.

ABSTRACT

The increasing demand for cage-free (CF) poultry farming raises concerns regarding air pollutant emissions in these housing systems. Previous studies have indicated that air pollutants such as particulate matter (PM) and ammonia (NH_3) pose substantial risks to the health of birds and workers. This study aimed to evaluate the efficacy of electrostatic particle ionization (EPI) technology with different lengths of ion precipitators in reducing air pollutants and investigate the relationship between PM reduction and electricity consumption. Four identical CF rooms were utilized, each accommodating 175 hens of 77 weeks of age (WOA). A Latin Square Design method was employed, with four treatment lengths: T1= control (0 m), T2 = 12 ft (3.7 m), T3=24 ft (7.3 m), and T4= 36 ft (11.0 m), where room and WOA are considered as blocking factors. Daily PM concentrations, temperature, and humidity measurements were conducted over 24 hours, while NH_3 levels, litter moisture content (LMC), and ventilation were measured twice a week in each treatment room. Statistical analysis involved ANOVA, and mean comparisons were performed using the Tukey HSD method with a significance level of $P \leq 0.05$. This study found that the EPI system with longer wires reduced $PM_{2.5}$ concentrations ($P \leq 0.01$). Treatment T2, T3, and T4 led to reductions in $PM_{2.5}$ by 12.1%, 19.3%, and 31.7%, respectively, and in small particle concentrations (particle size >0.5μm) by 18.0%, 21.1%, and 32.4%, respectively. However, no significant differences were observed for PM_{10} and large particles (particle size >2.5 μm) ($P<0.10$), though the data suggests potential reductions in PM_{10} (32.7%) and large particles (33.3%) by the T4 treatment. Similarly, there was no significant impact of treatment on NH_3 reduction ($P= 0.712$), possibly due to low NH_3 concentration (<2 ppm) and low LMC (<13%) among treatment rooms. Electricity consumption was significantly related to the length of the EPI system ($P \leq 0.01$), with longer lengths leading to higher consumption rates. Overall, a

longer-length EPI corona pipe is recommended for better air pollutant reduction in CF housing. Further research should focus on enhancing EPI technology, assessing cost-effectiveness, and exploring combinations with other PM reduction strategies.

Keywords: Cage-free, Air pollutant concentration, Mitigation strategy, Electrostatic-ionization technology.

8.1 INTRODUCTION

Livestock and poultry production generated air pollutants of ammonia (NH_3), greenhouse gases, and particulate matter (PM) are risks to the environment and ecosystem (Fabbri et al., 2007; Cambra-López et al., 2010; Dai et al., 2019; Ni, 2021; Xie et al., 2021, 2022; Ni et al., 2023). Cage-free (CF) housing systems in the USA have gained popularity as an ethical and humane poultry farming method (Mintus, 2021; UEP, 2022; Bist et al., 2023d). However, the concentration of air pollutants inside CF housing poses a major concern, particularly regarding particulate matter (PM) and ammonia (NH_3) (Chai et al., 2018; Bist and Chai, 2022; Bist et al., 2023b; Ni et al., 2023). These air pollutants can threaten bird health and worker safety (Senthilselvan et al., 2011; Ni, 2015). Various studies have shown that birds exposed to these air pollutants experienced adverse effects on health and welfare and increased mortality rates (Viegas et al., 2013). Exposure to high air pollutant levels can result in respiratory issues and decrease productivity in laying hens (Almuhanna, 2011; Bist and Chai, 2022; Bist et al., 2023d). Moreover, farm workers exposed to these air pollutants are at higher risk of developing chronic respiratory diseases like bronchitis, asthma, and airway obstruction (Donham et al., 2002; Viegas et al., 2013; EPA, 2022). The presence of air pollutants in the air not only endangers the safety, health, productivity, and behavior of the animals (Ni et al., 2023) but also causes significant damage to the surrounding ecosystem

and contributes to the formation of regional haze (EPA, 2022, 2023). Therefore, implementing an effective mitigation strategy can help reduce air pollutants and the adverse effects caused by their emissions.

Various mitigation technologies have been developed based on their working principles, including managerial, microbiological, biochemical, chemical, physical, and physiological principles, to enhance the air quality in poultry housing (Ni, 2015; Bist et al., 2023b). However, the effectiveness of these technologies has shown variation (Zhao et al., 2011), and there remains a pressing need for technically efficient, economically feasible, and user-friendly solutions to mitigate air pollutants in poultry housing (Bist et al., 2023b; Ni et al., 2023). One such technology involves spraying an oil/water mixture (Kocaman et al., 2005; Aarnink et al., 2011; Ogink et al., 2012; Zheng et al., 2012; Winkel et al., 2016; Bist and Chai, 2022; Bist et al., 2023b). Previous study have demonstrated that oil and water spraying systems can remove PM by 18-64% and NH_3 by up to 65% (Ogink et al., 2012). Similarly, acidic electrolyzed water spraying systems have reduced total PM by 89% (Chai et al., 2019). However, using an oil and water mixture can result in the trapping of PM on floors, walls, and cages, requiring frequent cleaning of the entire house to prevent worker hazards (Winkel et al., 2016). This cleaning process requires significant labor. Moreover, spraying oil and water can introduce moisture into the production environment. If this oil and water come into contact with metal objects, it can initiate corrosion and lead to the formation of rust (Chai et al., 2019). Another commonly employed method for controlling PM in poultry housing is wet scrubbers, particularly those with packed-bed configurations. These scrubbers have achieved high removal efficiencies of up to 93% for PM_{10} (PM with aerodynamic diameter $\leq$10 μm), 90% for $PM_{2.5}$ (PM with aerodynamic diameter $\leq$2.5 μm), 100% for ammonia,

and 85% for airborne bacteria (Zhao et al., 2011). However, wet scrubbers can be costly and prone to clogging despite their effectiveness. The cleaning of these scrubbers requires large amounts of water and has been criticized for shifting the pollution issue from air to liquid waste (Zhao et al., 2011). Similarly, filter and biofilter systems represent another prevalent approach for mitigating air pollutants in poultry housing (Pearson et al., 1992; Melse and Ogink, 2005; Van der Heyden et al., 2015; Forero et al., 2018; Bist et al., 2023b). These systems have been tested or employed in pig and layer farms in Iowa (Zhao et al., 2018). Previous studies have shown that installing such systems can reduce total suspended particles from 79-96% (Seedorf and Hartung, 1999) and reduce NH_3 from 36-97% (Bist et al., 2023b). However, they are prone to frequent clogging and particle resuspension (Strohmaier et al., 2018), so the filters and biofilters need regular cleaning and have a relatively short lifespan, necessitating periodic replacement (Tan and Zhang, 2004; Wood and Van Heyst, 2016). Furthermore, employing proper manure-handling procedures has significantly reduced air pollutants (Aillery et al., 2005; Chai et al., 2017). However, the installation of manure removal or collecting equipment presents challenges, particularly in CF floor-raised hen houses, due to the difficulty and expense associated with their implementation. A recent study applied a top layer of bedding materials over the existing litter and found that PM2.5, PM10, and total suspended particles were reduced by 36.5%, 39.4%, and 38.7%, respectively (Bist et al., 2023a).

The electrostatic particle ionization (EPI) system is an increasingly promising technology that has gained popularity across various industries as an effective solution for reducing air pollutant emissions (Mitchell and Waltman, 2003; Richardson et al., 2003; Mitchell et al., 2004; Ritz et al., 2006; Mitchell and Baumgartner, 2007a; Cambra-López et al., 2009; Chai et al., 2009; Manuzon et al., 2014; Knight et al., 2021; Bist and Chai, 2022). These charging systems are simple,

environmentally friendly, and harmless to animals, poultry, and humans. In addition, previously, charging systems had significantly reduced airborne dust, NH_3, and associated microorganisms from the farm (Mitchell, 1998; Mitchell et al., 2004; Ritz et al., 2006; Mitchell and Baumgartner, 2007b). This technology uses an electric charge to attract and capture PM particles and associated NH_3 molecules, causing them to cluster and form larger particles or molecules in the air (Ritz et al., 2006). One study demonstrated the effectiveness of charging systems in reducing airborne dust by 43% and NH_3 by 13% (Ritz et al., 2006). Another study by Mitchell et al. (2004) reported reductions of 61% in airborne dust, 56% in NH_3, and 67% in airborne bacteria. Additionally, Cambra-Lopez et al. (2009) reported reductions of 36% for PM_{10} and 10% for $PM_{2.5}$. A study by Mitchell and Waltman (2003) evaluated the effectiveness of an electrostatic charging system with a voltage of -30 K Vdc and a current of 0.2 mA in reducing dust within hatching cabinets. The results demonstrated a reduction in dust levels from 77% to 79%. In a recent study, a prototype electrostatic precipitator was tested under different weather and ventilation conditions (hot, warm, and cold weather), and it was found to be effective in reducing $PM_{2.5}$ and PM_{10} levels by up to 97.8% and 99.0%, respectively (Knight et al., 2021). Therefore, implementing charging systems has brought about a revolutionary approach to mitigating air pollutants, enhancing air quality, and promoting poultry and caretakers' overall health and well-being.

Previous studies have employed different spacing configurations relative to the floor area, providing valuable insights into the specific approaches used. For example, measurements include 5.5 m per 44.6 m^2 (Cambra-López et al., 2009), 5.8 m per 44.6 m^2 (Ritz et al., 2006), 8.6 m per 44.6 m^2 (Lim et al., 2008), 10.7 m per 44.6 m^2 (Martel et al., 2023), and 12.8 m per 44.6 m^2 (Jerez et al., 2013) have been utilized. However, the impact of EPI technology on PM reduction in CF

hen houses concerning varying lengths has not been fully explored. Therefore, there is a need to comprehensively investigate the impact of EPI technology on air pollutant reduction in CF henhouses.

To address the gap in research regarding the impact of EPI technology with varying lengths on PM reduction in CF hen houses, this study aims to investigate the influence of varying lengths of the EPI system (control, 3.7 m, 7.3 m, and 11 m per 44.6 m^2) on air pollutant reduction. Thus, the primary objectives of this study are: a) to evaluate the effectiveness of EPI technology by comparing different lengths of EPI systems in their capacity to reduce air pollutants, and b) to establish a correlation between the extent of PM reduction and the corresponding electricity consumption associated with operating the EPI systems of different lengths. By achieving these objectives, valuable insights will be gained for farmers and researchers seeking effective methods to mitigate PM in CF hen rooms, ultimately leading to improved health and productivity for poultry and caretakers. Furthermore, the study's outcomes will contribute to the development of optimal strategies for managing air pollutants and inform the decision-making processes concerning the implementation of EPI technology, thereby enhancing overall air quality and promoting the well-being of birds and workers within these housing systems.

8.2 MATERIALS AND METHODS

8.2.1 Housing and management

This experiment follows the same housing and bird management practices as described in Chapter 2 of section 2.2.1.

8.2.2 Experimental design

In this research, the Latin Square Design (LSD) method was employed due to the limited availability of four experimental CF rooms to conduct the four treatments across four WOA (Table 8.1). EPI systems (EPI Air, LLC, Columbia, MO, USA) were thoroughly cleaned each week after the experiment. The EPI systems operated continuously during each WOA. The varying lengths used in the study provide valuable insights into the specific spacing approaches utilized in previous research. The EPI systems were positioned at 8 feet instead of the standard 9-foot height in our experimental CF rooms. This adjustment was necessary to accommodate room equipment, such as heaters, circulating fans, and water supply pipes. Bird-repellent spikes (Bird-X, Inc., Elmhurst, IL, USA) were attached above the corona pipe using adhesive glue to prevent hens from perching on the corona pipes. Maintaining a minimum distance of 1 foot between the EPI system and the ceiling and walls is important to avoid any electric field effects on nearby objects. The corona pipes were positioned 1 foot (0.3 m) away from the side walls and 8 feet (2.4 m) away from the front and back walls, with a gap between the corona pipes, as depicted in Figure 8.1.

Table 8.1: Implementation of a Latin Square Design in the study design.

Weeks of Age	Room 1	Room 2	Room 3	Room 4
77	T1	T2	T4	T3
78	T4	T3	T1	T2
79	T2	T4	T3	T1
80	T3	T1	T2	T4

Where T1, T2, T3, and T4 are control (0 m), 12 ft (3.7 m), 24 ft (7.3 m), and 36 ft (11.0 m) lengths of the EPI corona pipe, respectively. EPI- electrostatic particle ionization.

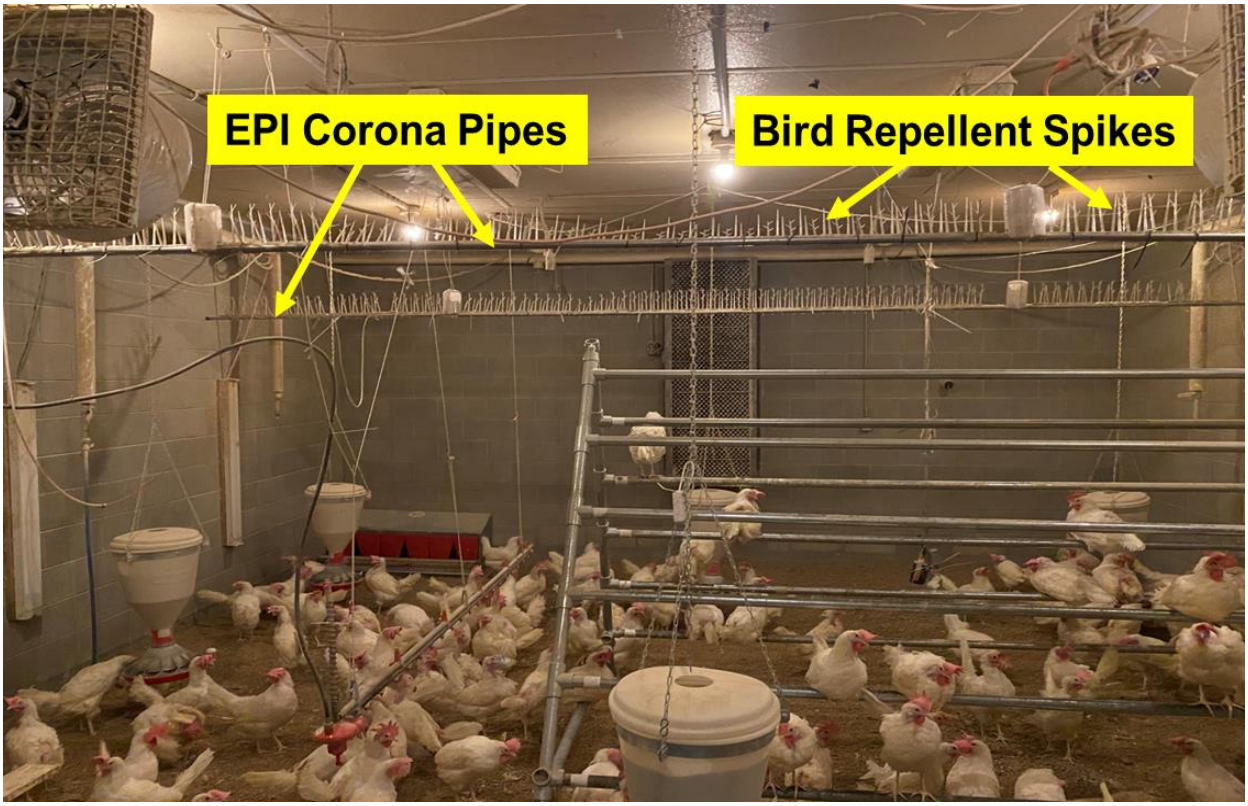

Figure 8.1: Experimental setup for EPI system in cage-free hen environment. EPI- electrostatic particle ionization.

8.2.3 Environment Parameter Measurements

8.2.3.1 Temperature and relative humidity

Temperature and humidity were measured inside and outside treatment rooms using Onset HOBO data loggers (Onset Computer Corporation, Bourne, Massachusetts, USA) programmed to collect data every 10 minutes for 24 hours daily. The inside sensor was placed 1.2 m above the floor in the middle of each room, while the outside was placed 1.8 m above the ground. Data were checked daily to ensure a comfortable environment for the birds.

8.2.3.2 Ventilation measurement

Small (12-inch opening Aerotech Vortex circulating fan, Munter Corporation, Mason, MI, USA) and large exhaust fans (24-inch opening Aerotech Vortex circulating fan, Munter Corporation, Mason, MI, USA) were installed in each room. The ventilation rate in each room was assessed twice a week by measuring the airflow at two air exhaust fan openings outside each rooms. Measurements were taken using a TSI anemometer (Alnor velometer thermal anemometer AVM410, TSI Incorporated, Shoreview, Minnesota, USA) positioned 5cm away from the exhaust fan. The TSI anemometer has a measurement range of 0-20 m/s (0-4000 ft/min) with an accuracy of ±3% of reading or ±0.015 m/s and a resolution of 0.01 m/s. The airflow speed (W) in m/s was recorded, along with the opening area (A; m^2) of the small (0.0723 m^2) and large exhaust fan (0.292 m^2). These measurements were later analyzed based on the airflow rate (Q; m^3 min^{-1}) using equations 1 and 2 as described in the study by Ni et al., 2023.

$$Q_{small} = 0.0723\ m^2 \times W \quad (1)$$

$$Q_{large} = 0.292\ m^2 \times W \quad (2)$$

Where, Q_{small} is the airflow rate of small ventilation, and Q_{large} is the airflow rate of large ventilation.

8.2.3.3 Litter moisture content

The moisture content of the litter (LMC) plays a significant role in influencing the levels of air pollutants within poultry housing. To assess the LMC of the litter in the rooms, samples weighing 100 g were collected weekly from four locations within each room into Ziplock bags (Great Value freezer bags, Walmart.com). These samples were then transported to a laboratory for analysis. The collected samples were thoroughly mixed in the laboratory, and two separate 10

g samples were extracted from each bag. One sample was used for testing purposes, while the other was a validation sample. The samples were weighed and heated in a THELCO Laboratory oven (Precision Scientific; Chicago, IL, USA) at 105 °C for 24 hours. After heating, the final litter weights were recorded. The litter moisture content was calculated using Equation (3).

$$LMC\ (\%) = \frac{LWW - LDW}{LWW} \times 100 \qquad (3)$$

Where, LMC is the percentage of moisture in the litter, LWW is the initial wet litter weight, and LDW is the final dry litter weight. This calculation helps determine the amount of moisture present in the litter samples.

8.2.4 Ammonia Measurement

Ammonia concentration was measured using the Drager DOL-53 NH_3 sensor (Dol-sensors A/S, Aarhus N, Denmark) connected to Onset's HOBO RX3000 (Onset Computer Corporation, Bourne, MA, USA). A single DOL sensor was positioned 0.91 m above the floor litter in each room. The NH_3 sensor was programmed to collect data every minute continuously until the completion of the study. However, it was observed that these sensors were sensitive to the effects of the EPI system, which could impact the readings and the device itself. Consequently, the DOL sensors were replaced with four compact ToxiRae Pro NH_3 sensors (RAE Systems by Honeywell, San Jose, CA, USA) used in previous studies (Gassman, 2015; Williams Ischer et al., 2017). These sensors were placed at the center of each room for 15 minutes twice a week. The ToxiRae Pro sensors recorded data at 1-minute intervals, covering a range of 0-100 ppm with a resolution of 1 ppm. The sensors were not left in place for extended periods to prevent damage by the EPI system.

8.2.5 PM Measurement

To monitor PM concentrations, we utilized five Dylos optical particle monitors (Model DC1700, Dylos Corporation, Riverside, California, USA). At the center of each room, one Dylos monitor was positioned at a height of 0.5 m from the ground. The Dylos monitors operated continuously every day, with a sampling period set at 1-minute intervals. These monitors measured PM mass ($PM_{2.5}$ and PM_{10} in $\mu g/m^3$) and particle concentrations for small particles (particle size>0.5μm) and large particles (particle size>2.5 μm) per 0.01 cubic foot of air in each treatment room. Every week, these Dylos monitors were collected from each room, and data were transferred to a hard drive for storage for further analysis. The difference between the readings for large and small particles allowed us to determine the particle count within 0.5 μm to 2.5 μm (Ni et al., 2023). We chose to use these Dylos sensors because they have been successfully employed in previous studies conducted in broilers (Yasmeen et al., 2019) and layer houses (Ni et al., 2023).

8.2.6 Working Principle of EPI

Electrostatic Particle Ionization technology improves air quality by charging the particles in the air, leading to PM precipitation. EPI systems comprise a 2.0 mA power supply, a corona pipe with precipitator corona points, a manual winch, insulators, and a negatively charged high-voltage direct current (-30 KV; 1.6×10^{12} electrons/second) with a current limited to 2 mA or lower to ensure safety (EPIAir, 2023). The power consumption of each EPI power supply is similar to that of a 100-watt light bulb, making it highly cost-effective to operate. It can connect to a standard 110-220 Volt, 50-60 Hz electrical service. The system uses a power supply to release ions into the air through stainless steel corona points. The ions are delivered at high pressure into the air consistant over length of the study, and the corona line is insulated from the ground to ensure

safe operation. EPI Air systems emit up to a thousand trillion negative ions every second, which saturate the particles and cause charge shifts.

The airspace is treated with negative ions released from the corona pipe points. These negative ions naturally attract and surround particles in the air, making them more likely to be attracted to grounded or positively charged surfaces. This attraction causes them to collide, polarizing the particles and giving them a positive and negative charge. This magnetic-like effect causes the particles to stick together and adhere to any surface they encounter, as shown in Figure 8.2. The result is a negatively charged ionized airspace that is a harsh environment for pathogens like bacteria and viruses. Additionally, air chemistry reactions occur that help reduce noxious gases. In summary, EPI technology works by saturating the air with negative ions, which charge the PM and cause it to bind to surfaces or fall to the ground.

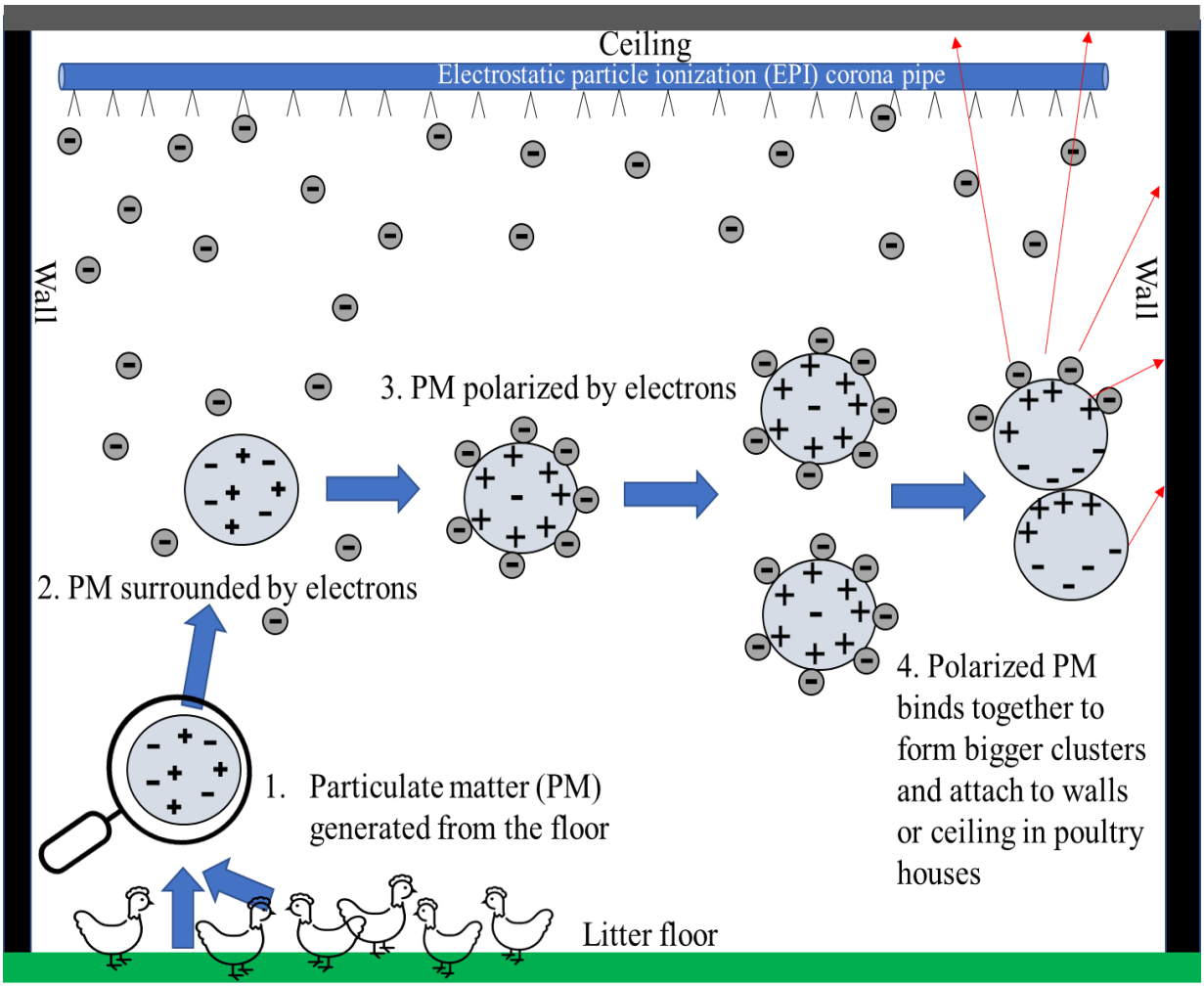

Figure 8.2: Working mechanism of EPI systems in cage-free hen rooms. EPI- electrostatic particle ionization; PM- particulate matter.

8.2.7 Electricity Consumption by EPI System

The study aimed to determine the power consumption of the EPI system and its correlation with the length of the corona pipe. This information is essential for poultry producers to choose the appropriate EPI length for their facilities based on housing size, considering both effectiveness and energy expenditure. A digital power monitor meter (Zhengzhou Paiji Technology, Zhengzhou, China) was used for each treatment room to measure the electricity consumption. This device

operates at a voltage of 120V, frequency of 60Hz, and operating current of up to 15A. The power consumption analysis was performed at the end of the study. The power consumption of the EPI system is estimated to be similar to a 100-watt bulb, but it depends on the length of the corona pipe used (EPIAir, 2023). By monitoring the electricity usage in kilowatt-hours (KWh), valuable insights were obtained regarding the power requirements and efficiency of the EPI system in different configurations.

8.2.8 Statistical Analysis

In this research, the four CF rooms were arranged in a Latin Square Design (LSD), with room and WOA treated as a blocking factor, and four EPI lengths were considered treatments. Statistical analyses were performed using R-studio (4.1.0). The ventilation rates, LMC, NH_3, PM, and electricity consumption data collected from each room were analyzed using an analysis of variance (ANOVA). The means were separated using the LSMeans Tukey HSD method, and any differences observed were considered significant at a $P \leq 0.05$. Similarly, the treatment comparison was made using contrasts (1) control vs EPI treatments and (2) the linear and quadratic polynomial trends across the three EPI lengths, excluding the control. The general linear model equation (Eq. 4) for ventilation rates, LMC, NH_3, PM, and electricity consumption data can be expressed as:

$$\boldsymbol{Y_{ijl} = \mu + \alpha_i + \beta_j + \gamma_l + \varepsilon_{ijl}} \quad (4)$$

Where: i=1,.., K; j=1,.., K, l=1,.., K; K represents the Latin letter for treatment in the $(i,j)^{th}$ cell of the Latin Square; Y_{ijk} represents the ventilation rates, LMC, NH_3, PM, or electricity consumption corresponding to K^{th} Latin letter in the $(i,j)^{th}$ cell; μ is the overall mean of the ventilation rates, LMC, NH_3, PM, or electricity consumption; α_i is the effect of i^{th} Rooms; β_j is the effect of j^{th} WOA; γ_l is the effect of l^{th} EPI lengths; and ε_{ijk} represents the random error term corresponding to K^{th} Latin letter in the $(i,j)^{th}$ cell.

8.3 RESULTS

8.3.1 Environment Parameters

8.3.1.1 Temperature and relative humidity

The treatment rooms displayed daily average temperature and relative humidity (RH) fluctuations during the study. The outdoor temperature generally increased significantly, while the RH resulted in a fluctuating pattern. Compared with treatment rooms, the outside temperature and RH significantly differed ($P < 0.01$). In contrast, the indoor temperature remained consistent throughout the treatment, showing no significant differences ($P = 0.342$). However, the RH inside the rooms appeared to increase from February 4 to March 4, resulting in significant differences among WOA ($P < 0.001$), but did not show significant differences among treatments ($P = 0.492$). The average temperatures of the outside, T1, T2, T3, and T4 rooms were 14.19±5.29, 22.60±0.74, 23.77±0.71, 23.34±1.09, and 23.14±1.07 °C, respectively. Similarly, the average RH of the outside, T1, T2, T3, and T4 rooms were 77.77±12.61, 51.67±11.55, 49.95±12.22, 51.55±11.35, 51.93±10.98 %, respectively.

8.3.1.2 Ventilation rates

The ventilation rates of all test rooms were controlled in the same way. However, a significant difference was observed between the two different ventilation fan sizes ($P < 0.001$). Large ventilation exhibits higher airflow rates than small ventilation. The airflow rate for the small ventilation fans typically falls between 8 and 17 cubic meters per minute, while the large ventilation fans typically range from 30 to 53 cubic meters per minute.

8.3.1.3. Litter moisture content

The results of LMC between treatments and WOA are presented in Table 8.2. The data show no significant difference between the treatments (P= 0.182). However, this study significantly differed in LMC with WOA (P= 0.001). The LMC was found to be highest at 80 WOA (12.10 ± 0.44 %) but lowest with no significant difference between 77 to 79 WOA.

Table 8.2: Effect of treatments and hens' age on litter moisture content (%, mean ± standard deviation).

Weeks of age	Treatments				Overall
	T1	T2	T3	T4	
77	11.18 ± 3.02	9.15 ± 1.12	10.38 ± 2.74	10.50 ± 2.40	10.30 ± 0.85[a]
78	11.32 ± 2.90	10.92 ± 3.50	9.77 ± 1.35	11.76 ± 2.69	10.94 ± 0.85[a]
79	10.39 ± 2.26	10.24 ± 2.89	9.79 ± 0.19	10.00 ± 2.59	10.11 ± 0.26[a]
80	11.49 ± 1.53	12.51 ± 2.20	12.32 ± 0.47	12.07 ± 1.99	12.10 ± 0.44[b]
Average	11.10 ± 0.49	10.71 ± 1.41	10.57 ± 1.20	11.09 ± 0.99	10.86 ± 0.90

Different alphabets within a column indicate significant mean differences ($p \leq 0.05$); n = 4;

Where T1, T2, T3, and T4 are control (0 m), 12 ft (3.7 m), 24 ft (7.3 m), and 36 ft (11.0 m) lengths of the EPI corona pipe, respectively.

8.3.2 Ammonia Concentration

Figure 8.3 illustrates no significant difference in the NH_3 concentrations among the control and EPI treatments (P= 0.451). The NH_3 levels were consistently low in each treatment room, measuring less than two ppm. The study indicates that NH_3 concentrations were consistently below any concerning thresholds, ensuring air quality in the treatment rooms.

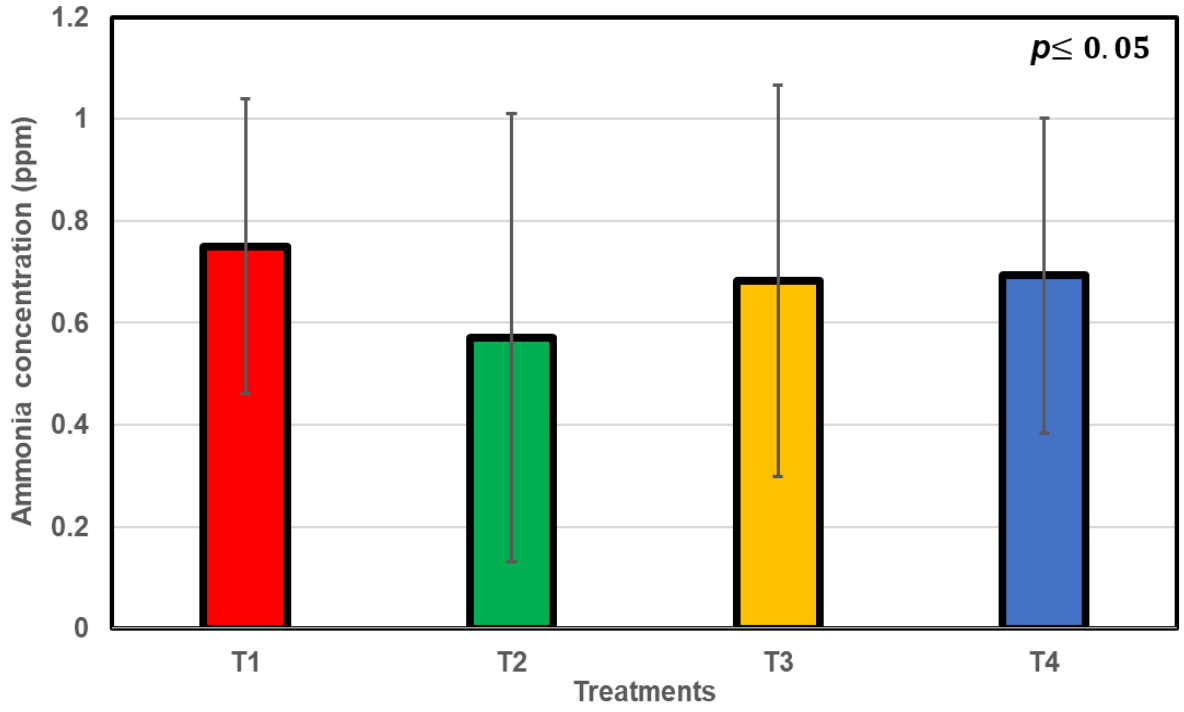

Figure 8.3: Overall ammonia concentration in testing rooms. Different alphabets within a column indicate significant mean differences ($P \leq 0.05$). The error bar represents the standard deviation (n = 4). Where T1, T2, T3, and T4 are control (0 m), 12ft (3.7 m), 24 ft (7.3 m), and 36 ft (11.0 m) lengths of the EPI corona pipe, respectively.

8.3.3 Effects of EPI on PM Reduction

8.3.3.1 Temporal variation of PM mass

The average PM mass for $PM_{2.5}$ and PM_{10} over 24 hours differed among the treatment rooms (T2, T3, and T4) than in the control room (T1). The concentrations for PM2.5 and PM10 seem to be highest in the control (T1) room, and the lowest average concentrations were found in the T3 and T4 rooms. The concentration of both $PM_{2.5}$ and PM_{10} concentrations resulted in lowest during the light-off (dark) period compared to the light period ($P < 0.001$). The highest PM mass observed from 12:30 to 14:00 hrs was due to daily farm activities such as egg collection and equipment checks. Besides these timelines, the highest daily mean $PM_{2.5}$ (84 to 239 µg m^{-3}) and PM_{10} (343 to 2944 µg m^{-3}) concentrations in the T1 room were observed throughout the sampling period. However, the concentrations of $PM_{2.5}$ (ranging from 68 to 217 µg m^{-3} and 46 to 182 µg m^{-3}) and PM_{10} (ranging from 207 to 2311 µg m^{-3} and 102 to 1994 µg m^{-3}) were found to be lower in T3 and T4 rooms than other two treatments. After 20:00 hrs, there seemed to be a decrease in PM mass concentrations as birds were ready for dark periods.

8.3.3.2 Temporal variation of PM concentrations

The average particle concentrations over a 24-hour in the three treatment rooms (T2, T3, and T4) differed from those in the control room (T1) for both small and large particles. In terms of particle concentrations, the daily mean of the T1 room showed the highest levels for both small and large particle counts, measuring between 33 and 104 particles cm^{-3} for small particles and between 5 and 71 particles cm^{-3} for large particles. In contrast, the T3 and T4 rooms exhibited the lowest concentrations of small and large particles. For T3, the values ranged from 20 to 81 particles cm^{-3} for small particles and from 3 to 53 particles cm^{-3} for large particles. In

the case of T4, the concentrations ranged from 13 to 79 particles cm^{-3} for small particles and from 1 to 45 particles cm^{-3} for large particles. The concentration of both small and large particle counts resulted in the lowest during the dark period compared to the light period ($P < 0.001$). The peak particle counts between 12:30 and 14:00 hrs resulted from routine farm activities, specifically egg collection. Besides these timelines, the highest particles in the air were observed when the light was turned on from 5:00 to 5:30, 11:00 to 12:30, and 17:00 to 20:00 hrs. After 20:00 hrs, there was a gradual decline in particle counts, which can be attributed to a decrease in bird activity as they prepared for the dark period.

8.3.3.3 PM levels and reductions

The study showed that the $PM_{2.5}$ concentration significantly differed among treatment rooms ($P = 0.006$; Table 8.3). When comparing the treatments, this study found a significant difference between the control and EPI treatment for $PM_{2.5}$ ($P = 0.003$) and PM_{10} ($P = 0.025$). Similarly, the linear trend between three EPI lengths was significant for $PM_{2.5}$ ($P = 0.01$). However, this research did not find a significant trend in evaluating quadratic polynomial trends for $PM_{2.5}$ ($P = 0.589$) and PM_{10} ($P = 0.596$). The T4 treatment room had the lowest $PM_{2.5}$ and PM_{10} concentrations, while the T1 treatment room had the highest (Figure 8.4). T2, T3, and T4 resulted in $PM_{2.5}$ reductions of 12.2, 19.3, and 31.7%, respectively, compared to the T1 control room. Therefore, these findings suggest that employing a longer length of the corona pipe in CF rooms can improve the air quality inside the housing.

Table 8.3: Effect of four treatments on two different PM mass (mean ± standard deviation) concentrations in cage-free rooms.

PM levels ($\mu g\ m^{-3}$)	Treatments				*P-value*
	T1	T2	T3	T4	
$PM_{2.5}$	161.59±11.58^{a}	142.04±33.92^{ab}	130.46±10.08^{bc}	110.30±26.50^{c}	0.006
PM_{10}	1404.53±761.00	1075.34±662.97	1083.69±506.39	944.70±603.16	0.098

Different alphabets indicate significant mean differences ($p \leq 0.05$). Where T1, T2, T3, and T4 are control (0 m), 12 ft (3.7 m), 24 ft (7.3 m), and 36 ft (11.0 m) lengths of the EPI corona pipe, respectively. PM- particulate matter.

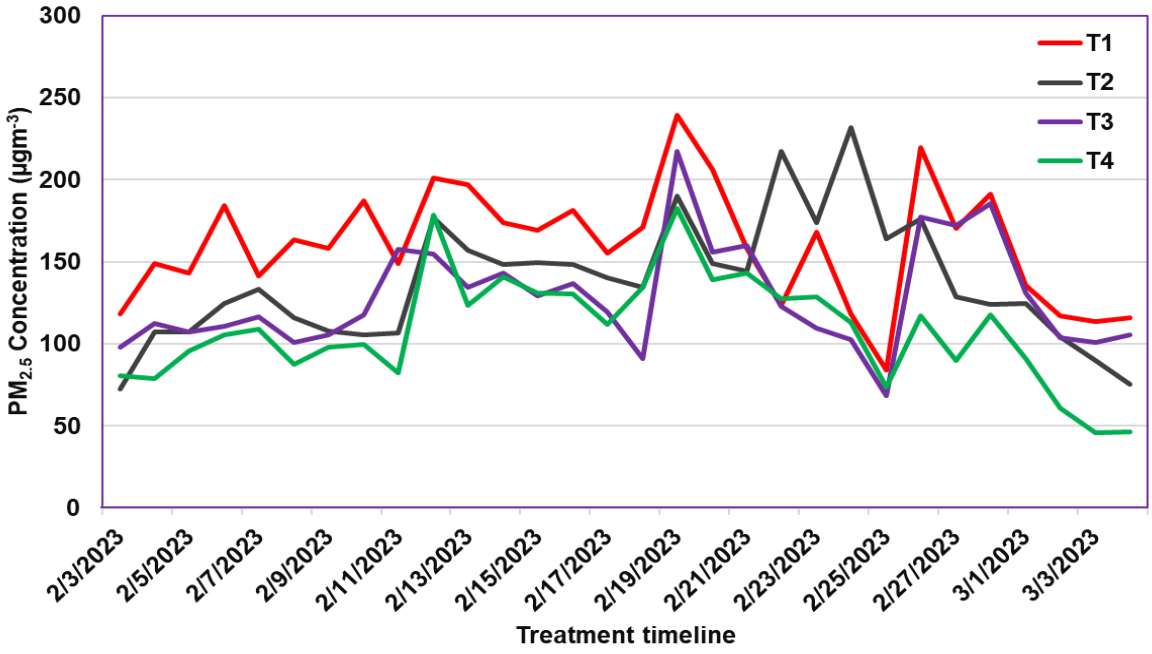

Figure 8.4: Comparison of daily mean concentrations of $PM_{2.5}$ in four treatment cage-free rooms from February 3 to March 4 (n = 4).

Where T1, T2, T3, and T4 are control (0 m), 12 ft (3.7 m), 24 ft (7.3 m), and 36 ft (11.0 m) lengths of the EPI corona pipe, respectively.

8.3.3.4 PM concentration

The data analysis in Table 8.4 revealed a significant difference in small particle concentrations among the treatment rooms (P= 0.002). When comparing the treatments, this study found a significant difference between the control and EPI treatment for small particles (P= 0.001) and large particles (P= 0.027) concentrations. Similarly, the linear trend between three EPI lengths was significant for small particle concentrations (P= 0.018). However, this research did not find a significant trend in evaluating quadratic polynomial trends for small particle (P= 0.329) and large particle (P= 0.594) concentrations. The T4 treatment room exhibited the lowest small and large particle concentrations, while the T1 treatment room showed the highest concentrations (Figure 8.5). Treatments T2, T3, and T4 resulted in 18.0%, 21.1%, and 32.4% reductions in small particle concentrations compared to the T1 control room. Thus, these findings suggest that employing a longer corona pipe in CF rooms can improve air quality.

Table 8.4: Effect of different EPI corona pipe lengths on PM concentrations (mean ± standard deviation) of small and large particle sizes in an experimental cage-free hen room.

PM concentrations (particles cm^{-3})	Treatments				*P-value*
	T1	T2	T3	T4	
Small particle	67.88 ± 19.93^{a}	55.68 ± 15.27^{b}	53.55 ± 9.92^{b}	45.87 ± 16.05^{b}	0.002
Large particle	29.63±19.93	22.14±16.01	22.62±12.29	19.77±14.19	0.102

Note: Different alphabets indicate significant mean differences ($p \leq 0.05$); n = 4; Where T1, T2, T3, and T4 are control (0 m), 12 ft (3.7 m), 24 ft (7.3 m), and 36 ft (11.0 m) lengths of the EPI corona pipe, respectively. Small particles = particle size >0.5 µm, and large particles = particle size >2.5µm.

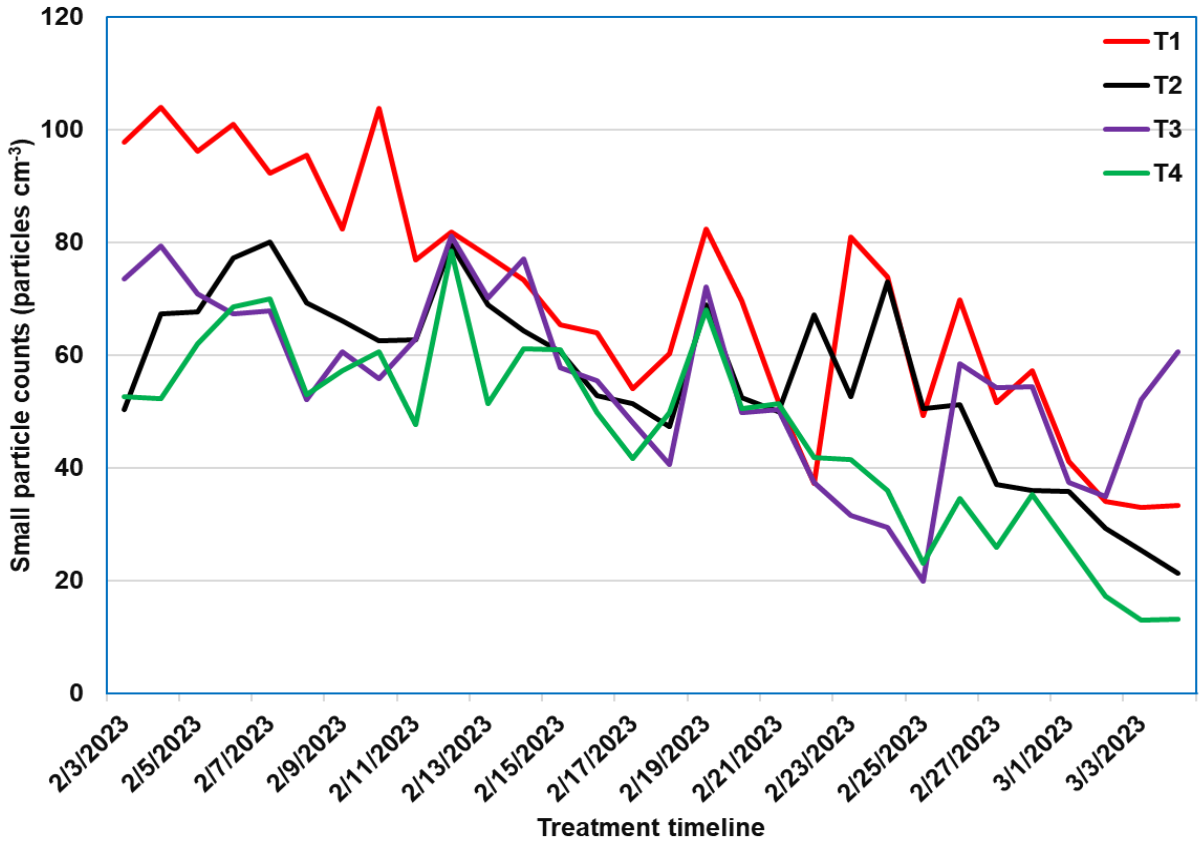

Figure 8.5: Comparison of daily mean particle counts of small particles in four treatment cage-free experimental rooms from February 3 to March 4 (n = 4).

Where T1, T2, T3, and T4 are control (0 m), 12 ft (3.7 m), 24 ft (7.3 m), and 36 ft (11.0 m) lengths of the EPI corona pipe, respectively. Small particles = particle size >0.5 µm, and large particles = particle size >2.5µm.

8.3.3.5 Electricity consumption

The study revealed a significant difference in electricity consumption based on the length of the EPI corona pipe used ($P < 0.001$; Figure 8.6). As the length of the corona pipe increased, so did the electricity consumption and associated costs. Based on this study, introducing a 12 ft (3.7 m) corona pipe to the existing EPI corona pipe led to an estimated increase of 0.034 KWh or

approximately 10% in daily electricity consumption compared to the initial 12 ft (3.7 m) corona pipe for each additional 12 ft (3.7 m) corona pipe. In addition, it can be calculated by Equation 5;

$$\textbf{Electricity consumption per day (KWh)} = 0.339 + (N \times 0.034) \quad (5)$$

Where, 0.339 KWh was the electricity consumed by 12 ft (3.7 m) corona pipe, N is the number of 12 ft (3.7 m) corona pipe added to an existing system, and 0.034 KWh is the electricity consumption difference between the initial 12 ft or 24ft (7.3 m) corona pipes and after adding 12 ft corona pipe to initial 12 ft or 24 ft corona pipes.

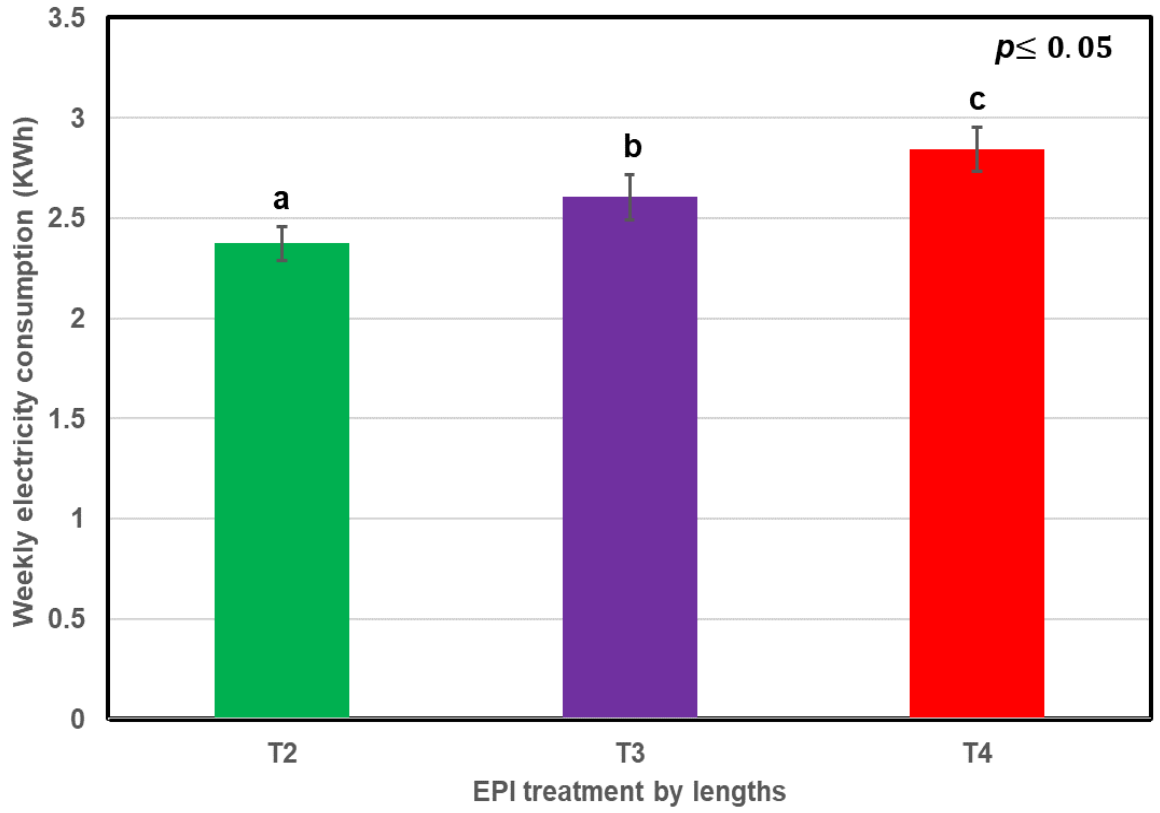

Figure 8.6: Comparison of weekly electricity consumption between control and three other treatments in an experimental cage-free layer room.

Different alphabets indicate significant mean differences ($P \leq 0.05$). The error bar represents the standard deviation ($n = 4$). Where T1, T2, T3, and T4 are control (0 m), 12 ft (3.7 m), 24 ft (7.3 m), and 36 ft (11.0 m) lengths of the EPI corona pipe, respectively

8.4 DISCUSSIONS

8.4.1 Environment Parameter

Temperature is a crucial factor that can significantly influence hen behavior (Lara and Rostagno, 2013) and indoor air quality (Kocaman et al., 2006; Bist et al., 2023b; d). In this study, we maintained consistent and similar temperatures across all treatment rooms throughout the experiment. This result was achieved through environmentally controlled housing, where the temperature was carefully regulated and maintained close to the desired setpoint per Hy-Line W36 management guidelines (Hy-Line, 2020). It is noteworthy that temperature and RH are interrelated but exhibit an inverse relationship (Elijah and Adedapo, 2006; Bist et al., 2023b). As temperature increases, RH tends to decrease, and vice versa. However, the RH inside the housing is influenced by both indoor and outdoor temperatures.

Previous studies have indicated that higher RH levels can increase NH_3 production in poultry housing (Chai et al., 2017, 2019; Lee et al., 2020; Bist et al., 2023b). However, in this study, we did not observe any significant differences in RH among the treatments, likely due to the controlled indoor environment with consistent inlet conditions. Additionally, increased RH can lead to higher LMC (Francesch and Brufau, 2004). Factors such as RH, manure deposition, and management issues like water leakage can affect LMC in poultry housing. However, our study encountered no management issues, and manure deposition was uniform across all treatments. As a result, the LMC did not exhibit significant differences. It is worth noting that as the WOA increased, there was an observed increase in LMC, which can be attributed to continuous manure deposition on the litter (Francesch and Brufau, 2004). Nevertheless, the LMC recorded in this

study remained below 13%, indicating that the litter remained sufficiently dry, which likely affected the volatilization of NH_3 gas.

The ventilation system is crucial in maintaining good air quality in poultry housing by effectively removing moisture, NH_3, and PM (Bist et al., 2023b; Ni et al., 2023). Previous research in the United Kingdom reported high NH_3 concentrations of up to 160 ppm in broiler houses linked to humidity and ventilation conditions (Chai et al., 2012). The emission rate of air pollutants is susceptible to variations in the ventilation rate, which is inversely proportional to the outside ambient temperature (Less et al., 2019). Studies have shown that higher outside temperatures and increased ventilation rates can significantly reduce air pollutant concentrations in the exhaust air (Vranken et al., 2003). Vranken et al. (2003) demonstrated that aligning the ventilation rate with the animals' thermal neutral zone at higher ambient temperatures can lead to an 8-13% decrease in NH_3 concentration. In this study, since the ventilation rates were set up to be similar for each treatment, we did not observe any differences in airflow rates between the treatment rooms. However, differences in airflow rates were noted between small and large ventilation fans with each room, which can be attributed to their respective sizes. In general, larger ventilation fans result in higher airflow rates.

Overall, this study provides insights into the role of temperature, RH, LMC, and ventilation in relation to indoor air quality in poultry housing. By maintaining controlled temperature, RH, and appropriate ventilation, it is possible to create an environment that minimizes NH_3 concentrations and promotes better air quality for the well-being of the poultry.

8.4.2 Ammonia Concentrations

The study's findings indicate that the treatments did not significantly affect NH_3 concentration. This lack of significance can be attributed to several factors observed during the experiment. One such factor is the LMC of the litter, which plays a crucial role in preventing NH_3 release (Miles et al., 2011; Chai et al., 2017, 2019; Bist et al., 2023b; Ni et al., 2023). The LMC remained below 13%, ensuring the litter was sufficiently dry and thereby reducing NH_3 concentration. Another contributing factor is the presence of heaters in each housing unit, which created a warm environment and effectively lowered the RH and LMC within the litter. Additionally, the continuous operation of the indoor circulatory fan facilitated the rapid drying of the litter and manure, further minimizing the NH_3 concentration. Out of these factors, the most important factor affecting room NH_3 concentration was the highest air flow rate of the exhaust fans (Van Wicklen and Allison, 1989). The highest speed of the exhaust fan pulls out all the NH3 gas inside the house. These factors explain why the treatments did not significantly impact the NH_3 concentration during the study.

While numerous studies have reported significant reductions in NH_3 concentration through the application of an EPI system (Mitchell and Waltman, 2003; Ritz et al., 2006), the findings of this particular study did not reveal a significant difference with the EPI treatment. This outcome could be attributed to the low NH_3 concentration levels observed in each experimental room. It is important to note that if the initial NH_3 concentration had been higher, it might have allowed for a more apparent distinction between the treatments. Therefore, this study's lack of a significant difference could be attributed to the relatively low baseline NH_3 levels, suggesting that the EPI system's effectiveness may be more pronounced in environments with higher PM concentrations.

8.4.3 PM Reduction Efficiency

8.4.3.1 Temporal variations of PM

The results of this study provide insights into the variations in average PM mass and particle concentrations among treatment rooms (T2, T3, and T4) and the control room (T1) over 24 hours. Notably, the control room (T1) exhibited the highest concentrations of both $PM_{2.5}$ and PM_{10}, while the lowest concentrations were observed in the T3 and T4 rooms. Likewise, the control room (T1) displayed the highest particle counts for small and large particles, whereas the lowest was found in the T4 and T3 rooms. Previous research also found similar results, with EPI treatment having the lowest dust particle concentration than control (Ritz et al., 2006; Mitchell and Baumgartner, 2007b). A noteworthy pattern emerged across all treatments, with $PM_{2.5}$ and PM_{10} concentrations and particle counts at their lowest during the dark period compared to the light period. This pattern suggests that reduced light exposure could positively impact minimizing the presence of airborne particles (Huneau-Salaün et al., 2012). Furthermore, the peak PM mass and particle counts observed between 12:30 and 2:00 pm can be attributed to routine farm activities, particularly egg collection. During these periods, increased human activity and disturbances within the treatment rooms likely contributed to higher particles in the air.

Additionally, the results emphasize that the control room (T1) consistently demonstrated elevated PM concentrations and particle counts throughout the light period, highlighting the need for improved ventilation or air quality management strategies during that time. Conversely, the T3 and T4 rooms exhibited the lowest concentrations of PM and particles, indicating the effectiveness

of the implemented treatments in reducing airborne particles. It is worth mentioning that a gradual decline in both PM mass and particle counts was observed after 8:00 pm across all rooms. This decline can be attributed to decreased bird activity as they prepared for the dark period, resulting in reduced disturbances and lower particle concentrations.

8.4.3.2 PM levels and concentrations comparison

The results of this study indicate that using a longer corona pipe in the CF rooms can effectively enhance the air quality inside poultry rooms. Specifically, the treatment room (T4) with the longest corona pipe showed the lowest PM2.5 and PM10 concentrations. The reductions achieved with the T4 treatment were notably greater than those in the other treatment rooms. The significant difference observed in $PM_{2.5}$ and small particle concentrations among the treatment rooms highlights the effectiveness of the corona pipe length in reducing airborne PM. However, the differences in PM_{10} and large particle concentrations did not reach the conventional level of statistical significance; the trend towards reduction suggests a potential advantage of the longer corona pipe in mitigating these larger particles. This study shows that PM size and concentration decreased as the treatment period increased, supported by previous research on high-rise layer barns (Lim et al., 2008).

These findings support the idea that incorporating appropriate design modifications, such as increasing the length of the corona pipe, can be an effective strategy for enhancing air quality in poultry housing. By reducing the concentrations of $PM_{2.5}$ (small particles) and potentially PM_{10} (large particles), these modifications can positively affect the health and well-being of poultry and workers in such environments.

8.4.3.3 Electricity consumption

As expected, the study findings demonstrated that longer corona pipe lengths in the EPI were also associated with increased electricity consumption. The increase in electricity consumption can be attributed to various factors, including the higher energy requirements for generating and maintaining the necessary electrostatic charge in longer corona pipes. Additionally, longer pipe lengths may introduce greater resistance and energy loss during the charging process, contributing to the overall rise in electricity consumption. Although longer corona pipes have the potential to enhance the effectiveness of the EPI system in reducing air pollutants, it is crucial to acknowledge the trade-off of increased energy consumption. Therefore, poultry producers and facility managers should carefully consider the optimal length of the corona pipe to strike a balance between effective air quality improvement and energy efficiency.

Future research endeavors in this field could focus on exploring alternative designs or materials for the corona pipe that minimize energy requirements without compromising the performance of the EPI system. Such research could involve investigating innovative approaches to efficiently generate and maintain the necessary electrostatic charge. Additionally, conducting assessments of the long-term economic benefits and environmental impacts associated with different corona pipe lengths would provide valuable insights for decision-making in poultry production facilities. In summary, this study underscores the significance of corona pipe length in influencing electricity consumption in the EPI system. It highlights the importance of a thoughtful approach in determining the optimal design and length of the corona pipe to manage energy costs effectively while achieving desired air quality outcomes in poultry housing facilities. By

optimizing these factors, poultry producers can strike a balance between air quality improvement and energy efficiency, ensuring the adoption of sustainable and cost-effective practices in poultry production.

8.4.4 Limitations and Future Directions

EPI is considered a safe and effective way to enhance the air quality in poultry houses (Mitchell and Waltman, 2003; Ritz et al., 2006). Using these systems requires a change in perspective regarding barn cleanliness, as the system allows a layer of dust to accumulate on surfaces (Ritz et al., 2006). Although this may appear less clean, dust collected on surfaces is better than dust suspended in the air. In addition, this system improves air quality (Ritz et al., 2006) and potentially reduces respiratory stress (Bist et al., 2023b).

Despite the benefits of EPI systems, there are certain drawbacks associated with their use. One of the main challenges is the cost involved in installing and maintaining these systems. Additionally, EPI systems can generate static electricity, potentially damaging electronic equipment. In poultry houses, dust accumulates above perches, which can affect perching behaviors and pose challenges for maintaining and cleaning equipment such as lighting systems, heaters, and circulatory fans. Regular cleaning, including lighting systems, is necessary to ensure the efficient operation of these systems and prevent blockage of light intensity falling at the bird level. If not cleaned promptly, this might decrease the light intensity and result in a potential production decline. The blocking of light or uneven light intensity over rooms might induce several problematic behaviors, such as piling and pecking (Bist et al., 2023c), and may increase the chances of mislaid eggs (Bist et al., 2023c; Subedi et al., 2023).

Despite its limitations, EPI can enhance air quality in poultry houses. Researchers must identify new ways to make EPI more effective and economical, including developing new materials that resist static electricity, using safer and more efficient charging methods, and regulating the amount of charge applied to materials. Developing improved EPI can further enhance air quality control in poultry production. In addition, research into dust collection of all the charged PM in the air to reduce PM accumulation on other useful farm equipment is needed. Future studies can also assess the impact of EPI technology on chicken health and productivity, evaluate the long-term benefits and costs of using this technology on a commercial scale, and explore the potential of combining EPI technology with other mitigation strategies such as air filtration and mechanical ventilation to achieve greater reductions in PM concentrations in CF hen houses.

Further research is needed to evaluate the effectiveness of EPI technology in different environmental conditions and with different numbers and breeds of chickens. Continued investigation and development of EPI systems will contribute to improved air quality control in poultry production, ensuring the well-being and productivity of the birds while minimizing the environmental impact.

8.5 CONCLUSIONS

This study provides a practical solution for reducing PM in CF hen rooms. Using longer corona pipes, we improved air quality by significantly reducing $PM_{2.5}$ (small particle) concentrations ($P \leq 0.01$). T3 and T4 treatments showed notable reductions compared to the

control room (T1). While no significant differences were observed for PM_{10} (large particle) concentrations, encouraging trends indicated potential reductions ($P \leq 0.10$). These findings demonstrate the promising potential of longer corona pipes in enhancing air quality within poultry housing environments. This study found no significant differences in NH_3 concentrations among the treatments, likely due to the low NH_3 levels and LMC observed across all treatments.

Implementing EPI systems does come with challenges and costs, requiring regular cleaning and maintenance for optimal operation. Future research should focus on enhancing EPI technology, evaluating its impact on chicken health and productivity, and assessing its cost-effectiveness on a larger scale. Exploring combinations with other mitigation strategies may yield even greater reductions in PM concentrations. Continued research and development of EPI systems will contribute to improved air quality control in poultry production, promoting bird welfare and minimizing environmental impact while striving for sustainable and responsible practices in animal agriculture.

8.6 REFERENCES

Aarnink, A., J. van Harn, T. Van Hattum, Y. Zhao, and N. Ogink. 2011. Dust reduction in broiler houses by spraying rapeseed oil. Transactions of the ASABE 54:1479–1489.

Aillery, M. P., N. R. Gollehon, R. C. Johansson, J. D. Kaplan, N. D. Key, and M. Ribaudo. 2005. Managing manure to improve air and water quality.

Almuhanna, E. 2011. Characteristics of air contaminants in naturally and mechanically ventilated poultry houses in Al-Ahsa, Saudi Arabia. Transactions of the ASABE 54:1433–1443.

Bist, R. B., and L. Chai. 2022. Advanced strategies for mitigating particulate matter generations in poultry houses. Applied Sciences 12:11323.

Bist, R. B., P. Regmi, D. Karcher, Y. Guo, A. K. Singh, C. W. Ritz, W. K. Kim, D. R. Jones, and L. Chai. 2023a. Bedding management for suppressing particulate matter in cage-free hen houses. AgriEngineering 5:1663–1676.

Bist, R. B., S. Subedi, L. Chai, and X. Yang. 2023b. Ammonia emissions, impacts, and mitigation strategies for poultry production: A critical review. Journal of Environmental Management 328:116919.

Bist, R. B., X. Yang, S. Subedi, and L. Chai. 2023c. Mislaying behavior detection in cage-free hens with deep learning technologies. Poultry Science:102729.

Bist, R. B., X. Yang, S. Subedi, M. K. Sharma, A. K. Singh, C. W. Ritz, W. K. Kim, and L. Chai. 2023d. Temporal variations of air quality in cage-free experimental pullet houses. Poultry 2:320–333.

Cambra-López, M., A. J. Aarnink, Y. Zhao, S. Calvet, and A. G. Torres. 2010. Airborne particulate matter from livestock production systems: A review of an air pollution problem. Environmental Pollution 158:1–17.

Cambra-López, M., A. Winkel, J. Van Harn, N. Ogink, and A. Aarnink. 2009. Ionization for reducing particulate matter emissions from poultry houses. Transactions of the ASABE 52:1757–1771.

Chai, M., M. Lu, T. Keener, S.-J. Khang, C. Chaiwatpongsakorn, and J. Tisch. 2009. Using an improved electrostatic precipitator for poultry dust removal. Journal of Electrostatics 67:870–875.

Chai, L., J.-Q. Ni, C. A. Diehl, I. Kilic, A. Heber, Y. Chen, E. Cortus, B. Bogan, T. Lim, and J.-C. Ramirez-Dorronsoro. 2012. Ventilation rates in large commercial layer hen houses with two-year continuous monitoring. British Poultry Science 53:19–31.

Chai, L., H. Xin, Y. Wang, J. Oliveira, K. Wang, and Y. Zhao. 2019. Mitigating particulate matter generation in a commercial cage-free hen house. Transactions of the ASABE 62:877–886.

Chai, L., H. Xin, Y. Zhao, T. Wang, M. Soupir, and K. Liu. 2017. Mitigating ammonia emissions from liquid-sprayed litter of cage-free hen house with a solid litter additive. Page 1 in American Society of Agricultural and Biological Engineers.

Chai, L., H. Xin, Y. Zhao, T. Wang, M. Soupir, and K. Liu. 2018. Mitigating ammonia and PM generation of cage-free henhouse litter with solid additive and liquid spray. Transactions of the ASABE 61:287–294.

Dai, C., S. Huang, Y. Zhou, B. Xu, H. Peng, P. Qin, and G. Wu. 2019. Concentrations and emissions of particulate matter and ammonia from extensive livestock farm in South China. Environmental Science and Pollution Research 26:1871–1879.

Donham, K. J., D. Cumro, and S. Reynolds. 2002. Synergistic effects of dust and ammonia on the occupational health effects of poultry production workers. Journal of Agromedicine 8:57–76.

Elijah, O. A., and A. Adedapo. 2006. The effect of climate on poultry productivity in Ilorin Kwara State, Nigeria. International Journal of Poultry Science 5:1061–1068.

EPA, O. 2022. Health and environmental effects of particulate matter (PM). Available at https://www.epa.gov/pm-pollution/health-and-environmental-effects-particulate-matter-pm (verified 15 June 2023).

EPA, O. 2023. NAAQS table. Available at https://www.epa.gov/criteria-air-pollutants/naaqs-table (verified 15 June 2023).

EPIAir. 2023. FAQ's about EPI air system | Agricultural dust reduction. EPI AIR Available at https://epiair.com/faqs/ (verified 15 June 2023).

Fabbri, C., L. Valli, M. Guarino, A. Costa, and V. Mazzotta. 2007. Ammonia, methane, nitrous oxide and particulate matter emissions from two different buildings for laying hens. Biosystems Engineering 97:441–455.

Forero, D., C. Pena, P. Acevedo, M. Hernandez, and I. Cabeza. 2018. Biofiltration of acetic acid vapours using filtering bed compost from poultry manure-pruning residues-rice husks. Chemical Engineering Transactions 64:511–516.

Francesch, M., and J. Brufau. 2004. Nutritional factors affecting excreta/litter moisture and quality. World's Poultry Science Journal 60:64–75.

Gassman, R. G. 2015. Effect of dust filtration control on CO2 and NH3 concentrations in a swine farrowing room. The University of Iowa.

Huneau-Salaün, A., N. Rousset, L. Balaine, N. Homo, and C. Aubert. 2012. Daily variations of dust concentration in the air of poultry houses for laying hens. Emissionsof Gasand Dust from Livestock:139.

Hy-Line. 2020. 36 COM ENG.pdf. Available at https://www.hyline.com/filesimages/Hy-Line-Products/Hy-Line-Product-PDFs/W-36/36%20COM%20ENG.pdf (verified 10 September 2022).

Jerez, S. B., S. Mukhtar, W. Faulkner, K. D. Casey, M. S. Borhan, and R. A. Smith. 2013. Evaluation of electrostatic particle ionization and BioCurtain^{TM} technologies to reduce air pollutants from broiler houses. Applied Engineering in Agriculture 29:975–984.

Knight, R. M., L. Zhao, and H. Zhu. 2021. Modelling and optimisation of a wire-plate ESP for mitigation of poultry PM emission using COMSOL. Biosystems Engineering 211:35–49.

Kocaman, B., N. Esenbuga, A. Yildiz, E. Laçin, and M. Macit. 2006. Effect of environmental conditions in poultry houses on the performance of laying hens. International Journal of Poultry Science 5:26–30.

Kocaman, B., A. V. Yaganoglu, and M. Yanar. 2005. Combination of fan ventilation system and spraying of oil-water mixture on the levels of dust and gases in caged layer facilities in Eastern Turkey. Journal of Applied Animal Research 27:109–111.

Lara, L. J., and M. H. Rostagno. 2013. Impact of heat stress on poultry production. Animals 3:356–369.

Lee, M., P. Li, J. A. Koziel, H. Ahn, J. Wi, B. Chen, Z. Meiirkhanuly, C. Banik, and W. S. Jenks. 2020. Pilot-scale testing of UV-A light treatment for mitigation of NH3, H2S, GHGs, VOCs, odor, and O3 inside the poultry barn. Frontiers in Chemistry 8:613.

Less, B. D., S. M. Dutton, I. S. Walker, M. H. Sherman, and J. D. Clark. 2019. Energy savings with outdoor temperature-based smart ventilation control strategies in advanced California homes. Energy and Buildings 194:317–327.

Lim, T. T., A. J. Heber, J. Ni, L. Zhao, and S. H. Hanni. 2008. Effects of electrostatic space charge system on particulate matter emission from high-rise layer barn. Page 1 in American Society of Agricultural and Biological Engineers.

Manuzon, R., L. Zhao, and C. Gecik. 2014. An optimized electrostatic precipitator for air cleaning of particulate emissions from poultry facilities. ASHRAE Transactions 120.

Martel, M., S. Kirychuk, B. Predicala, R. Bolo, Y. Yang, B. Thompson, H. Guo, and L. Zhang. 2023. Improving air quality in broiler rooms using an electrostatic particle ionization system. Journal of the ASABE:0.

Melse, R. W., and N. Ogink. 2005. Air scrubbing techniques for ammonia and odor reduction at livestock operations: Review of on-farm research in the Netherlands. Transactions of the ASAE 48:2303–2313.

Miles, D., D. Rowe, and T. Cathcart. 2011. Litter ammonia generation: Moisture content and organic versus inorganic bedding materials. Poultry Science 90:1162–1169.

Mintus, C. 2021. More states in the united states to switch to cage-free eggs. Available at https://www.thepoultrysite.com/news/2021/06/more-states-in-the-united-states-to-switch-to-cage-free-eggs (verified 1 April 2023).

Mitchell, B. 1998. Effect of negative air ionization on ambient particulates in a hatching cabinet. Applied Engineering in Agriculture 14:551–555.

Mitchell, B. W., and J. W. Baumgartner. 2007a. Electrostatic space charge system for reducing dust in poultry production houses and the hatchery.Pages 23–24 in International Conference How to improve air quality. Citeseer.

Mitchell, B. W., and J. W. Baumgartner. 2007b. Electrostatic space charge system for reducing dust in poultry production houses and the hatchery.Pages 23–24 in International Conference How to improve air quality. Citeseer.

Mitchell, B., L. Richardson, J. Wilson, and C. Hofacre. 2004. Application of an electrostatic space charge system for dust, ammonia, and pathogen reduction in a broiler breeder house. Applied Engineering in Agriculture 20:87.

Mitchell, B., and W. Waltman. 2003. Reducing airborne pathogens and dust in commercial hatching cabinets with an electrostatic space charge system. Avian Diseases 47:247–253.

Ni, J.-Q. 2015. Research and demonstration to improve air quality for the US animal feeding operations in the 21st century–A critical review. Environmental Pollution 200:105–119.

Ni, J.-Q. 2021. Factors affecting toxic hydrogen sulfide concentrations on swine farms—sulfur source, release mechanism, and ventilation. Journal of Cleaner Production 322:129126.

Ni, J.-Q., M. Erasmus, D. R. Jones, and D. L. Campbell. 2023. Effectiveness and characteristics of a new technology to reduce ammonia, carbon dioxide, and particulate matter pollution in poultry production with artificial turf floor. Environmental Technology & Innovation 29:102976.

Ogink, N., J. van Harn, R. van Emous, and H. Ellen. 2012. Top layer humidification of bedding material of laying hen houses to mitigate dust emissions: effects of water spraying on dust, ammonia and odor emissions. Page 3 in American Society of Agricultural and Biological Engineers.

Pearson, C., V. Phillips, G. Green, and I. Scotford. 1992. A minimum-cost biofilter for reducing aerial emissions from a broiler chicken house.Pages 245–254 in Studies in Environmental Science. Elsevier.

Richardson, L., B. Mitchell, J. Wilson, and C. Hofacre. 2003. Effect of an electrostatic space charge system on airborne dust and subsequent potential transmission of microorganisms to broiler breeder pullets by airborne dust. Avian Diseases 47:128–133.

Ritz, C., B. Mitchell, B. Fairchild, M. Czarick III, and J. Worley. 2006. Improving in-house air quality in broiler production facilities using an electrostatic space charge system. Journal of Applied Poultry Research 15:333–340.

Seedorf, J., and J. Hartung. 1999. Reduction efficiencies of a biofilter and a bio-scrubber as bio-aerosols in two piggeries. Berliner und Munchener Tierarztliche Wochenschrift 112:444–447.

Senthilselvan, A., J. Beach, J. Feddes, N. Cherry, and I. Wenger. 2011. A prospective evaluation of air quality and workers' health in broiler and layer operations. Occupational and Environmental Medicine 68:102–107.

Strohmaier, C., A. J. Schmithausen, M. S. Krommweh, B. Diekmann, and W. Büscher. 2018. Evaluation of a dry filter for dust removal under laboratory conditions in comparison to practical use at a laying hen barn. Environ Sci Pollut Res 25:29511–29517 Available at https://doi.org/10.1007/s11356-018-2981-3 (verified 15 June 2023).

Subedi, S., R. Bist, X. Yang, and L. Chai. 2023. Tracking floor eggs with machine vision in cage-free hen houses. Poultry Science:102637 Available at https://www.sciencedirect.com/science/article/pii/S003257912300161X (verified 10 March 2023).

Tan, Z., and Y. Zhang. 2004. A review of effects and control methods of particulate matter in animal indoor environments. Journal of the Air & Waste Management Association 54:845–854.

UEP. 2022. Retailers, restaurants continue cage-free commitments. United Egg Producers Available at https://unitedegg.com/retailers-restaurants-continue-cage-free-commitments/ (verified 11 May 2023).

Van der Heyden, C., P. Demeyer, and E. I. Volcke. 2015. Mitigating emissions from pig and poultry housing facilities through air scrubbers and biofilters: State-of-the-art and perspectives. Biosystems Engineering 134:74–93.

Van Wicklen, G., and J. Allison. 1989. Aerosol and ammonia concentrations in broiler houses using mechanical and natural ventilation. Journal of Agricultural Engineering Research 42:97–109.

Viegas, S., V. M. Faísca, H. Dias, A. Clérigo, E. Carolino, and C. Viegas. 2013. Occupational exposure to poultry dust and effects on the respiratory system in workers. Journal of Toxicology and Environmental Health, Part A 76:230–239.

Vranken, E., S. Claes, and D. Berckmans. 2003. Reduction of ammonia emission from livestock buildings by the optimization of ventilation control settings. Air Pollution from Agricultural Operations III, Proceedings:167–173.

Williams Ischer, S., M. Farnell, G. Tabler, M. Moreira, P. O'Shaughnessy, and M. Nonnenmann. 2017. Evaluation of a sprinkler cooling system on inhalable dust and ammonia concentrations in broiler chicken production. Journal of Occupational and Environmental Hygiene 14:40–48.

Winkel, A., J. Mosquera, A. J. Aarnink, P. W. G. Koerkamp, and N. W. Ogink. 2016. Evaluation of oil spraying systems and air ionisation systems for abatement of particulate matter emission in commercial poultry houses. Biosystems Engineering 150:104–122.

Wood, D. J., and B. J. Van Heyst. 2016. A review of ammonia and particulate matter control strategies for poultry housing. Transactions of the ASABE 59:329–344.

Xie, Q., J.-Q. Ni, J. Bao, and Z. Su. 2021. Correlations, variations, and modelling of indoor environment in a mechanically-ventilated pig building. Journal of Cleaner Production 282:124441.

Xie, Q., J.-Q. Ni, E. Li, J. Bao, and P. Zheng. 2022. Sequential air pollution emission estimation using a hybrid deep learning model and health-related ventilation control in a pig building. Journal of Cleaner Production 371:133714.

Yasmeen, R., Z. Ali, S. Tyrrel, and Z. A. Nasir. 2019. Estimation of particulate matter and gaseous concentrations using low-cost sensors from broiler houses. Environmental Monitoring and Assessment 191:1–10.

Zhao, Y., A. Aarnink, M. De Jong, N. Ogink, and P. G. Koerkamp. 2011. Effectiveness of multi-stage scrubbers in reducing emissions of air pollutants from pig houses. Transactions of the ASABE 54:285–293.

Zhao, Y., L. Chai, B. Richardson, and H. Xin. 2018. Field evaluation of an electrostatic air filtration system for reducing incoming particulate matter of a hen house. Transactions of the ASABE 61:295–304.

Zheng, W., B. Li, W. Cao, G. Zhang, and Z. Yang. 2012. Application of neutral electrolyzed water spray for reducing dust levels in a layer breeding house. Journal of the Air & Waste Management Association 62:1329–1334.

CHAPTER 9

SUMMARY

The dissertation presents a comprehensive investigation into the use of innovative technologies and strategies to improve conditions within cage-free poultry farming systems. The research findings are significant, demonstrating the potential of precision farming technologies to address the most pressing challenges in poultry farming: air quality, abnormal behaviors, and animal welfare.

Air Quality Improvement: The study successfully showed that electrostatic particle ionization (EPI) technology, particularly when utilized with longer ion precipitators, significantly reduces particulate matter (PM) levels in cage-free hen rooms. This reduction is crucial for enhancing the health and welfare of hens and the working conditions of farm workers. The effectiveness of EPI technology varied with the length of ion precipitators, highlighting the importance of system configuration for optimal air quality management.

Behavior and Footpad Health Detection: The use of advanced deep learning models, such as YOLOv5, YOLOv6, YOLOv7, and YOLOv8, for the early detection of health issues, floor egg-laying behavior, piling behavior, bumblefoot, and footpad dermatitis represents a groundbreaking step towards automated health and welfare monitoring in poultry farming. The detection accuracy was up to 95.5% or 100%.

Conclusion: This dissertation underscores the transformative potential of integrating precision farming technologies with innovative management practices to improve the welfare and ethical standards of poultry farming. The findings advocate for a holistic approach to poultry farm

management, where technology-driven solutions enhance production efficiency and prioritize the animals' health and welfare. The successful application of EPI technology for air quality management, alongside the strategic use of environmental modifications and AI-driven health monitoring, sets a new benchmark for the future of cage-free poultry farming, emphasizing the need for continuous innovation and adaptation in agricultural practices.

APPENDIX A

CURRICULUM VITAE

A.1 EDUCATION & TRAINING

- **Ph.D. Poultry Science**- Department of Poultry Science, University of Georgia, Athens, GA (GPA of 3.77; Expected to graduate in May 2024) (2021- 2024).

  Dissertation: Precision Farming Technologies for Enhancing Air Quality, Floor Egg Management, and Animal Welfare in Cage-Free Hens. ***Advisor:*** Dr. Lilong Chai
- **MS in Agriculture - Animal Science** at the Arkansas State University in Jonesboro, Arkansas (GPA of 3.70) (2016-2018).
- **BS in Zoology** from Tribhuvan University, Nepal, with first division (2011-2014).
- **Proficiency Certificate in Science (Major: Biology)** from Florida International Higher Secondary School with first division (2008-2010).
- **School Leaving Certificate** from Florida International Higher Secondary School with first division (2007-2008).

A.2 PROFESSIONAL EXPERIENCE

- **Graduate Research Assistantship:** University of Georgia – Department of Poultry Science, Athens, GA 30605, USA (2021 – Present).

  Research Activities- Researched, tested, and implemented machine learning models for poultry behavior detection. Developed automated systems for assessing footpad and feather conditions. Utilized precision technology like accelerometers to gauge bird activity levels and correlated data with environmental parameters for improved animal health and welfare. Innovated solutions to reduce air pollutants in poultry housing.

  Teaching Experience- Served as a Teaching Assistant for the course "Effects of Global Agriculture on World Culture." Assisted the professor in grading student assignments and

provided constructive feedback to enhance their academic performance in future assignments.

- **Evisceration Sorter**: PECO Foods, Inc., Arkansas, USA (2019 – 2020).

  Hands-on experience- Demonstrated hands-on expertise as an approved Evisceration Sorter in a poultry processing company. Extensive knowledge spans the entire processing plant, from first to further processing. Worked in harmony with diverse groups of employees.

- **Science and Math Teacher:** Prabhat Vidhya Niketan Higher Secondary School, Kanchanpur, Nepal (2012 – 2014).

  Teaching Experience- Provide instruction in science and math courses to lower secondary school students. Fostered an inclusive environment, ensuring equal opportunities for students with diverse backgrounds to thrive in their learning.

A.3 EXTENSION EXPERIENCES

- **Research Extension volunteer** at the University of Georgia under Dr. Lilong Chai (2021-cont.)- Helped Dr. Chai in organizing extension conferences like "Georgia Precision Poultry Farming Conference" and "Georgia Layer Conference."

  Output: Over the last three years, these conferences have offered online training to 1200+ attendees, spanning poultry producers, farmers, researchers, tech managers, government officials, extension agents, and students from 40+ countries.

- **Volunteer** with Dr. Lilong Chai at the Georgia 4-H and FFA youth education program (2021-cont.)- Assisted Dr. Chai in the youth education program, actively involved in egg collection and storing for quality analysis.

A.4 RESEARCH INTERESTS:

- Develop, test, and apply machine learning models and statistical tools to support precision livestock farming.
- Integrate machine learning techniques with sensor-enabled data to streamline and optimize livestock management processes.
- Develop and find innovative technologies to improve air quality inside livestock housing.
- Develop an Artificial Intelligence model to differentiate normal and abnormal behavior, facilitating early detection of health issues to improve animal welfare.
- Implement and develop technologies to enhance farming efficiency and environmental sustainability.

A.5 RECENT PUBLICATIONS

A.5.1 Peer-Reviewed Articles

19. **Bist, R. B.,** Subedi, S., Chai, L., Ritz, C. W., Kim, W. K., and Yang, X. (2024). Electrostatic particle ionization for suppressing air pollutants in cage-free layer facilities: Dust suppressing for cage-free hens. Poultry Science, 103494. https://doi.org/10.1016/j.psj.2024.103494.
18. **Bist, R. B.,** Subedi, S., Chai, L., and Yang, X. (2023). Illuminating solutions to reduce mislaid eggs in cage-free layers. AgriEngineering, 5(4), 2170-2183. https://doi.org/10.3390/agriengineering5040133.

17. **Bist, R. B.,** Regmi, P., Karcher, D., Guo, Y., Singh, A. K., Ritz, C. W., Kim, W. K., Jones, D., and Chai, L. (AgriEngineering; 2023). Bedding Management for Suppressing Particulate Matter in Cage-Free Hen Houses. https://doi.org/10.3390/agriengineering5040103.
16. **Bist, R. B.,** Subedi, S., Chai, L., and Yang, X. (AgriEngineering; 2023). Automatic Detection of Cage-free Dead Hens with deep learning methods. https://doi.org/10.3390/agriengineering5020064.
15. **Bist, R. B.,** Subedi, S., Chai, L., and Yang, X. (Poultry Science; 2023). Mislaying behavior detection in cage-free hen house with deep learning technologies. https://doi.org/10.1016/j.psj.2023.102729.
14. **Bist, R. B.,** Subedi, S., Chai, L., and Yang, X. (Poultry; 2023). Effective Strategies for Mitigating Feather Pecking and Cannibalism in Cage-Free W-36 Pullets. https://doi.org/10.3390/poultry2020021.
13. **Bist, R. B.,** Subedi, S., Chai, L., and Yang, X. (Poultry; 2023). Temporal Variations of Air Quality in Cage-Free Experimental Pullet Houses. https://doi.org/10.3390/poultry2020024.
12. **Bist, R. B.,** Subedi, S., Chai, L., and Yang, X. (AgriEngineering; 2023). A novel benchmark of YOLOv6 object detector for piling behavior detection in cage-free laying hen facilities. https://doi.org/10.3390/agriengineering5020056.
11. **Bist, R. B.,** Subedi, S., Chai, L., Regmi, P., Ritz, C. W., Kim, W. K., and Yang, X. (Poultry; 2023). Effects of Perching on Poultry Welfare and Production: A Review. Poultry, 2(2), 134-157. https://doi.org/10.3390/poultry2020013.

10. **Bist, R. B.,** Subedi, S., Chai, L., and Yang, X. (Journal of Environmental Management; 2023). Ammonia emissions, impacts, and mitigation strategies for poultry production: A critical review. Journal of Environmental Management, 328, 116919. https://doi.org/10.1016/j.jenvman.2022.116919
9. **Bist, R. B.,** and Chai, L. (Applied Sciences; 2022). Advanced Strategies for Mitigating Particulate Matter Generations in Poultry Houses. https://doi.org/10.3390/app122211323.
8. Chai, L., Subedi, S., **Bist, R. B.,** and Yang, X. (Journal of the NACAA, 2023). Artificial Intelligence Technologies for Monitoring Poultry Pecking. ISSN 2158-9459, 16-1.
7. Guo, Y., Chai, L., **Bist, R. B.,** Regmi, P., and D, Yi (Poultry Science; 2023). Automatic Tracking of Lohmann Brown Hens on the Litter Floor of Cage Free Houses with Deep Learning Methods. https://doi.org/10.1016/j.psj.2023.102784.
6. Subedi, S., **Bist, R. B.,** Yang, X., and Chai, L. (Computers and Electronics in Agriculture, 2023). Tracking pecking behaviors and damages of cage-free laying hens with machine vision technologies. https://doi.org/10.1016/j.compag.2022.107545.
5. Subedi, S., **Bist, R. B.,** Yang, X., and Chai, L. (Poultry Science, 2023). Tracking Floor Eggs with Machine Vision in Cage-free Hen Houses. https://doi.org/10.1016/j.psj.2023.102637.
4. Yang, X., **Bist, R. B.,** Subedi, S., and Chai, L. (Animal; 2023). A computer vision based automatic system for egg grading and defect detection. https://doi.org/10.3390/ani13142354.
3. Yang, X., **Bist, R. B.,** Subedi, S., and Chai, L. (Engineering Applications of Artificial Intelligence; 2023). An automatic classifier for monitoring applied behaviors of cage–free laying hens with deep learning. https://doi.org/10.1016/j.engappai.2023.106377.

2. Yang, X., **Bist, R. B.,** Subedi, S., and Chai, L. (Artificial Intelligence in Agriculture; 2023). A Deep Learning Method for Monitoring Spatial Distribution of Cage-Free Hens. https://doi.org/10.1016/j.aiia.2023.03.003.
1. Yang, X., Chai, L., **Bist, R. B.,** Subedi, S., and Wu, Z. (Animal; 2022). A Deep Learning Model for Detecting Cage-Free Hens on the Litter Floor. Animals, 12(15), 1983. https://doi.org/10.3390/ani12151983.

A.5.2 Preprint

- Yang, X., Dai, H., Wu, Z., **Bist, R. B.,** Subedi, S., Sun, J., and Chai, L. (ArXiv; 2023). SAM for Poultry Science. arXiv preprint arXiv:2305.10254. https://doi.org/10.48550/arXiv.2305.10254.

A.5.3 Papers Under Review

1. **Bist, R. B.,** Subedi, S., Chai, L., and Yang, X. Automatic detection of cage-free hens bumblefoot with computer vision technologies.
2. **Bist, R. B.,** Subedi, S., Chai, L., and Yang, X. Comparative Assessment of Pullet Hen Age and Dust Concentration using Accelerometer-based Activity Monitoring.
3. **Bist, R. B.,** Bist, K., and Chai, L. Sustainable Poultry Farming Practices: A Review of Current Strategies and Future Prospects.
4. **Bist, R. B.,** Subedi, S., Chai, L., and Yang, X. Automatic footpad dermatitis scoring in poultry using FPD models.

5. **Bist, R. B.,** Subedi, S., Chai, L., and Yang, X. Synergistic Effect of Electrostatic Space charging and Bedding Management on Particulate Matter and Ammonia Control for Cage-Free Hen.
6. **Bist, R. B.,** Subedi, S., Chai, L., and Yang, X. Effectiveness of electrostatic particle ionization in reducing particulate matter in cage-free hen houses with varying heights and durations.
7. **Bist, R. B.,** Subedi, S., Paneru, B., Yang, X., and Chai, L. Individual hen detection and tracking using Machine Learning.
8. **Bist, R. B.,** Subedi, S., Chai, L., and Yang, X. Artificial Intelligence in Poultry Science: A Review.
9. **Bist, R. B.,** Subedi, S., Chai, L., and Yang, X. Automated Feather Damage Scoring in Cage-Free Laying Hen Houses Using machine learning.
10. **Bist, R. B.,** Subedi, S., Chai, L., and Yang, X. Individual laying hen detection, segmentation, and tracking using YOLOv8.
11. **Bist, R. B.,** Subedi, S., Chai, L., and Yang, X. Effect of the dimmer on laying hen perching behavior.
12. **Bist, R. B.,** Subedi, S., Chai, L., and Yang, X. Effect of topping bedding on ammonia and particulate matter concentrations.
13. Subedi, S., **Bist, R. B.,** Yang, X., and Chai, L. Multiple Behaviors Classification of Cage-free Laying Hens Using Deep Learning.

14. Yang, X., **Bist, R. B.**, Paneru, B., Liu. T., Applegate, T., Ritz, C.W., Kim, W. K., Regmi, P., and Chai, L. Revolutionizing Poultry Management with Advancements in Computer Vision.

15. Yang, X., **Bist, R. B.**, Paneru, B., and Chai, L. Deep learning methods for tracking the locomotion of individual chickens.

16. Yang, X., Haixing Dai., Zihao Wu., **Bist, R. B.**, Subedi, S., Guoyu Lu., Changying Li., Tianming Liu., and Chai, L. An Innovative Segment Anything Model for Precision Poultry Monitoring.

17. Yang, X., **Bist, R. B.,** Subedi, S., and Chai, L. A deep learning framework for monitoring wild birds on poultry farms to prevent avian influenza.

18. Paneru B., **Bist, R. B.,** Chai, L., and Yang, X. Tracking dustbathing behavior of cage-free laying hen with machine vision technologies.

19. Paneru B., **Bist, R. B.,** Chai, L., and Yang, X. Perching behavior detection based on age and height using machine learning model.

20. Paneru B., **Bist, R. B.,** Chai, L., and Yang, X. Male hen detection in cage-free hen housing.

21. Poudel, S., **Bist, R. B.,** Chai, L., and Mani, S. Current State and Future Landscape of Digital Agriculture Technologies in Crop and Livestock farming.

22. Saeidifar, S., Li, G., Chai, L., **Bist, R. B**., Rasheed, K. M., Lu, J., Banakar, A., and Liu, T. (2024). Zero-Shot Image Segmentation for Monitoring Thermal Conditions of Individual Cage-Free Laying Hens.

A.5.4 Papers Published in Proceedings

1. **Bist, R. B.,** Subedi, S., Chai, L., and Yang, X. (ASABE, 2023). Effects of artificial dusk lighting on perching behaviors of cage-free laying hens. In 2023 ASABE Annual International Meeting (p. 1). doi:10.13031/aim.202300120.
2. **Bist, R. B.,** Subedi, S., Chai, L., and Yang, X. (ASABE, 2023). Cage Free Hens' Feather Pecking Management. In 2023 ASABE Annual International Meeting (p. 1). doi: 10.13031/aim.202300119.
3. **Bist, R. B.,** Chai, L., Yang, X., Subedi, S., and Guo, Y. (ASABE, 2022). Air Quality in Cage-free Houses during Pullets Production. In 2022 ASABE Annual International Meeting (p. 1). American Society of Agricultural and Biological Engineers. http://dx.doi.org/10.13031/aim.202200329.
4. Yang, X., Chai, L., **Bist, R. B.,** Subedi, S., and Guo, Y. (ASABE, 2022). Variation of litter quality in cage-free houses during pullet production. In 2022 ASABE Annual International Meeting (p. 1). American Society of Agricultural and Biological Engineers. http://dx.doi.org/10.13031/aim.202200925.

A.5.5 Abstracts and Presentations

1. **Bist, R. B.,** Paneru, B., Yang, X., and Chai, L. (2024). Automatic Detection and Scoring of Footpad Dermatitis in Laying Hens Using Machine Learning Models. (Poster Presentation), ASABE Annual International Meeting 2024, Anaheim, CA, USA.
2. **Bist, R. B.,** Paneru, B., Yang, X., and Chai, L. (2024). Comparative Assessments of Cage-Free Pullet Age, Activities, and Impacts on Dust Concentration Using

Accelerometer-Based Activity Sensor. (Poster Presentation), ASABE Annual International Meeting 2024, Anaheim, CA, USA.

3. **Bist, R. B.,** Paneru, B., Yang, X., and Chai, L. (2024). Automatic Detection and Scoring of Footpad Dermatitis in Laying Hens Using Machine Learning Models. (Poster Presentation), ASABE Annual International Meeting 2024, Anaheim, CA, USA.
4. **Bist, R. B.,** Subedi, S., Yang, X., Paneru, B., and Chai, L. (2024). Machine Learning Model for Detection, Segmentation, and Tracking of Individual Cage-Free Laying Hens. (Oral presentation), IPSF/ IPPE 2024, Atlanta, Georgia, USA.
5. **Bist, R. B.,** Subedi, S., Chai, L., and Yang, X. (2023). Synergistic effect of electrostatic particle ionization and bedding management on particulate matter and ammonia reduction in cage-free hen houses. (Oral presentation). 2023 Poultry Science Association Annual Meeting, Philadelphia, PA, USA.
6. **Bist, R. B.,** Subedi, S., Chai, L., and Yang, X. (2023). Detecting cage-free hens bumblefoot with deep learning models. (Poster presentation). 2023 Poultry Science Association Annual Meeting, Philadelphia, PA, USA.
7. **Bist, R. B.,** Subedi, S., Chai, L., and Yang, X. (2023). Effects of artificial dusk lighting on perching behaviors of cage-free laying hens. (Poster presentation). ASABE Annual International Meeting 2023, Omaha, Nebraska, USA.
8. **Bist, R. B.,** Subedi, S., Chai, L., and Yang, X. (2023). Poultry pecking management: a case study. (Poster presentation). ASABE Annual International Meeting 2023, Omaha, Nebraska, USA.

9. **Bist, R. B.,** Subedi, S., Chai, L., and Yang, X. (2023). Monitoring Cage-free Laying Hens on Litter Floor with Machine Vision. (Oral Presentation). US Precision Livestock Farming Conference 2023. Knoxville, Tennessee, USA.
10. **Bist, R. B.,** Subedi, S., Chai, L., and Yang, X. (2023). Early Detection of Bumblefoot in Poultry: A Novel Approach to Improve Welfare. (Poster). 2023 International Conference on Integrative Precision Agriculture, Athens, Georgia, USA.
11. **Bist, R. B.,** and Chai, L. (2023). Floor egg laying behavior detection in cage-free housing. (Oral Presentation), UGA Poultry Science scientific writing proposal presentation, Athens, Georgia, USA.
12. **Bist, R. B.,** Subedi, S., Chai, L., and Yang, X. (2023). An integrated engineering method for mitigating air pollutant emissions from cage-free hen houses. (Poster), UGA Cleantech Symposium, Athens, Georgia, USA.
13. **Bist, R. B.,** Subedi, S., Chai, L., and Yang, X. (2023). Monitoring mislaying behaviors of cage-free hens with deep learning. (Oral Presentation), UGA Poultry Science Seminar, Athens, Georgia, USA.
14. **Bist, R. B.,** Subedi, S., Chai, L., and Yang, X. (2023). Monitoring mislaying behaviors of cage-free hens with deep learning. (Poster), IPSF/ IPPE, Atlanta, Georgia, USA.
15. **Bist, R. B.,** Subedi, S., Chai, L., and Yang, X. (2022). Effects of Hy-line W-36 pullet age on air pollutant concentration in a cage-free housing system. (Oral Presentation), IPSF/ IPPE, Atlanta, Georgia, USA.
16. **Bist, R. B.,** Subedi, S., Chai, L., and Yang, X. (2022). Bedding management for suppressing particulate matter in cage-free layer house. (Oral Presentation), PSA Annual Meeting, San Antonio, Texas, USA.

17. **Bist, R. B.,** Subedi, S., Chai, L., and Yang, X. (2022). Bedding management for suppressing particulate matter in the cage-free layer house. (Poster), ASABE Annual International Meeting, Houston, Texas, USA.
18. **Bist, R. B.,** Subedi, S., Chai, L., and Yang, X. (2022). Bedding management for suppressing particulate matter in the cage-free layer house. (Poster), UGA Graduate Research Forum, Athens, Georgia, USA.
19. **Bist, R. B.,** Subedi, S., Chai, L., and Yang, X. (2022). Preventing feather pecking and cannibalism for W-36 pullets in cage-free houses. (Poster), PSA Annual Meeting, San Antonio, Texas, USA.
20. Yang, X., **Bist, R. B.,** Paneru, B., and Chai, L. (2024). Advanced Machine Learning Techniques for Monitoring Poultry Movement Patterns. (Oral Presentation), ASABE Annual International Meeting 2024, Anaheim, CA, USA.
21. Yang, X., **Bist, R. B.,** Subedi, S., Paneru, B., and Chai, L. (2024). Deep learning algorithm for tracking individual chicken for locomotion analysis (Oral presentation), IPSF/ IPPE 2024, Atlanta, Georgia, USA.
22. Yang, X., **Bist, R. B.,** Subedi, S., and Chai, L. (2023). A computer vision based automatic system for egg grading and defect detection in cage-free facilities. (Oral presentation). 2023 Poultry Science Association Annual Meeting, Philadelphia, PA, USA.
23. Yang, X., **Bist, R. B.,** Subedi, S., and Chai, L. (2023). Monitoring cage-free laying hens on litter floor with machine vision. (Oral Presentation). US Precision Livestock Farming Conference 2023. Knoxville, Tennessee, USA.

24. Yang, X., **Bist, R. B.,** Subedi, S., and Chai, L. (2022). A deep learning model to detect cage-free laying hens on the litter floor. (Oral Presentation), PSA Annual Meeting, San Antonio, Texas, USA.
25. Yang, X., **Bist, R. B.,** Subedi, S., and Chai, L. (2023). (Poster). A computer vision-based automatic system for egg grading and defect detection. 2023 International Conference on Integrative Precision Agriculture, Athens, Georgia, USA.
26. Yang, X., **Bist, R. B.,** Subedi, S., and Chai, L. (2023). Tracking cage-free laying hens on litter floor with machine vision. (Oral Presentation), IPSF/ IPPE, Atlanta, Georgia, USA.
27. Yang, X., **Bist, R. B.,** Subedi, S., and Chai, L. (2022). Monitoring litter quality in cage-free facilities with W-36 pullets. (Poster), PSA Annual Meeting, San Antonio, Texas, USA.
28. Yang, X., **Bist, R. B.,** Subedi, S., and Chai, L. (2022). Tracking cage-free laying hens on litter floor with machine vision (Oral Presentation), UGA Graduate Research Forum, Athens, Georgia, USA.
29. Paneru, B., **Bist, R. B.,** Yang, X., and Chai, L. (2024). Tracking dustbathing behavior of cage-free laying hen using machine vision technologies (Poster presentation), IPSF/ IPPE 2024, Atlanta, Georgia, USA.
30. Paneru, B., **Bist, R. B.,** Yang, X., and Chai, L. (2024). Using Machine Learning Models to Detect Dustbathing Behavior of Cage-Free Laying Hens Automatically. (Poster Presentation), ASABE Annual International Meeting 2024, Anaheim, CA, USA.
31. Paneru, B., **Bist, R. B.,** Yang, X., and Chai, L. (2024). Detecting Perching Behavior of Cage-Free Laying Hens with Machine Vision Technologies. (Poster Presentation), ASABE Annual International Meeting 2024, Anaheim, CA, USA.

32. Subedi, S., **Bist, R. B.,** Yang, X., and Chai, L. (2023). Multiple Behavior Classification of Cage-Free Laying Hens Using Deep Learning. (Oral presentation). 2023 Poultry Science Association Annual Meeting, Philadelphia, PA, USA.
33. Subedi, S., **Bist, R. B.,** Yang, X., and Chai, L. (2023). Floor Egg Detection with Machine Vision in Cage-Free Houses. (Oral Presentation). US Precision Livestock Farming Conference 2023, Knoxville, Tennessee, USA.
34. Subedi, S., **Bist, R. B.,** Yang, X., and Chai, L. (2023). Multiple Behavior Classification of Cage-free Laying Hens using Deep Learning. (Poster). 2023 International Conference on Integrative Precision Agriculture, Athens, Georgia, USA.
35. Subedi, S., **Bist, R. B.,** Yang, X., and Chai, L. (2023). Detecting Floor Eggs with Machine Vision Technologies. (Poster), IPSF/ IPPE, Atlanta, Georgia, USA.
36. Subedi, S., **Bist, R. B.,** Yang, X., and Chai, L. (2022). Pecking Behavior and Damages Detection Using Machine Vision Technology. (Oral Presentation), PSA Annual Meeting, San Antonio, Texas, USA.
37. Saeidifar, S., Li, G., Chai, L., and **Bist, R. B.** (2024). Zero-shot image segmentation for monitoring thermal conditions of individual laying hens. (Oral Presentation), IPSF/ IPPE 2024, Atlanta, GA, USA.

A.6 ROLES IN PROFESSIONAL SOCIETIES AND OTHERS

- **Education and Career Development Committee Member** of Poultry Science Association Hatchery (2023 - present).
- **Vice-President** of Nepali Student Association at the University of Georgia (2023 - 2024).

- **Poultry Science Association member** (2021 - cont.).
- **World Poultry Science Association member** (2021- cont.).
- **American Society of Agricultural and Biological Engineers member** (2023 - cont.).
- **Canadian Society for Bioengineering member** (2023 - cont.).
- **Volunteer** at different programs organized by Nepali Student Association (2021 - cont.).
- **Certified evisceration sorter** at PECO Foods, Inc., Arkansas, 2019.
- **ECO Club Advisor** at Prabhat Vidhya Niketan Higher Secondary School (2012 - 2014).
- **President** of Biological Science Association Nepal at Siddhanath Science Campus (2011 - 2012).
- **Pasture-raised livestock farmer** at a family-owned farm in Nepal (2000 - 2014).

A.7 HONORS/AWARDS

- Winner of **Outstanding Graduate Student Research Presentation**, 2023 International Poultry Scientific Forum (IPSF/IPPE, 2023).
- Winner of **2023 Summer Travel Grant**, University of Georgia.
- Awarded "**Employee of Plant**" and "**Employee of the Month**" at PECO Foods, Inc., Arkansas, 2019.
- **Educating Children in Nepal Scholarship** at Florida International Higher Secondary Boarding School (2003-2010).

A.8 JOURNAL / CONFERENCE REVIEWER

- Applied Computing and Informatics (2024-cont.) [**CiteScore- 24.2**].

- Artificial Intelligence in Agriculture (2023-cont.) [**CiteScore 15.1**].
- Computers and Electronics in Agriculture Journal (2023-cont.) [**Impact Factor- 8.3, CiteScore- 13.6**].
- Poultry Science Journal (2023-cont.) [**Impact Factor- 4.4, CiteScore- 7.4**].
- ASABE Applied Engineering in Agriculture (2023-cont.) [**Impact Factor- 0.9, Cited Half-Life- 13.1**].
- 2nd US Precision Livestock Farming Conference (USPLF 2023).

A.9 LEADERSHIP TRAINING

- University of Georgia "**Leadership Summit**" (2023).
- Georgia Research Alliance "**Greater Yield Cohort 3- Session 1**" (2023).
- University of Georgia Innovation District "**I-Corps Cohort 13**" (2021).

A.10 SKILLS

- **Statistical software:** R, Python, and JMP
- **Programming languages:** R and Python
- **Operational systems:** Windows

A.11 GRANT APPLIED

1. **UGA- Summer Research Grant.** "An automated footpad dermatitis detection and scoring system with machine vision technologies." (Not Funded; 2023).

2. **Graduate Student Travel Grant** from the Graduate School at the University of Georgia (Funded: $550; 2023).